

Role of Transcriptional and Translational Gene Regulation in the Mechanism of Doxorubicin Cardiotoxicity

Thesis submitted for the degree of
Doctor of Philosophy (PhD)
at the University of Leicester

By

Amy Victoria Pointon
MRC Toxicology Unit
University of Leicester

September 2009

ABSTRACT

Role of Transcriptional and Translational Gene Regulation in the Mechanism of Doxorubicin Cardiotoxicity

Amy V Pointon, MRC Toxicology Unit, University of Leicester

Doxorubicin, one of the most widely used and effective anticancer drugs, is limited in its therapeutic use by cardiotoxicity. Multiple hypotheses have been advanced to explain the cardiotoxicity. In this project I utilised novel global genomic analysis of mRNA and miRNA transcription and mRNA translation to investigate the mechanism of doxorubicin cardiotoxicity *in vivo*. A comparator naphthoquinone was employed in parallel to specifically investigate the potential role of redox activity in the mechanism of cardiotoxicity. For both compounds mouse models were used where cardiac damage was characterised at several dose levels (acute and chronic repeat dosing for 7 weeks). A major transcriptionally and translationally affected pathway was the electron transport chain, this was further confirmed biochemically. These changes were reflected by a rapid loss of ATP and an associated increase in the AMP:ATP ratio and associated activation of AMPK indicating a change in cellular energy dynamics. In tandem mtDNA copy number and caspase 3 were rapidly increased. Comparison of all the data led to the hypothesis that the mechanism of doxorubicin toxicity was via interference with the electron transport chain, possibly through electron shuttling, leading to mitochondrial damage and activation of the intrinsic pathway of apoptosis. In further analysis miRNA alterations associated with the cardiotoxicity of both compounds were investigated. Several miRNAs appeared to be intrinsically involved and one of these, miR-181a was followed up *in vitro* in HL-1 cells and showed an association with susceptibility to doxorubicin cardiotoxicity. The findings provide a novel insight into doxorubicin cardiotoxicity, through the utilization of genomics and suggest the major mechanism of doxorubicin toxicity is via interference with the electron transport chain, and unrelated to the pharmacological action. These data offer the possibility of molecule alteration to retain the pharmacological profile without the associated cardiotoxicity.

ACKNOWLEDGMENTS

It is extremely hard to know where to start; so many people have helped, motivated, supported and guided me throughout the past three years. Without the funding from the BBRSC, GSK and MRC this thesis would have not been possible. I would like to thank and convey my sincere gratitude to my academic supervisor at the MRC Toxicology Unit, Tim Gant for whom I would have not completed this thesis without his guidance, help and support over the past three years. Tim has been incredibly supportive.

A number of people at the MRC Toxicology Unit have been a huge help from day one, they have offered both scientific assistance and friendship. In particular all members of the Systems Toxicology Group past and present, they have put up with me, my questions and allowed scientific discussion (thanks Josh), taught me how to 'deal' with all the microarray data (thanks JinLi and Shu-Dong) but most importantly were always willing to go for coffee! Two members have had a massive role, Kate and Joan. Thanks Kate for all your help and the hours stuck upstairs waiting for the time course to finish; I would still be there if it was not for your assistance. And last but no means least, Joan, you are always up for a laugh and a wealth of information – a hidden gold mine! My gratitude and thanks go out to you for all you have done.

I would also like to thank and show my appreciation to my industrial supervisor, Jon Lyon, at GSK for all the opportunities you have given me and support and advice offered, I have been able to conduct experiments I could have only dreamed of! Hopefully I will be able to return the favours one day. Also Joel Parry and Tracy Walker from GSK have been a great help, in conducting the quinone HPLC assay and providing assistance and expert help during the development of the mitochondrial complex activity assays.

I would also like to thank my family and friends, in particular my Mum Jean, for your support and encouragement over the years, finally I would like to dedicate this thesis to my late Dad, Mike, he would have been proud of his little Amy.

P.S. Thanks to various coffee producers and Cadburys for beverages and food stuff that have kept me going!

CONTENTS

ABSTRACT	1
ACKNOWLEDGMENTS	2
CONTENTS	3
LIST OF FIGURES	8
LIST OF TABLES	12
ABBREVIATIONS	14
CHAPTER 1: THESIS INTRODUCTION	17
1.1 Introduction to quinone	18
1.2 Doxorubicin	19
1.2.1 Mechanism of anti-cancer activity of doxorubicin	20
1.2.2 Clinical presentation of the associated cardiotoxicity	21
1.2.3 Hypothesised mechanisms of doxorubicin cardiotoxicity	21
1.2.4 Modulation of doxorubicin cardiotoxicity	26
1.3 Cardiac biomarkers	30
1.4 Quinone energy dynamics in the heart and the role of mitochondria	32
1.4.1 Energy dynamics in mitochondria	33
1.4.1.1 Mitochondrial replication	35
1.4.2 The mitochondrial permeability transition pore	37
1.4.3 Mitochondrial genomics	39
1.4.4 Transcriptional response to mitochondrial damage	40
1.4.5 Cell death	42
1.4.5.1 Cardiomyocyte cell death	45
1.5 Transcriptomics and microarrays	45
1.5.1 Transcription and translation of mRNA	45
1.5.2 microRNAs and their role in controlling translation	47
1.5.3 Modulation of miRNA in disease and toxicology	49
1.5.4 Role of miRNA in cardiac disease	50
1.5.5 Additional small non-coding RNA species	52
1.5.6 Transcriptional profiling and the use of expression microarrays	52
1.5.7 Data analysis	56
1.6 Thesis aims and objectives	58
CHAPTER 2: MATERIALS AND METHODS	59
2.1 Animals	60
2.1.1 Preparation of dosing solutions	60
2.1.2 Development of an <i>in vivo</i> model of toxicity	60
2.2 Cardiac cells non-primary	61
2.2.1 Transfection of HL-1 with microRNAs knockdown probes	62
2.3 Primary cardiomyocytes	63
2.4 Measurement of tissue and cell protein content	63
2.5 Assessment of cell viability using the MTS assay	64
2.6 Determination of DMNQ and MNQ levels by HPLC	64
2.7 Assessment of cardiac damage by measurement of plasma creatine kinase activity	65
2.8 Assessment of cardiac damage by measurement of plasma troponin I levels	66

2.9 Assessment of cardiac damage by measurement of AST levels	67
2.10 Measurement of glutathione and reduced glutathione	67
2.11 Measurement of caspase 3 activity	68
2.11.1 Caspase 3 assay	69
2.11.2 Caspase 3 western blotting	69
2.12 Measurement of ATP/ADP/AMP activity by HPLC	70
2.13 Measurement of ventricular width	70
2.14 Nucleic acid extraction	70
2.15 Quantification and quality control of nucleic acid extraction	71
2.16 Transcriptional profiling using microarrays	72
2.16.1 Microarray hybridization	74
2.16.2 Post hybridization slide washing	74
2.16.3 Scanning of microarrays and primary analysis	74
2.17 Quantitative Real time PCR	74
2.17.1 First strand cDNA synthesis	75
2.17.2 Primer design, optimisation and validation	75
2.17.3 Running qRT-PCR	77
2.17.4 Statistical analysis of qRT-PCR data	77
2.18 mtDNA copy number	77
2.19 microRNA expression profiling	77
2.20 microRNA qRT-PCR	78
2.21 microRNA northern blotting	79
2.22 Separation of RNA and verification for translational analysis	80
2.23 Translational profiling using microarrays	82
2.24 Transcription factor binding	83
2.25 Mitochondrial complex activities	85
2.25.1 Mitochondrial complex activity – sample preparation	86
2.25.2 Complex I activity	86
2.25.3 Complex II-III activity	87
2.25.4 Complex IV activity	88
2.25.5 Complex V activity	89
2.26 Citrate synthase activity	89
2.27 ANT/VDAC western blotting	90
2.28 Lactate dehydrogenase assay	90
2.29 Glutamate dehydrogenase assay	91
2.30 Methemoglobin assay	91
2.31 DNA and protein synthesis	92
2.32 Cell culture media composition	92
2.33 Statistical Analysis	93
CHAPTER 3: TOXICOKINETICS OF DMNQ AND MNQ IN MICE AND THE APPLICATION OF DMNQ FOR STUDYING CARDIOTOXICITY <i>IN VIVO</i>.	94
3.1 Introduction	95
3.1.1 Plan of investigation	95
3.1.2 Hypothesis and Aims	96
3.2 Results	97
3.2.1 Dose selection	97
3.2.2 Toxicokinetics and bio-distribution of DMNQ or MNQ in a mouse model	97

3.2.3 Metabolomic analyse	99
3.2.4 Cardiac GSH/GSSG and plasma CK-MB activity	99
3.2.5 Cardiac transcription profiling	102
3.2.6 De novo DNA and protein synthesis	103
3.3 Discussion	104
3.3.1 Summary	106
CHAPTER 4: EVALUATION OF THE RELATIVE CARDIOTOXICITY OF DOXORUBICIN AND DMNQ IN A MOUSE MODEL	107
4.1 Introduction	108
4.1.1 Plan of investigation	109
4.1.2 Hypothesis and Aims	110
4.2 Experimental design	111
4.3 Results	111
4.3.1 Dose response experiments	111
4.3.2 Body mass to heart mass ratios	117
4.3.3 Biochemical endpoints	119
4.3.4 Cellular imaging	120
4.4 Discussion	127
4.4.1 Summary	129
CHAPTER 5: TRANSCRIPTIONAL RESPONSE OF THE HEART <i>IN VIVO</i> FOLLOWING DOXORUBICIN AND DMNQ EXPOSURE	130
5.1 Introduction	131
5.1.1 Plan of investigation	131
5.1.2 Hypothesis and Aims	132
5.2 Results	134
5.2.1 Transcriptional profiles	134
5.2.2 Identification of mechanism specific expression	134
5.2.3 Pathway analysis	137
5.2.3.1 KEGG pathway analysis	137
5.2.3.2 Pathway analysis: Ingenuity pathway analysis	140
5.2.4 Transcriptional response in oxidative phosphorylation genes	145
5.2.5 Transcription response in NRF-1 target genes	147
5.2.6 qRT-PCR confirmation of microarray data	148
5.2.7 Genomic consequences of cardiac damage	154
5.2.7.1 AMPK activity	154
5.2.7.2 mtDNA copy number	156
5.2.8 Activity of proteolipid complexes on the mitochondrial membrane	158
5.2.9 Investigation of the rapid induction of transcription	159
5.3 Discussion	162
5.3.1 Comparison of transcriptional expression profiles	162
5.3.2 Identification of a mechanistic cardiotoxic gene signature	163
5.3.3 Expression of <i>Tcap</i>	166
5.3.4 Pathway analysis	167
5.3.5 Transcriptional response to oxidative phosphorylation	168
5.3.6 Transcriptional response to mitochondrial damage	171
5.3.7 Summary	173

CHAPTER 6: microRNA RESPONSE OF THE HEART <i>IN VIVO</i> FOLLOWING DOXORUBICIN AND DMNQ EXPOSURE	175
6.1 Introduction	176
6.1.1 Plan of investigation	177
6.1.2 Hypothesis and Aims	177
6.2 Results	178
6.2.1 miRNA expression profiles	178
6.2.2 Genomic localization of miRNA coding sequences	183
6.2.3 qRT-PCR and northern blotting confirmation of microarray data	185
6.2.4 Plasma expression of miRNAs	190
6.3 Discussion	192
6.3.1 Genomic localization of miRNAs	195
6.3.2 miRNA expression in plasma	197
6.3.3 miRNA target prediction	199
6.3.4 Summary	199
 CHAPTER 7: TRANSLATIONAL RESPONSE OF THE HEART <i>IN VIVO</i> FOLLOWING DOXORUBICIN AND DMNQ EXPOSURE	 200
7.1 Introduction	201
7.1.1 Plan of investigation	203
7.1.2 Hypothesis and Aims	204
7.2 Results	205
7.2.1 mRNA translational profiling	205
7.2.2 Pathway analysis	208
7.2.3 Translational response in oxidative phosphorylation genes	209
7.2.4 qRT-PCR confirmation of microarray data	212
7.2.5 Correlation of mRNA translational profiles with miRNA expression profiles	215
7.3 Discussion	217
7.3.1 Pathway analysis	219
7.3.2 Verification of translational modulation	219
7.3.3 miRNA-mRNA predicted interactions	221
7.3.4 Summary	222
 CHAPTER 8: EFFECT OF DOXORUBICIN AND DMNQ ON MITOCHONDRIA AND THE UTILIZATION OF <i>IN VITRO</i> MODELS TO INVESTIGATE microRNA FUNCTION	 223
8.1 Introduction	224
8.1.1 Plan of investigation	224
8.1.2 Hypothesis and Aims	225
8.2 Results	226
8.2.1 Comparison of cardiac <i>in vitro</i> and <i>in vivo</i> models	226
8.2.1.1 <i>In vitro</i> dose selection	227
8.2.1.2 Transcriptional and miRNA profiling <i>in vitro</i>	227
8.2.2 miRNA knockdown	231
8.2.3 Electron transport chain complex activity	232
8.2.4 Assessing mitochondrial integrity	242

8.2.5 Mechanistic consequences	246
8.3 Discussion	250
8.3.1 Establishing a cardiac <i>in vitro</i> model system	250
8.3.2 Doxorubicin and DMNQ challenge of HL-1 cells with suppressed miR-181a expression	252
8.3.3 Affects on mitochondria and energy dynamics	253
8.3.4 Summary	257
CHAPTER 9: THESIS DISCUSSION	258
9.1 Study design and data analysis	261
9.2 Mechanisms of toxicity	263
9.3 Specificity of doxorubicin as a cardiotoxin	275
9.4 The potential role of miRNAs	276
9.5 Possible strategies to modulate doxorubicin cardiotoxicity	278
9.6 Other cardiotoxic anti-cancer agents	279
9.7 Future work	281
9.8 Conclusions	281
REFERENCES	283

ADDENDA CONSISTING OF ONE DATA CD

LIST OF FIGURES

Figure 1.1	Chemical structure of doxorubicin, its sister compound DNR, epirubicin and mitoxantrone	20
Figure 1.2	Fenton reaction equation	27
Figure 1.3	Illustration of the process of oxidative phosphorylation	34
Figure 1.4	Schematic summary of the mechanisms of cellular energy production	35
Figure 1.5	Overview of the previous and current knowledge of the molecular composition of the mPTP	38
Figure 1.6	Summary of the proposed mechanisms of mitochondrial damage following doxorubicin	39
Figure 1.7	Role of PCG-1 α in the activation of transcription factors involved in energy metabolism	41
Figure 1.8	Schematic representation of the major events of the apoptotic pathway	44
Figure 1.9	Summary of the process of RNA translation	46
Figure 1.10	Summary of the mechanism of miRNA processing	49
Figure 1.11	Known roles of miRNAs in cardiac dysfunction	50
Figure 1.12	Differential expression profiles of miRNAs in cardiac hypertrophy and myocardial infarction	51
Figure 1.13	Schematic diagram of the microarray production and processing utilised in this thesis	54
Figure 1.14	Translational profiling experimental design	55
Figure 2.1	Principle of the AST assay	67
Figure 2.2	Principle of the GLDH assay	91
Figure 3.1	DMNQ and MNQ exposure kinetics in male C57BL/6J mice following a single dose of 25mg/kg	98
Figure 3.2	Urinary metabolite profiling	100
Figure 3.3	Cardiac GSH and GSSG levels following a single dose of 25mg/kg DMNQ in 10ml/kg arachis oil or 10ml/kg arachis oil	101
Figure 3.4	Plasma CK-MB levels following a single dose of 25mg/kg DMNQ or 25mg/kg MNQ	101
Figure 3.5	PCA of DMNQ (25mg/kg) and MNQ (25mg/kg)	103
Figure 3.6	DNA and protein synthesis following DMNQ and doxorubicin exposure for 24 hours in HL-1 cells	103
Figure 4.1	Structure of doxorubicin and DMNQ with their associated chemical properties	110
Figure 4.2	Schematic diagram of the experimental design of the chronic models of dosing	111
Figure 4.3	Dose response organ:body weight ratios <i>in vivo</i>	114
Figure 4.4	Creatine kinase muscle/brain (CK-MB) activity during dose response experiments	115
Figure 4.5	Number of genes significantly differentially expressed during dose response experiments	116
Figure 4.6	Heart:Body weight ratios <i>in vivo</i>	118
Figure 4.7	Acute creatine kinase measurement	121
Figure 4.8	Chronic creatine kinase measurement	122
Figure 4.9	Troponin I activity	123

Figure 4.10	AST activity following acute doxorubicin and chronic DMNQ and doxorubicin	124
Figure 4.11	Pathophysiological characterisation of cardiac damage	125
Figure 4.12	Ventricular width	126
Figure 5.1	Summary of the process of transcriptional data analysis	133
Figure 5.2	PCA of transcriptional data	135
Figure 5.3	Significantly affected KEGG pathways following acute DMNQ and doxorubicin	139
Figure 5.4	Signature of pathways affected by both doxorubicin and DMNQ in a chronic model of toxicity	140
Figure 5.5	HCL of genes encoding the complexes of the ETC involved in oxidative phosphorylation	146
Figure 5.6	HCL of genes that were targeted or regulated by the transcription factor NRF-1.	147
Figure 5.7	Confirmation of selected differentially regulated genes in an acute model of DMNQ toxicity	149
Figure 5.8	Confirmation of selected differentially regulated genes in a chronic model of DMNQ toxicity	150
Figure 5.9	Confirmation of selected differentially regulated genes in an acute model of doxorubicin toxicity	151
Figure 5.10	Confirmation of selected differentially regulated genes in a chronic model of doxorubicin toxicity	152
Figure 5.11	<i>Tcap</i> gene expression in plasma and cardiac tissue	153
Figure 5.12	Transcription of genes encoding AMPK	155
Figure 5.13	HCL of genes that are encoded by the mitochondrial genome	156
Figure 5.14	mtDNA copy number	157
Figure 5.15	Western blots probed for ANT and VDAC	158
Figure 5.16	NRF-1 activity, protein expression level and DNA binding	160
Figure 5.17	Methemoglobin activity following a single dose of doxorubicin (15mg/kg) and DMNQ (25mg/kg)	161
Figure 5.18	GSH and GSSG activity following a single dose of doxorubicin (15mg/kg)	161
Figure 5.19	Summary of pathway activation following a single dose of either DMNQ (25mg/kg) or doxorubicin (15mg/kg)	168
Figure 5.20	Schematic summary of the possible mechanisms of doxorubicin cardiotoxicity with transcriptional modulated genes highlighted	173
Figure 6.1	Clustering of miRNAs significantly affected in an acute model of doxorubicin and DMNQ toxicity	180
Figure 6.2	Clustering of miRNAs significantly affected in a chronic model of doxorubicin and DMNQ toxicity	181
Figure 6.3	Clustering of miRNAs significantly affected by doxorubicin and DMNQ	182
Figure 6.4	Clustering of miRNAs significantly affected in all models of toxicity	183
Figure 6.5	Representation of the relative location from where significantly expressed miRNAs are encoded from in an acute model of toxicity	184
Figure 6.6	Representation of the relative location from where significantly expressed miRNAs are encoded in the genome that are differentially expressed in all models of toxicity	185
Figure 6.7	Confirmation of down-regulated miR-181a in cardiac tissue	186

Figure 6.8	Confirmation of up regulated miR-29a	187
Figure 6.9	Further qRT-PCR confirmation of selected differentially regulated miRNAs in an acute model	188
Figure 6.10	qRT-PCR confirmation of selected differentially regulated miRNAs in a chronic model	189
Figure 6.11	Plasma expression of miR-181a and miR-29a in a model of acute doxorubicin (15mg/kg) and DMNQ (25mg/kg) toxicity	191
Figure 6.12	Summary of the role of miRNAs in cardiac function with those affected in these studies highlighted	194
Figure 6.13	Role of miR-29 and miR-34 in the activation of p53 induced apoptosis	195
Figure 7.1	Representation of the experimental design employed to carry out translational microarray analysis	204
Figure 7.2	RNA fractionation profiles, from HL-1 cells, cardiac tissue + EDTA and cardiac tissue	207
Figure 7.3	PCA of doxorubicin and DMNQ translational profiles in an acute and chronic modle of toxicity	208
Figure 7.4	Significantly affected translational KEGG pathways	210
Figure 7.5	HCL of translationally affected genes encoding the complexes of the ETC	211
Figure 7.6	Verification of more efficiently translated mRNAs,	213
Figure 7.7	Verification of less efficiently translated mRNAs	214
Figure 7.8	Correlation of mRNA-miRNA interactions following acute doxorubicin (15mg/kg) and DMNQ (25mg/kg) treatment	216
Figure 7.9	Correlation of mRNA translational profiles and miRNA expression profiles	217
Figure 8.1	Venn diagrams of HL-1 and primary cardiomyocyte gene expression changes compared to cardiac <i>in vivo</i> gene expression profiles	226
Figure 8.2	Cell viability following 24 hours exposure of doxorubicin or DMNQ	227
Figure 8.3	Venn diagrams of <i>in vitro</i> and <i>in vivo</i> gene transcriptional expression changes following doxorubicin or DMNQ	229
Figure 8.4	Signature of miRNAs affected <i>in vitro</i>	230
Figure 8.5	Venn diagrams of <i>in vitro</i> and <i>in vivo</i> miRNA expression changes following doxorubicin or DMNQ	231
Figure 8.6	miR-181a expression, LDH release and CK-MB release in HL-1 cells exposed to doxorubicin or DMNQ exposure following miR-181a knockdown	233
Figure 8.7	Complex I activity	237
Figure 8.8	Complex II activity	238
Figure 8.9	Complex III activity	239
Figure 8.10	Complex IV activity	240
Figure 8.11	Complex V activity	241
Figure 8.12	Summary of the activity of each complex of the oxidative phosphorylation pathway	242
Figure 8.13	Citrate synthase activity	244
Figure 8.14	GLDH activity	245
Figure 8.15	ATP/ADP/AMP HPLC spectra	247
Figure 8.16	ATP, ADP, AMP measurement	248
Figure 8.17	Caspase 3 activity	249

Figure 8.18	Overview of the possible diversion of electrons from the ETC	256
Figure 9.1	Overview of the possible shuttling effect of electrons following doxorubicin and DMNQ	267
Figure 9.2	Illustration of the relationship between cardiotoxicity and redox potential	269
Figure 9.3	Cardiac distribution <i>in vivo</i> and structure of the quinone lapachol	269
Figure 9.4	Summary of the influence of AMPK on doxorubicin induced cardiotoxicity	274
Figure 9.5	Schematic of the proposed mechanism of doxorubicin toxicity resulting from inhibition of ATP production from the ETC	276

LIST OF TABLES

Table 1.1	Example of quinones mammals are exposed to in the environment, diet and medicine	19
Table 1.2	Summary of a number of available biochemical biomarkers associated with cardiac damage	31
Table 2.1	Volumes of tissue culture reagents used for different tissue culture vessels	62
Table 2.2	Native protein gel composition	66
Table 2.3	Caspase 3 polyacrylamide gel composition	69
Table 2.4	Post hybridization microarray wash solutions	74
Table 2.5	Forward and reverse primer concentrations used to optimise primer pairs	76
Table 2.6	qRT-PCR cycling conditions	76
Table 2.7	Post hybridization microarray wash solutions	78
Table 2.8	miRNA northern blotting gel composition	80
Table 2.9	PCR conditions used to generate probes for northern blotting	81
Table 2.10	EMSA gel composition	85
Table 2.11	NRF-1 western blot polyacrylamide gel composition	85
Table 2.12	Details of reaction buffers for complexes I-V assays	87
Table 2.13	ANT and VDAC polyacrylamide gel composition	90
Table 3.1	Summary of DMNQ and MNQ exposure following a single 25mg/kg dose in a mouse model	98
Table 4.1	Selected dose levels and time points used in doxorubicin first dose response	112
Table 4.2	Doxorubicin first dose response, body, heart, liver and kidney weight at the point of sacrifice	112
Table 4.3	Calculated organ to body weight ratios 48 hours following a single dose of doxorubicin	112
Table 4.4	Selected dose levels and time points used to select dose levels for mechanic characterisation	113
Table 4.5	The concentration of compounds and point of sacrifice used for all further work	117
Table 5.1	Concentration of compounds used for all transcriptional profiling	132
Table 5.2	Gene transcriptional signature affected by doxorubicin and DMNQ in an acute and chronic model of toxicity	136
Table 5.3	Number of transcriptional modulated genes included in subsequent pathway analysis	137
Table 5.4	Number of transcriptional modulated genes included in IPA analysis	140
Table 5.5	IPA networks transcriptionally affected by both DMNQ and doxorubicin in an acute model of toxicity	142
Table 5.6	IPA networks transcriptionally affected by both DMNQ and doxorubicin in a chronic model of toxicity	144
Table 5.7	Time points used to verify transcriptional microarray data by qRT-PCR	148
Table 7.1	Table stating the time points of sacrifice for translational profiling experiments	203
Table 7.2	Doxorubicin and DMNQ translationally modulated genes in an acute and chronic model	206

Table 7.3	Time points used to verify translational microarray data by qRT-PCR	212
Table 8.1	Concentration range of doxorubicin and DMNQ tested in dose selection experiments <i>in vitro</i>	227
Table 8.2	Significantly affected KEGG pathways following doxorubicin (1 μ M) and DMNQ (5 μ M) in HL-1 cells for 24 hours	229
Table 8.3	Table stating the time points of sacrifice for mitochondrial enzyme activity assays <i>in vivo</i>	234
Table 8.4	ATP/ADP and AMP/ATP ratios	249

ABBREVIATIONS

%	Percent
~	Approximately
<	Less than
>	More than
±	Plus or minus
≤	Less than or equal to
≥	Greater than or equal to
μCi	Microcurie
μg	Microgram
μl	Microlitre
μM	Micromolar
ADP	Adenine diphosphate
AMP	Adenine monophosphate
AMPK	AMP-activated protein kinase
ANT	Adenine nucleotide translocator
AST	Aspartate aminotransferase
ATP	Adenine triphosphate
AUC	Area under the curve
BAD	Bcl-2 antagonist of cell death
BAX	Bcl-2 associated x protein
bp	Base pair
BSA	Bovine serum albumin
cDNA	Complementary DNA
CK	Creatine kinase
CK-MB	Creatine kinase muscle brain isoform
C _{max}	Maximum concentration
CoA	Coenzyme A
C _t	Cycle threshold
cTnI	Cardiac troponin I
Cy	Cyanine dye
CYP-D	Cyclophilin-D
Cyt c	Cytochrome c
DMNQ	2,3-dimethoxy-1,4-Naphthoquinone
DMSO	Dimethylsulphoxide
DMSO	Dimethyl sulfoxide
DNA	Deoxyribonucleic acid
DNR	Daunorubicin
Dox	Doxorubicin
dpm	Disintegrations per minute
dsRBD	Double stranded RNA binding domain
dUTP	Deoxyuridine triphosphate

e ⁻	Electron
e.g.	For example
EDTA	Ethylenediaminetetraacetic acid
ETC	Electron transport chain
FADH ₂	Flavin adenine dinucleotide
Fe ²⁺	Ferrous iron
Fe ³⁺	Ferric iron
g	Gram
GSH	Reduced glutathione
GSSG	Oxidized glutathione
GST	Glutathione-S-transferase
H ⁺	Proton
H ₂ O ₂	Hydrogen peroxide
HCL	Hierarchical cluster
HO•	Hydroxyl radical
HPLC	High performance liquid chromatography
i.p.	Intraperitoneal
IPA	Ingenuity pathway analysis
IRP	Iron regulatory protein
kDa	Kilodalton
KEGG	Kyoto Encyclopedia of Genes and Genomes
kg	Kilogram
LDH	Lactate dehydrogenase
log P	Logarithm of the partition coefficient
M	Molar
m ²	Meters squared
MDH	Malate dehydrogenase
mg	Milligrams
miRNA	microRNA
ml	Millitre
mM	Millimolar
MNQ	2-methyl-1 4-naphthoquinone (Menadione)
mPTP	Mitochondrial permeability transition pore
mRNA	Messenger RNA
mtDNA	Mitochondrial DNA
mTOR	Mammalian target of rapamycin
NAD ⁺	Nicotinamide adenine dinucleotide
NADH	Reduced nicotinamide adenine dinucleotide
NADPH	Reduced nicotinamide adenine dinucleotide phosphate
ng	Nanogram
nM	Nanomolar
NOAEL	No observed adverse effect levels

NQO1	NAD(P)H:Quinone oxidoreductase 1
nt	Nucleotide
O ₂	Molecular oxygen
O ₂ ^{•-}	Superoxide anion
OD	Optical density
Oligo(s)	Oligonucleotide(s)
p53	p53 tumor suppressor
PAGE	Polyacrylamide gel electrophoresis
PBS	Phosphate buffered saline
PCA	Principle component analysis
PCD	Programmed cell death
PCR	Polymerase chain reaction
piRNA	Piwi-interacting RNA
pM	Picomolar
RISC	RNA-induced silencing complex
RNA	Ribonucleic acid
RNAi	RNA interference
ROS	Reactive oxygen species
rpm	Revolutions per minute
RT	Room temperature
qRT-PCR	Quantitative Real time PCR
SDS	Sodium dodecyl sulfate
siRNA	Small interfering RNA
SOD	Superoxide dismutase
TCA cycle	Tricarboxylic acid cycle
TFAM	Transcription factor A mitochondrial
tiRNA	Transcription initiation RNA
T _m	Melting temperature
T _{max}	Time to maximum
UTR	Untranslated region
UV	Ultraviolet
VDAC	Voltage dependent anion channel
wk	Week

Chapter 1: Thesis Introduction

1.1 INTRODUCTION TO QUINONES

Doxorubicin is a member of the quinone class of chemicals. Quinones are a group of naturally occurring compounds derived from aromatic hydrocarbons present in all respiring animal and plant cells (Long and Jaiswal 2000; O'Brien 1991; Smith 1985). They represent a class of toxicological intermediates which can cause a wide range of hazardous effects, mediated through chemical reactivity and redox cycling (Parry et al. 2009; Bolton et al. 2000). Biologically quinones are broadly divided into two classes, endogenous and physiological quinones. Endogenous quinones are produced via oxidative metabolism of estrogens and catecholamine (E.g.: dopamine, adrenaline, noradrenalin), or through alkylation (transfer of an alkyl group from one molecule to another) (Monks et al. 2002). Physiological quinones are however utilised as redox-active cofactors. For example, within the electron transport chain (ETC) during aerobic respiration in mammals (Saraste 1999).

Mammals are exposed to quinones through diet, medicines and the environment (Table 1.1). Quinones are often found as the active ingredient of many herbal remedies and dyes due to their presence as a secondary metabolite in plants from which they are derived, e.g.: the natural dye henna contains the quinone 2-hydroxy-1, 4-naphthoquinone. Exposure to quinone-associated compounds can result in a range of toxicities, despite a number of quinones having a clear therapeutic benefit e.g. doxorubicin. They exert their toxicity predominantly through two mechanisms; covalent binding to vital cellular macromolecules (Floreani and Carpenedo 1991), or oxidative stress via redox cycling (Bolton et al. 2000). The importance of these two mechanisms varies depending on a number of factors, including, the redox potential of the quinone, the susceptibility of electrophilic centres and the degree of oxidation of protein thiols by superoxide radicals (O'Brien 1991). The molecular basis for the activation of quinone cytotoxicity in terminally differentiated cells e.g.: cardiomyocytes has been attributed to the alkylation or oxidation of essential protein thiol or amine groups.

Compound	Quinone Class	Exposure
Doxorubicin	Anthracycline	Clinical use to treat cancer
Tetracenoycin	Anthracycline	Clinical use - antibiotic
1,4-naphthoquinone	Naphthoquinone	Diesel exhaust fumes ¹
5-hydroxy-1,4-naphthoquinone	Naphthoquinone	Diet

Table 1.1: Example of quinones mammals are exposed to in the environment, diet and medicine.

¹ Pan et al. 2004

1.2 DOXORUBICIN

Doxorubicin is an anthracycline antibiotic, and amongst the most successful of broad spectrum anticancer agents developed (Sun et al. 2001), first isolated from *Streptomyces peucetius* during the 1960's along with daunorubicin (DNR) (Figure 1.1). It has been used since particularly in the treatment of solid tumours and haemophilic carcinomas. Despite this important anticancer pharmacology, the clinical value is severely jeopardized by two factors; firstly drug resistance arising primarily as a result of over-expression of ABC gene family members and secondly cumulative and irreversible dose dependent cardiotoxicity.

Doxorubicin is metabolised to form an alcohol via a carbonyl reduction and several aglycone derivatives, though little of this metabolism is conducted in the heart (Berthiaume and Wallace 2007a). The parent compound is partially eliminated through the faeces and urine; in addition to undergoing bio-reduction (Berthiaume and Wallace 2007a).

Bio-reduction occurs by one-electron reduction through metabolic activation, by NADPH-dependent cytochrome P450 reductase, in the endoplasmic reticulum and complex I of the ETC in the mitochondria resulting in the formation of a semiquinone via a univalent reduction. This semiquinone is capable of autoxidising using molecular oxygen as an electron acceptor, resulting in oxidation to the parent quinone (Kang et al 1996).

Over 2000 analogs of doxorubicin have been developed, including structural modifications (e.g.: epirubicin); structurally related drugs (e.g.: mitoxantrone) and incorporation into liposomes (e.g.: liposomal doxorubicin).

Three have clinical approval, epirubicin (EPI), mitoxantrone and liposomal doxorubicin (Wu 2008). Often these analogs need to be used in greater quantities for the same pharmacological effect and at these levels cardiotoxicity arises. Thus the pharmacological to toxicological ratio is little altered to that of doxorubicin (Alderton et al. 1992). The anti-cancer and cardiotoxic actions of doxorubicin are thought to be exerted through distinct mechanisms; however, both may share common effectors, for example oxidative stress (Tokarska-Schlattner et al. 2006).

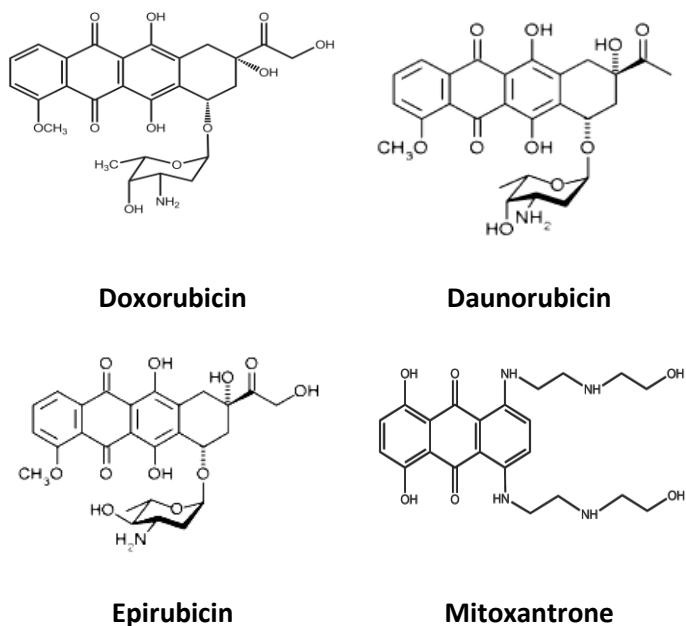


Figure 1.1: Chemical structure of doxorubicin, its sister compound DNR, and analogs epirubicin and mitoxantrone, two analogs of doxorubicin with clinical approval. Doxorubicin has a tetracycline moiety containing a quinone and a conjugated amino sugar residue (Berthiaume and Wallace 2007a).

1.2.1 MECHANISM OF ANTI-CANCER ACTIVITY OF DOXORUBICIN

Despite extensive clinical utilisation the mechanism of doxorubicin's pharmacological action remains controversial (Minotti et al. 2004). However, it is widely accepted that DNA damage is the most probable mechanism. Doxorubicin is highly effective as a DNA synthesis inhibitor by obstructing and inhibiting topoisomerase II (Fornari et al. 1994; Tarr and van Helden 1990). Topoisomerase II is responsible for catalysing the double strand breaks and subsequent rejoining of DNA during replication and repair of the

genome, thus inhibition results in DNA damage (Tarr and van Helden 1990). Direct interaction with genomic DNA, by intercalating between base pairs on the DNA strand resulting in the formation of DNA adducts is also thought to be involved in doxorubicin's anti-cancer activity. These adducts interfere with the binding of proteins and enzymes for instance transcription factors and RNA polymerase by denying access to their binding sites (Cutts et al. 1996). This initiates RNA and DNA inhibition arresting cell proliferation in the S-phase of the cell cycle resulting in a lack of transcription and cell death (Ashley and Poulton 2009; Wallace 2003).

1.2.2 CLINICAL PRESENTATION OF THE ASSOCIATED CARDIOTOXICITY

Both acute and chronic cardiomyopathy occur following doxorubicin treatment (Belham et al. 2007). The major risk factor affecting occurrence is the total cumulative dose received leading to a lifetime limit of $450\text{mg}/\text{m}^2$. An increase to $550\text{mg}/\text{m}^2$ results in a 7% increased risk of developing cardiac damage at some point, suggesting that the resultant toxicity is cumulative and dose-dependent, and also irreversible with time (Takemura and Fujiwara 2007; Horan et al. 2006; Tokarska-Schlattner et al. 2006; Wallace 2003).

Pathologically the cardiotoxicity is manifest as a loss of left ventricular function resulting in cardiomyocyte vacuolation and cell death (apoptotic, autophagic or necrotic).

The gross clinical features associated with doxorubicin cardiomyopathy include hypertension, arrhythmia, myocardial infarction, cardiomyopathy and cardiac failure (Kim et al. 2003). Symptoms typically occur within days to years following treatment (Takemura and Fujiwara 2007). Severe chronic cardiotoxicity is observed in >20% of patients receiving doxorubicin. Additionally standard heart failure treatments of angiotensin-converting enzyme (ACE) inhibitors and β -blockers have little impact on symptoms (Minotti et al. 1999).

1.2.3 HYPOTHESISED MECHANISMS OF DOXORUBICIN CARDIOTOXICITY

The mechanism of doxorubicin cardiotoxicity has not been conclusively determined despite over 30 years of research. It has been proposed that the resultant cardiotoxicity is multifunctional with many mechanisms functioning in co-ordination (Arola et al. 2000).

Redox stress

The majority of hypothesised mechanisms for doxorubicin toxicity have an element of oxidative stress and the subsequent production of reactive oxygen species (ROS). Oxidative stress results from excessive production of ROS above the capacity of cellular antioxidant systems (Gustafsson and Gottlieb 2008). ROS are produced as a consequence of redox cycling through either one or two electron reduction. Two-electron reduction is mediated by NAD(P)H:quinone oxidoreductase (NQO1) and is considered a detoxification pathway resulting in the formation of a stable hydroquinone. These are cleared from the body by conjugation with either sulphate or glucuronic acid and excreted into urine (Munday 2001). Despite this, hydroquinones produced via NQO1 detoxification are capable of autoxidizing, resulting in ROS generation (Munday 2001). However, doxorubicin does not appear to be a substrate for NQO1, based on its inability to oxidize NADH at 100 μ M drug concentrations, thus suggesting that two-electron reduction by NQO1 is not a prominent route of metabolism for doxorubicin (Gutierrez 2000). One-electron reduction is mediated by microsomal NADPH P450 reductase, NADH cytochrome b5 reductase and mitochondrial NADH-oxidoreductase (Parry et al. 2009). This results in production of the semiquinone radical, which is readily autoxidised back to the parent quinone in the presence of molecular oxygen, resulting in the production of a superoxide anion ($O_2^{\bullet -}$). $O_2^{\bullet -}$ is then able to undergo further one-electron reduction, enzymatically through the utilisation of superoxide dismutase (SOD) or spontaneously to form the highly reactive species, hydrogen peroxide (H_2O_2). If H_2O_2 is not reduced by catalase or glutathione peroxidase, a hydroxyl radical ($HO\bullet$), is formed in the presence of trace amounts of iron or other transition metal ions (Bolton et al. 2000; Thannickal and Fanburg 2000). This results in oxidative damage to lipids, proteins and nucleic acids and in some cases apoptosis of cardiomyocytes by indirectly triggering modifications of mitochondrial membranes (Thorburn and Frankel 2006; Marnett 1999). Healthy adult cardiac tissue has a low abundance of endoplasmic reticulum, an organelle key in the expression of cytochrome P450. This results in an increased proportion of redox cycling in the mitochondria in cardiac tissue, making this organelle more susceptible to damage

(Berthiaume and Wallace 2007a). In addition cardiomyocytes have low levels of the anti-oxidant enzymes, catalase and SOD, increasing the susceptibility of cardiomyocytes to oxidative stress (O'Brien 1991).

The quinone moiety on the anthracycline ring that has the potential to act as an alternative electron acceptor undergoing one-electron reduction by complex I of the ETC, followed by re-oxidation strongly suggests a redox hypothesis. Redox cycling has two effects, diversion of electrons from the ETC and production of ROS from the semiquinone, if the production of ROS exceeds cellular detoxification pathways oxidative stress results (Tokarska-Schlattner et al. 2006; Weinstein et al. 2000; Toxopeus et al. 1994; Toxopeus et al. 1993; Doroshov and Davies 1986). The oxidative damage thought to be caused by doxorubicin is complex and results in effects on mitochondria, lipid peroxidation, sarcoplasmic reticulum, lysosomes and microfibers (Yi et al. 2006). However, doxorubicin's redox potential of, -328mV, means that for eukaryotic cells it is not an optimal redox cycling agent. The optimal range is -210 to -160mV (Wallace and Starkov 2000; Powis and Appel 1980). At these redox potentials the relative rates of reduction and oxidation relative to cellular reducing centres and molecular oxygen are relatively balanced. As a result of doxorubicin's negative redox potential, it will be reduced relatively slowly. Doxorubicin reduction to the semiquinone followed by re-oxidation by molecular oxygen results in the formation of ROS, which react with cellular molecules as described earlier. However, the exact consequences of this process on cell signalling and the oxidation of lipids and proteins has not been substantively established (Kang et al. 1997). Furthermore one ROS member, $O_2^{\bullet -}$, can undergo further reactions to form the hydroxyl free radical, resulting in further cellular damage. The majority of studies conducted to identify the mechanism of doxorubicin cardiotoxicity have used concentrations of doxorubicin that exceed clinically relevant doses, making the observed effects difficult to translate to the clinical setting (Tokarska-Schlattner et al. 2006). Additionally a large proportion of studies have been carried out solely *in vitro*; cells in culture are at a higher oxygen tension than those in tissues thus the kinetics of redox reactions *in vitro* do not mirror those which might occur *in vivo* at physiological oxygen tensions. These higher doxorubicin and oxygen concentrations may predispose cells to redox action which

may not occur clinically. While this does not preclude redox cycling as a mechanism of toxicity it suggests that others may be more important.

Mitochondria and cardiolipin

Doxorubicin is known to accumulate in the mitochondria of cardiomyocytes and appears to have an affinity for cardiolipin (Oliveira et al. 2004). Cardiolipin is an acidic phospholipid specific to the mitochondrial inner membrane and is primarily found in cardiac and skeletal muscle cells. It has a vital role in the allosteric regulation (binding effector molecules to cardiolipin) of a number of mitochondrial enzymes including those of the ETC and mitochondrial membrane transporters (Goormaghtigh et al. 1990; Goormaghtigh et al. 1986; Huart et al. 1984). Doxorubicin-cardiolipin binding is thought to interfere with a number of cardiolipin dependent proteins including, pyruvate, phosphate transporters and elements of the ETC by altering membrane kinetics (Wallace 2003). Binding also increases concentrations of doxorubicin near to complex I of the ETC that may facilitate redox action. The effect of doxorubicin localisation in the mitochondrial inner membrane is compounded by the high energy demands of the heart in comparison to other organs. The heart achieves this higher energy demand by increasing the number of mitochondria (~35% of total cell volume) and hence increasing the availability of complex I of the ETC to doxorubicin (Gustafsson and Gottlieb 2008; Tokarska-Schlattner et al. 2005; Lebrecht et al. 2003). However, to date doxorubicin has not been shown to affect the ETC complexes downstream of complex I *in vivo* at clinically relevant concentrations. The effects on complex I may result in the reduction of doxorubicin to the semiquinone and subsequent re-oxidization resulting in oxidative stress and loss of ETC function. This loss of ETC function may trigger caspase 3 activation and cytochrome c release through the activation of the intrinsic pathway of apoptosis (Section 1.4.5). Both have been reported in a rat model of doxorubicin toxicity, however, the dose level used in this analysis exceeded that used clinically (Childs et al. 2002). In addition Wallace (2003) suggested that doxorubicin disrupts mitochondrial function by inducing the mitochondrial permeability transition pore (mPTP), disturbing the proton gradient across the inner mitochondrial membrane, as a result ADP and

phosphate cannot be converted to ATP resulting in uncoupling of oxidative phosphorylation and release of mitochondrial contents into the cellular space (e.g.: cytochrome c, Smad), activating apoptosis leading to a loss of cardiomyocytes.

The role of iron

Limited metabolism of doxorubicin occurs in the heart, except for the reduction of the ketone side chain to the secondary alcohol to form doxorubicinol (Olson et al. 1988). This metabolism is thought to release iron from cytoplasmic aconitase, which converts aconitase to the iron regulatory protein (IRP). IRP causes increased protein levels of the iron transport protein transferrin by mRNA stabilisation and decreased levels of ferritin iron storage protein by decreased mRNA translation (Rouault 2006). Conversely doxorubicin may also inhibit the IRP formation in addition to preventing binding to the IRP element. Thus the effects of doxorubicin on iron regulation in cells is complex and the role played in the mechanism of toxicity is not clear (Minotti et al. 1999). Iron overload is a known mediator of heart failure (Rouault 2001), therefore cardiotoxicity maybe a result of interactions with cellular iron metabolism or an effect of redox cycling.

DNA damage

Another proposed mechanism is direct DNA damage and/or interference with DNA repair (Arola et al. 2000). It is accepted that this is the main mechanism of anti-cancer activity but has also been proposed to contribute to the cardiotoxic phenotype. The anthracycline segment of doxorubicin is thought to insert itself between neighbouring base pairs on the DNA strand, thus single strand breaks and DNA damage occur rendering the DNA stand unable to act as a template during DNA synthesis (Thorburn and Frankel 2006; Zhang et al. 1996). However, clinically DNA damage has not been widely observed in cardiomyocytes, despite activation of p53 and partial DNA repair *in vitro* (L'Ecuyer et al. 2006). Hence it is questionable whether these *in vitro* models of cardiotoxicity mirror the mechanism of action *in vivo*.

Transcription factors

Doxorubicin treatment may affect the expression and activation of a number of transcription factors, affecting gene expression. Altered transcription factor expression may result in activation of apoptosis or necrosis or increased susceptibility to ROS. Doxorubicin treatment has been reported to decrease the expression of the transcription factor GATA-4 (Kim et al. 2003). GATA-4 is a survival factor for cardiomyocytes and an upstream regulator of *Bcl-X*, an anti-apoptotic gene (Aries et al. 2004). Consequently down-regulation of GATA-4 could possibly result in the induction of cardiac myocyte apoptosis, manifesting as cardiac failure.

Uncertainty about the relative role of each of these mechanisms in the induction of doxorubicin cardiotoxicity has led to the hypothesis that doxorubicin induced cardiomyopathy develops as a result of several contributing factors.

1.2.4 MODULATION OF DOXORUBICIN CARDIOTOXICITY

A range of chemicals and compounds have been tested to reduce the cardiotoxicity following doxorubicin administration. The iron chelator and free radical scavenger dexrazoxane (a derivative of EDTA) is the only clinically approved agent for co-administration (Horan et al. 2006). Dexrazoxane is able to bind free iron, Fe^{2+} (ferrous iron) and Fe^{3+} (ferric iron), and could therefore act to reduce free iron in the cell, reducing the level of ROS formation and generation of $HO\bullet$ through Fenton reactions (Figure 1.2), thus reducing oxidative stress. However, there is only very limited amount of free iron in the cell and so the effective target for dexrazoxane is limited. Also it does not appear to confer absolute cardio protection. The cardiovascular biomarker troponin T is still significantly elevated in 35% of patients receiving doxorubicin co-administered with dexrazoxane. The overall risk of developing cardiotoxicity thus is comparable between patients receiving dexrazoxane and those that do not (Lebrecht et al. 2007; L'Ecuyer et al. 2006; Lipshultz et al. 2004; Lopez et al. 1998).



Figure 1.2: Fenton reaction equation, ferrous iron (II) is oxidized by hydrogen peroxide, a ROS, resulting in the formation of ferric iron (III), a hydroxyl radical and a hydroxyl anion.

Similarly in a rat model, dexrazoxane did not provide any protection when clinically relevant concentrations of doxorubicin were utilised (Héon et al. 2003). These data thus bring into question the effectiveness of this agent in preventing doxorubicin induced cardiotoxicity. In addition dexrazoxane is administered as a closed ring structure which is subsequently metabolised to an open ring iron chelating form. However, the closed ring structure has been found to interfere with the pharmacological activity of doxorubicin by stabilising topoisomerase II complexes, preventing DNA damage and tumour cell death, consequently reducing the pharmacological activity of doxorubicin (Bird and Swain 2008; Swain et al. 1997). Other iron chelating agents, e.g.: deferiprone *in vitro* produce similar results (Xu et al. 2006), thus opening the question of the effectiveness of these agents to prevent the occurrence of cardiotoxicity.

Metallothionein is a low molecular weight, thiol-rich protein that functions as an antioxidant and has been implicated with scavenging of hydroxyl radicals, reducing doxorubicin associated cardiotoxicity (Kang et al 1997). An increase in metallothionein in the heart prevents doxorubicin induced apoptosis, possibly through inhibition of the doxorubicin activated p38 mitogen-activated protein kinase (MAPK) pathway. Transgenic mice over-expressing metallothionein, treated with doxorubicin, do not develop cardiotoxicity (Sun et al. 2001). Despite this promising evidence, all studies have utilised super clinical concentrations of doxorubicin; hence translation of this research to the clinical setting is questionable. A number of pharmaceutical agents have been identified that increase metallothionein levels in cardiac tissue, including bismuth subnitrate, isoproterenol and tumour necrosis factor- α . This indicated that increasing metallothionein levels in the heart is possible, providing a novel opportunity to overcome doxorubicin induced cardiotoxicity (Sun et al. 2001; Kang et al. 1997). However, before these approaches are pursued, *in vivo* transgenic studies need to be

repeated with clinically relevant concentrations. Interestingly, Yin et al. (1998) reported that a single clinically relevant (15mg/kg) dose of doxorubicin induces physiological metallothionein expression in the heart, suggesting that activation is an acute response to toxicity.

The free radical scavenger N-acetylcysteine (an antioxidant) has also been found to protect against doxorubicin induced cardiotoxicity in animal models, when administered prior to doxorubicin. Such protection is thought to result from reduced lipid peroxide formation, and free radical scavenging of ROS (Doroshov et al. 1981). It has also been suggested that the antioxidants, vitamin E and flavonoids reduce the toxic effects *in vivo*; however, their activity is limited and is not clinically effective. Similarly the use of FP15, a peroxynitrite decomposition catalyst has been found to prevent doxorubicin induced cardiotoxicity by reducing peroxynitrite (a ROS) production (Pacher et al. 2003). However, all studies utilizing such compounds have been carried out using elevated concentrations of doxorubicin, thus the occurrence of these ROS may arise due to gross cytotoxicity not directly a result of doxorubicin, thus questioning the clinical use of these compounds.

Transgenic mice over-expressing catalase (an enzyme involved in the detoxification of H_2O_2) by 60-100 fold in the heart appear to be protected against doxorubicin-induced toxicity, possibly through utilisation of the free radicals produced during redox cycling of doxorubicin. However, transgenic mice over-expressing catalase by 200-500 fold were not protected; conversely, a slight elevation was observed (Kang et al. 1996). These results may occur due to an imbalance between SOD and catalase, resulting in the chelation of heme iron by catalase and the subsequent release of iron after degradation (Kang et al. 1996; Demant 1984). This illustrates the delicate balance required to maintain cells in a normal physiological state. Due to the toxicity observed with high levels of catalase it is unlikely that administration could occur safely in the clinical setting. This variation and limited success of antioxidant compounds may be due to the unspecific nature of their reactions. Antioxidants reduce oxidative stress in general without being specific to cardiac tissue. This may

not only result in a lack of effect on the cardiotoxicity, but may also interfere with the pharmacological effects of doxorubicin, reducing the effectiveness of these agents (L'Ecuyer et al. 2006; Hensley et al. 1999).

During the early 1980's a continuous infusion of doxorubicin, over 48-96 hours rather than a bolus dose delivered over 15 minutes, appeared effective in reducing the pathological changes in the heart, without affecting the pharmacological action (Minotti et al. 2004). This data implied that the plasma and tissue C_{max}, was more predictive of the development of cardiotoxicity, rather than the AUC (Danesi et al. 2002). Despite this promising evidence, a growing amount of clinical data is available contradicting this idea (Lipshultz et al. 2002). Currently it has been hypothesised that the predictive benefit obtained by lowering the peak dose is offset by damage due to the longer exposure of cardiomyocytes to doxorubicin, suggesting the overall dose level and not the C_{max}, is responsible for the observed cardiotoxicity (Minotti et al. 2004).

Co-administrations of either cyclosporine A or tacrolimus with doxorubicin, both of which are immunosuppressants, appear to provide protection against doxorubicin induced cardiotoxicity (Al-Nasser 1998). Cyclosporine A prevents the mPTP from opening, thus inhibiting cytochrome c release and the subsequent activation of the intrinsic pathway of apoptosis, maintaining cardiomyocyte function (Section 1.4.5). Tacrolimus is thought to act in a similar manner. This highlights the importance of mitochondria in the manifestation of doxorubicin cardiotoxicity. It is possible to postulate that the cardiotoxicity may be a consequence of increased inner mitochondrial membrane permeability transition, resulting in disruption of the mitochondria membrane potential and release of any accumulated calcium from the mitochondria, thus affecting the dynamics and contractility of the heart (Marks 2003; Al-Nasser 1998).

A number of these compounds provide promising insight into the mechanism of doxorubicin cardiotoxicity and provide a potential opportunity for reduction. However, translation of this research to the clinical setting is critical. Small scale clinical trials have not proved successful. Despite the reported cardiotoxicity, and limited modulation, wide spread use of doxorubicin will however continue until effective and safer

alternatives are identified (Horan et al. 2006). Greater targeting to cardiomyocytes may prove successful in reducing the cardiotoxicity without interfering with the potent anti-cancer activity (L'Ecuyer et al. 2006).

1.3 CARDIAC BIOMARKERS

A biomarker is as a measurable biological product whose level is directly correlated to a tissue or cell injury.

Heart failure can be characterised by neurohumoral activation and a decline in cardiac output, a number of phenotypic and biochemical markers are affected resulting in their release into circulating plasma

(Barringhaus and Zamore 2009). Identification of cardiac disease biomarkers provides insight into the pathogenesis of the phenotype allowing an earlier and more accurate diagnosis (Marian and Nambi 2004).

However a number of cardiac biomarkers have a limited half life, therefore the timing of sample collection is important in the diagnosis of cardiac dysfunction (Walker 2006). In addition the amount of activity, the age of

the patient or animal, food consumption and in the case of pre-clinical studies animal handling prior to blood collection can artificially raise a number of clinical chemistry biomarkers, in particular those that lack high

levels of specificity (Walker 2006; Baetz and Mengeling 1971). These issues can be reduced pre-clinically by

consistent experimentation and are of lower priority when comparing vehicle treated control and treated animals as long as handling is consistent. In order to assess cardiac function during and after doxorubicin

treatment a number of cardiac function parameters can be assessed. Cardiac damage can be assessed by imaging, electrophysiology (ECG or ECHO) or clinical chemistry measurement (Table 1.2). However many

cardiac biomarkers are not specific to the heart and elevation is difficult to detect in the early stages of myocardial damage/failure (Naraoka et al. 2005). The 'gold standard' in the clinical setting is the

measurement of Troponin I following a suspected cardiac event (O'Brien 2008). The utility of troponin I in the clinical and pre-clinical diagnosis of cardiac dysfunction is attributed to its high specificity and sensitivity for

cardiac myocyte injury and lack of cross species differences (Walker 2006). This specificity can be accredited to the addition of 10-30 amino acid residues to the troponin T and I proteins compared to troponin C present

in skeletal muscle, allowing efficient differentiation of the three proteins (Wallace et al. 2004). Measurement

also consistently translates to the peak concentrations and half life of biological or chemical compounds and the development of histopathological changes present in humans following cardiac injury or toxicity (York et al. 2007; Wallace et al. 2004; Bertinchant et al. 2000; O'Brien et al. 1997).

Marker of cardiotoxicity	Summary
Creatine kinase	Two subunits (M and B) that dimerise to form three isoenzymes (MM, MB, BB) within the cytoplasm. MM form is found predominately in skeletal muscle, BB the brain and MB within cardiac tissue. Leakage from damaged tissue results in increased plasma levels. The serum half life is ~0.5-1 hour in rats (Walker 2006).
Troponin	Complex of three regulatory proteins (C, I and T) that are essential for muscle contraction in skeletal (C) and cardiac muscle (I and T). The proteins are controlled by changes in intracellular calcium concentrations resulting in the production of myosin cross bridges and increased plasma concentrations of these proteins following damage.
Aspartate aminotransferase (AST)	Two isoenzymes, a mitochondrial and cytoplasmic form. It catalyses the reverse transfer of an amino group to α -oxoglutarate producing keto acid and oxaloacetate, found in heart, liver, skeletal muscle and kidney thus it is an unspecific marker of cardiac damage, elevations maybe a result of non-cardiac origins.
Lactate dehydrogenase (LDH)	A tetrameric protein consisting of two subunits (M and H). The M form found in skeletal muscle and the H form present in the heart. It is localised with the cytoplasm and is released from damaged tissues results in increased plasma levels. It is an unspecific marker of cardiac damage.
Myoglobin	Present in the cytoplasm of cardiac and skeletal muscle and is released into the plasma upon tissue damage. However higher proportions are present in skeletal muscle than cardiac muscle making this an unspecific marker of cardiotoxicity.
B-type natriuretic peptide (BNP)	Neurohormone synthesised primarily in ventricle tissue. It is released into circulating plasma in response to ventricular wall stress, ischemia or infarction (Kasap et al. 2007). The gene encoding this hormone is a 'fetal' gene expressed in the heart prior to birth, upon cardiac hypertrophy the fetal gene signature is re-activated.
Heart fatty acid binding protein (H-FABP)	Predominately expressed in cardiac tissue within the cytoplasm and is responsible for the transport and delivery of fatty acyl-coenzyme A for oxidation within the mitochondria. H-FABP is released from damaged tissue into the circulating plasma following damage (Marian and Nambi 2004). Peak plasma concentrations occur within 15 minutes in the rat and are proportional to the damage observed by microscopy. Due to this rapid release sampling times need great thought (Walker 2006).

Table 1.2: Summary of a number of available biochemical biomarkers associated with cardiac damage. A number of the above are used in the clinical setting to aid the diagnosis of cardiac disease and dysfunction.

The recently identified biochemical biomarkers brain-type natriuretic peptide (BNP) and atrial natriuretic peptide (ANP) provide promise for the identification of further biomarkers of cardiac dysfunction (Kasap et al. 2007). These two novel biomarkers are structurally related hormones secreted from the heart, into circulating blood as pro-hormones in response to both atrial and ventricular myocardial wall tension, respectively (Doust et al. 2005). These allow the identification of the section of the heart that is damaged, thus possibly enabling biomarkers to guide specific treatment (Brügger-Andersen et al. 2008; Gerszten and Wang 2008). Both of these hormones are also expressed in other tissues, limiting their utility as specific cardiac biomarkers. Nevertheless, a large amount of concordance with troponin I has been reported, indicating a high level of specificity to the heart.

Before the wide spread use of these hormones as biomarkers, further data regarding species variation and extrapolation is required. As a number of biochemical biomarkers have now been identified; it would be helpful to measure multiple markers from one sample allowing a more definitive diagnosis.

Recent technological advances (gene microarray, nuclear magnetic spectroscopy (NMR) and tandem mass spectrometry) allow the transcriptome, proteome and metabolome to be screened in the search for possible biomarkers (Marian and Nambi 2004). This technology may identify further novel biomarkers of cardiac dysfunction, allowing improved and earlier diagnosis of a decline in cardiac function.

1.4 QUINONE ENERGY DYNAMICS IN THE HEART AND THE ROLE OF MITOCHONDRIA

Mitochondria perform pivotal activities that are essential for a range of processes including energy metabolism, embryonic development, cell signalling, cell cycle control and cell death (Hamilton et al. 2008). The inner membrane is relatively impermeable; molecules have to enter through transporter proteins, whereas the outer membrane is permeable to molecules up to 1.5kDa. Along the length of the membranes there are a number of positions where the two membranes meet allowing influx and efflux of molecules to

and from the matrix. The inner membrane creates cristae structures in which oxidative phosphorylation is contained (Hom and Sheu 2009).

1.4.1 ENERGY DYNAMICS IN MITOCHONDRIA

Oxidative phosphorylation is the metabolic process which couples the oxidation of reduced nicotinamide adenine dinucleotide (NADH) and flavin adenine dinucleotide (FADH₂) to the phosphorylation of ADP to ATP, by utilisation of the ETC (a series of five enzyme complexes) in the inner membrane (Figure 1.3) (Muravchick and Levy 2006; Thannickal and Fanburg 2000). Oxidative phosphorylation is consistently (seconds to minutes) regulated primarily by substrate availability and allosteric control (inhibition or activation of each enzyme complex by a small regulatory molecule that interacts with the enzyme) (Wagner et al. 2008). Electrons are passed through the complexes of the ETC, intrinsically linked to this process, is the generation and maintenance of a hydrogen ion gradient across the inner membrane. This gradient is established by protons being pumped out of the ETC complexes across the inner membrane. This proton gradient across the inner membrane allows the flow of hydrogen ions to pass through complex V allowing the phosphorylation of ADP and phosphate to ATP (Muravchick and Levy 2006). Complex V is a reversible enzyme and under certain conditions can act as an ATPase to hydrolyze ATP produced in the cytosol by glycolysis and produce a proton gradient (Shen et al. 2009; Wallace and Starkov 2000). The proton gradient across the membrane can be dissipated by proton leakage back into the matrix through the inner membrane, thus bypassing complex V (Muravchick and Levy 2006).

ATP within the cell is produced by oxidative phosphorylation through the ETC, but also glycolysis, fatty acid oxidation, and the TCA cycle or a combination of these mechanisms. However both glycolysis and fatty acid oxidation are not efficient energy generators. Glycolysis results in the formation of two ATP molecules for every molecule of glucose. Both glycolysis and fatty acid oxidation result in the production of acetyl CoA which can enter the TCA cycle, allowing oxidation of the acetyl groups in the mitochondrial matrix and the generation of NADH and FADH₂, these electrons are transferred to the inner membrane and enter the ETC

through complex I or in the case of FADH₂ complex II (Figure 1.4). In a state of uncoupled oxidative phosphorylation or inhibition, cellular energy production is reliant on glycolysis. However this process is unable to maintain correct cellular function for prolonged periods, resulting in cellular damage.

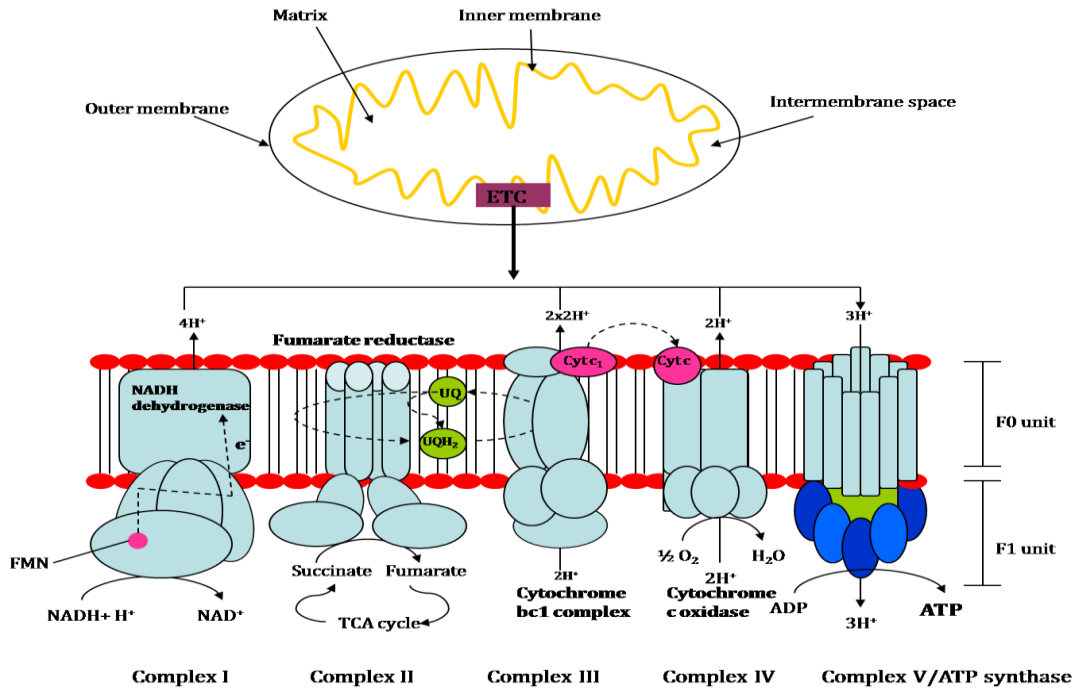


Figure 1.3: Illustration of the process of oxidative phosphorylation. Energy from the transfer of electrons through the complexes of the ETC is used to pump protons from the mitochondrial matrix into the intermembrane space. This creates an electrochemical proton gradient across the inner membrane allowing complex V to use the flow of hydrogen ions through the complex to generate ATP from ADP and inorganic phosphate. Electrons enter the chain through complex I (via NADH) or complex II (via FADH₂). Complex I or II then passes the electrons to coenzyme Q (a lipophilic ubiquinone) which passes two electrons through complex III. This results in electrons being passed to the next electron acceptor (cytochrome c), with the associated translocation of two protons into the inner membrane space. Cytochrome c passes the electrons to complex IV. Complex IV utilises the electrons and hydrogen ions to reduce molecular oxygen to water. The electrochemical gradient formed as protons are passed into the inner membrane space, allows the production of ATP in complex V.

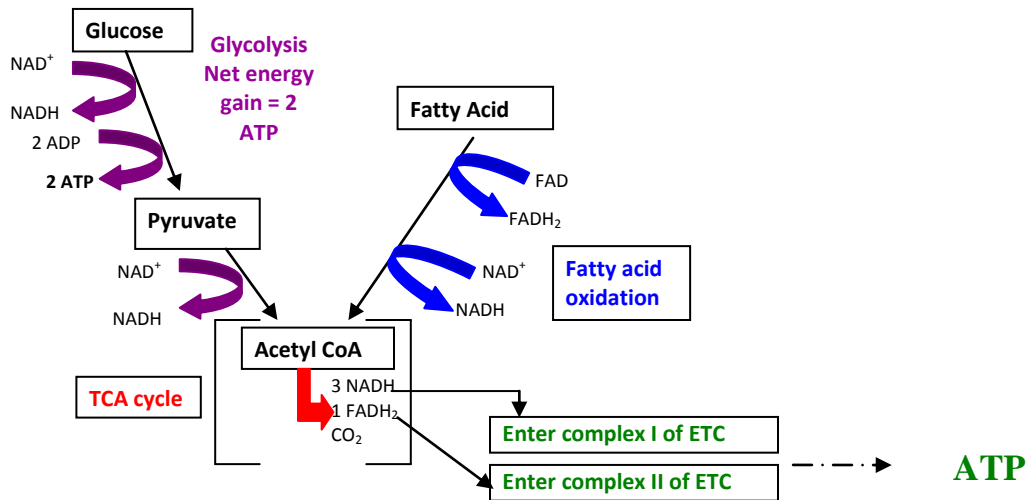


Figure 1.4: Schematic summary of the mechanisms of cellular energy production, involving the inter play between glycolysis, fatty acid oxidation, TCA cycle and oxidative phosphorylation.

1.4.1.1 MITOCHONDRIAL REPLICATION

Mitochondria are created from existing mitochondria through synthesis and division in addition to the import of proteins and lipids. They undergo fusion and fission on average every two minutes in a range of cell types and have a half life of five days to several weeks (Boldogh and Pon 2007; Dykens and Will 2007; Frederick and Shaw 2007; Shaw and Nunnari 2002). A decrease in mitochondrial fusion results in a decrease in oxygen consumption in mitochondria and a lack of membrane potential. Whereas inhibition of fission can delay or inhibit cytochrome c release; preventing the induction of the intrinsic pathway of apoptosis (Section 1.4.5) (Hom and Sheu 2009). It is this balance between fusion and fission that is critical to maintain normal biogenesis and turnover of mitochondria; little is currently known about this process in cardiomyocytes.

Mitochondria are key organelles in a number of disease states including cardiovascular disease (Armstrong 2007; Milagros Rocha and Victor 2007). Chronic hypoxia is known to produce a loss of mitochondrial bioenergetic capacity in the heart (Milagros Rocha and Victor 2007; Muravchick and Levy 2006). Doxorubicin may interfere with mitochondrial function at multiple levels by inhibiting different components of the ETC and oxidative phosphorylation or exerting partial uncoupling (Tokarska-Schlattner et al. 2006). Doxorubicin

has been found to interact with complex I, but to date the downstream complexes of the ETC have not been found to be affected. Interaction possibly reduces complex I activity resulting in interruption of the ETC affecting ATP production and elevating superoxide levels (Wallace and Starkov 2000). Additionally doxorubicin's interaction with complex I and accumulation within mitochondria could adversely affect the mitochondrial genome (Lebrecht et al. 2003). Doxorubicin is known to intercalate into mtDNA possibly contributing to the cardiotoxicity (Ashley and Poulton 2009). The chronic cardiotoxicity associated with doxorubicin may also be explained through imprinting effects on mtDNA. This may result in permanent alterations and defects in genetic material, thus affecting protein expression that can be maintained months to years after the cessation of treatment (Berthiaume and Wallace 2007b; Lebrecht et al. 2003).

Over 90% of the ATP used by cardiomyocytes is produced by the ETC; therefore any effect on the mitochondria will have a prolonged effect on cardiac function (Tokarska-Schlattner et al. 2006). Abnormal mitochondria have recently been demonstrated to be one of the earliest and most prominent histomorphological features following doxorubicin administration (Ashley and Poulton 2009). Mitochondria are not only central to oxidative phosphorylation but also serve as biosensors for oxidative stress and an effector organelle for apoptosis (Guzy and Schumacker 2006; Muravchick and Levy 2006). They are involved in these processes by monitoring the presence of growth factors, ROS, oxygen and DNA damage within the cell and respond accordingly (Gustafsson and Gottlieb 2008).

A major by product of oxidative phosphorylation is superoxide production, a ROS (Toogood 2008). ROS can degrade and destroy mitochondria by modulating the activity of the mitochondrial enzyme complexes, affecting membrane integrity by either direct contact or lipid peroxidation (Muravchick and Levy 2006). Superoxide is detoxified by a combination of mitochondrial antioxidant enzymes, which allows quick conversion to hydrogen peroxide by manganese superoxide dismutase (MnSOD). Hydrogen peroxide is then converted to water by catalase and glutathione peroxidase (GPx) or by peroxiredoxins (a group of thioredoxin-dependent antioxidant peroxidases) removing any toxic consequences (Gustafsson and Gottlieb

2008; Muravchick and Levy 2006). The production of ROS at levels above the capacity of the detoxification system result in oxidative modification of mitochondrial proteins, lipids and mitochondrial DNA leading to mitochondrial dysfunction and apoptotic activation (Gustafsson and Gottlieb 2008).

1.4.2 THE MITOCHONDRIAL PERMEABILITY TRANSITION PORE (mPTP)

Mitochondrial membrane protein ion channels function to transfer selected metabolites across the membrane; this structure is collectively referred to as the mPTP. A large proportion of mitochondrial damage arises as a result of increased permeability of the inner membrane allowing influx of ions into the mitochondria or by inhibiting the membrane proteins contained in the mPTP. This results in a lack of transport of essential macromolecules into and out of the mitochondria (Wallace and Starkov 2000). Mitochondria regulate cell death through the mPTP. The change of mitochondria to mediators of cell death is activated through the release of cytochrome c, Smac/Diablo and Omi/Htr2A from the mitochondria into the cytoplasm through opening of the mPTP. mPTP opening disrupts the proton gradient, leading to decreased ATP synthesis and enhanced ROS production leading to cellular swelling and membrane rupture activating the intrinsic pathway of apoptosis (Section 1.4.5) (Baines 2009). The mPTP opens in response to a number of stimuli including calcium, oxidative stress, inorganic phosphate and decreased ATP (Lim et al. 2007). The mPTP has a number of core components including a voltage-dependent anion channel (VDAC), adenine nucleotide translocator (ANT) and cyclophilin-D (CYP-D) all of which have been implicated in the control of the mPTP (Figure 1.5). ANT is reported to be the most prominent in the inner membrane (Oliveira and Wallace 2006). It regulates the movement of ADP and ATP in opposite directions across the inner membrane, whereas VDAC facilitates this movement across the outer membrane and is also involved in the regulation of apoptosis by interacting with Bcl-2 protein family members on the outer membrane (Armstrong 2007). ANT and VDAC deliver ADP to complex V of the ETC and ATP to high energy requiring sites in the cytosol (Muravchick and Levy 2006).

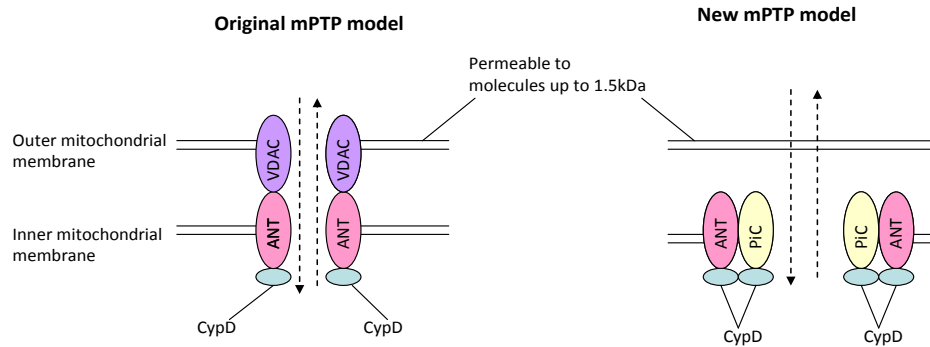


Figure 1.5: Overview of the previous and current knowledge of the molecular composition of the mPTP. Current knowledge implicates the proteins, ANT, CYP-D and PiC as key modulators of the mPTP. VDAC is thought to have a protective role allowing removal of toxins through the outer membrane. Adapted from Baines 2009.

Over the past year, this classic structure of the mPTP has been questioned. Transgenic mice have been used to investigate the role of CYP-D, VDAC and ANT. CYP-D $-/-$ mice are resistant to mPTP opening induced by either calcium or oxidative stress, thus highlighting a central role for this protein in the mPTP (Lim et al. 2007). VDAC consists of three isoforms VDAC1, VDAC2 and VDAC3. An *in vitro* triple knockout model exposed to oxidative stress and calcium appeared to activate the mPTP and initiate the intrinsic pathway of apoptosis, suggesting that VDAC is not necessary to induce the mPTP (Baines et al. 2007; Cheng et al. 2003). However these cells did demonstrate an increased sensitivity to oxidative stress, postulating that the function of VDAC is one of a protective nature allowing removal of toxins from the cell to preserve correct cellular function (Baines 2009). As the outer membrane is permeable to molecules up to 1.5kDa it maybe that there are no regulatory proteins of the mPTP on the outer membrane. ANT knockout studies revealed that ANT acts more as a peripheral regulatory protein of ATP/ADP transport than previously thought (Baines 2009). Through these studies a number of possible proteins maybe involved in the mPTP have been identified including the mitochondrial phosphate carrier (PiC). PiC is a family member of ANT and is ubiquitously expressed in all tissues (Palmieri 2004). It has been widely accepted that inorganic phosphate sensitises the mPTP to induction by calcium and oxidative stimuli. This suggests that a phosphate binding site must be present

within the pore. PiC is able to bind to phosphate binding sites and thus sensitise the mPTP (Figure 1.5) (Baines 2009). Before the full potential of PiC can be determined further knockout experiments are required to identify if PiC is vital to the opening of the mPTP or other regulatory proteins e.g.: ANT.

1.4.3 MITOCHONDRIAL GENOMICS

Mitochondria are the only organelle outside of the nucleus to process a unique genome. The mitochondrial genome consists of a small circular genome of approximately 16569 bp, entirely maternally inherited. Each mitochondria contains multiple copies (~1000) of the genome that encodes 13 peptides that form part of subunits of complexes I, III, IV and V of the ETC, 2 ribosomal RNA's and 22 tRNA's (Scatena et al. 2007). The majority of mitochondrial genes and proteins required for mitochondrial function are however encoded by nuclear DNA, including the mitochondrial transcription factor A (TFAM), this transcription factor is required for mitochondrial genome expression. The organization of the mtDNA is unlike nuclear encoded DNA. Genes have no 5' or 3'- non coding sequences and no introns or spacer regions (Wallace 2005). Point mutations in mtDNA can result in many diseases (e.g.: diabetes, cardiomyopathy) and defective or dysfunctional oxidative phosphorylation impacting on mitochondrial function, possibly resulting from doxorubicin (Figure 1.6) (Hom and Sheu 2009; Wallace 2005).

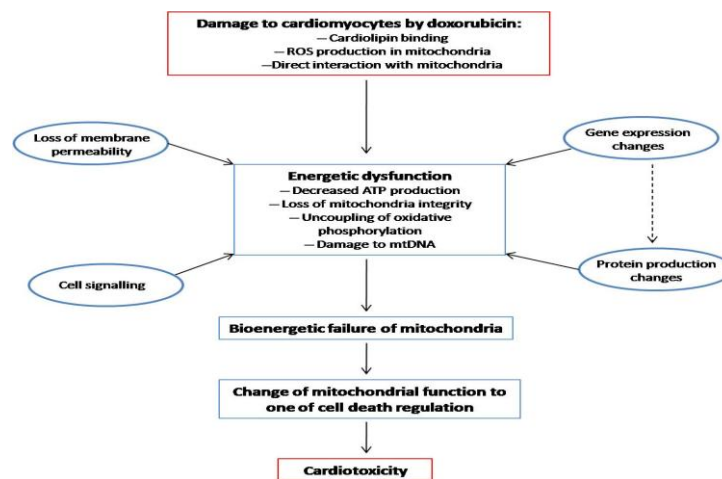


Figure 1.6: Summary of proposed mechanisms of mitochondrial damage following doxorubicin (Ashley and Poulton 2009; Tokarska-Schlattner et al. 2006; Wallace 2003).

1.4.4 TRANSCRIPTIONAL RESPONSE TO MITOCHONDRIAL DAMAGE

The transcription of a wide range of genes is modulated during mitochondrial dysfunction in cardiac tissue in both the nuclear and mitochondrial genomes. Nuclear encoded genes make up a major contribution to mitochondrial metabolic systems and molecular architecture. Interaction between the mitochondrial and nuclear genome is therefore critical in maintaining functional mitochondria. One of the key mechanisms through which the mitochondrial and nuclear genomes interact is through the activation of transcription factors encoded by the nuclear genome that are essential for mitochondrial genome transcription.

Peroxisome proliferator-activated receptor-gamma co-activator one alpha (PGC-1 α) is a transcriptional co-activator present in the nucleus that interacts with a wide range of transcription factors involved in a variety of biological processes including mitochondrial biogenesis, glucose metabolism and heart development (Liang and Ward 2006; Meirhaeghe et al. 2003). A co-activator of transcription can be defined as a protein, which increases the probability of a gene being transcribed, excreting its activity by interacting with transcription factors which directly bind to genes (Puigserver and Spiegelman 2003). PGC-1 α is expressed at high levels in metabolically active tissue e.g.: the heart and functions to increase the level of oxidative phosphorylation (Mudd and Kass 2008). Mechanistically PGC-1 α induces mitochondrial biogenesis by increasing the production of a number of transcription factors including the nuclear respiratory factor 1 (NRF-1), nuclear respiratory factor 2 (NRF-2), the estrogen-related receptor- α (ERR- α) and the proliferation activated receptor- α (PPAR- α). The transcription factors NRF-1, NRF-2 and ERR- α regulate the transcription of genes involved in mitochondrial bioenergetics whereas PPAR- α and ERR- α regulate the transcription of genes involved in fatty acid oxidation and glycolysis (Figure 1.7) (Vega et al. 2000). Both NRF-1 and NRF-2 additionally regulate expression of the only mitochondrial transcription factor, TFAM (Huss and Kelly 2005). Whereas, NRF-1 also transcriptionally controls a range of genes involved in mitochondrial function and biogenesis and is a vital mediator between the nuclear and mitochondrial genomes (Figure 1.7) (Scarpulla 2008; Scarpulla 2006; Kelly and Scarpulla 2004).

Following mitochondrial damage, a coordinated response is mediated by increasing transcription of genes whose proteins enhance production of antioxidants, DNA repair, glycolysis and mitochondrial uncoupling proteins while simultaneously decreasing the transcription of genes such as those encoding the complexes of oxidative phosphorylation preventing ATP production. The key pathway for gene regulation in mitochondria is oxidative phosphorylation. Oxidative phosphorylation is vital to the energy dynamics of a cell as described in section 1.4.1. Deregulation of this pathway results in the activation of alternative energy generation pathways, namely glycolysis. Mitochondrial dysfunction can be transcriptionally identified by differential expression of genes involved in oxidative phosphorylation, glycolysis and the TCA cycle.

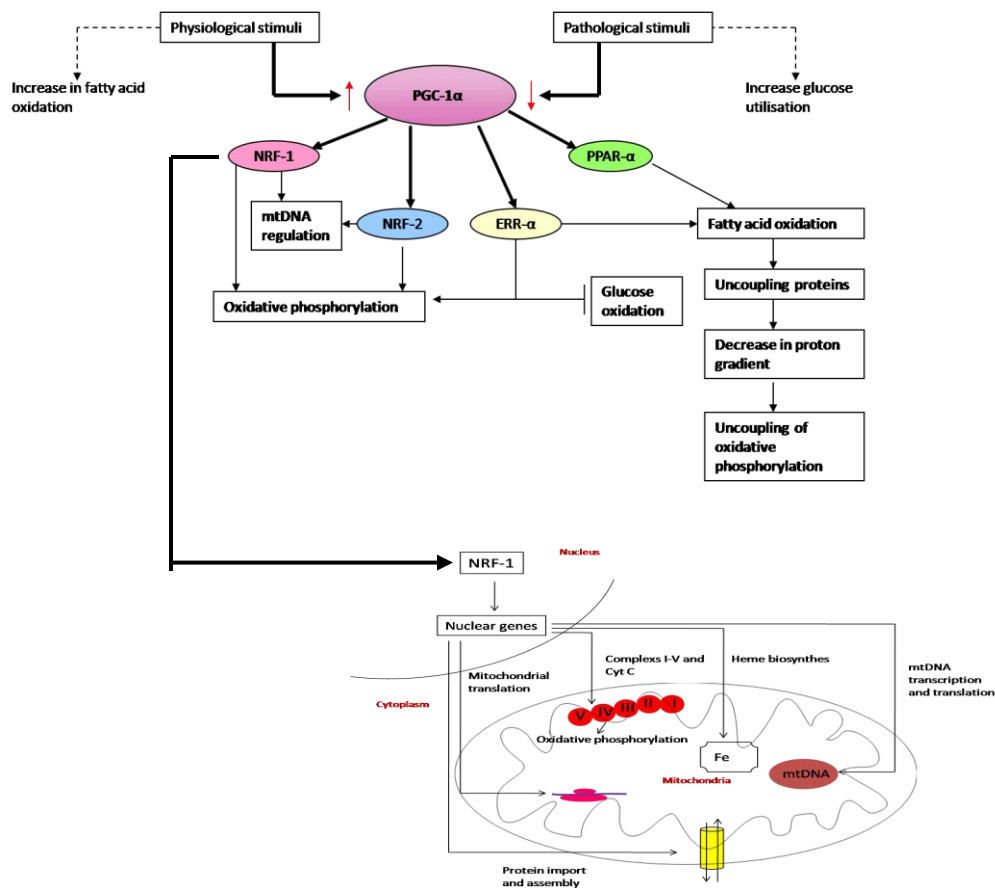


Figure 1.7: Role of PGC-1α in the activation of transcription factors involved in energy metabolism, detailing the processes that are regulated by the transcription factor NRF-1. PGC-1α co-regulates the transcription factors: NRF-1, NRF-2, PPAR- α and ERR-α. NRF-1 regulates genes involved in mitochondrial function and biogenesis and is a vital mediator between the nucleus and mitochondrial genomes. Increased ERR-α reduces glucose oxidation, thus impacting on oxidative phosphorylation. Adapted from Scarpulla (2008) and Liang and Ward 2006.

1.4.5 CELL DEATH

Cell death can be broadly divided into two classes, programmed cell death (PCD) and necrosis. There are two main types of PCD; apoptosis and autophagy. The timely execution of PCD is critical for a range of physiological processes including embryogenesis, development, aging, tissue homeostasis and removal of damaged cells. PCD is a common feature of many disease states including cancer, stroke, ischemic heart disease and as a response to a number of toxins (McClintock et al. 2002).

Apoptosis

Apoptosis was first described by Kerr et al. in 1972 and can be characterised by distinct morphology and an energy dependent biochemical mechanism (Elmore 2007). During apoptosis cells develop certain characteristics including chromatin condensation, nuclear fragmentation and shrinkage in cell size affecting single cells or small groups. Apoptotic cells do not release any cellular constituents into the surrounding tissue. Damaged cells are quickly phagocytosed by surrounding cells, and these engulfing cells do not produce any anti-inflammatory cytokines (Kurosaka et al. 2003; Savill and Fadok 2000).

In contrast, necrosis often affects multiple adjacent cells and can also be characterised by cell swelling, formation of cytoplasmic blubs resulting in disruption of cell membranes and leakage of cellular components into the cytoplasm with an associated inflammatory response (Elmore 2007). Many studies *in vivo* and *in vitro* show cells within the same tissue or culture undergoing both apoptosis and necrosis (McClintock et al. 2002). Thus the complex pathways involving both these forms of cell death can be activated within the same tissue.

In most cases apoptosis occurs via one of two biochemical pathways; the extrinsic or the intrinsic pathway. The extrinsic pathway (Figure 1.8) involves the activation of death receptors outside the cell that are members of FAS, TRAIL and tumour necrosis factor receptor gene super families (Zhang et al. 2004). Binding of these receptors to their respective ligands activates a caspase cascade that cleaves and activates the

effector caspase, caspase 3. This pathway of apoptosis is regulated by c-FLIP which is able to inhibit upstream caspases and inhibitor of apoptosis proteins (IAPs) which in turn, inhibit caspase 3, thus preventing cell death.

The intrinsic pathway of apoptosis (Figure 1.8) is activated by intracellular signals that act directly on targets within the cell or via p53, through mitochondrial-initiated events. Such stimuli can include the presence or absence of growth factors, hormones, cytokines, radiation, toxins, DNA damage, hypoxia and ROS. The tumour suppressor protein p53 is a key activator. p53 accumulates as a result of DNA or cellular damage and initiates apoptosis by transcriptionally activating pro-apoptotic and inhibiting anti-apoptotic Bcl-2 proteins. In healthy cells Bcl-2 is present on the outer membrane of the mitochondria, inhibiting apoptosis. Cellular damage results in Bax migrating to the outer mitochondrial membrane. This leads to inhibition of the anti-apoptotic protein Bcl-2 and binding of Bax to the outer membrane, thus disturbing the membrane (Figure 1.8). Cellular stimuli causes disruption of the mitochondrial inner membrane, leading to opening of the mPTP, resulting in loss of membrane potential, uncoupling of oxidative phosphorylation and release of cytochrome c, Smac/DIABLO and Omi/HtrA2 out of the mitochondria into the surrounding cytoplasm. Cytochrome c binds and activates Apaf-1 (apoptotic protease activating factor-1) and pro-caspase 9 forming an apoptosome (ATP-dependent formation of a macromolecule complex). This activates caspase 9, initiating the apoptotic caspase cascade, activating caspase 3, resulting in apoptotic cell death (McClintock et al. 2002). Some forms of cellular stress (e.g.: in sarcoplasmic reticulum) can activate caspase 12 thus activating caspase 3 and apoptotic cell death (Figure 1.8).

This process of apoptosis is tightly regulated by the Bcl-2 family of proteins (25 genes) that function as both pro- and anti-apoptotic molecules (Zhang et al. 2004). This family of proteins is regulated by p53 (Elmore 2004). Over-expression of the anti-apoptotic members e.g.: *Bcl-2* and *Bcl-xl* inhibits cytochrome c release, whilst the pro-apoptotic members, e.g.: *Bax*, *Bak*, *Bid*, *Puma*, *Noxa* and *Bim* promote cytochrome c release from the mitochondria.

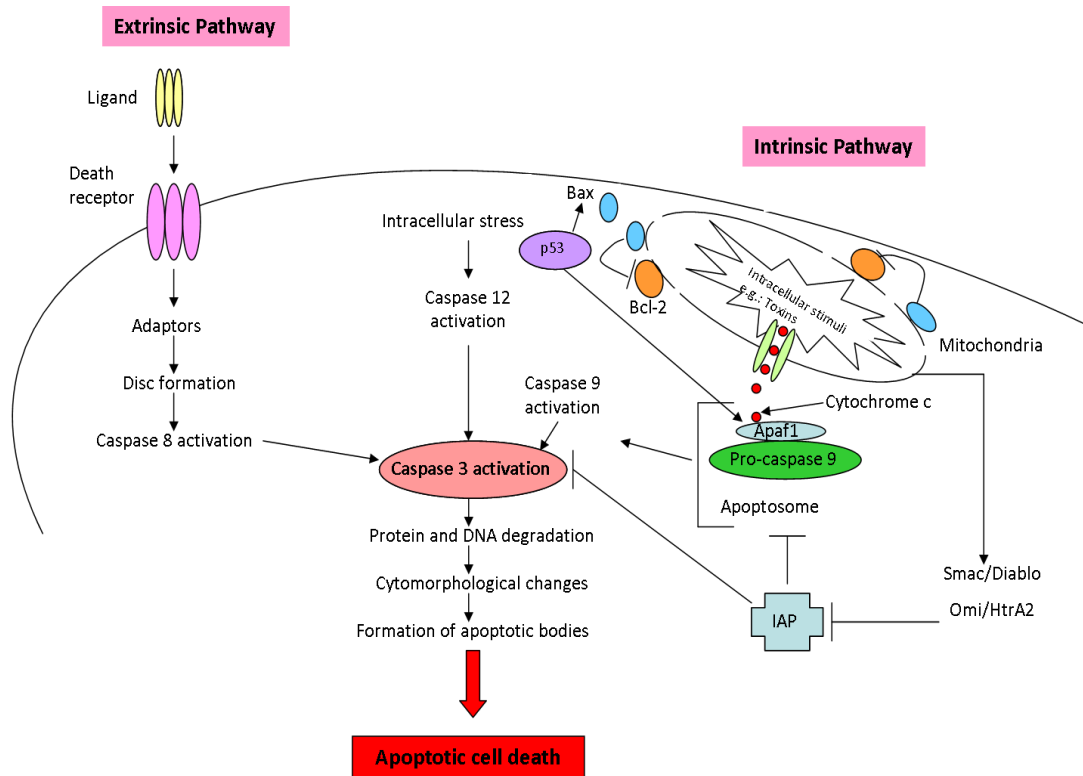


Figure 1.8: Schematic representation of the major events of the apoptotic pathway. The two main pathways of apoptosis are the extrinsic and intrinsic pathways. The extrinsic pathway is activated through receptor ligation activating caspase 8. The intrinsic pathway activates caspase 9 following Apaf2 and cytochrome c release from the mitochondria. Some forms of intracellular stress can directly activate caspase 12. Both pathways activate caspase 3 resulting in a cascade of events cumulating in apoptotic cell death. IAP (inhibitor of apoptosis proteins) can directly inhibit caspases 3 and 9 preventing apoptosis. Various mitochondrial proteins can inhibit IAP promoting apoptosis.

Autophagy

Another form of PCD is autophagy. Autophagy is a form of caspase independent PCD that can be characterised by the degradation of cellular components within dying cells involving vacuolisation, degradation of cytoplasmic content and slight chromatin condensation (Flink and Cookson 2005). A wide range of extracellular and intracellular stimuli are able to activate an autophagic response, including ROS (Yu et al. 2006; Yang et al. 2005). Autophagy is responsible for contributing to cell death during development and neurodegenerative diseases by regulating key cell functions including cell survival during substrate starvation; however the exact mechanism of autophagic cell death is unclear.

1.4.5.1 CARDIOMYOCYTE CELL DEATH

The heart is particularly sensitive to loss of cells and even relatively small increases in cardiomyocyte death results in cardiac pathology (Baines 2009). The survival of adult cardiomyocytes is regulated by extra cellular ligands, growth factors and cytokines that are able to bind to cell surface receptors and activate an intracellular signalling transduction cascade, controlling cell death and survival (Muslin 2008).

Over recent years a number of experimental systems have provided evidence for apoptosis, necrosis and autophagy in cardiac dysfunction. As apoptosis is an ATP dependent process it has been suggested that this high ATP requirement may result in cardiomyocytes being more prone to necrosis due to a lack of ATP during cardiac dysfunction. However the proportion of apoptosis to necrosis may depend on a number of factors including the cell death stimuli and the duration of the injury (Fliss and Gattinger 1996). A recent study using a rat model of myocardial ischemia identified the presence of apoptosis during the initial insult followed by necrosis in the long term. This model of cell death therefore accounts for the progressive nature of cardiac dysfunction (Fliss and Gattinger 1996; Gottlieb et al. 1994). *In vitro* models of doxorubicin toxicity have identified the activation of apoptosis; hypothesised to result from the production of hydrogen peroxide by doxorubicin, and subsequent p53 activation as a consequence of increased intracellular oxidant formation (Takemura and Fujiwara 2007; Tokarska-Schlattner et al.2006). *In vivo* apoptosis has only been found in acute models of doxorubicin cardiomyopathy suggesting the initial cell death that occurs is apoptotic, accumulation of which leads to myocardial dysfunction (Arola et al. 2000).

1.5 TRANSCRIPTOMICS AND MICROARRAYS

1.5.1 TRANSCRIPTION AND TRANSLATION OF mRNA

Two major processes have to occur to result in protein expression; transcription and translation.

Transcription is the synthesis of a single-stranded RNA copy of a segment of DNA involving three nuclear RNA polymerases synthesised from the 5' to 3' UTR. Transcription results in the production of mRNA, tRNA, rRNA and small nuclear RNA (snRNA). Transcription occurs through the utilisation of transcription factors that bind

to the DNA sequence and facilitate binding of the polymerase enzyme through recognition of the promoter sequence. Translation is the conversion of the resulting mRNA sequence to an amino acid sequence of a polypeptide (van der Beucken et al. 2006). This is achieved by the binding of the 40S and 60S ribosomal subunits to the mRNA strand, allowing the formation of the polypeptide (Figure 1.9).

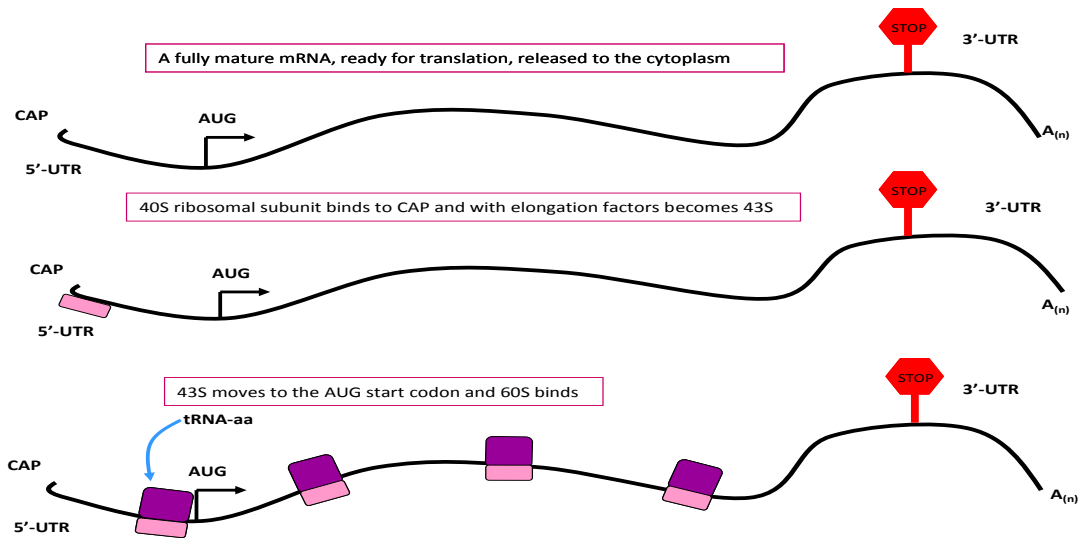


Figure 1.9: Summary of the process of RNA translation. A single stranded copy of DNA is cleaved from the genome, resulting in mRNA (transcription). This mRNA sequence is translated into an amino acid sequence.

Translation and transcription can be broadly divided into three phases, initiation, elongation and termination all of which are subject to control (Wilkie et al. 2003). Translation of mRNA requires the binding of eIF4E, an initiation factor (Richter and Sonenberg 2005). eIF4F complex contains the mRNA 5' cap binding proteins eIF4E, eIF4A and eIF4G. eIF4F is directed to the 5' UTR of the mRNA by eIF4E and functions in co-ordination with eIF4A to unwind the mRNA 5' UTR secondary structures. This allows the 40S ribosomal subunit to bind and subsequently the 60S ribosomal subunit. One such pathway/protein that controls translation is mammalian target of rapamycin (mTOR) (Mamane et al. 2006). mTOR is activated in response to extracellular signals and phosphorylates a large number of translation initiation factors. The 5' and 3' UTR are able to control gene expression by influencing the stability and translational efficiency of mRNA. One transcript that

is involved in post-transcriptional regulation and requires recognition sites at the 3' UTR are microRNA's (Section 1.5.2).

1.5.2 microRNAs AND THEIR ROLE IN CONTROLLING TRANSLATION

The discovery of microRNAs (miRNAs) 9 years ago has added another layer of complexity and regulation at the post-transcriptional level of replication (Callis and Wang 2008). miRNAs are natural, endogenous short (21-23nt) non-coding RNA molecules which have a fundamental role in controlling mRNA translation (Callis and Wang 2008; Thum et al. 2008; Kim and Nam 2006; Valencia-Sanchez et al. 2006). They are involved in a wide range of biological processes including development, apoptosis, immunity, toxicity and disease (Thum et al. 2008; Yang et al. 2008; Croce and Calin 2005). At present, 488 mouse and 695 human miRNAs have been registered in the Sanger miRBase database (<http://microrna.sanger.ac.uk/sequences>). The first miRNAs identified were Lin-4 and Let-7 in *Caenorhabditis elegans* (Williams 2007; Murchison and Hannon 2004). The vertebrate genomes may contain over 1000 miRNAs, representing >3% of the predicted human genes (Zhang 2008). These miRNAs are predicted to control the expression of 30% of protein-coding genes, each miRNA having hundreds of potential targets and each single protein-coding gene can be regulated by multiple miRNAs (Callis and Wang 2008; Wang et al. 2008; Yang et al. 2008). miRNAs tend to be clustered near other miRNAs and are transcribed from polycistronic clusters in the genome under the control of RNA polymerase II promoters or expressed as individual transcripts from intergenic or intronic locations (Cordes and Srivastava 2009; van Rooij et al. 2008; Kim and Nam 2006; Murchison and Hannon 2004). However the transcription of some miRNAs particularly those associated with short interspersed nuclear elements and those derived from viruses are dependent on RNA polymerase III promoters rather than II (Latronico and Condorelli 2009; Zhang 2008). miRNAs are transcribed from the genome as long fragments (pri-miRNA). These pri-miRNA transcripts can exceed 1Kb and may give rise to a number of different miRNAs (Taylor and Gant 2008; Thum et al. 2008). These are cleaved to the active miRNA in a two phase process involving two nuclear ribonuclease III (RNase III) enzymes (Chendrimada et al. 2005). Firstly, the enzyme *Drosha*, along with its

double stranded RNA binding domain (dsRBD) protein partner DGCR8, in the nucleus, cleaves genomic material and trims it into pri-miRNAs. These pri-miRNAs are characterised by a 33nt stem-loop or hairpin structure of 60-70 nts. The pri-miRNAs are then exported into the cytosol by exportin 5 and are cleaved by the enzyme *Dicer* and its dsRBD protein partner TRBP. Following action by *Dicer*, active pre-miRNA duplexes result (~22nt in length) (Cullen 2004). This resultant pre-miRNA duplex unwinds probably by helicase activity and one strand is degraded, the other interacts with argonaute to form the protein complex, RNA-induced silencing complex (RISC). The RISC is guided by argonaute to mRNA species containing miRNA recognition sites (~8 bp in length) and binds at the 3' untranslated region (UTR) (Chen et al. 2009; Wang et al 2009; Thum et al. 2008; Anderson and Mohler 2007). This complex may be sequestered away from the translational machinery in processing bodies (p-bodies), which act by recruiting poly (A) nucleases to help modulate deadenylation of mRNA, preventing translation (Barrington and Zamore 2009; Cordes and Srivastava 2009; Zhao and Srivastava 2007). The miRNA either induces degradation of the target mRNA, or its translation is inhibited by binding to an 8bp seed region (Figure 1.10) (Selbach et al. 2008; Bruneau 2005). The process which occurs is dependent on three factors; the overall degree of complementarity of the binding site, the number of binding sites on the target mRNA and the accessibility of the binding sites to the miRNA (Yang et al. 2008).

A number of questions regarding the stability of miRNAs remain unanswered; this could prove problematic when transferring miRNA expression profiles into potential therapeutics. Mature miRNAs are thought to be stable but one study in *Arabidopsis thaliana* found a family of exoribonucleases that could degrade miRNAs. Their presence has currently not been found in other species (Winter et al. 2009; Ramachandran and Chen 2008). In addition nothing is currently known about the turnover and half life of miRNAs.

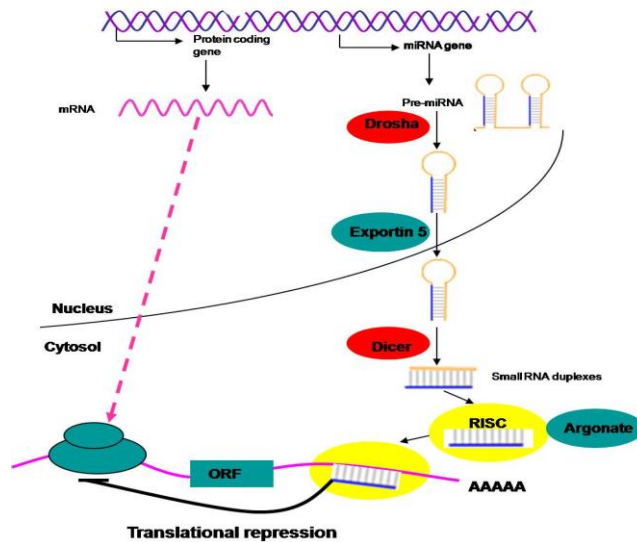


Figure 1.10: Summary of the mechanism of miRNA processing. miRNAs are cleaved into active miRNAs in a two phase process involving two nuclear ribonuclease III enzymes, drosha and dicer. Once processed by dicer the pre-miRNA is incorporated into the RNA induced splicing complex (RISC) complex and guided by argonate to binding recognition sites on the 3'UTR of mRNA (Selbach et al. 2008; Bruneau 2005; Chendrimada et al. 2005; Cullen 2004).

1.5.3 MODULATION OF miRNA IN DISEASE AND TOXICOLOGY

miRNA species are modulated in expression in a number of diseases. It is likely that their overall function is to modulate or fine tune cellular phenotypes (Valen 2009). The first published study linking miRNAs to disease was published in 2002, implicating miRNAs in B-cell leukaemia (Croce and Calin 2005; Calin et al. 2002). Differential miRNA expression has been associated with schizophrenia (Perkins et al. 2007), Alzheimer's disease (Lukiw 2007), hypoxia (Kulshreshtla et al. 2007), virus infection (Liu et al. 2008) and cardiac disease (van Rooij et al. 2006). Altered expression patterns of specific miRNAs in different tumour types have been observed, possibly allowing differentiation of cancers (Volinia et al. 2006; Lu et al. 2005). As miRNAs are transcribed from the genome under the control of RNA polymerase II promoters and some of these promoters often contain toxicological significant enhancer regions (Taylor and Gant 2007), it is logical to presume a role for miRNAs in toxicology. miRNA modulation has also been found following ethanol,

antimetabolite 5-fluorouracil and the estrogen receptor antagonist tamoxifen, indicating a role for miRNAs in response to chemical insult (Wang et al. 2009a; Pogribny et al. 2007; Rossi et al. 2007; Sathyan et al. 2007).

1.5.4 ROLE OF miRNA IN CARDIAC DISEASE

The expression profile of miRNAs appears to be tissue/cell specific allowing generation of miRNA expression profiles to aid in the diagnosis and prognosis of disease (Wang et al. 2008; Bruneau 2005). The role of miRNAs in the pathological process of the cardiovascular system is a rapidly emerging area of research (Latronico and Condorelli 2009; Wang et al. 2008). It has become increasingly evident that miRNAs are regulated in cardiac dysfunction and possibly have the capacity to create cardiac pathology. A small number of miRNAs have been found to be muscle specific in expression (miR-1, miR-208 and miR-133a), with others significantly modulated in expression during cardiac dysfunction (e.g.: miR-21, miR-29, miR-27b, miR-195 and miR-126). The mechanism for such specific alterations in expression is currently unknown (Thum et al. 2008; Yang et al. 2008; Bruneau 2005) (Figure 1.11).

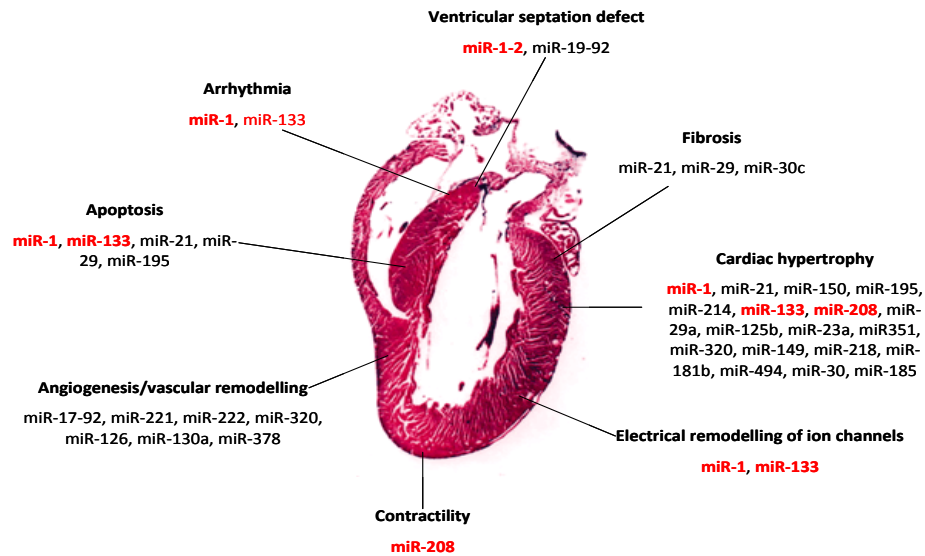


Figure 1.11: Known roles of miRNAs in cardiac dysfunction, discovered by miRNA profiling and/or genetic manipulation. Those miRNAs known to be highly expressed in cardiac tissue are highlighted in red (Latronico and Condorelli 2009; Callis and Wang 2008; Latronico et al. 2008; Scalbert and Bril 2008; van Rooij et al 2008).

The expression profiles in varying cardiac disease states are different suggesting the involvement of etiologic factors impacting on miRNA expression (Figure 1.12) (Latronico and Condorelli 2009; Yang et al. 2008).

However as this field of genomics is still in its infancy greater knowledge of all the factors that may affect the cardiac miRNA transcriptome are required. These miRNA expression profiles, unique to certain disease states, raises the possibility of miRNAs as biomarkers of disease, allowing distinction between different forms of cardiac dysfunction or allowing the monitoring of disease progression.

The fundamental importance of miRNAs in cardiac biology is rapidly developing. The use of transgenic mice containing a dicer knockout, specific to the heart, has revealed the development of abnormal heart function and embryonic lethality (Zhao and Srivastava 2007). Dicer knockout in adult hearts, reduced levels of contractility proteins and sarcomere reorganization resulting in the development of cardiomyopathy and heart failure (Callis and Wang 2008). Lowered expression of dicer has also been reported in clinical patients with heart failure highlighting the importance of miRNAs in cardiac biology (Callis and Wang 2008).

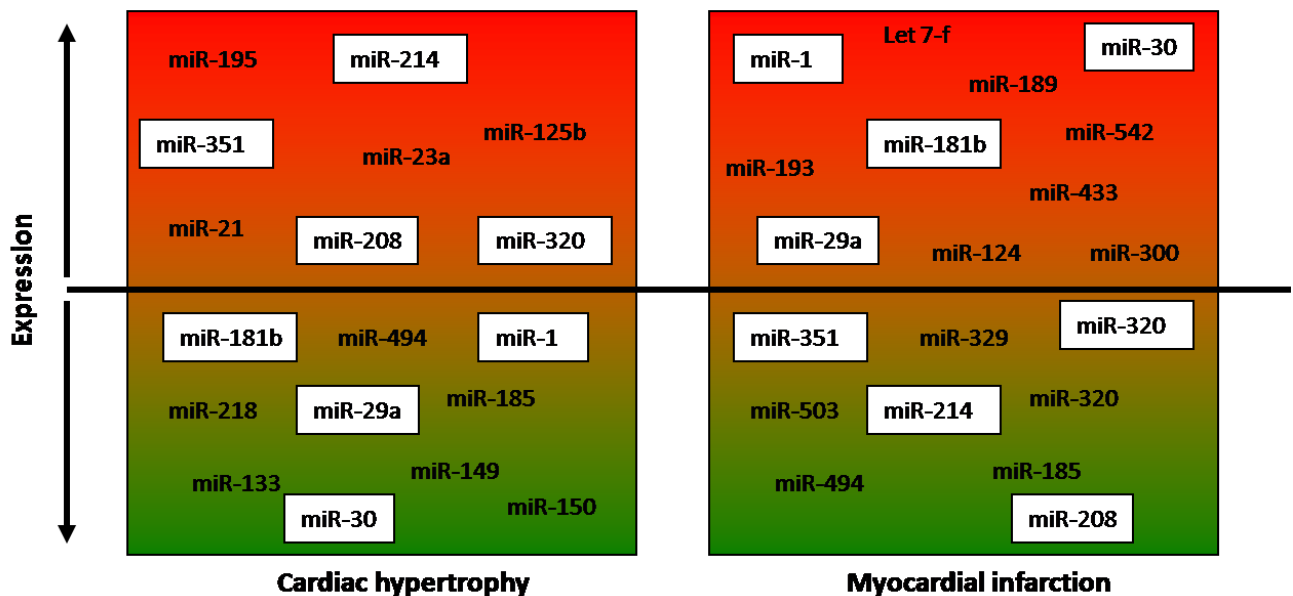


Figure 1.12: Differential expression profiles of miRNAs in cardiac hypertrophy and myocardial infarction. miRNAs above the line are up-regulated and below are down-regulated. miRNAs in white boxes indicate those that are differentially expressed in the two forms of cardiac dysfunction (Wang et al. 2009a; Yang et al. 2008).

1.5.5 ADDITIONAL SMALL NON-CODING RNA SPECIES

In addition to miRNAs there are a number of other small non-coding RNA species that have been identified including small interfering RNA (siRNA), piwi-interacting RNA (piRNA) and transcription initiation RNA (tiRNA). siRNAs are a similar length (20-25nt) to miRNAs but are derived from longer perfectly complementary double stranded RNA precursors normally of an exogenous nature. They guide mRNA cleavage at the sites to which they bind utilising the RNA interference pathway (RNAi) (Latronico et al. 2008; Wu et al. 2006). miRNAs are thought to be the physiological equivalent of siRNA (Gant et al. 2009). Since the discovery of siRNA in 2001 one siRNA molecule has clinical approval, fomivirsen, an anti-sense oligonucleotide used for the treatment of cytomegalovirus retinitis (Jason et al. 2004).

piRNAs are 26-31nt in length contained within large genomic clusters and are only present in the testes of mammals, suggesting an important role in epigenetic modifications that are transferred through the germ line. However little is currently known regarding how they are processed and function (Barringhaus and Zamore 2009; Malone et al. 2009).

The latest member of the small non-coding RNA family to be discovered are the tiRNAs. tiRNAs are 18nt in length and appear to be derived from a specific position near to transcription start sites on transcribed genes (Taft et al. 2009). They may offer another target for pharmacological exploration.

1.5.6 TRANSCRIPTIONAL PROFILING AND THE USE OF EXPRESSION MICROARRAYS

During the last 10 years the use of genomics has been widely utilised to allow insight into mechanisms and pathways involved in biological systems. Transcriptional profiling allows expression levels of genes in tissues or cells from 'control' and 'test' conditions to be generated. Multiple techniques are available to investigate transcriptional gene expression, including northern blotting, quantitative real time-PCR (qRT-PCR) and microarray analysis. Both northern blotting and qRT-PCR allow the study of a small number of genes, whereas microarray analysis allows simultaneous expression profiling of thousands of genes.

Microarrays have been used in a wide range of biological and medical fields, including toxicology, to further understand and provide additional insight into biological processes. Microarrays allow genome wide studies to be conducted on all organisms, producing a large volume of data quicker than previously.

Microarray platforms utilise the same principles. A nucleic acid is immobilised on a solid surface to hybridise with a RNA sample that is fluorescently labelled. Widely used microarray platforms including the Stanford microarray system, Affymetrix genechips and Illumina microarrays. Affymetrix genechips are manufactured by synthesising a 25-mer oligonucleotide probe onto a silicon chip using a photolithography method. The microarrays are hybridised with a single sample at one time. Illumina microarrays use microscopic beads instead of a solid support; both of these platforms are commercially available.

Stanford type microarrays

Stanford type microarrays were first produced and utilised by the Brown lab (Stanford University, California) in 1995. These microarrays are two colour arrays that utilise a glass slide that is coated with aldehyde or poly-L-lysine with either a PCR product (PCR amplified cDNA clones) or a DNA oligonucleotide (a short nucleic acid sequence) diluted in printing buffer (betaine SSC) spotted directly onto it. These probes bind to the glass slide by covalent binding. Up to 40,000 oligonucleotide or cDNA clones can be printed onto one slide. Oligonucleotides have better sensitivity and stability, are less labour intensive and the user has greater control; however they do have a higher cost. The microarrays used in this thesis have oligonucleotides printed onto them. Robotics are used to print the microarrays allowing a large number of replicate microarrays in a single run, with the bulk number dependent on the machine used (up to 1000 microarrays are possible). This high density of spots in a small area is achieved by using a print head containing 32 metallic microquills that deposit the probe onto the glass slide. Hybridisation of control and test RNA is carried out simultaneously, by one of two labelling techniques; direct or indirect labelling. Direct labelling involves incorporation of dUTP and a fluorescent cyanine dye (Cy-3 or Cy-5) during the reverse transcription reaction. Whereas indirect labelling involves incorporation of an amino-allyl dUTP during the reverse

transcription reaction followed by coupling with an esterized Alexa 555 or Alexa 647 dye. Cy-3 /Alexa 555 is labelled with the control RNA sample and Cy-5/Alexa 647 is labelled with the test RNA sample, thus combining a control and test sample allows the relative expression of genes between samples to be obtained. Slides are visualised by scanning at the appropriate two wavelengths (Cy-3/Alexa 555 = 532 nm and Cy-5/Alexa 647 = 635 nm). The relative abundance of the intensities of each spot results in a ratio of expression between the two samples. In order to account for any differences in dye binding, samples are labelled with the opposite dye to reduce any bias. Microarray technology such as this can be used to generate mRNA and miRNA transcriptional profiles (Figure 1.13).

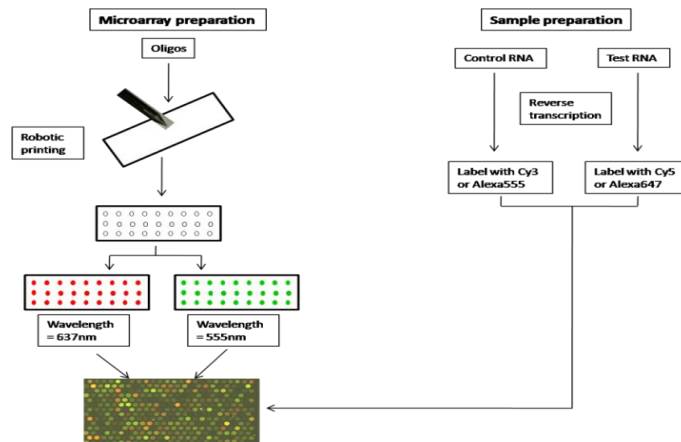


Figure 1.13: Schematic diagram of the microarray production and processing utilised in this thesis. Microarrays robotically printed onto a coated glass slide using oligonucleotide probes. RNA samples fluorescently labelled and applied to the microarray followed by scanning at the appropriate wavelength.

Measurement of total mRNA transcriptional profiles does not allow off-target changes in mRNA to be identified. One method to identify such occurrences and allow greater insight into the genomic changes following chemical exposure is to obtain mRNA translational profiles. mRNA global translational profiles using microarrays can be generated, but separation of mRNA has to be carried out. mRNA can be separated by mass on a sucrose gradient into RNA species that are not being actively translated, termed monosomes and those that are being actively translated, termed polysomes. The polysome fractions, contain cytoplasmic

mRNAs loaded with multiple ribosomes therefore are being actively translated in a cell and are of greater mass than non translated mRNAs. The monosome fractions contain the small 40S and larger 60S ribosomal subunits and messenger ribonucleoproteins ((mRNP) cytoplasmic mRNA which are either translationally inactive or translated at a reduced efficiency and are present as free cytoplasmic mRNP particles), these have only one or two ribosomes attached, so when separated on a sucrose gradient a distinct separation of the two mRNA species occurs (Figure 1.14).

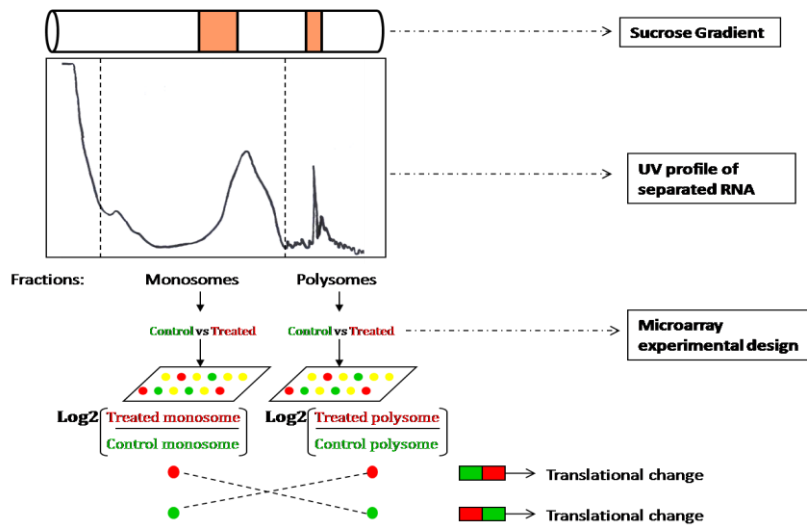


Figure 1.14: Translational profiling experimental design.

RNA is separated by sucrose density gradient centrifugation and then fractionated while monitoring the absorbance at 254nm generating a UV profile, the relative position of monosomal and polysomal mRNA is indicated. Microarrays are used by hybridising test and control monosomes on one slide and the same for the polysome fractions on another thus generating translational gene expression profiles.

Using this method one can determine the translational efficiency of a gene, and of the global mRNA

population. This approach has been widely utilised (over 50 publications) to generate mRNA translational profiles *in vitro* (Melamed and Arava 2007; Blais et al. 2004), but only limited *in vivo* application has been published (Iguchi et al. 2006).

1.5.7 DATA ANALYSIS

Following microarray scanning the raw microarray images are converted to pixel intensities by overlapping a template file indicating the position and gene name of each feature. Each template is fitted around the raw image; any defects were excluded to reduce the false discovery rate. The feature intensity is measured as the sum intensity of the pixels within the marked feature. The background intensity was set as zero, which allows the phenomenon of black holes (where the background intensity is higher than the spot) to be dealt with (Zhang and Gant 2005). MA plots (plot of the log-ratio of two expression intensities versus the mean log-expression of the two) were plotted in ArrayTrack to assess data quality. The relative intensity of each feature then needs to be normalised to adjust for differences in the intensities of each channel. Global normalisation was utilised to adjust for any systematic differences in the relative intensities of each channel, based on the assumption that the two channel intensities are related by a constant factor over the entire microarray slide. This was used for microarrays where reverse labelling had been carried out. Another method of normalisation is LOWESS. This method assumes the intensity of the two channels are not constant but vary as a function of signal intensity. When reverse labelling of microarrays has been used to address the dye bias the LOWESS normalisation principles do not hold true. Both types of normalisation assume that the majority of genes within a sample are not differentially expressed between the two samples on the microarray (Zhang and Gant 2004). ArrayTrack was utilised to carry out normalisation. Following normalisation data is presented in terms of a ratio of the median intensity of each wavelength (Log_2), thus indicating if specific genes are up- or down-regulated relative to the control sample (i.e. up-regulated genes have a positive number, down-regulated genes have a negative number). In order to apply statistical significance a one-sample two tailed t-test was carried out at each time point. Genes with a p-value of >0.05 were excluded from further downstream analysis.

These assumptions used in the normalisation of microarray data do not hold true when RNA is separated for translational profiling. Careful consideration is required as the assumption that the majority of genes within a

sample does not change in expression cannot be applied when comparing monosomal and polysomal RNA that is derived from the same biological sample. A novel approach has been applied to overcome this problem. Microarray hybridisations were conducted as in Figure 1.14. A one-sample student t-test was conducted on each set of expression data and any gene with a p-value of >0.05 was excluded. The relative expression of monosomal mRNA can then be subtracted from that of polysomal mRNA thus generating global mRNA translational profiles.

Once significant gene lists were generated, cluster analysis was conducted. A number of software packages are available to carry this out; within this thesis ArrayTrack was utilised. This organises gene expression data into groups that share related gene expression profiles. Two forms of clustering were used in this thesis, hierarchical clustering (HCL) and principle component analysis (PCA). HCL groups genes based on their expression similarity between samples, whereas PCA identifies directions termed “principal components” along which the variation in data is maximal (Ringnér 2008).

In order to fully understand microarray data, biological meaning needs to be applied to aid in the understanding of biological pathways and mechanisms. Pathway analysis was used to achieve this. Two programmes were used, the Gene Set Analysis Toolkit, which is a freely available web based application, and IPA (Ingenuity Inc) a proprietary analysis that must be subscribed to. Two different programs have been utilised as different programmes have different focuses (Kamburov et al. 2009). The Gene Set Analysis Toolkit was used to identify KEGG (Kyoto Encyclopaedia of Genes and Genomes) pathways that were affected. A modified Fisher exact test was applied to the data; this generates an enrichment probability score for each pathway. IPA separates significant genes into networks defined by known interactions from the literature (Ishigami et al. 2007). Biological themes are also conferred to the networks by using a modified version of the Fisher exact test.

1.6 THESIS AIMS AND OBJECTIVES

The overall aim of the project was to use a genomic approach at several levels of gene regulation to inform on the mechanism of doxorubicin cardiotoxicity. To achieve this, acute and chronic models of doxorubicin toxicity were established *in vivo* and *in vitro*. Furthermore another naphthoquinone (DMNQ) was employed to discern factors of the molecule specific to its pharmacology from those associated with toxicity. These models and compounds were coupled with global genomic methods at the transcriptional (mRNA and miRNA) and translational levels. Several bioinformatic methods were employed to identify pathways and relationships in the data that suggest mechanisms of toxicity. These were then investigated further through the utilisation of biochemical analysis.

Data within this thesis expands our knowledge of the mechanisms underlying doxorubicin's cardiotoxic effects and provides insight into the importance of genomics in toxicology.

Chapter 2: Materials and Methods

All reagents used were of the highest grade available and purchased from Sigma unless otherwise stated.

2.1. ANIMALS

All animal work was carried out in accordance with the Animal Scientific Procedures Act (1986) under project license 80/2048 and personal license 80/10212.

2.1.1. PREPARATION OF DOSING SOLUTIONS

Fresh solutions were prepared for each experiment. DMNQ (synthesized according to Gant et al. 1988) and MNQ were dissolved in arachis oil by heating and cooled before use. Doxorubicin was dissolved in 0.9% (v/v) saline. Working solutions of 2.5mg/ml DMNQ and MNQ and 1.5mg/ml doxorubicin were prepared.

2.1.2. DEVELOPMENT OF AN *IN VIVO* MODEL OF TOXICITY

Male C57BL/J mice were obtained from an inbred colony (supplied by Biomedical Services, University of Leicester) and housed with free access to food and water with a light/dark cycle of 12 hours. Mice initially weighing 20-25g (~8 weeks old) were randomly assigned to a treatment group and dosed by intraperitoneal injection (i.p.). In experiments requiring multiple doses, i.p. injections were rotated to minimize local tissue irritation. At dosing and at the end of treatment all animal body and heart weights were recorded. All animals were killed by overdose of isoflurane induced anaesthesia followed by blood withdrawal by cardiac puncture without thoracotomy, collected blood was placed into heparin tubes (Sarstedt) on ice. Following this a laparotomy was performed, the descending vena cava cut and organs perfused with 10ml PBS (pH 7.6) or 10ml PBS containing 100µg/ml cycloheximide. The heart, brain and liver were removed and snap frozen in liquid nitrogen. To obtain plasma, blood samples were centrifuged at 13,000rpm for 5 minutes, supernatant was stored at -80°C. For animals used for electron microscopy and determination of ventricular width, animals were killed by isoflurane induced anaesthesia. The body cavity was opened and a 1¼ inch butterfly cannula placed in the aorta and perfused with 0.9% (v/v) saline for 5 minutes, once perfusion had started the descending vena cava was cut, followed by perfusion with 2.5% (v/v) glutaraldehyde, 2% (v/v) formaldehyde in 0.1M PBS (pH 7.4) for hearts used for electron microscopy and 10% (v/v) neutral buffered formalin for

ventricular width determination both for 5 minutes. Hearts were removed and placed in appropriate fixative for long term storage. Electron microscopy was conducted by Dr David Dinsdale at the MRC Toxicology Unit.

2.2 CARDIAC CELLS NON-PRIMARY

HL-1 cells were obtained as a kind gift from William Claycomb (LSU Health Sciences, New Orleans, USA).

Pre-coating flasks

All tissue culture vessels used were pre-coated in gelatine/fibronectin (0.02% (w/v) gelatine/1ml fibronectin (1mg/ml)) as detailed in table 2.1, at 37°C overnight and removed immediately prior to use.

Culturing and passaging of cells

Complete media (Section 2.32) was changed daily (Table 2.1). Cells were only passaged when reached >90% confluency. Complete culture media was aspirated and cells briefly washed twice with PBS. An appropriate volume (Table 2.1) of 1x trypsin/EDTA solution (0.5g/L trypsin and 0.2g/L EDTA Invitrogen) was added to each culture vessel and incubated at 37°C for 2 minutes. An appropriate volume of complete media (Table 2.1) was added to each culture flask and centrifuged at 200rpm for 3 minutes, before aspiration of the supernatant, the resulting pellet was gently suspended in complete culture media followed by determination of cell number using a haemocytometer. An appropriate concentration of HL-1 cells (Table 2.1) was plated and incubated at 37°C with 5% CO₂.

Treatment of cells

Once each tissue culture vessel reached ~75-80% confluency, complete media was removed. An appropriate volume of freshly prepared treatment media was added to each culture vessel (Table 2.1). Treatment media was either vehicle control (complete media + 0.1% (v/v) dimethyl sulphoxide (DMSO) or DMNQ media or doxorubicin media (DMNQ or doxorubicin dissolved in 100% (v/v) DMSO, further dissolved in complete culture media). Cells were incubated for 24 hours at 37°C with 5% CO₂ prior to sampling.

Harvesting cells for nucleic acid generation

Cells were trypsinized as described above, cell pellets washed with PBS and centrifuged at 6000rpm for 3 minutes, the supernatant was removed and pellets stored at -80°C.

Harvesting cells for protein lysates

Cells were washed twice with ice cold PBS before 1ml RIPA buffer (25 mM Tris-HCl pH 7.6, 150 mM NaCl, 1% (v/v) NP-40, 1% (v/v) sodium deoxycholate, 0.1% (v/v) SDS) with protease inhibitor cocktail (Roche Diagnostics) was added to the culture vessel and incubated for 5 minutes at 4°C. Cells were collected by scrapping and centrifuged at 13,000rpm for 20 minutes at 4°C. The supernatant was stored at -80°C.

Plate/Flask Type	Seeding Density	Seeding Volume	PBS Wash Volume	Complete Media Volume	Treatment Media Volume	Trypsin/EDTA (1x)	Coating Volume
T25 Flask	5x10 ⁶ /ml	5ml	5ml	5ml	5ml	2ml	2ml
6 well plate	5x10 ⁶ /ml	2ml	2ml	2ml	2ml	1ml	1ml
96 well plate	5x10 ⁶ /ml	100µl	100µl	100µl	100µl	0.5ml	0.5ml

Table 2.1: Volumes of tissue culture reagents used for different tissue culture vessels.

2.2.1 TRANSFECTION OF HL-1 CELLS WITH microRNA KNOCKDOWN PROBES

Locked nucleic acid knockdown probes are able to associate with RISC and induce degradation of the complementary target of a miRNA sequence. This process results in decreased expression of the target miRNA.

Transfection Complex Preparation

Diluted Lipofectoamine 2000 (50µl, 1:50) was combined with 20nM locked nucleic acid miRNA knockdown probe (Exiqon) in a volume of 50µl in opti-MEM culture media (Invitrogen) and incubated at RT for 20 minutes.

Transfection of HL-1 Cells

HL-1 cells were cultured as described in Section 2.2, however seeding density was reduced to 3x10⁵ cells/ml and transfection complete media was used (Section 2.32). After 24 hours 100µl of appropriate transfection

complex was added to each well to be transfected and incubated at 37°C with 5% CO₂ for 48 hours to allow miRNA knockdown to occur. Treatment of cells was conducted as described in section 2.2.

2.3 PRIMARY CARDIOMYOCYTES

Primary cardiomyocytes were isolated from 3 day old Wistar rats. Rats were decapitated and the heart was rapidly removed. 10 hearts were pooled into 10ml primary cardiomyocyte complete media (Section 2.32); the connective tissue was trimmed and discarded. Ventricles were finally minced and transferred to 10ml collagenase (Type II, Lorne laboratories, section 2.32) pre-warmed to 37°C and placed into a shaking water bath at 60 cycles per minute for 5 minutes. The supernatant was transferred to a fresh falcon tube containing 10mls of collagenase stopping media (Section 2.32) and placed on ice. An additional 10ml of collagenase was added to the tissue and placed in a shaking water bath for 5 minutes at 37°C, this process was repeated until all tissue was digested. Resulting supernatants were centrifuged for 7 minutes at 1000rpm at RT. The supernatant was removed and the resultant pellets suspended in 4mls of primary cardiomyocyte complete media, and transferred to a 6 well plate pre-coated with collagen (BD Biosciences). Plates were incubated at 37°C with 5% CO₂ for 1 hour. Media was removed and cells counted and seeded at a density of 2x10⁵ cells per well in a 24 well plate pre-coated with collagen in 2mls of primary cardiomyocyte complete media and incubated at 37°C with 5% CO₂. 3 days following isolation cells were collected by scrapping into 1ml Tri reagent and stored at -80°C.

2.4 MEASUREMENT OF TISSUE AND CELL PROTEIN CONTENT

Protein concentrations were determined using the Bradford method; this is a colorimetric assay that relies on binding of coomassie blue G-250 dye to protein. An absorbance shift in coomassie dye occurs as it binds to protein by donating a free proton to the ionisable protein group, thus exposing hydrophobic structures allowing non-covalent binding to non-polar regions of coomassie dye via Van Der Waals forces. The proportion of protein is directly proportional to dye protein binding at 595nm. The concentration of protein within a sample was derived by reference to a BSA standard curve.

Running Bradford Assay

A standard curve was prepared by diluting 1mg/ml BSA to the following concentrations: 0, 0.5, 1, 2, 5, 10, 15, 20, 25, 30, 40, 50µg/ml in sample relevant buffer. Lysis buffer (796µl) or water (796µl) was mixed with 4µl test sample or standard of interest. Two hundred microlitres Bio-Rad protein assay reagent (BioRad) was added, and transferred to a cuvette (Sarstedt, 10x4x45 mm). The absorbance was measured at 595nm.

2.5 ASSESSMENT OF CELL VIABILITY USING THE MTS ASSAY

Cell viability following treatment was assessed by an MTS (3-(4,5-dimethylthiazol-2-yl)-5-(3-carboxymethoxyphenyl)-2-(4-sulfophenyl)-2H-tetrazolium) assay. The CellTiter 96® Aqueous One Solution Cell Proliferation Assay (Promega) was utilised. Cells were incubated with a novel tetrazolium compound and an electron coupling reagent, these compounds are bio-reduced in living cells resulting in the formation of formazan that has an absorbance at 490nm. The amount of formazan in culture is directly proportional to the number of viable living cells.

All reagents were used as supplied. Cells were seeded in a 96 well plate and treated as described in section 2.2. Following 23 hours of treatment 20µl of CellTiter 96® Aqueous One Solution reagent was added per well and incubated at 37°C for 1 hour. The absorbance at 490nm was recorded using a SPECTRAMax PLUS 384 spectrophotometer.

2.6 DETERMINATION OF DMNQ AND MNQ LEVELS BY HPLC

The tissue distribution of DMNQ and MNQ was determined using a HPLC assay, conducted by Joel Parry, GSK, Ware.

Sample Preparation

~100mg of tissue or 100µl plasma was mixed with two times the volume of water and homogenised using an Ultra-Turrax at RT. Two times the volume of acetonitrile was added and shaken for 30 minutes at RT before centrifugation at 13,000rpm. The resultant supernatant was dried in a Speed Vac Dryer on a medium heat.

HPLC Assay

Dried samples were suspended in 50µl 50% (v/v) methanol per 100mg or 100µl of starting sample and centrifuged at 13,000rpm for 1 minute. The supernatant was loaded into a total recovery HPLC vial (Water). HPLC was performed as described in Parry et al. (2009) on a 150x2.1mm C18 3.5µm column.

2.7 ASSESSMENT OF CARDIAC DAMAGE BY MEASUREMENT OF PLASMA CREATINE KINASE ACTIVITY

The creatine kinase MB assay (Randox CK-1296) was used, this is an immunoinhibition assay. An antibody incorporated in the CK reagent binds to and inhibits the activity of the M subunit, the kit measures the activity of the B subunit and the activity is multiplied by a factor of two to result in total CK-MB activity. In addition native protein gels were ran with plasma and probed with a CK-MB antibody.

Creatine Kinase Assay

All reagents were used as supplied. Working solutions were prepared by reconstituting one vial of R1b with 2.5ml of assay buffer. 1ml was then mixed with 40µl of plasma and incubated at 25°C for 10 minutes before being transferred to a cuvette (Sarstedt, 10x4x45mm). Using a UV/Vis spectrometer Lambda 2S (Perkin Elmer) the absorbance at 340nm was recorded (A1) and again 5 minutes later (A2). CK-MB activity was then calculated:

$$\Delta A = A2 - A1$$
$$\text{CK-MB} = 1651 \times \Delta A$$

Creatine Kinase Native Protein Gels

Protein concentration of plasma was determined (Section 2.4). Plasma samples containing 35µg protein were diluted with water to 10µl and mixed with 6x loading buffer (50% (v/v) glycerol, 1xtris/glycine running buffer, 0.25% (w/v) xylene cyanol) and separated on 7.5% polyacrylamide (PAGE) gel, with a 3.5% stacking gel (Table 2.2) in tris/glycine running buffer (250mM Tris-base, 1.9M glycine, pH 8.6) at 150V at 4°C and transferred onto nitrocellulose membranes (Hybond-ECL, Amersham Biosciences) by semi dry blotting. After blocking in 5% (v/v) non-fat milk in TBST (10mM Tris, 150mM NaCl, 0.1% (v/v) Tween 20) for 2 hours, the membranes

were incubated with a specific antibody to CK-MB diluted in 5% (v/v) non-fat milk in TBST (1:200) (sc-28898, Santa Cruz Biotechnology) for 2 hours at RT. Membranes were washed three times in TBST for 5 minutes each, and incubated with anti-rabbit IgG antibody (Cell Signalling Technology) conjugated to horseradish peroxidase in 5% (v/v) non-fat milk in TBST (1:1000) for 1 hour again at RT and then washed three times with TBST for 5 minutes each. Bands were visualised by chemiluminescence (GE Healthcare), for 2 minutes without shaking. The membranes were wrapped in plastic wrap and placed in a film cassette in the dark and exposed to x-ray film (ECL hyperfilm, GE Healthcare) for 30 seconds to 2 minutes and developed. Band intensities were measured by computerized image analysis software.

In order to assess equal protein loading, gels were stained with Coomassie Brilliant Blue R-250 (Bio-Rad) for 30 minutes while shaking and destained with 40% (v/v) methanol (Fisher Scientific) and 10% (v/v) glacial acetic acid (Fisher Scientific) solution for 1 hour, with changes to solution every 10 minutes. An image of the gel was then obtained by scanning.

Reagent	Volume (ml)	
	Resolving gel (7.5%)	Stacking gel (3.5%)
Water	7.87	3.14
Acrylamide:bisacrylamide (30% (v/v))	4	0.58
1.5M Tris-HCL pH 8.8 (resolving gel), 0.5M Tris-HCL pH 6.8 (stacking gel)	4	1.25
TEMED	0.008	0.005
10% (v/v) ammonium persulfate	0.12	0.025

Table 2.2: Native protein gel composition

2.8 ASSESSMENT OF CARDIAC DAMAGE BY MEASUREMENT OF PLASMA TROPONIN I LEVELS

Measurement of circulating troponin I in plasma is frequently used for the diagnosis of cardiac dysfunction. The mouse cardiac troponin-I (cTnI) ELISA kit (2010-1-HSP Life Diagnostics) was used to determine cTnI levels in circulating plasma. This kit employs an ELISA method utilising two antibodies that react with plasma resulting in cTnI being bound to horseradish peroxidase (HRP) that subsequently reacts with a HRP substrate that has an absorbance at 450nm. The concentration of cTnI within a sample is directly proportional to the absorbance at 450nm.

Troponin I Assay

All reagents were used as supplied. Plasma samples were diluted 1:3 with plasma diluent®, 100µl of this was mixed with 100µl of cTnI horseradish peroxidase conjugate and placed into a single well in an anti-cTnI-coated 96 well plate. Each plate was shaken at RT for 1 hour. Following shaking plates were washed with water six times before 100µl of TMB reagent was added to each well and again incubated at RT for 20 minutes while shaking. To stop the reaction 100µl of stop solution was added to each well and gently mixed. The absorbance was read at 450nm using a SPECTRAMax PLUS 384 spectrophotometer. A series of standards were run at the same time. All samples were run in triplicate. cTnI levels were calculated with reference to the standard curve and multiplied by the dilution factor.

2.9 ASSESSMENT OF CARDIAC DAMAGE BY MEASUREMENT OF AST LEVELS

The AST assay kit (Randox AS 1202) was used to determine circulating AST levels. The principle of the assay relies on the measurement of NADH oxidation (Figure 2.1).

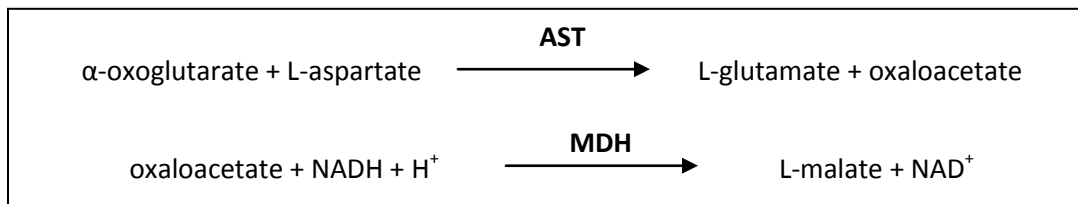


Figure 2.1: Principle of the AST assay, AST activity is directly proportional to the rate of NADH oxidation at 340nm, (malate dehydrogenase (MDH)).

The AST Assay

All reagents were used as supplied. Working solutions were prepared by reconstituting one vial of R1b with 2ml assay buffer, 1ml was then mixed with 100µl of plasma and incubated at 25°C for 1 minute before measuring the absorbance at 340nm every minute for 4 minutes using a UV/Vis spectrometer Lambda 2S (Perkin Elmer). AST activity was then calculated as follows: $U/l = 1746 \times \Delta A_{340nm}/\text{minute}$

2.10 MEASUREMENT OF GLUTATHIONE (GSH) AND REDUCED GLUTATHIONE (GSSG)

The Bioxytech GSH/GSSG-412 assay kit (371757, Calbiochem) was used. All reagents were used as supplied.

This kit utilises 1-methyl-2-vinylpyridinium trifluoromethanesulfonate (M2VP), a thiol-scavenging reagent. To

measure total GSH (GSH_t), GSH reacts with the chromogen 5,5' -dithiobis-(2-nitrobenzoic acid) (DTNB) to emit a detectable product at 412nm. Determination of the rate at which the product is formed is directly related to the concentration of glutathione within a sample with reference to standards. GSSG levels are then measured by scavenging GSH with M2VP

Sample Preparation

100mg of frozen tissue was added to 20µl of ice cold 5% (v/v) meta-phosphoric acid/mg tissue and homogenised using an Ultra-Turrax on ice. Samples were centrifuged at 13,000rpm at 4°C.

Running the GSH/GSSG Assay

All reagents were used as supplied. Total (GSH_t) samples were prepared by diluting 10µl of tissue lysate (above) 1:10 with GSH assay buffer. GSSG samples were prepared by mixing 50µl of tissue lysate (above) with 10µl of assay scavenger solution and incubated for 30 minutes at 4°C, before diluting 1:3 in GSSG assay buffer. Two hundred microlitres of blank (assay buffer), standard (as supplied) or sample were added to a cuvette (Sarstedt 10x4x45mm). To this 200µl of chromogen and 200µl of enzyme was added and incubated at RT for 5 minutes, followed by 200µl of NADPH. The absorbance at 412nm for 3 minutes was measured using a UV/Vis spectrometer Lambda 2S (Perkin Elmer). GSH_t and GSSG levels were then related to the standard curves ran in conjunction. All results were expressed in terms of nmol/mg of tissue.

2.11 MEASUREMENT OF CASPASE 3 ACTIVITY

Activated caspase 3 levels were assessed to indicate the overall activation of apoptosis. The BD ApoAlert™ Caspase 3 colorimetric assay kit (630215, BD Biosciences Clontech) and western blotting were utilised. The assay uses the spectrophotometric detection of chromophore p-nitroaniline (pNA) after its cleavage by caspase 3, the amount of pNA is directly proportional to caspase 3 activity.

2.11.1 CASPASE 3 ASSAY

All reagents were used as supplied in the kit. 100mg of frozen tissue was homogenised in 250µl of lysis buffer. Lysate was centrifuged at 13,000rpm for 10 minutes at 4°C. Tissue lysate (50µl) was mixed with 50µl of 2xreaction buffer/DTT mix and 5µl of 1mM caspase-3 substrate (DEVD-pNA) and incubated at 37°C for 1 hour. PBS (900µl) was added to each sample and transferred to a cuvette (Sarstedt, 10x4x45mm). Absorption was measured at 405nm using a UV/Vis spectrometer Lambda 2S (Perkin Elmer).

2.11.2 CASPASE 3 WESTERN BLOTTING

To further confirm the activation of caspase 3 western blotting was conducted using an antibody against activated 3. Western blots were also probed for GAPDH to assess equal protein loading.

Western Blot Sample Preparation

50mg of heart tissue was homogenised in 1ml of RIPA buffer (25 mM Tris-HCl pH 7.6, 150 mM NaCl, 1% (v/v) NP-40, 1% (v/v) sodium deoxycholate, 0.1% (v/v) SDS) and protease inhibitor cocktail (Roche Diagnostics). Samples were incubated on ice for 30 minutes before centrifugation at 13,000rpm for 20 minutes at 4°C. Protein concentration of the resultant supernatant was determined (Section 2.4).

Caspase 3 Western Blotting

35µg protein (above) was separated by SDS-PAGE on a 12.5% polyacrylamide gel, with a 3.5% stacking gel (Table 2.3) at 100V and transferred onto nitrocellulose membranes (Hybond-ECL, Amersham Biosciences) by wet transfer at 100V for 1 hour.

Reagent	Volume (ml)	
	Resolving gel (12.5%)	Stacking gel (3.5%)
Water	5.05	3.09
Acrylamide:bisacrylamide (30%T, 2.6%C)	6.67	0.58
1.5M Tris-HCL pH 8.8 (resolving gel), 0.5M Tris-HCL pH 6.8 (stacking gel)	4	1.25
10% (w/v) SDS	0.16	0.05
TEMED	0.008	0.005
10% (w/v) ammonium persulfate	0.12	0.025

Table 2.3: Caspase 3 polyacrylamide gel composition

Membranes were blocked and probed with a mouse monoclonal IgG₁ caspase 3 antibody (Sc-56055, Santa Cruz Biotechnology) or a mouse monoclonal IgG₁ GAPDH antibody (Sc-47724, Santa Cruz Biotechnology) followed by incubation with a goat anti-mouse IgG antibody conjugated to horseradish peroxidase (SC-2005, Santa Cruz Biotechnology) as described in section 2.7.

2.12 MEASUREMENT OF ATP/ADP/AMP ACTIVITY BY HPLC

50mg of heart tissue was homogenised in 1ml of 10% (v/v) perchloric acid. Samples were centrifuged at 10,000rpm for 15 minutes at 4°C. The resultant supernatant was neutralised to pH7.5 with 1M KOH and stored at -80°C. Spiked samples were prepared by adding 60µM of each ATP/ADP/AMP to 1ml 10% (v/v) perchloric acid, tissue extracts were prepared as above.

ATP/ADP/AMP HPLC Assay

HPLC was performed on a BDS-Hypersil 250x4.6mm C₁₈ 5µm column using a Transgenomic HPLC Analyser. Buffer A was 83.3mM triethylammonium phosphate (TEAP) pH 6.0 and Buffer B was HPLC grade methanol. The flow rate was set at 1ml/min. The injection volume was 10µL. ATP/ADP/AMP was monitored at 206nm and the amount of ATP/ADP/AMP in each sample determined by calibration of the system with standards of known concentration and the data analysed with reference to the standards and expressed as µM/g tissue.

2.13 MEASUREMENT OF VENTRICULAR WIDTH

Hearts were fixed in 10% (v/v) neutral buffered formalin as described in section 2.1. Cross sectional sections were cut in a 5µm serial step manner through the heart starting at the apex, 10 sections were stained by hematoxylin and eosin from each heart and the ventricular width was measured at three separate locations using Axiovision software, the mean of which was taken as the ventricular width.

2.14 NUCLEIC ACID EXTRACTION

Total RNA extraction

To each tissue sample (100mg) or cell pellet 1ml Tri Reagent was added and homogenised and incubated at RT for 5 minutes before 200µl of 1-bromo-3-chloro-propane was added to each sample. Lysates were shaken

for 20 seconds and vortexed before incubation for 3 minutes at RT. Followed by centrifugation at 13,000rpm for 15 minutes at 4°C; this separates the lysate into two aqueous phases. The upper aqueous phase was transferred to a new tube and 600µl of isopropanol added and incubated at RT for 10 minutes, before centrifugation at 13,000rpm for 10 minutes at 4°C. The supernatant was removed and the resulting pellet was washed twice in 1ml 75% (v/v) ethanol and centrifuged at 13,000rpm for 10 minutes at 4°C. The supernatant was removed and pellets dried and suspended in 20µl water. Extracted RNA was quantified (Section 2.15) and stored at -80°C.

RNA extraction from plasma

Total RNA was extracted from 250µl plasma using the miRCURY RNA Isolation Kit, cell and plant (Exiqon), according to the manufacturer's instructions.

Total DNA extraction

DNA was extracted using a Qiagen kit (QIAamp® DNA micro). All reagents were used as supplied and DNA extracted from 10mg heart tissue. Extracted DNA was then quantified as described in section 2.15.

2.15 QUANTIFICATION AND QUALITY CONTROL OF NUCLEIC ACID EXTRACTION

UV spectrophotometer (NanoDrop) was used to determine the concentration and purity of nucleic acid (RNA and DNA) extractions.

Quantification by UV Spectrophotometry

A NanoDrop ND-1000 UV (NanoDrop technologies) spectrophotometer was used to determine RNA and DNA concentrations. Quality control of extracted RNA and DNA was carried out by calculating the OD_{260/280} ratio (260nm, peak nucleic acid absorbance, 280nm, peak protein absorbance). An OD_{260/280} ratio of between 1.9 and 2.2 was classified as good quality for RNA and between 1.7 and 2.0 for genomic DNA.

2.16 TRANSCRIPTIONAL PROFILING USING MICROARRAYS

Two colour microarrays with reverse labelling were carried out using a full genome mouse oligo array (70mers), using exon centred probes (Mouse Exonic Evidence Based Oligonucleotide (MEEBO) set, Invitrogen), a total of 39,000 oligos were covered including spliced variants, positive, negative and doped controls. These probes were printed onto aldehyde slides (Genetix) using a Stanford type microarray spotter in house.

Pre-washing of microarray slides and cover slips

Before use the required number of microarray slides were racked and washed in 0.2% (w/v) SDS for 2 minutes while shaking before two washes in water for 2 minutes each. Slides were dried by centrifugation for 4 minutes at 1000rpm. Cover slips were racked and washed in 1% (w/v) SDS for 30 minutes before being washed five times in water for 5 minutes each and dried at 42°C overnight.

Microarray reverse transcription

Total RNA was diluted to 7µg in 13µl water before the addition of 1.0µl of oligo dT₂₃N₂ (8µg/µl) and 1µl of random pentadecamers (10nmol/µl), and incubated at 95°C for 5 minutes and 70°C for 10 minutes. Samples were snap cooled on ice for 1 minute. Labelling mix (14µl) (dATP 0.5mM, dGTP 0.5mM, dCTP 0.5mM, dTTP 0.2mM, aadUTP 0.3mM, 1xfirst strand buffer (Invitrogen), DTT 0.01M) and 1µl of Superscript III (Invitrogen) were added and samples incubated at 50°C for 3 hours resulting in cDNA with incorporated amino-allyl dUTP.

RNA hydrolysis

Any remaining RNA was hydrolysed by the addition of 10µl of 0.5M EDTA and 10µl of 1M NaOH to each sample. Samples were incubated at 65°C for 15 minutes before being neutralised by the addition of 25µl of 1M HEPES (pH7.0).

Purification of cDNA

The resultant cDNA was cleaned up using Microcon YM-30 filters (Millipore). Water (400µl) was added to each cDNA sample and added to an assembled Microcon YM-30 filter and centrifuged at 12,000rpm for 7 minutes, the resultant flow through was discarded, and an addition 450µl of water was applied to each filter.

Filters were centrifuged at 12,000rpm for 10 minutes. Each filter was then inverted into a fresh tube and centrifuged at 13,000rpm for 30 seconds to collect the filtrate. The resultant sample was dried in a speedvac on a medium heat. The dried sample was re-dissolved in 3.5µl of water and 0.5µl of sodium carbonate buffer (0.1M, pH 9.0) to ensure the pH remains between 8.5 and 9 during dry incorporation.

The next series of steps attach the Alexa fluorophore (Molecular Probes, Invitrogen) to the aadUTP by means of a covalent condensation reaction between the carboxylic acid group on the dye and the amine group in the aadUTP.

cDNA/dye coupling and clean up

The resulting cDNA was coupled to Alexa fluorophore 555 or 647 (Molecular Probes, Invitrogen); forward labeling: control Alexa 555, test Alexa 647; reverse labeling: control Alexa 647, test Alexa 555. Light exposure to Alexa dyes was reduced to prevent bleaching.

DMSO (4µl) was added to one tube of Alexa 555/647 dye and dissolved, 2µl of each Alexa dye solution was added to half the samples and incubated for 1 hour at RT in the dark before the addition of 4.5µl of 4M hydroxylamine to quench the reaction and incubated for a further 15 minutes in the dark at RT. One Alexa 555 sample was combined with the respective Alexa 647 sample before the addition of 35µl of 0.1M NaOAc (pH 5.2). Alexa labelled cDNA was cleaned up using the Qiagen PCR purification kit (Qiagen). All reagents were used as supplied according to the manufacturer's instructions, samples were eluted in 40µl of elution buffer.

Quantification of labelling and pre-hybridization

Dye incorporation was assessed using a NanoDrop ND-1000 UV (NanoDrop technologies) spectrophotometer using the microarray application within the manufacturer's software and blanked against water.

2x enhanced hybridisation buffer (40µl) (Genesphere) and 1µl of Yeast tRNA (4µg/µl, Invitrogen) was added to each sample, and denatured at 95°C for 2 minutes and incubated at 42°C for 30 minutes.

2.16.1 MICROARRAY HYBRIDIZATION

A coverslip was gently lowered onto the slide to be hybridized. 40µl sample was pipetted onto the edge of the coverslip and allowed to flow under by capillary flow. Slides were placed in a humidified hybridization chamber (Genetix) and hybridized overnight at 42°C.

2.16.2 POST HYBRIDIZATION SLIDE WASHING

Following hybridization microarray slides were removed from the hybridization chamber and racked. One litre of each of the three wash solutions described in table 2.4 were prepared. The racked slides were placed in each wash solution depicted in table 2.4 for the time indicated. Followed by centrifugation at 1000rpm for 4 minutes, slides were placed in an opaque box to protect from light prior to scanning.

Wash solution 1	Wash solution 2	Wash solution 3
1.0xSSC 0.03% (w/v) SDS	0.2xSSC	0.05xSSC
10 minutes	5 minutes	5 minutes

Table 2.4: Post hybridization microarray wash solutions

2.16.3 SCANNING OF MICROARRAYS AND PRIMARY ANALYSIS

Microarray slides were scanned using an Axon 4200A scanner with GenePix 6.0 software. GenePix 6.0 software was opened and one microarray slide loaded onto the scanner. Scanning was carried out using the auto PMT function at 80% power, at a resolution of 5µm at 532nm and 647nm. Downstream analysis of transcriptional data was carried out using software as described in Chapter 1.

2.17 QUANTITATIVE REAL TIME PCR (qRT-PCR)

qRT-PCR is used to quantify the expression levels of selected transcripts. It is widely utilised as an acceptable method to confirm microarray analysis and provides greater sensitivity and requires smaller amounts of RNA compared to microarray platforms. qRT-PCR monitors the progression of a PCR reaction in real time by measuring the emission increase of a fluorescent dye. As the amount of PCR product increases so does the emission rate. This allows characterisation of samples by identifying the point at which the PCR product can

be detected; this is known as the cycle threshold (C_t). qRT-PCR was carried out on a ABI PRISM[®] 7000 real-time PCR System (Applied Biosystems) using Power Syber Green Master Mix (Applied Biosystems), which emits a fluorescent signal when bound to cDNA.

2.17.1 FIRST STRAND cDNA SYNTHESIS

100ng RNA was diluted in 4.5 μ l water mixed with 0.5 μ l 90OD random hexamers and heated to 95°C for 5 minutes and snap cooled on ice. 1 μ l of RNA (100ng) random hexamer mixture was then reversed transcribed using 8.25 μ l of RT master mix (5xPCR buffer, 100mM dATP, 100mM dCTP, 100mM dGTP, 100mM dTTP, and 0.1M DTT), 0.25 μ l of RNasin (Promega), and 0.5 μ l of Superscript III (Invitrogen) and incubated at 50°C for 1 hour then 70°C for 15 minutes before storage at -20°C.

2.17.2 PRIMER DESIGN, OPTIMISATION AND VALIDATION

Primers for RT-PCR were designed to cross exon-intron boundaries to eliminate the detection of any contaminating genomic DNA. Transcript information was obtained from Ensembl (www.ensembl.org) before being imported to Primer Express[®] software v2.0 (Applied Biosystems) to design primer pairs. Primers were designed using the default settings. Selected primer pairs were blast searched to ensure the correct transcript was amplified (www.ncbi.nlm.nih.gov/BLAST).

Primers were obtained from Sigma-Aldrich, upon arrival they were suspended in water to obtain a 1nM concentration. The concentrations of forward and reverse primers in each qRT-PCR reaction were optimized, table 2.5 primer concentrations were added to 12.5 μ l of Power Syber Green Master Mix (Applied Biosystems), 1 μ l of cDNA (Section 2.17.1) and made up to 25 μ l with water per well. Each reaction was placed in triplicate in a 96 well plate (MicroAmp[™] Optical 96-well reaction plate and adhesive film, Applied Biosystems), and centrifuged at 1000rpm for 2 minutes prior to being loaded onto a ABI PRISM[®] 7000 real-time PCR System (Applied Biosystems).

Forward Primer Concentration (nM)	Reverse Primer Concentration (nM)
50	50
50	300
50	900
300	50
300	300
300	900
900	50
900	300
900	900

Table 2.5: Forward and reverse primer concentrations used to optimise primer pairs.

The qRT-PCR was run on the default thermal program for the detector (Table 2.6) with a dissociation protocol at 60°C to check for the presence of non-specific amplification. The primer concentration that gave rise to the lowest mean C_t value was used for all further qRT-PCR reactions for that primer pair.

Time	Temperature (°C)	Stage
<i>For 1 cycle</i>		
2 minutes	50	Initial denature
10 minutes	95	Annealing
<i>For 40 cycles</i>		
15 seconds	95	Denature
1 minute	60	Anneal, extend and read
15 seconds	95	Denature
20 seconds	60	Dissociation protocol and read
15 seconds	95	

Table 2.6: qRT-PCR cycling conditions

Validation of the primers was then conducted to ensure qRT-PCR amplifies at the same efficiency with different amounts of cDNA. RNA was diluted to 10, 20, 50, 100, 200 and 500ng in water and reverse transcribed as described in section 2.17.1. qRT-PCR was conducted using optimised primer concentrations as described earlier. Calculation of the gene of interest minus the endogenous housekeeping gene to the \log_{10} was determined to calculate the regression (R_2) value. An R_2 value of near 1 indicated that the primer pair amplifies at the same rate regardless of the starting RNA concentration.

2.17.3 RUNNING qRT-PCR

1µl of the first strand cDNA (100ng) prepared as in section 2.17.1 was used in each qRT-PCR reaction as described in 2.17.2 for the gene of interest and an endogenous housekeeping gene.

2.17.4 STATISTICAL ANALYSIS OF qRT-PCR DATA

Once a qRT-PCR run was complete, the presence of a single dissociation curve for each primer pair used was checked, before the C_t values were exported as a tab-delimited text file. Relative quantification of gene expression was performed using the $\Delta\Delta C_t$ relative quantitation method. The mean C_t value was calculated for each gene and normalised to the endogenous housekeeping gene. Each gene from treated samples was then normalised against the control data.

2.18 mtDNA COPY NUMBER

mtDNA copy number was measured using a qRT-PCR based technique. Primers were designed using Primer Express and optimized as described in section 2.17.2, but genomic DNA was used in place of cDNA.

qRT-PCR to Assess mtDNA Copy Number

Per well of a 96 well plate, 1µl (100ng) genomic DNA (Section 2.14) was added and qRT-PCR was conducted as in 2.17.3. Statistical analysis was carried out as described in section 2.17.4, data was normalized to a nuclear encoded gene.

2.19 microRNA EXPRESSION PROFILING

Two colour microarrays with reverse labelling were carried out using in house printed microarrays. Arrays were printed on a Stanford design printer onto aldehyde coated slides (Genetix). Locked nucleic acid (LNA) miRNA probes (miCURAY Exiqon) version 208010V8.1 were utilised to cover all identified miRNAs to Sanger version 8.1. Due to the short length of miRNAs conventional microarray labelling techniques cannot be utilised, instead a Flashtag™ kit (Genisphere) was used.

miRNA Microarrays - Poly A Tailing

Microarray slides and coverslips were washed as in 2.16. All reagents were used as supplied. Total RNA was diluted to 1.5µg in 5µl water, before the addition of 0.75 µl of 10xreaction buffer, 0.75 µl of MnCl₂, 0.5 µl of diluted ATP solution (1:500 from stock in water) and 0.5 µl of poly(A)polymerase enzyme, and incubated at 37°C for 15 minutes.

miRNA Microarrays - Ligation of Fluorophore and Hybridization

2µl of the appropriate dye solution (6xAlexa fluor 3[®] Rapid Ligation Mix or 6xAlexa fluor 5[®] Rapid Ligation Mix) and 1µl of T4 DNA Ligase was added to each sample and incubated at RT for 30 minutes in the dark. The reaction was quenched with 1.25µl of Stop Solution. One sample of opposite dyes were pooled together and 2.5µl of BSA solution and 26µl of enhanced cDNA hybridisation buffer was added to each sample, and incubated at 65°C for 10 minutes. Hybridisation was conducted as outlined in 2.16.1, but hybridised at 52°C.

miRNA Microarrays - Post Hybridization Slide Washing, Scanning and Primary Analysis

Following hybridization microarray slides were washed as described in 2.16.2, but the solutions depicted in table 2.7 were used instead. Microarray scanning and data analysis was conducted as described in 2.16.3.

Wash solution 1	Wash solution 2	Wash solution 3
2.0xSSC 0.2% (w/v) SDS	0.5xSSC	0.2xSSC

Table 2.7: Post hybridization microarray wash solutions

2.20 microRNA qRT-PCR

The small length of miRNAs (~22nt) means conventional PCR approaches are not able to be used. To overcome this problem the SuperScript[®] III First-Strand Synthesis System (Invitrogen) and mirVana qRT-PCR primer set (Ambion) kits were utilised.

miRNA qRT-PCR

All reagents were used as supplied. Total RNA was diluted to 25ng in 8µl of water before the addition of 1µl of 1xappropriate dtPrimer (mirVana qRT-PCR primer set) and 1µl of dNTP and incubated at 65°C for 5 minutes and snap cooled on ice for 1 minute. Following this 2µl of 10xRT Buffer, 4µl of 25mM MgCl₂, 2µl of 0.1M DTT, 1µl of RNase out and 1µl of superscript III was added to each sample and incubated at 50°C for 50 minutes, then 85°C for 5 minutes.

1µl of the first strand cDNA specific to the miRNA of interest (above) was added to 12.5µl of Power Syber Green Master Mix (Applied Biosystems), 11µl of water and 0.5µl of appropriate miRNA primer (from mirVana qRT-PCR primer set) and placed in one well of a 96 well plate (MicroAmp™ Optical 96-well reaction plate and adhesive film, Applied Biosystems). Samples were analyzed in triplicate. In addition to the miRNA of interest 5S rRNA was also ran in conjunction to allow sample normalization. qRT-PCR reaction and data analysis was as described in 2.17.3 and 2.17.4.

2.21 microRNA NORTHERN BLOTTING

miRNA northern blotting was conducted using miRCURY LNA™ microRNA Detection Probes (Exiqon). These probes allow high affinity binding and enable specific and sensitive miRNA detection.

Total RNA diluted to 20µg in 10µl water was mixed with 10µl 2xloading buffer (98% (v/v) deionised formamide, 2% (v/v) 0.5 M EDTA pH8, 0.25% (w/v) bromophenol blue and 0.25% (w/v) xylene cyanol) and denatured at 95°C for 5 minutes and separated on a 15% polyacrylamide/urea gel (Table 2.8) at 100V for 1 hour. Followed by transfer to a positively charged nylon membrane (Genetix) by capillary transfer using 20xSSC overnight. The membranes were UV cross linked at 120 mJ/cm² for 60 seconds. LNA™ miRNA detection probes (Exiqon) were end labelled with ³²P(δ)ATP, incorporation was measured by scintillation counting. Membranes were hybridised overnight at 37°C with 1x10⁶ dpm/ml probe. Following hybridisation membranes were washed twice in 2xSSC and 0.1% (w/v) SDS for 10 minutes followed by a further two washes in 1xSSC and 0.1% (w/v) SDS for 10 minutes before a final two washes in 0.2xSSC and 0.1% (w/v) SDS again for

10 minutes, membranes were exposed on Phosphor screens for up to 48 hours and scanned on a Storm™ Scanner (Amersham).

Reagent	Volume
Acrylamide:bisacrylamide (30% v/v)	7.50ml
Urea	6.30g
5 x TBE	1.50ml
10% (v/v) ammonium persulfate	0.15ml
TEMED	0.01ml

Table 2.8: miRNA northern blotting gel composition

2.22 SEPARATION OF RNA AND VERIFICATION FOR TRANSLATIONAL ANALYSIS

Sample Preparation

50mg of heart tissue perfused with 100µg/ml cycloheximide (Section 2.1.2) was homogenised in 250µl ice cold lysis buffer (15mM Tris-HCl pH8, 300mM NaCl, 15mM MgCl₂, 1% (v/v) Triton X-100, 100µg/µl cycloheximide, 1mg/ml heparin, 80 U/ml RNAsin). Samples were incubated on ice for 15 minutes followed by centrifugation at 12,000rpm for 5 minutes at 4°C. The protein concentration of the resultant supernatant was determined (Section 2.4) and 300µg protein was loaded directly onto each sucrose gradient.

Sucrose Gradient Preparation and Centrifugation

8ml of 65% (w/v) sucrose solution in lysis buffer (15mM Tris-HCl pH7.5, 300mM NaCl, 15mM MgCl₂, 100µg/µl cycloheximide, 1mg/ml heparin, 1mM DTT) and 8ml lysis buffer was prepared and cooled to 4°C. A linear 10-65% sucrose gradient was prepared using a gradient station machine in Beckman ultra-clear centrifuge tubes (14x95mm). The sample lysates (above) were loaded directly onto the top of a gradient and centrifuged at 200,000g for 2 hours at 4°C.

Fractionation of Gradients and RNA Extraction

Gradients were fractionated by upward displacement into 1ml aliquots (15 in total). The absorbance at 254nm was monitored throughout; samples were collected into 1ml TRI[®] Reagent. RNA was extracted from each sample as described in 2.14. Equal volumes of each fraction were used for further analysis.

Verification of Fractionated RNA

To ensure RNA was separated the proportion of β -actin in each fraction was measured by qRT-PCR and northern blotting to identify polysomal fractions. Monosomal fractions were identified by the 40S and 60S peaks on the A_{254} profile and treating tissue lysate with 100mM EDTA. 100mM EDTA was added to tissue lysate prior to gradient centrifugation, gradients were processed as described above. EDTA disaggregates ribosomes from the mRNA leaving free mRNA, so marking the position of the monosomal mRNA.

qRT-PCR on Fractionated RNA

Equal volume of RNA (1 μ l) from each fraction (up to 100ng) was reverse transcribed and subjected to qRT-PCR as described in section 2.17. The percentage translation of the gene was calculated to determine the amount of the gene of interest in each fraction.

Northern Blotting Using Fractionated RNA - Preparation of Probes

Probes for northern blotting were generated by PCR using total RNA of mouse origin utilising primers designed in Primer Express as described in section 2.17.2. 100ng RNA was added to 50pM of forward and reverse primer in 50 μ l of 1xPCR Master Mix (Promega) and subjected to PCR (Table 2.9).

Temperature (°C)	Time
<i>For 1 cycle</i>	
50	2 minutes
95	10 minutes
<i>For 40 cycles</i>	
95	15 seconds
60	1 minute

Table 2.9: PCR conditions used to generate probes for northern blotting

PCR samples were then purified using the QIAquick PCR purification kit (Qiagen). The manufacture's instructions were followed; the PCR product was eluted in 30 μ l of elution buffer. The resultant DNA sample was sequenced in house by PNCAL (University of Leicester) via the Big Dye reaction to ensure the genomic sequence was correct.

Northern Blotting Using Fractionated RNA

A 1% denaturing agarose gel with 18% (v/v) formaldehyde in 1xMOPS (0.2M MOPS (pH 7.0), 80mM NaOAc, 10mM EDTA) was prepared by melting 80mg agarose in 57.7ml of water prior to the addition of 8ml of 10xMOPS and 14.3ml of formaldehyde and cast. Once set, the gel was submerged in 1xMOPS in an electrophoresis tank. An equal volume of each fraction (5.5µl) was mixed 1:1 with denaturing buffer (70% (v/v) deionised formamide, 25% (v/v) formaldehyde, 1xMOPS and 30µg ethidium bromide) and incubated at 95°C for 15 minutes and snap cooled on ice. 2µl RNA loading buffer (50% (v/v) deionised formamide, 1 mM EDTA, 0.25% (w/v) bromophenol blue and 0.25% (w/v) xylene cyanol) was added to each sample, prior to samples being loaded into the gel and separated overnight at 20V. Gel images were obtained with a UVP BioImaging System (UVP, Cambridge, UK). RNA was transferred from the gel onto a positively charged nylon membrane (Genetix, New Milton, UK) by capillary transfer overnight in 3xSSC. The membrane was UV cross-linked at 120 mJ/cm² for 60 seconds. Probes for β-actin were labelled with ³²P using Klenow fragment, incorporation was measured by scintillation counting. Membranes were hybridised overnight at 42°C with 1x10⁶ dpm/ml probe. Followed by, washing and exposure, as described in section 2.21.

2.23 TRANSLATIONAL PROFILING USING MICROARRAYS

All microarray slides and coverslips were prewashed as described in section 2.16.

Translational Profiling - Purification of RNA

Equal amounts of RNA from appropriate fractions (i.e. polysomes or monosomes) were pooled (10µl from each fraction) and precipitated with 1x3M NaOAc pH 5.0 and 3x100% (v/v) ice cold ethanol at -20°C overnight. Followed by centrifugation at 13,000rpm for 15 minutes at 4°C, the resultant pellets were washed twice in 1ml of 75% (v/v) ethanol by centrifugation at 13,000rpm for 5 minutes at 4°C each and suspended in 10µl of water.

Translational Profiling - Reverse Transcription and Labelling

A direct labelling method was used; this involves reverse transcribing the RNA at the same time as labelling the resultant cDNA with Cy3- or Cy5-dUTPs (GE Healthcare). Cy3 and Cy5 have a wavelength of 532 and 647 nm, respectively. 10µl of the purified RNA sample (above) was incubated at 95°C for 3 minutes and snap cooled on ice for 1 minute. 1.0µl of oligo dT₂₃N₂ (8µg/µl) was added to each sample and incubated at 70°C for 8 minutes. 6.5µl of direct labelling mix (dATP 0.5mM, dGTP 0.5mM, dCTP 0.5mM, dTTP 0.2mM, 1xfirst strand buffer (Invitrogen) and DTT 0.01M) and 1µl of Superscript III (Invitrogen), 0.5µl of RNAsin (Promega) and 2µl of the appropriate Cy dye were added to each sample and incubate at 50°C for 2 hours.

Translational Profiling - RNA Hydrolysis and cDNA Purification

Any remaining RNA was hydrolysed by the addition of 20.5µl water, 1µl of 0.5M EDTA, 1µl of 10% (w/v) SDS and 3µl of 3M NaOH to each sample and incubated at 70°C for 10 minutes and neutralised by the addition of 10µl of 1M Tris-HCL (pH 7.5) and 3µl of 2M HCL (Fisher). The resultant cDNA was purified as described in 2.16 and suspended in 20µl water.

Translational Profiling - Hybridization and Scanning

Labelling efficiency was measured (Section 2.16) and equal amounts of labelled cDNA (Cy-3 and Cy-5) were combined. Samples were made up to a volume of 40µl with water, 1µl of Yeast tRNA (4µg/µl, Invitrogen) and 40µl of 2xenhanced cDNA hybridisation buffer (Genisphere) was added to each sample and incubated at 42°C for 30 minutes. Hybridization was conducted as described in section 2.16.1. Following hybridization slides were washed and analyzed as described in 2.16.2 and 2.16.3.

2.24 TRANSCRIPTION FACTOR BINDING

Transcription factor binding was assessed by electrophoretic mobility shift assay (EMSA) and western blotting. An EMSA allows the investigation of DNA-protein interactions, utilising electrophoresis to detect 'shifts' in bands.

Transcription factor binding - protein extraction

Total protein was isolated from tissue as described in section 2.11.2. Nuclear protein was extracted from 50mg of powdered heart tissue and homogenised in 1ml of ice cold lyses buffer (10mM HEPES, 10mM KCl, 0.1mM EDTA, 0.4% (v/v) Triton x100, 1mM DTT and protease inhibitor cocktail) and incubated on ice for 10 minutes. Samples were centrifuged at 13,000rpm for 3 minutes at 4°C, the resultant pellet was suspended in 150µl of nuclear extraction buffer (20mM HEPES, 0.4M NaCl, 1mM EDTA, 10% (v/v) glycerol, 1mM DTT and protease inhibitor cocktail) and shaken vigorously for 2 hours at 4°C. Samples were centrifuged at 13,000rpm for 5 minutes at 4°C. The protein concentration of the supernatant was determined as in section 2.4.

Transcription factor binding - EMSA NRF-1

EMSA was conducted using the LightShift® Chemiluminescent EMSA kit (20148, Pierce) according to the manufacturer's instructions. Single stranded oligonucleotides were designed against NRF-1 using Primer Express as described in 2.17.2. The complementary sequence of the designed primers was determined and biotin end-labelled double stranded oligonucleotides were obtained from Sigma-Aldrich. A non biotin end-labelled double stranded oligonucleotide was also obtained.

EMSA was carried out on a 6% polyacrylamide gel in 0.5xTBE (Table 2.10). Binding reactions were prepared (per 20µl) containing 35µg of nuclear protein (above), 2µl of 10x binding buffer, 1µl of 1µg/µl poly (dI-dC), 1µl of 50% (v/v) glycerol, 1µl 1mg/ml BSA, 1µl of 1% (w/v) NP-40, 1µl of 1M KCl, 1µl of 100mM MgCl₂ and 30nM biotin end-labelled double stranded oligonucleotide. Two additional binding reactions were prepared as above but, with the addition of 30nM double stranded oligonucleotide and protein extract was omitted.

These two additional binding reactions ensure that any shift observed is a result of DNA:protein interaction. All binding reactions were incubated at RT for 20 minutes. Following incubation 5µl of 5x loading buffer was added to each sample; samples were subjected to electrophoresis at 100V for 45 minutes and transferred to a positively charged membrane (Genetix) by wet transfer at 100V for 30 minutes and UV cross linked at 120mJ/cm² for 60 seconds. Biotin labelled DNA was then detected by chemiluminescence using a

streptavidin-horseradish peroxide conjugate according to the manufacturer's instructions (20148, Pierce). Following blocking and conjugation membranes were placed in a film cassette in the dark and exposed to x-ray film (ECL hyperfilm, GE Healthcare) for 5 seconds to 30 seconds and developed.

Reagent	Volume (ml)
5 x TBE	2.000
Acrylamide:bisacrylamide (30% v/v)	2.500
Glycerol	2.000
10% (w/v) ammonium persulfate	0.150
TEMED	0.017
Water	3.500

Table 2.10: EMSA gel composition

Transcription factor binding - western blotting of NRF-1

35µg total or nuclear protein from tissue (above) was separated by SDS-PAGE on a 10% polyacrylamide gel, with a 3.5% stacking gel (Table 2.11) as described in 2.7 and probed with a mouse monoclonal IgG₁ NRF-1 antibody (Sc-33771, Santa Cruz Biotechnology) followed by incubation with a goat anti-rabbit IgG antibody conjugated to horseradish peroxidase (SC-2004, Santa Cruz Biotechnology).

Reagent	Volume (ml)	
	Resolving gel (10%)	Stacking gel (3.5%)
Water	6.38	3.09
Acrylamide:bisacrylamide (30% v/v)	5.33	0.58
1.5M Tris-HCL pH 8.8 (resolving gel), 0.5M Tris-HCL pH 6.8 (stacking gel)	4	1.25
10% (w/v) SDS	0.16	0.05
TEMED	0.008	0.005
10% (w/v) ammonium persulfate	0.12	0.025

Table 2.11: NRF-1 western blot polyacrylamide gel composition

2.25 MITOCHONDRIAL COMPLEX ACTIVITIES

The electron transport chain and ATP synthase are positioned in the mitochondria inner membrane as described in Chapter 1. In order to investigate the activity of complex I-V kinetic based assays were

developed. The developed assays are able to detect both direct acting inhibitors and indirect effects on complex activity.

2.25.1 MITOCHONDRIAL COMPLEX ACTIVITY - SAMPLE PREPARATION

~ 200mg heart tissue was homogenised in 250µl PBS and centrifuged at 4°C for 1 minute at 6000rpm; the resultant supernatant was stored at -80°C. HL-1 cells were seeded, treated and harvested into PBS at a concentration of 2×10^6 /ml as described in section 2.2 and stored at -80°C. Protein concentrations of samples were determined (Section 2.4).

2.25.2 COMPLEX I ACTIVITY

The oxidation of NADH formed in the TCA cycle is catalysed by complex I. Complex I can be inhibited by rotenone, an isoflavonoid of plant origins. Rotenone binds to the ubiquinone binding site on complex I preventing oxidation of NADH. Activity was measured as a rotenone-sensitive decrease in NADH concentration at 340nm (Barrientos 2002).

Complex I Assay - Biological Lysate Preparation

A 1:1 dilution of sample (Section 2.25.1) with 0.5% (v/v) triton X100 in PBS were prepared and incubated on ice for 1 hour. 3µl of the resulting lysate was added to each well of a 96 flat bottomed plate (Greiner bio-one), this equated to ~130ug protein/well.

Complex I Assay

Each sample was measured in triplicate and each triplicate was duplicated, to the duplicate samples 4µl of 1mM rotenone (in 100% (v/v) ethanol) was added to inhibit any complex I activity. Reaction buffer (Table 2.12) was added to each well. Absorbance of each 96 well plate was measured at 340nm every 9 seconds for 10 minutes at 37°C on a SPECTRAmax PLUS 384 spectrophotometer.

Calculation of Complex I Activity

Complex I activity was calculated for each sample when the change in absorbance of NADH at 340nm against time was linear. This change was taken as the maximum rate of reaction (V_{max}) where the regression value is equal to 1. The absorbance of the rotenone inhibited samples was subtracted from the corresponding non-inhibited samples to obtain the V_{max} of complex I activity in each sample. Data was normalized to the amount of protein in each sample and expressed as $\Delta Abs/min(V_{max})/\mu g$ protein. The inverse $V_{max}/\mu g$ protein was plotted to avoid confusion over the change in activity.

Reaction buffer per well			
Complex I	Complex II-III	Complex IV	Complex V
In 200 μ l: 25mM K_2HPO_4 titrate to pH 7.4 with KH_2PO_4 , 12.5 μ l of 50mg/ml fatty acid free BSA, 7.5 μ l of 5mM NADH, 12.5 μ l of 40mM sodium azide, 3.75 μ l of 5mM coenzyme Q10 (in 100% (v/v) ethanol) and 13.75 μ l of dd H_2O , pre-warmed to 37 $^{\circ}C$	In 150 μ l: 166mM K_2HPO_4 titrate to pH 7.4 with KH_2PO_4 , 12.5 μ l of 40mM sodium azide, 3 μ l of 0.5M succinate, 3 μ l of rotenone, 25 μ l of 0.1% (w/v) BSA and 31.5 μ l of 10.4mg/ml cytochrome c, pre-warmed to 37 $^{\circ}C$	In 62.5 μ l: 40mM K_2HPO_4 titrate to pH 6.5 with KH_2PO_4 , 1M sucrose and 4mg/ml fatty acid free BSA, 18 μ l of 6.25mM lauryl maltoside and 10 μ M reduced cytochrome C in a volume of 205 μ l	Per well: 20 μ l of 0.5M Tris-HCL (pH 8.0), 2 μ l of 0.5M $MgCl_2$, 20 μ l of 10mM NADH, 12.5 μ l of 100mM PEP, 20 μ l of 50mg/ml fatty acid free BSA, 4 μ l of 1mM rotenone, 3 μ l of 1mM antimycin-A, 6 units of LDH and 5 units of PK and pre warmed to 37 $^{\circ}C$

Table 2.12: Details of reaction buffers for complexes I-V assays

2.25.3 COMPLEX II-III ACTIVITY

Complex II-III can be measured following the reduction of cytochrome c by complex III coupled to succinate oxidation (Gellerich et al. 2004). Complex II oxidises succinate to fumarate in the TCA cycle and transfers electrons to ubiquinone, which are subsequently reduced to ubiquinol by complex III. Complex II-III activity was measured by a succinate-dependent antimycin-A or 2-thenoyltrifluoroacetone (TTFA) sensitive reduction of cytochrome c at 550 nm allowing measurement of combined activities of complex II and III (King et al. 1967). Antimycin-A is an inhibitor of complex III and TTFA is an inhibitor of complex II, both were used in separate wells (Barrientos 2002).

Complex II-III Assay

~ 20µg protein was placed in each well of a 96 well plate (Section 2.25.1) each sample was measured in triplicate. 18µl of 0.5% (v/v) tween 20 in PBS was added to each well containing biological material. To one set of triplicate samples 3µl of 1mM antimycin-A (in 100% (v/v) ethanol) was added. In another set of triplicate samples 5µl of 500mM TTFA (in 100% (v/v) ethanol) was added. Reaction buffer (Table 2.12) was added to each well. Absorbance of each 96 well plate was measured at 550nm every 9 seconds for 10 minutes at 37°C on a SPECTRAMax PLUS 384 spectrophotometer. Activity was calculated as in Section 2.25.2

2.25.4 COMPLEX IV ACTIVITY

Complex IV is the terminal member of the ETC, coupling the transfer of electrons from cytochrome c to molecular oxygen. Complex IV activity can be measured by following the oxidation of reduced cytochrome c at 550nm (Gellerich et al. 2004). Complex IV activity can be competitively inhibited by the addition of sodium azide.

Preparation of Reduced Cytochrome C

Reduced cytochrome c was prepared by making a 2.742mg/ml cytochrome c solution in water and reduced with ascorbic acid until the solution was light pink in colour. This solution was desalted by passing through a PD-10 Sephadex desalting column (Amersham Biosciences). The absorbance at 550nm of the reduced cytochrome c was determined. The amount of reduced cytochrome c added per well to give a final concentration of 10µM was then calculated.

Complex IV Assay

~ 10µg protein was placed in each well of a 96 well plate (Section 2.25.1), each sample was measured in triplicate and each triplicate was duplicated, to the duplicate samples 25µl of 8mM sodium azide was added to inhibit any complex IV activity. Reaction mix (Table 2.12) was added to each well. Absorbance was measured at 550nm every 9 seconds for 10 minutes at 37°C on a SPECTRAMax PLUS 384 spectrophotometer. Activity was calculated as in section 2.25.2.

2.25.5 COMPLEX V ACTIVITY

This enzyme catalyses the formation of ATP from ADP and phosphate, using the proton gradient generated, by downstream complexes (Gellerich et al. 2004). Complex V activity can be inhibited by oligomycin by blocking its proton channel preventing the conversion of ADP and phosphate to ATP (Zheng and Ramirez 1999).

Complex V Sample Preparation

Samples were prepared as in section 2.25.1, but were homogenised in 250mM sucrose, 2mM EGTA, and 20mM Tris pH 7.4 at 4°C instead of PBS. 15µg protein was added into each well of a 96 flat bottomed plate.

Complex V Assay

Each sample was measured in triplicate and each triplicate was duplicated, to the duplicate samples 3µl of 1mM oligomycin (in 100% (v/v) ethanol) was added to inhibit complex V activity. Reaction buffer (Table 2.12) was added to each well. Absorbance was measured at 340nm every 9 seconds for 5 minutes at 37°C on a SPECTRAMax PLUS 384 spectrophotometer, this constitutes the pre-read plate. Following this 75µl of 10mM MgATP was added per well and again the absorbance was measured at 340nm every 9 seconds for 10 minutes. Activity was determined as described in 2.25.2 but prior to calculation the pre-read plate V_{max} was subtracted from the post ATP plate.

2.26 CITRATE SYNTHASE ACTIVITY

Citrate synthase is involved in the tricarboxylic acid cycle (TCA) and is widely used as a measure of mitochondrial mass. Citrate synthase catalyses the reaction of acetyl CoA and oxaloacetate to form coenzyme A. The production of coenzyme A was monitored by the reaction with 5, 5'-dithiobis 2-nitrobenzoic acid (DTNB) at 412nm.

Citrate Synthase Activity - Sample Preparation

100µg protein (Section 2.25.1) was mixed 1:1 with 0.5% (v/v) triton X 100 in PBS and incubated on ice for 1 hour. 3µl of the resulting lysate was added to each well of a 96 well plate, reaction buffer (per well, containing 25µl of 0.4mg/ml DTNB (dissolved in 1M Tris-HCl pH 8.1), 7.5µl of 10mg/ml acetyl CoA (dissolved

in acidified water pH 5.0) and 165µl water) was added to each well. Absorbance was measured at 412nm every 9 seconds for 3 minutes on a SPECTRAmax PLUS 384 spectrophotometer, this constitutes the pre read plate. Following this 12.5µl of 0.5mM oxaloacetic acid was added per well and the plate was again read at 412nm every 9 seconds for 5 minutes. Activity was determined as described in 2.25.2 but prior to calculation the pre-read plate Vmax was subtracted from the post oxaloacetic acid plate.

2.27 ANT/VDAC WESTERN BLOTTING

35µg total protein from tissue (2.11.2) was separated by SDS-PAGE on a 15% polyacrylamide gel, with a 3.5% stacking gel (Table 2.13) as outlined in 2.7 and probed with a monoclonal IgG₁ ANT or VDAC antibody (Sc-11433 or Sc-8829 Santa Cruz Biotechnology) followed by incubation with a goat anti-rabbit IgG or donkey anti-goat IgG antibody both conjugated to horseradish peroxidase (Sc-2004 or Sc-2020 Santa Cruz Biotechnology).

Reagent	Volume (ml)	
	Resolving gel (15%)	Stacking gel (3.5%)
Water	3.710	3.090
Acrylamide:bisacrylamide (30%T, 2.6%C)	8.000	0.580
1.5M Tris-HCL pH 8.8 (resolving gel), 0.5M Tris-HCL pH 6.8 (stacking gel)	4.000	1.250
10% (w/v) SDS	0.160	0.050
TEMED	0.008	0.005
10% (w/v) ammonium persulfate	0.120	0.025

Table 2.13: ANT and VDAC polyacrylamide gel composition

2.28 LACTATE DEHYDROGENASE (LDH) ASSAY

LDH is used to assess cell viability as a marker of cell breakdown and damage. LDH is released into the plasma or cell culture media upon damage. A Konelab T series LDH assay kit (IFCC) was utilised. In this assay LDH catalyses the conversion of L-lactate to pyruvate in reducing NAD⁺ to NADH, allowing measurement at 340nm.

LDH Assay

Samples were prepared as in 2.25.1. A Konelab T series LDH assay kit (IFCC) kit was used to measure LDH on a Thermo Konelab 20XT clinical auto analyser. Reagents were prepared according to the manufacturers instructions. 200µl of each sample was loaded onto the auto analyser. The absorbance was measured at 340nm. Data was normalized to the amount of protein and expressed as Units of activity/ug protein.

2.29 GLUTAMATE DEHYDROGENASE (GLDH) ASSAY

Glutamate dehydrogenase (GLDH) is a mitochondrial enzyme bound to the inner mitochondrial membrane that catalyzes the conversion of α-oxoglutarate to glutamate (Figure 2.2). Upon tissue damage GLDH is released into plasma, and is a biomarker for mitochondrial damage.

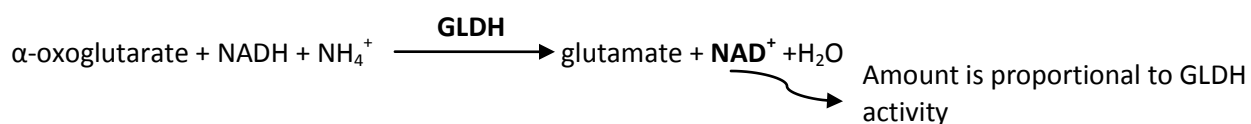


Figure 2.2: Principle of the GLDH assay

GLDH Assay

Samples were prepared as in 2.25.1. A randox kit was used to measure GLDH (GL441) on a Thermo Konelab 20XT clinical auto analyser as described in section 2.28.

2.30 METHEMOGLOBIN ASSAY

Methemoglobin was measured according to Anders and Chung (1984). In duplicate 25µl of blood (Section 2.1.2) was mixed with 2mls of water and incubated at RT. Following incubation 25µl of 30g/L hydrogen peroxide was added to one of the samples (A1) and 10µl of 50g/L sodium nitrite to the other (A2). 8ml PBS (pH 6.6) was added to all samples and 1ml of each sample placed into a cuvette (Sarstedt, 10x4x45mm). 5ml of the control sample was further diluted with an additional 5ml PBS (pH 6.6) and 1 ml placed in a cuvette (Sarstedt, 10x4x45mm); this sample was used as a blank. The absorbance at 405nm was recorded. Results were calculated as follows: methemoglobin % = (A1/A2) x 100.

2.31 DNA AND PROTEIN SYNTHESIS

De novo protein and DNA synthesis was assessed in HL-1 cells by measuring the incorporation of L-[4, 5-³H]-leucine or [6-³H] – thymidine, respectively. Cells were seeded into a 96 well plate and treated (Section 2.2). After treatment, media was removed and replaced with complete media containing labelled leucine or thymidine to a final concentration of 1uCi/well and incubated at 37°C for 2 hours. Following this media was removed and replaced with 200µl of 10% (w/v) trichloroacetic acid and again incubated at 37°C for 10 minutes before being aspirated, followed by the addition of 200µl of 1M NaOH to each well. The plate was incubated at 37°C overnight. One hundred and fifty microlitres of the resulting solution was assessed for leucine or thymidine incorporation by scintillation counting. Results were expressed as a percentage of the control incorporated.

2.32 CELL CULTURE MEDIA COMPOSITION

HL-1 cells complete media

Component	Volume (ml)	Final Concentration
Claycomb media	87	-
Fetal bovine serum (Sigma Batch 027K8414)	10	10%
Penicillin/Streptomycin (Invitrogen)	1	100 U/ml:100 µg/ml
Norepinephrine (10mM in 30mM ascorbic acid)	1	0.1mM
L-Glutamine (200mM)	1	2mM

HL-1 cells transfection media

Component	Volume (ml)	Final Concentration
Claycomb media	87	-
Fetal bovine serum (Sigma Batch 027K8414)	10	10%
Norepinephrine (10mM in 30mM ascorbic acid)	1	0.1mM
L-Glutamine (200mM)	1	2mM

Primary cardiomyocyte complete media

Component	Volume (ml)	Final Concentration
Minimal essential medium (Invitrogen)	90	-
Fetal calf serum	10	10%
Penicillin/Streptomycin (Invitrogen)	1	100 U/ml:100 µg/ml

Collagenase

Component	Amount/Volume
Collagenase Type II	0.25g
Ca ²⁺ /Mg ²⁺ free media	83.00ml

Collagenase stopping media

Primary complete media supplemented with 5mg gentamycin per 100ml media pre cooled to 4°C before use.

2.33 STATISTICAL ANALYSIS

Microarray data analysis was conducted as described in chapter one. All other data was subjected to a one way ANOVA and post hoc Dunnett's t-test using GraphPad Prism.

Chapter 3: Toxicokinetics of DMNQ and MNQ in mice and the application of DMNQ for studying cardiotoxicity *in vivo*

3.1 INTRODUCTION

Doxorubicin has several chemical properties that individually or in combination could be responsible for its toxicity. One favoured hypothesis for the mechanism of cardiotoxicity is via redox cycling and oxidative stress. In order to investigate the role of redox cycling and oxidative stress in doxorubicin cardiotoxicity, model compounds that redox cycle but are largely devoid of other chemical activity have been utilised to try and gain mechanistic knowledge into doxorubicin cardiotoxicity. Two quinones 2, 3-dimethoxy-1, 4-naphthoquinone (DMNQ) and 2-methyl-1, 4-naphthoquinone (MNQ) have been widely utilised as model compounds to investigate redox cycling and oxidative stress (Gant et al. 1988; Miller et al. 1986). The advantage of using these model compounds was to isolate the redox properties of doxorubicin from the pharmacological effects for hypothesis testing. DMNQ has a single electron redox potential of -183mV making it a near ideal redox cycling agent and lacks confounding chemical reactivity with nucleophiles, a feature of MNQ. DMNQ can redox cycle more effectively than doxorubicin but is thought not to inhibit DNA synthesis to the same extent as doxorubicin.

The majority of studies have been conducted *in vitro* and no data was present in the literature concerning DMNQ administration *in vivo*, prior to the publication of this study (Parry et al. 2009).

3.1.1 PLAN OF INVESTIGATION

In order to assess the suitability of DMNQ as a model compound *in vivo* I first had to establish the toxicokinetics and bio-distribution of DMNQ in a mouse model. MNQ was also profiled in this manner to act as a comparison to the results obtained with DMNQ. Following bio-distribution analysis the marker of cardiac dysfunction CK-MB and transcriptional profiling of the heart using MEEBO (Mouse Exonic Evidence Based Oligonucleotide) microarrays were used to assess the impact of both these quinones on cardiac tissue. In addition the assessment of cardiac glutathione levels (reduced glutathione (GSH) and oxidised (GSSG)) was conducted to assess the impact of these quinones on the oxidative response of the heart. These studies allowed the determination of the suitability of both DMNQ and MNQ as model compounds for studying the

redox cycling of doxorubicin. As both DMNQ and MNQ are thought not to affect DNA and protein synthesis to the same extent as doxorubicin, de novo DNA and protein synthesis rates were also determined *in vitro*. Toxicokinetic experiments were not conducted following doxorubicin, as a number of studies have previously determined the distribution and toxicokinetics of this compound *in vivo* (Al-Abd et al. 2009; Urva et al. 2009; Colombo et al. 1999).

All high-performance liquid chromatography (HPLC) based assays in this chapter were conducted by Joel Parry (GSK). Tissue extracts were supplied for this purpose.

3.1.2 HYPOTHESIS AND AIM

The overall aim of this study was to define the toxicokinetics and bio-distribution of DMNQ and MNQ *in vivo* following a single dose and assess the suitability of these as model compounds to study doxorubicin cardiotoxicity.

3.2 RESULTS

3.2.1 DOSE SELECTION

Male C576B/AJ mice were utilised in all studies. Preliminary investigations conducted by Dr. T. Gant revealed oral administration of 200mg/kg DMNQ resulted in poor bioavailability (data not reported). Consequently it was decided to evaluate intraperitoneal (i.p.) administration of DMNQ using arachis oil as a vehicle to increase the systematic availability. Arachis oil was utilised as the vehicle due to the insolubility of DMNQ in water. Dr. T. Gant identified a single dose of 25mg/kg DMNQ in 10ml/kg arachis oil dosed i.p. in C576B/AJ mice as the no observed adverse effects level (NOAEL). Toxicity at dose levels above this rapidly manifested and was evident by piloerection and withdrawal. The toxicity at this dose level however appeared transient in nature resolving approximately 45 minutes following dosing.

3.2.2 TOXICOKINETICS AND BIODISTRIBUTION OF DMNQ OR MNQ IN A MOUSE MODEL

Mice were dosed with a single dose of 25mg/kg DMNQ or MNQ in 10ml/kg arachis oil or arachis oil alone and sacrificed at 5, 10, 15, 20, 30, 45 minutes and 1, 1.5, 2, 5 hours following a single dose (n=3 per compound and time point). Plasma, heart, liver and brain extracts were subjected to HPLC analysis for the presence of DMNQ or MNQ. Mean quinone exposure data was imported into WinNonlin version 1.4 (Pharsight Corporation) and the data analysed as in Parry et al. (2009) to gain exposure metrics. The observed transient toxicity 45 minutes following dosing correlates with the pharmacokinetic data. DMNQ is almost entirely eliminated by 60 minutes following dosing (Table 3.1). The pharmacokinetic data for the plasma is comparable for both DMNQ and MNQ, with a Cmax of 8.97ng/ml and 11.1ng/ml, respectively, with a Tmax of 10 minutes and half life of 18 and 20 minutes respectively. However tissue distribution was considerably different for the two quinones of interest. DMNQ was more widely distributed than MNQ and was found distributed to the heart and crossed the blood brain barrier, in addition there was only a slight absorption phase in any of the tested tissues following DMNQ (Figure 3.1), this maybe a reflection of the dosing route.

The T_{max} was reached in the heart within 10 minutes with a C_{max} of 2.74ng/mg following DMNQ; however a prolonged half life of 126 minutes was present, compared to 18 minutes in the plasma.

Quinone	Tissue	C _{max} (ng/ml or mg)	C _{max} (nM)	T _{max} (minutes)	Half life (minutes)
DMNQ	Heart	2.74	12.6	10	126
	Plasma	8.97	41.1	15	18
	Liver	9.75	44.7	10	51
	Brain	1.35	6.2	10	70
MNQ	Plasma	11.1	64.5	10	20
	Liver	3.31	19.2	20	24

Table 3.1: Summary of DMNQ and MNQ exposure following a single 25mg/kg dose in a mouse model.

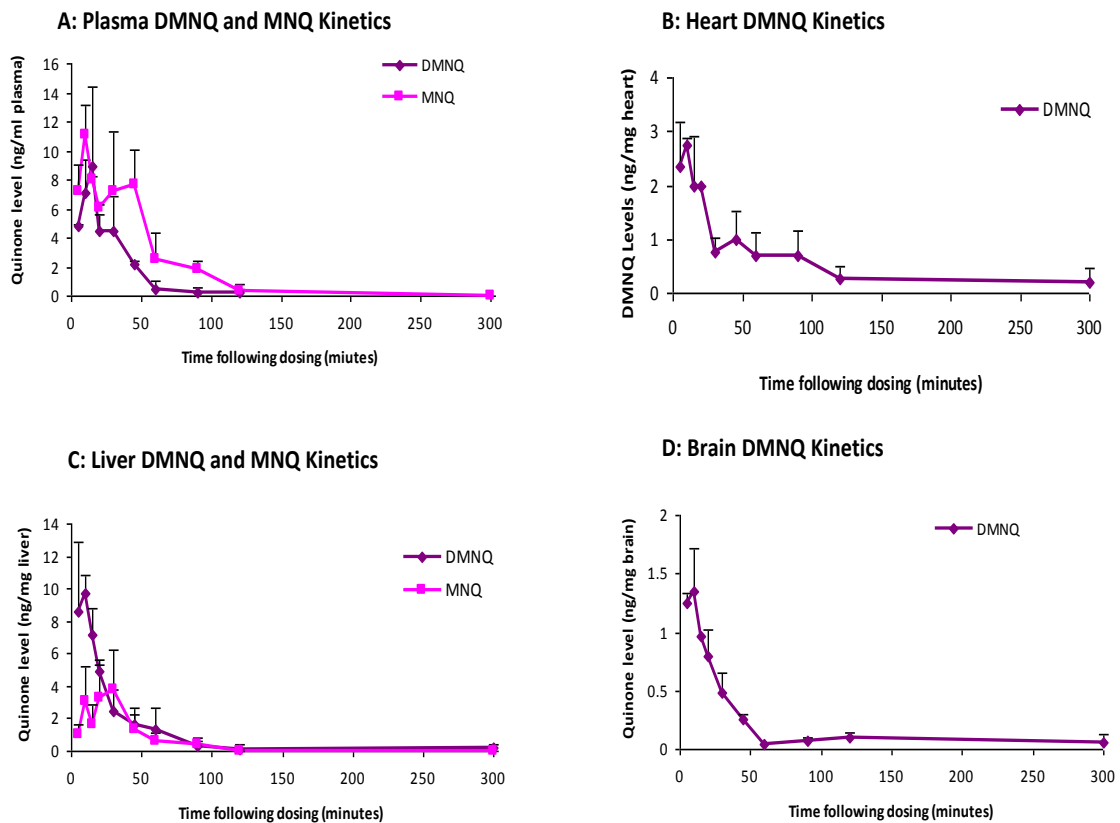


Figure 3.1: DMNQ and MNQ exposure kinetics in male C57BL/6J mice following a single dose of 25mg/kg in plasma (A), heart (B), liver (C) and brain (D). Mean quinone concentrations (n=3 ±S.D. apart from MNQ treated liver samples n=2 ±S.D.)

3.2.3 METABOLITE PROFILING

To investigate the metabolism of DMNQ *in vivo*, quadrupole linear ion trap mass spectrometry was used in conjunction with Dr. U. Lutz and Dr. W. Lutz as described in Parry et al. (2009); samples were supplied for this purpose. This allowed detection and characterisation of the metabolites in the urine 4 hours following a single 25mg/kg dose of DMNQ or arachis oil. Data obtained was compared using metabolite ID software, identifying a list of peaks present in DMNQ treated samples (Figure 3.2). These were further examined (Figure 3.2 A and B). The metabolism appeared to occur by two electron reduction to the dihydronaphthoquinone (H₂DMNQ) followed by conjugation of the hydroxyl groups prior to excretion in the urine (Figure 3.2A and B). Minor metabolites included sulphate-glucuronide double conjugates of H₂DMNQ and demethylation products at the methoxy group of DMNQ (Parry et al. 2009). Following metabolism in the liver, secretion into the bile is an important excretion route for acidic conjugates e.g.: GSH, however metabolic profiling of bile ducts revealed no conjugates of this nature following DMNQ treatment (Parry et al. 2009). The main route of elimination appeared to be via a renal route through the urine.

3.2.4 CARDIAC GSH/GSSG AND PLASMA CK-MB ACTIVITY

To investigate if a single dose of DMNQ resulted in a redox challenge to the heart, GSH and GSSG levels were measured (Section 2.10). No significant change in GSH or GSSG was apparent compared to control animals (Figure 3.3).

In order to examine if either DMNQ or MNQ resulted in cardiotoxicity CK-MB levels in plasma from animals treated with 25mg/kg DMNQ or 25 mg/kg MNQ were measured (Section 2.7). No significant change in plasma CK-MB levels occurred following MNQ, but DMNQ resulted in a significant ($p \leq 0.01$) increase in CK-MB levels throughout the time course, indicating the presence of cardiotoxicity (Figure 3.4).

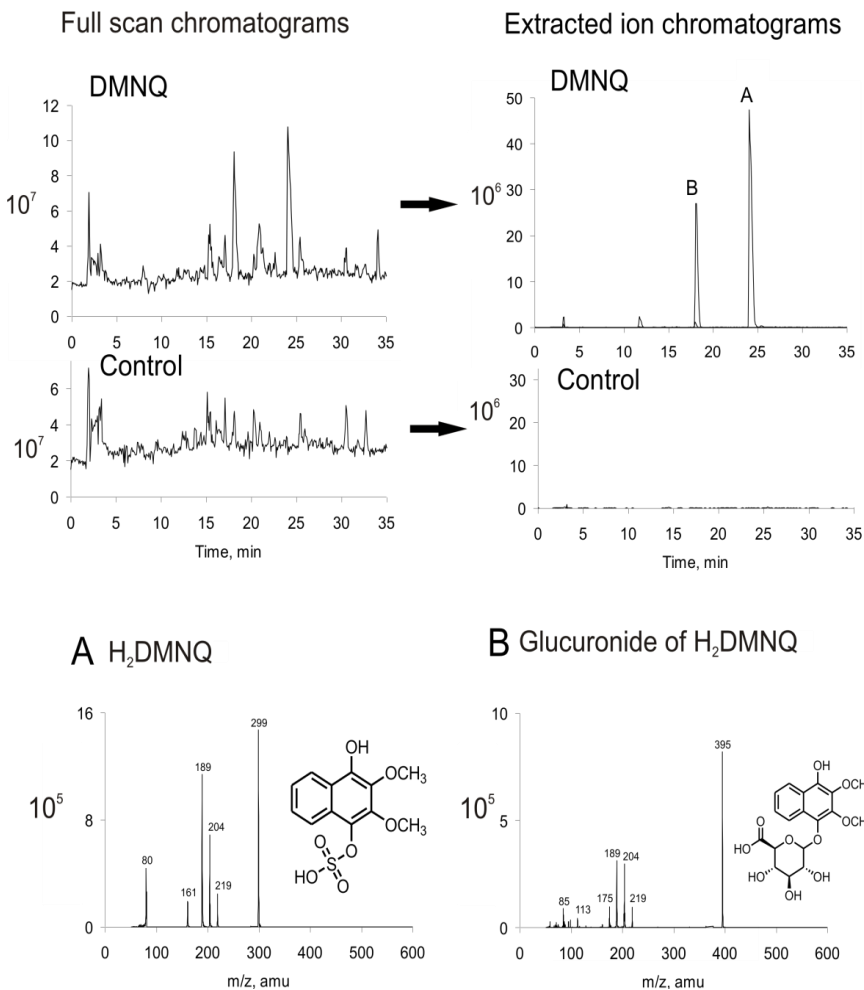
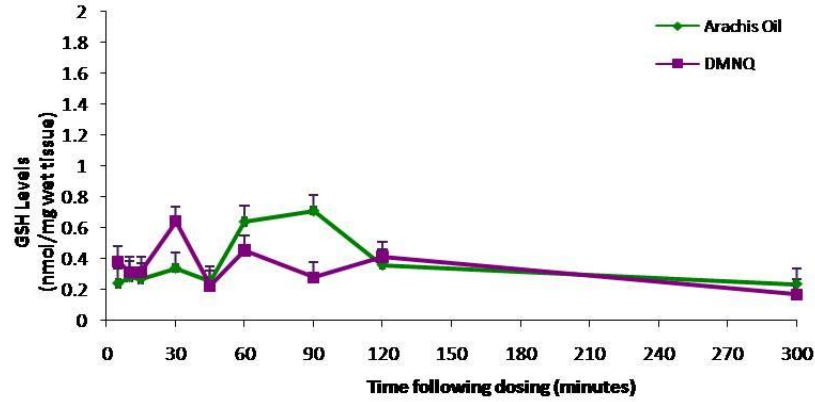


Figure 3.2: Urinary metabolite profiling, 4 hours following a single i.p. dose of 25mg/kg DMNQ or 10ml/kg arachis oil. This identified a number of peaks following DMNQ. The most prominent were (A) and (B). (A), showed characteristic fragments for a sulphate conjugate of the H₂DMNQ. (B) is the glucuronide of H₂DMNQ. Intensities of the signal (CPS) are shown on the vertical axis with the multiplication factor shown for each group. All experiments n=3. Adapted from Parry et al. (2009).

A



B

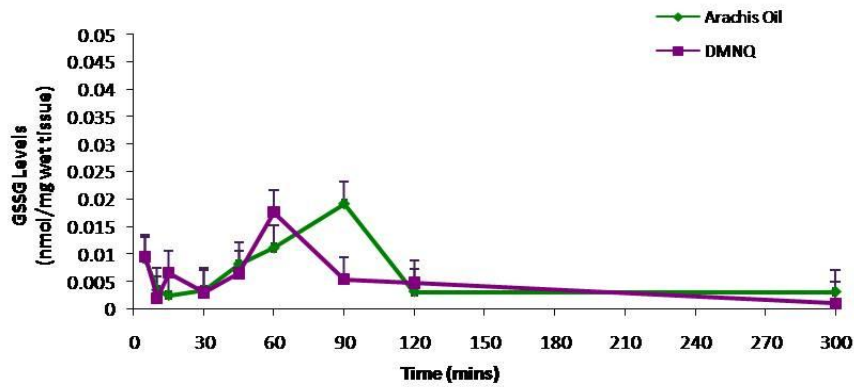


Figure 3.3: Cardiac GSH (A) and GSSG (B) levels following a single dose of 25mg/kg DMNQ in 10ml/kg arachis oil or 10ml/kg arachis oil. Results are means (n=3) \pm S.D.

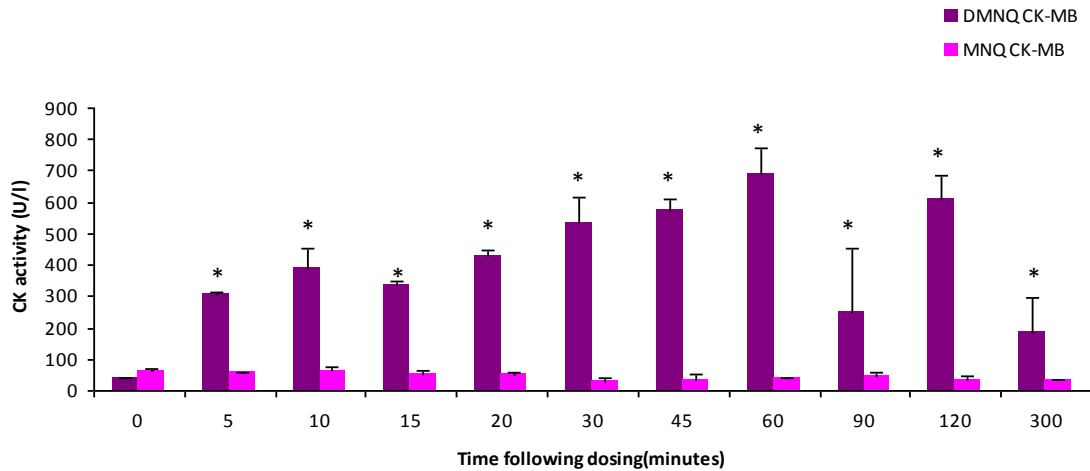


Figure 3.4: Plasma CK-MB levels following a single dose of 25mg/kg DMNQ or 25mg/kg MNQ. Results are means (n=3) \pm S.D. One way ANOVA and post-hoc Dunnett's T-test * $p \leq 0.01$.

3.2.5 CARDIAC TRANSCRIPTIONAL PROFILING

Cardiac transcriptional profiles following a single dose of 25mg/kg DMNQ or 25mg/kg MNQ were generated. Total RNA was extracted from cardiac tissue from mice sacrificed at 5, 10, 15, 20, 30 and 45 minutes and 1, 1.5, 2, and 5 hours following a single dose. Microarrays were conducted (Section 2.17) using cardiac RNA from arachis oil treated animals time matched against either 25mg/kg DMNQ or 25mg/kg MNQ cardiac RNA. Data was analysed as described in Chapter 1, MNQ did not produce any significant ($p \leq 0.05$) gene expression changes. Principal component analysis (PCA) was carried out to further identify shared mechanisms of action. PCA is a multivariate analysis allowing the identification of similarities and differences between different data sets. It groups data sets around 'principle components', hence the closer one data set is to another, the more alike the two data sets are (Chapter 1). PCA of transcriptional profiles following 25mg/kg DMNQ and 25mg/kg MNQ indicated three clusters, the first contained the early DMNQ time points, the second contained the later DMNQ time points and the third contained all the MNQ time points. This indicated a difference between the effects of DMNQ and MNQ on the heart (Figure 3.5), reflecting the different disruption of the two compounds. As MNQ is not systemically distributed to the heart and results in no change in CK-MB or cardiac transcription this compound was not further utilised.

3.2.6 DE NOVO DNA AND PROTEIN SYNTHESIS

The rate of DNA and protein synthesis was measured using thymidine and leucine incorporation, respectively, in HL-1 cells exposed to DMNQ and the anticancer agent doxorubicin, (Section 2.31) (Figure 3.6). Doxorubicin and DMNQ resulted in a dose dependent reduction in DNA and protein synthesis. However the reduction in DNA synthesis occurred at lower concentrations following doxorubicin.

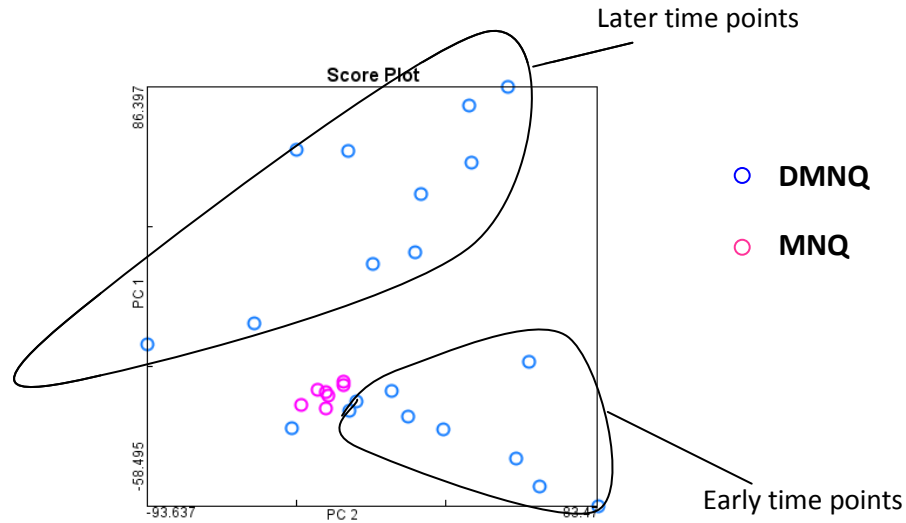


Figure 3.5: PCA of DMNQ (25mg/kg) and MNQ (25mg/kg). All genes on the microarray were included as MNQ resulted in no significant gene changes. Results are mean expression values (n=3).

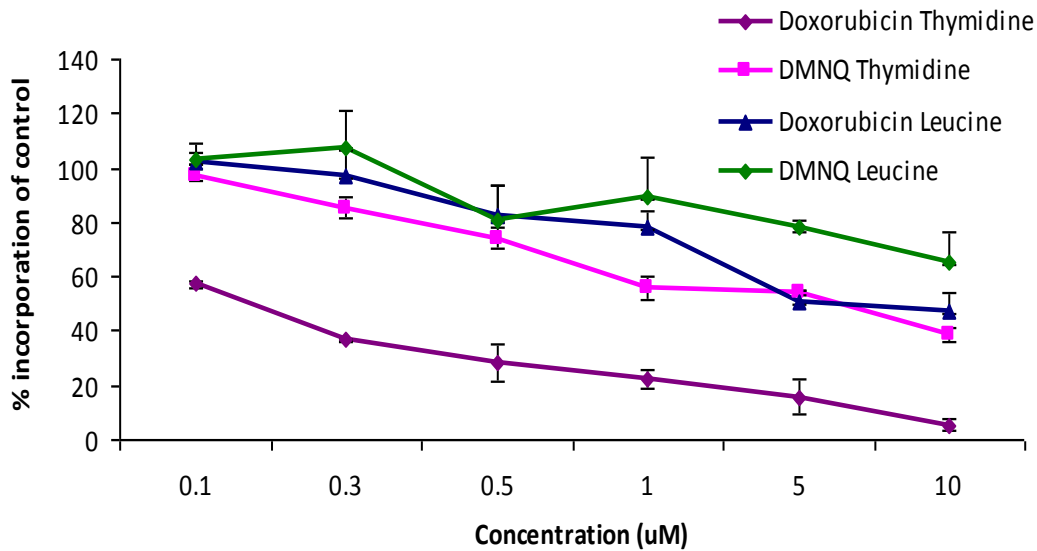


Figure 3.6: DNA and protein synthesis following DMNQ and doxorubicin exposure for 24 hours in HL-1 cells. Thymidine incorporation measures DNA synthesis and leucine incorporation measures protein synthesis. Results are means of n=3 ± S.D.

3.3 DISCUSSION

The overall aim of this study was to define the toxicokinetics and bio-distribution of DMNQ *in vivo* following a single dose and secondly to assess the suitability for use as a mimic of doxorubicin cardiotoxicity in male C57B6/AJ mice. As mentioned previously (Section 3.1) the majority of studies utilising DMNQ have been conducted *in vitro* and no data was present in the literature concerning DMNQ administration *in vivo*, prior to the publication of this study (Parry et al. 2009). The related naphthoquinone, MNQ however has been extensively used both *in vitro* and *in vivo*; despite this no toxicokinetic data was available in the public domain. MNQ was thus included in these studies to aid as a comparison for DMNQ and fill in the knowledge gap that appeared to exist. A dose of 25mg/kg i.p. in male C57B6/AJ mice was found to be close to the maximum tolerated dose with 100% lethality occurring at dose levels of 200mg/kg i.p. for both DMNQ (data not reported) and MNQ (Molitor and Robinson 1940). This was a surprise finding as MNQ appears to be one magnitude more cytotoxic *in vitro* (Gant et al. 1988). DMNQ was more widely distributed to all major organs tested including the heart and crossed the blood brain barrier, despite the plasma concentrations of the two compounds being comparable (Figure 3.1). The wider distribution of DMNQ was an unexpected finding as it was postulated that MNQ would have greater systemic distribution due to the difference in lipophilicity of DMNQ and MNQ. DMNQ has a partition coefficient ($\log P$) of 1.67 compared to 2.24 for MNQ (Buffinton et al. 1989; Hodnett et al. 1983), thus suggesting MNQ has greater lipophilic properties suggestive of better tissue distribution. The lack of MNQ distribution to the heart and brain was perhaps a consequence of MNQ's chemical reactivity with arylate soft nucleophiles (Bellomo et al. 1987; Ross et al. 1985). The formation of arylate soft nucleophilic-MNQ conjugates in tissue would reduce the amount of free MNQ measured in these assays. As DMNQ does not react with nucleophiles, levels of DMNQ were detectable until elimination from the organ, thus indicating possible retention of MNQ on macromolecules (Parry et al. 2009)

Metabolite profiling conducted in conjunction with this study identified that both DMNQ and MNQ were eliminated via a renal route (Figure 3.2). Metabolism occurred by two electron reduction to the

dihydronaphthoquinone of DMNQ and MNQ followed by conjugation of the hydroxyl groups prior to excretion in the urine (Parry et al. 2009). This result therefore supports the hypothesis of two electron reduction as a detoxification route. *Nqo1* knockout mice provide further evidence of this finding; they elicit increased sensitivity to naphthoquinones (Munday 2001; Radjendirane et al. 1998). The lack of significant changes in GSH or GSSG activity in the heart following DMNQ indicates that the heart is not the site of redox activity *in vivo* (Figure 3.3). However GSSG levels in liver from the same study indicated a transient increase but no change in GSH suggesting the liver to be the site of redox activity *in vivo* (Parry et al. 2009). This effect on the liver was not studied further as the dose of 25mg/kg was close to the maximum tolerated, thus it was not possible to saturate the reduction or conjugation routes and observe the effects on redox activity.

To investigate if a single dose of 25mg/kg DMNQ was cardiotoxic CK-MB levels in plasma from treated animals was measured. This indicated the activation of acute cardiotoxicity from 5 minutes following dosing; levels remained elevated 300 minutes following a single dose suggesting the development of profound cardiac dysfunction (Figure 3.4). In order to investigate the effects of DMNQ and MNQ on the heart further transcriptional microarray analysis was also conducted. No significant changes in gene expression were observed following MNQ administration, thus reinforcing the pharmacokinetic data. DMNQ resulted in significant ($p \leq 0.05$) differential gene expression in 4766 genes throughout the time course from 5 to 300 minutes. PCA was conducted to investigate the similarities and differences between the gene expression profiles following DMNQ and MNQ, this resulted in a distinction between DMNQ and MNQ, again further confirming the difference between the two compounds (Figure 3.5).

As DMNQ appears to be distributed to the heart and results in elevated CK-MB levels and differential cardiac gene transcription it is suggestive that DMNQ impacts on the heart. These results indicate the possibility of DMNQ's utility to mimic doxorubicin's cardiotoxic effects possibly allowing greater insight into the pharmacological and toxicological actions of doxorubicin.

3.3.1 SUMMARY

These studies have established the pharmacokinetics of DMNQ and MNQ in a mouse model. The wider tissue distribution of DMNQ to the heart, coupled with increased CK-MB levels, a marker of cardiotoxicity and cardiac differential transcription profiles suggests DMNQ to be a suitable model compound to allow a greater insight into doxorubicin's cardiotoxicity.

Chapter 4: Evaluation of the Relative Cardiotoxicity of Doxorubicin and DMNQ in a Mouse Model

4.1 INTRODUCTION

Doxorubicin is a broad spectrum anticancer agent used in the treatment of blood and solid tumours (Weiss 1992). In spite of being first used over 30 years ago it is still considered as a first line anti-cancer treatment (Outomuro et al. 2007). Its pharmacological activities result from doxorubicin being a highly effective DNA synthesis inhibitor through its inhibition of topoisomerase II, (Fornari et al. 1994) and promotion of DNA doxorubicin adducts initiating RNA inhibition (Swift et al. 2006). Despite doxorubicin's important anticancer pharmacology, the clinical value of this chemotherapeutic agent is severely jeopardized by cumulative and irreversible dose dependent cardiotoxicity. The significance of this cardiotoxicity is becoming increasingly evident as the survival rate of cancer patients increases. However the widespread use is likely to continue until effective and safer alternatives have been identified (Horan et al. 2006).

Both acute and chronic cardiomyopathies occur following doxorubicin, from days to years following the cessation of treatment (Belham et al. 2007). The major risk factor affecting occurrence is the total cumulative dose received. Retrospective analysis reveals that dose levels above $550\text{mg}/\text{m}^2$ result in a significant elevation in the occurrence of cardiotoxicity. The incidence of cardiotoxicity increases by 18% when patients receive a cumulative dose of between $551\text{-}600\text{mg}/\text{m}^2$, and about 36% at doses of $601\text{mg}/\text{m}^2$ and higher, with an overall mortality rate of over 50% (Takemura and Fujiwara 2007). Other risk factors that appear to affect the development of cardiotoxicity are age (young and old at greater risk), history of cardiac disease, previous cancer therapies (e.g.: radiation) and the chemotherapy regimen (e.g.: co-administration with trastuzumab attenuates the cardiotoxicity) (Outomuro et al. 2007). Cardiotoxicity, however, does occur also in patients with no predisposing risk factors (Horan et al. 2006; Thorburn and Frankel 2006). The mechanism of the cardiotoxicity resulting from doxorubicin has not been conclusively determined despite over 30 years of research. However, the mechanism responsible is thought to be separate from the pharmacological activity, raising the possibility of designing treatment options that reduce the severity and occurrence of toxicity without affecting tumour efficiency (Takemura and Fujiwara 2007). The majority of hypothesised

mechanisms for cardiotoxicity have an element of redox stress and production of ROS, which result in effects on lipids, nucleic acids and protein macromolecules, altering gene transcription (Section 1.4.4).

4.1.1 PLAN OF INVESTIGATION

In order to investigate the role of redox cycling in doxorubicin toxicity, a novel quinone 2, 3-dimethoxy-1, 4-naphthoquinone (DMNQ) was utilised (Figure 4.1). The pharmacokinetics of DMNQ *in vivo* were recorded in Chapter 3. The purpose of using DMNQ was to isolate the redox properties of doxorubicin from the pharmacological effects, allowing the cardiotoxicity of doxorubicin to be separated from its pharmacological action, by comparing common changes. Before mechanistic characterisation of the resultant cardiotoxicity could be carried out, acute and chronic models of doxorubicin toxicity and its potential mimic DMNQ, needed to be established and quantification of any cardiac damage evaluated.

As cardiac hypertrophy and end-stage heart failure are known to affect the whole heart, mouse models were established of doxorubicin cardiotoxicity and DMNQ, to ensure the dynamic interactions that occur *in vivo* are not diminished allowing a 3-dimensional study of cardiotoxicity (Molkentin and Robbins 2009). As doxorubicin cardiotoxicity can occur both acutely and chronically, two models were established. The acute model of toxicity allowed an in depth analysis of the cardiotoxicity and the mechanism responsible, before gross morphological alterations became detectable and quantifiable (Robert 2007). The hypothesis to be tested was that this would allow the mechanism of toxicity to be identified, prior to the occurrence of gross cytotoxicity. A chronic model of both doxorubicin and DMNQ was also established. Recent evidence suggests that it is the overall dose of doxorubicin received, not the time over which it is administered that is most important to the development of cardiotoxicity (Danesi et al. 2002). It is also thought that any protective benefit of lowering doxorubicin doses to be given over a period of weeks is offset by the occurrence of damage occurring due to the longer exposure of cardiomyocytes to doxorubicin (Minotti et al. 2004). Thus, indicating that an acute model of doxorubicin cardiotoxicity can mirror the toxicity that occurs at all time points following treatment.

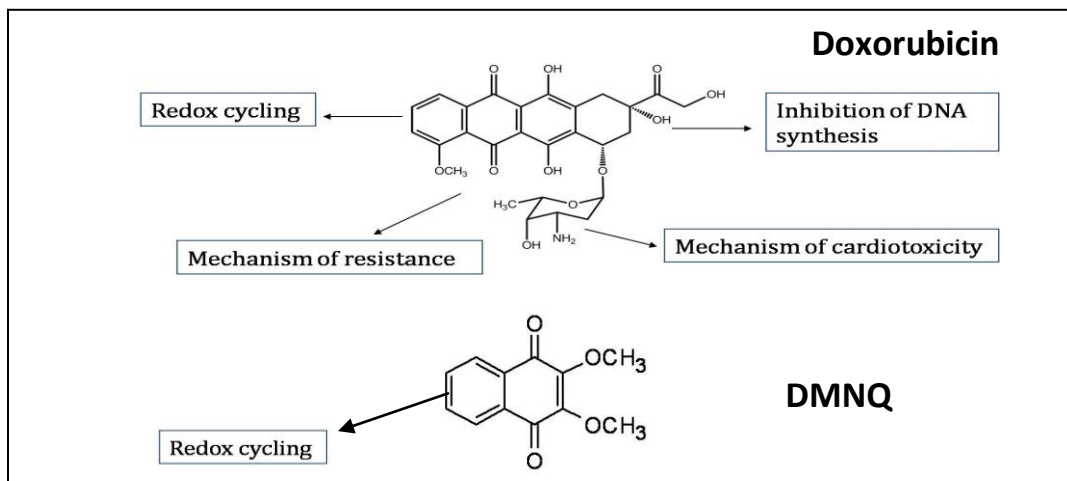


Figure 4.1: Structure of doxorubicin and DMNQ with their associated chemical properties. Doxorubicin has a range of known chemical properties, it is able to inhibit DNA synthesis, redox cycle and cause both cardiotoxicity and resistance. However DMNQ is much simpler and currently is only known to redox cycle.

Before measurement of cardiac dysfunction can be assessed suitable dose levels need to be established where the overall level of toxicity in the animal is minimal allowing specific cardiotoxicity to be mechanistically characterised.

4.1.2 HYPOTHESIS AND AIMS

It was hypothesised that the pharmacological and toxicological properties of doxorubicin are distinguishable, allowing the use of a simpler quinone, DMNQ to provide a novel insight into the associated cardiotoxicity. The overall aim of this study was to define the cardiac effects following a single i.p. dose of doxorubicin or DMNQ, or following chronic dosing of both compounds in male C57BL/6J mice and the progression to the cardiotoxic state.

4.2 EXPERIMENTAL DESIGN

Dose response experiments were carried out to select suitable concentrations of each compound, in an acute and chronic model (Figure 4.2) of toxicity in C57B6/AJ mice. At the point of sacrifice organ and body weight were recorded and plasma CK-MB levels were assayed. To assist in the selection of dose levels transcriptional gene expression profiling was conducted. Liver to body weight ratios of above 5% were deemed to result in a state of gross toxicity. In a model of known hepatic injury, a liver to body weight ratio of 10% resulted in gross hepatic toxicity both morphologically and transcriptionally (Davies et al. 2005). As a result, a cut off of 5% (liver:body weight) was deemed to result in minimal hepatic toxicity. Cytotoxic effects were evaluated over a broad range of dose levels. Once specific dose levels were selected cardiac damage was characterised.

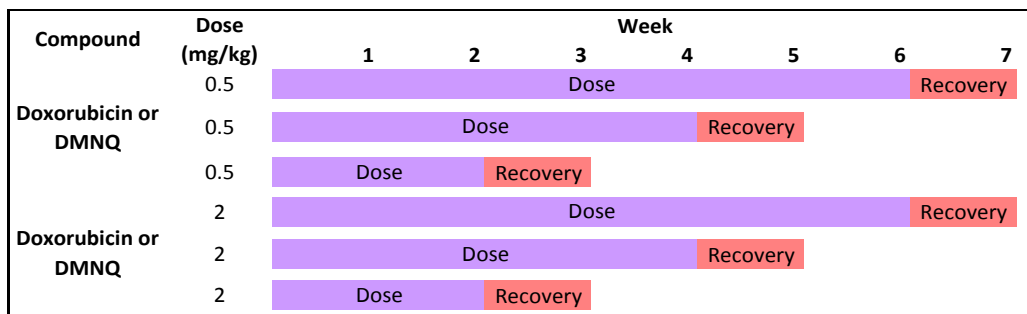


Figure 4.2: Schematic diagram of the experimental design of the chronic models of dosing.

4.3 RESULTS

4.3.1 DOSE RESPONSE EXPERIMENTS

Dose response experiments were carried out in order to identify the maximum acceptable dose i.p. of doxorubicin and DMNQ over an acute and chronic time course. Literature was consulted to guide appropriate dose levels for doxorubicin treatment (Yi et al. 2006; Delgado et al. 2004; Forrest et al. 2000; Kang et al. 1997). A preliminary dose response experiment using doxorubicin was carried out in order to gain an insight into the appropriate dose level (Table 4.1). Post dosing animals were observed for any signs of gross toxicity, observations were recorded (Table 4.2). A dose of 75mg/kg resulted in mortality at 24 hours

post dosing. At the point of sacrifice body, heart, liver and kidney weights were measured (Table 4.2) and the corresponding organ to body weight ratio calculated (Table 4.3). This indicated a substantial increase in heart weight to body weight 48 hours following a single dose at 15, 25 and 50 mg/kg, but increases in liver (above 5% total body weight) and kidney (above 1.5% total body weight) to body weight were also observed 48 hours following dosing at 25 and 50 mg/kg indicating gross toxicity to the animal. These dose levels are therefore unsuitable for further genomic investigation, as the gross toxicity may mask the underlining mechanisms predisposing to the cardiotoxic phenotype.

Compound	Model of Toxicity	Dose Level (mg/kg)	Time Point of Sacrifice
Doxorubicin	Acute	0, 15, 25, 50 and 75	48 hours

Table 4.1: Selected dose levels and time points used in doxorubicin first dose response.

Dose (mg/kg)	Weight at point of sacrifice				Observations
	Weight (g)	Heart weight (g)	Liver weight (g)	Kidney weight (g)	
0	25.9	0.14	1.2	0.31	Healthy
15	22.6	0.16	1.1	0.3	Isolated immediately after dosing resolved within 1 hour
25	29	0.21	1.57	0.45	Hunched and isolated
50	26	0.19	1.45	0.41	Limping, hunched and isolated
75	-	-	-	-	Mortality 24 hours following dosing

Table 4.2: Doxorubicin first dose response, body, heart, liver and kidney weight at the point of sacrifice.

Signs of gross toxicity were observed with an i.p. dose of 25 and 50 mg/kg doxorubicin. Results are means of n=2, except the 75mg/kg dose (n=1).

Dose (mg/kg)	Heart:body weight ratio (%)	Liver:body weight ratio (%)	Kidney:body weight ratio (%)
0	0.54	4.63	1.19
15	0.71	4.87	1.32
25	0.72	5.41	1.55
50	0.73	5.58	1.57

Table 4.3: Calculated organ to body weight ratios 48 hours following a single dose of doxorubicin. A dose of 15mg/kg appears to affect the heart but only minimally affect the liver and kidney indicating specific cardiac toxicity and not gross toxicity as appears to occur at doses above this level. Results are means of n=3.

A second dose response experiment over 120 hours for an acute model, and over 7 weeks for a chronic model was conducted; selected dose levels for both DMNQ and doxorubicin are illustrated in Table 4.4. The maximum dose level of DMNQ used was that found to be just below the threshold for overt toxicity in Chapter 3. In order to assess toxicity, heart, liver and kidney weights were measured (Figure 4.3). A dose dependent increase in heart :body weight was observed throughout the time course following both doxorubicin and DMNQ. Additionally the liver and kidney weights remained constant, indicating a lack of gross cytotoxicity. CK-MB activity (Figure 4.4) was assessed in duplicate animals using the method outlined in section 2.7. Again a dose dependent increase in activity was observed following both doxorubicin and DMNQ. Transcriptional profiling was also conducted to assess the genomic impact at the selected doses.

Compound	Model of Toxicity	Dose Level (mg/kg)	Time Point of Sacrifice
Doxorubicin	Acute	0, 2.5, 5, 7.5, 10, 15	120 hours
DMNQ	Acute	0, 2.5, 5, 7.5, 10, 20, 25	120 hours
Doxorubicin	Chronic	0, 0.5, 2 (per week)	Week 3, 5, and 7
DMNQ	Chronic	0, 0.5, 2 (per week)	Week 3, 5, and 7

Table 4.4: Selected dose levels and time points used to select dose levels for mechanic characterisation.

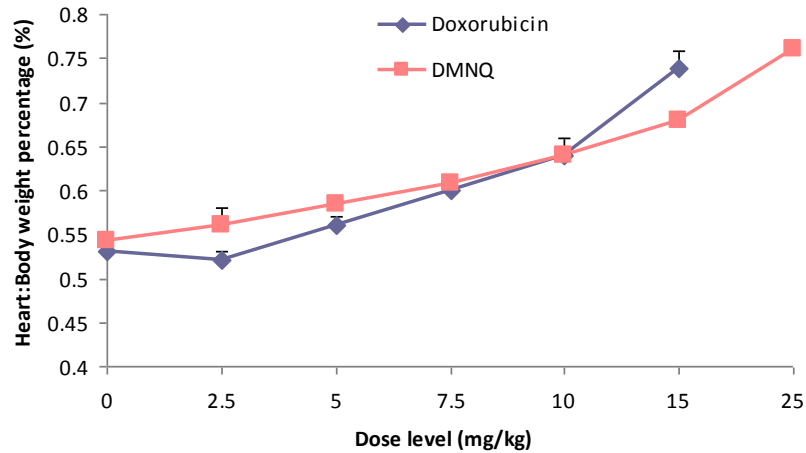
Transcriptional Profiles

In order to aid in the selection of dose levels, transcriptional profiles were generated 120 hours following a single dose in an acute model and 3, 5, and 7 weeks following the start of dosing in a chronic model. Cardiac RNA was isolated following acute and chronic treatment with doxorubicin and DMNQ and subjected to two colour microarray analyses (Section 2.16). Data generated was subjected to global normalization and filtering ($\text{Log}_2 \leq 1.5$ or $\text{Log}_2 \geq 1.5$) in order to calculate the number of genes up and down-regulated in expression as described in Chapter 1 (Figure 4.5). An increase in the number of genes differentially expressed is observed with increasing doses in all models of toxicity, suggestive of increasing damage. Interestingly, acute and chronic doxorubicin and chronic DMNQ treatment resulted in a greater proportion of genes decreased in expression.

A

Compound	Dose (mg/kg)	Heart:body weight ratio (%)	Liver:body weight ratio (%)	Kidney:body weight ratio (%)
Doxorubicin	0	0.53	4.49	1.35
	2.5	0.52	4.8	1.64
	5	0.56	4.68	1.76
	7.5	0.6	4.88	1.4
	10	0.64	4	1.52
	15	0.74	4.78	1.82
DMNQ	0	0.54	4.79	1.63
	2.5	0.56	4.69	1.47
	5	0.58	4.92	1.28
	7.5	0.6	4.75	1.25
	10	0.64	4.4	1.44
	15	0.68	4.84	1.32
	25	0.76	4.75	1.49

B



C

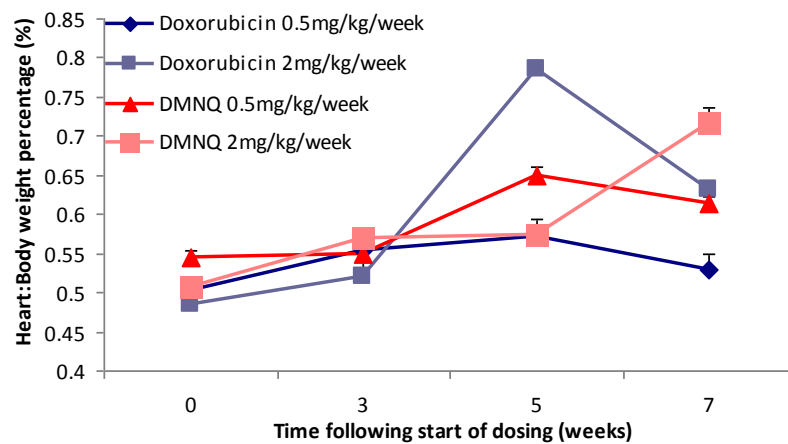
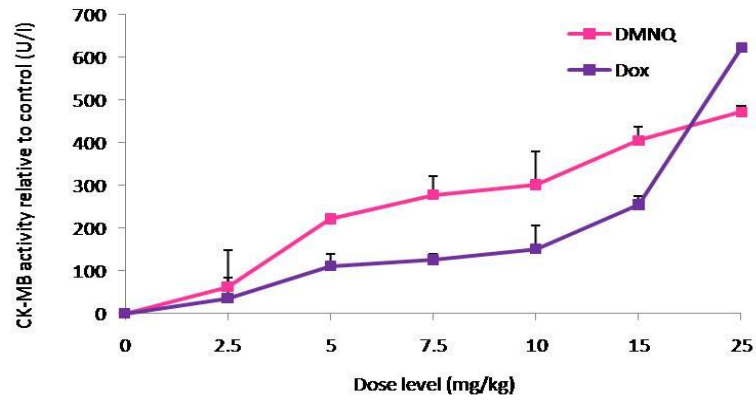


Figure 4.3: Dose response organ:body weight ratios *in vivo*, in response to doxorubicin or DMNQ in an acute model 120 hours following a single dose (A) and graphical representation of the Heart:Body weight ratio in an acute (B) and chronic model (C) of toxicity. A dose of 15mg/kg doxorubicin and 25mg/kg DMNQ in an acute model and 2mg/kg in a chronic model appears to affect the heart but only minimally affect the liver and kidney indicating specific cardiotoxicity (n=3).

A



B

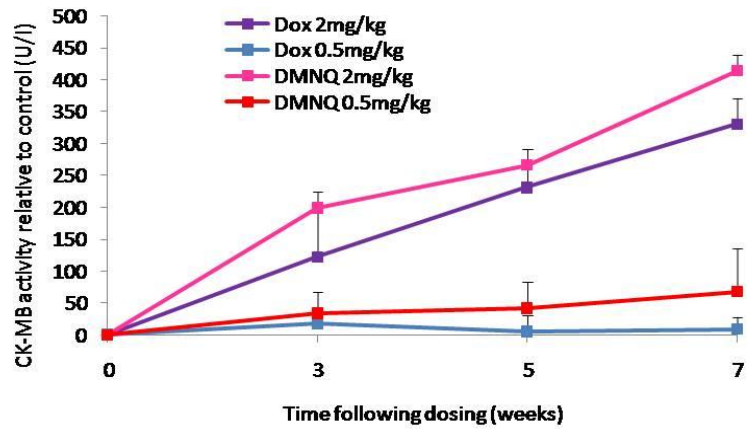


Figure 4.4: Creatine kinase muscle/brain (CK-MB) activity during dose response experiments, in response to doxorubicin or DMNQ in an acute (A) and chronic model (B) of toxicity. Results are means, $n=2 \pm$ S.D.

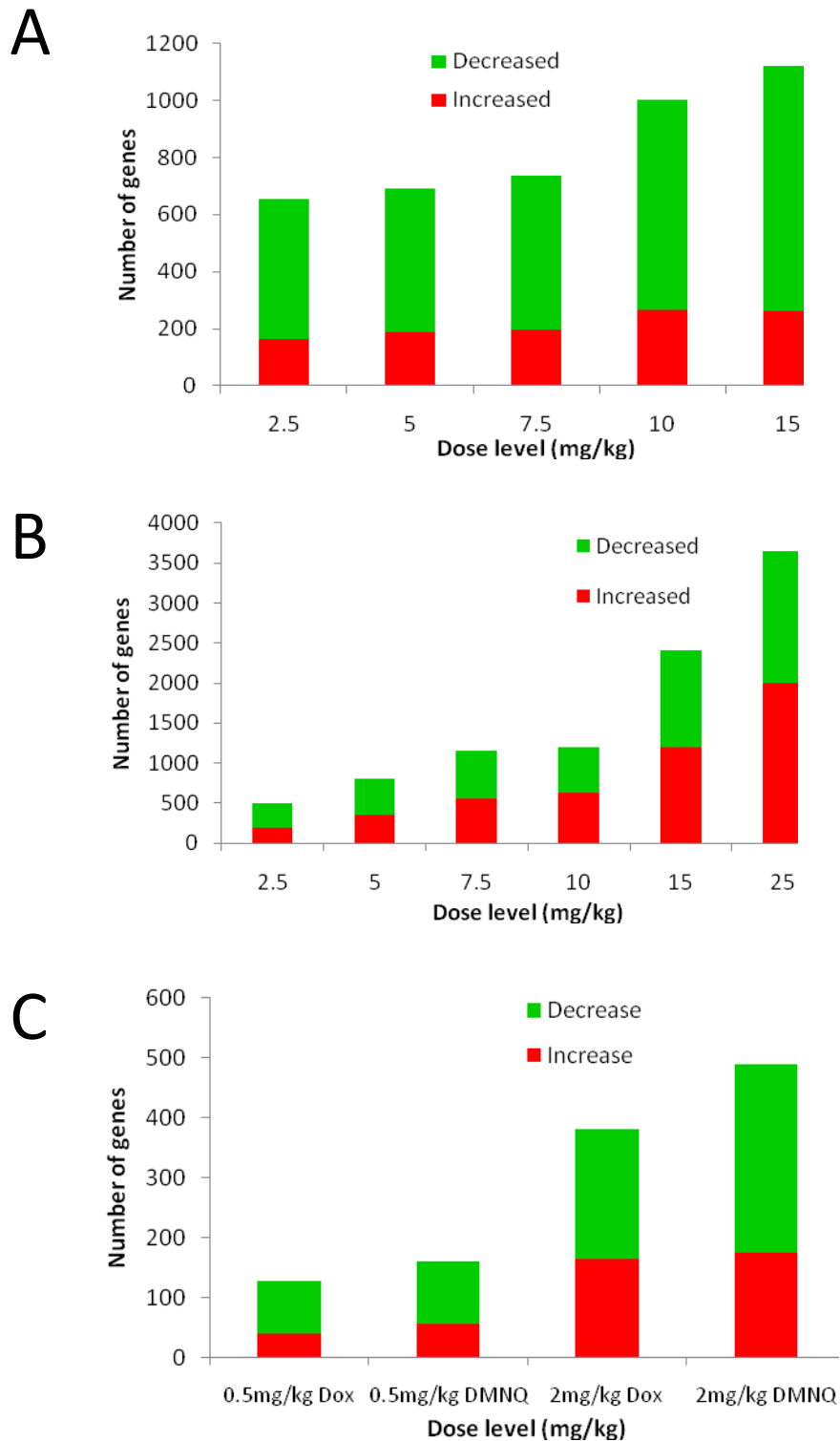


Figure 4.5: Number of genes significantly differentially expressed during dose response experiments, by $\text{Log}_2 \leq 1.5$ or $\text{Log}_2 \geq 1.5$ following acute doxorubicin (A) and acute DMNQ (B) at 120 hours following a single dose and chronic DMNQ and doxorubicin (C) 7 weeks after the start of dosing. Results are means of reverse labeling $n=1$.

A dose level of 15mg/kg doxorubicin in 10ml/kg saline i.p. and 25 mg/kg DMNQ in 10ml/kg arachis oil i.p. were selected to mimic an acute model of toxicity and 2mg/kg/week of doxorubicin or DMNQ i.p. were selected to mimic a chronic model of toxicity. Dose levels above the selected, either resulted in substantial gross toxicity in this study or had been previously reported (Table 4.5). At these selected dose levels via this dosing route in C57B6/AJ mice in an acute model the overall level of toxicity was minimal allowing genetic mechanistic characterisation to take place without overtly elevated levels of toxicity in the whole animal.

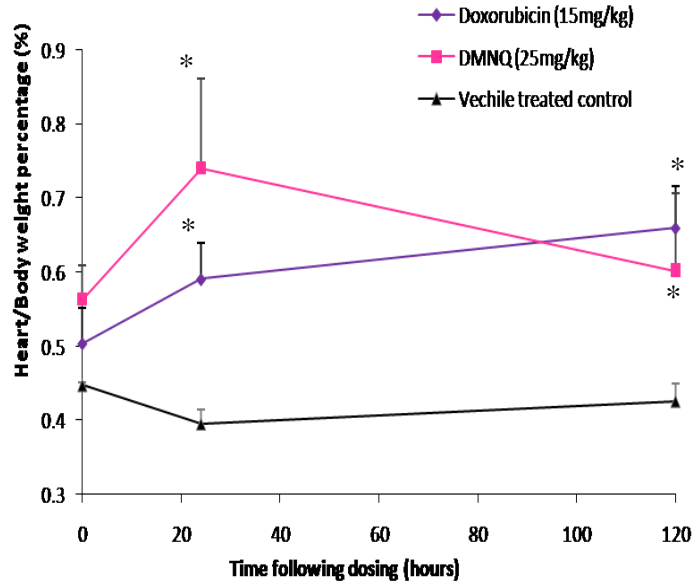
Compound	Model of Toxicity	Dose Level	Time Point of Sacrifice
Doxorubicin	Acute	15mg/kg	0.5, 1, 2, 12, 24 and 120 hours
DMNQ	Acute	25mg/kg	5, 10, 15, 20, 30 minutes and 1, 2, 5, 12, 24, 120 hours
Doxorubicin	Chronic	2mg/kg/wk	3, 5 and 7 weeks
DMNQ	Chronic	2mg/kg/wk	3, 5 and 7 weeks

Table 4.5: The concentration of compounds and point of sacrifice used for all further work.

4.3.2 BODY MASS TO HEART MASS RATIOS

As an overall measure of the health of the animal and a crude measure of cardiac damage, mouse body and heart weights were measured at the point of sacrifice. Heart:Body weight ratios increased ($p \leq 0.01$) following both compounds indicating an effect on the overall health of the animal, in particularly the heart (Figure 4.6). In an acute model of toxicity a significant ($p \leq 0.01$) elevation in Heart:Body weight was apparent from 0.5 hours following a single dose of doxorubicin or DMNQ. This elevation above control levels was still apparent 120 hours following dosing, indicating an acute prolonged effect on the heart following a single dose of either compound. In a chronic model of toxicity again a significant ($p \leq 0.05$) increase in Heart:Body weight was recorded from week 5 to week 7 following the start of dosing, indicating that both compounds affected the heart.

A



B

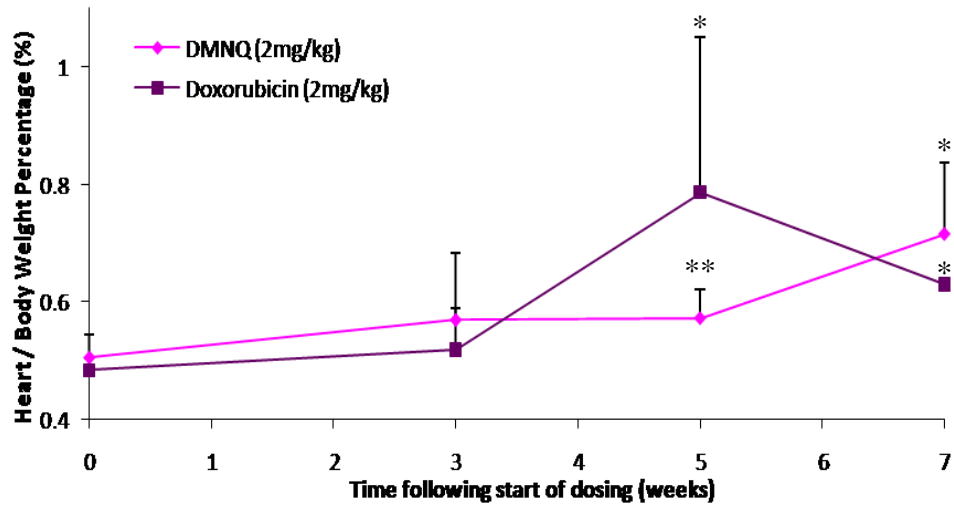


Figure 4.6: Heart:Body weight ratios in an acute (A) (n=4) and chronic (B) (n=3) model of toxicity. Results are a mean \pm S.D., one way ANOVA and post-hoc Dunnett's T-test * $p \leq 0.01$, ** $p \leq 0.05$.

4.3.3 BIOCHEMICAL ENDPOINTS

Creatine kinase muscle/brain (CK-MB), troponin I (cTnI) and aspartate aminotransferase (AST) were determined in plasma from treated animals as described in sections 2.7, 2.8 and 2.9, respectively. CK-MB and cTnI, both markers of cardiac damage were elevated. The brain (BB), skeletal muscle (MM) and cardiac (MB) isoforms of creatine kinase (CK) were determined in the plasma from doxorubicin and DMNQ (acute and chronic) treated animals. CK-MB isoform was increased following acute (Figure 4.7) and chronic (Figure 4.8) treatment. Both acute doxorubicin (15mg/kg) and DMNQ (25mg/kg) caused an elevation in the MB isoform of about 6 fold (Figure 4.7) within 5 minutes of administration with a maximum at 0.5 to 1 hour of more than 10 fold over control. This elevation was still apparent 120 hours following a single dose ($p \leq 0.01$). Chronic doxorubicin and DMNQ (2mg/kg/wk) treatment resulted in a significant ($p \leq 0.01$) cumulative increase in CK-MB with time. All assay data were further confirmed by native protein gels, indicating elevated levels of CK-MB following acute DMNQ and acute and chronic doxorubicin. However some of the increase in CK-MB measurement following chronic DMNQ treatment (2mg/kg/wk) was likely to be a result of elevated B subunit only, as confirmed by native protein gels. In all models of toxicity a slight elevation in the CK-BB isoform was also identified. Measurement of CK-MB overall indicated a significant effect on cardiac muscle.

Troponin I levels were significantly ($p \leq 0.01$) raised 0.5 hours following acute dosing of both doxorubicin and DMNQ and were continually elevated at 120 hours (Figure 4.9). Chronic doxorubicin treatment resulted in elevation of cTnI of 3 fold over control from week 3 to week 7 following the start of dosing. This along with elevated CK-MB levels indicated that both compounds were having a rapid and prolonged effect on the heart resulting in cardiotoxicity. AST levels were also measured following acute and chronic doxorubicin and DMNQ exposure. AST is abundantly distributed in a range of tissues including the heart, liver and kidneys; hence is an unspecific marker of cardiotoxicity (Figure 4.10). Elevated levels above control were observed following acute doxorubicin and chronic DMNQ treatment. Acute doxorubicin treatment resulted in peak AST levels one hour following dosing ($p \leq 0.01$), which is in co-ordination with peak troponin I and CK-MB activity. AST

levels were still elevated at 120 hours ($p \leq 0.05$). Following chronic DMNQ (2mg/kg/wk) AST activity peaked at week 5 following dosing ($p \leq 0.01$). However, this was reversed by week 7 of the entire dosing period, resulting in decreased AST activity ($p \leq 0.01$). Chronic doxorubicin resulted in a marked decrease in the level of AST ($p \leq 0.01$) throughout the time course. The biological consequence of decreased AST activity is unknown. Acute DMNQ resulted in no significant change. These altered AST levels may reflect hepatic, nephronic or cardiotoxicity.

4.3.4 CELLULAR IMAGING

Electron microscopy was conducted on fixed tissue 24 hours following a single dose of 15mg/kg doxorubicin or 25mg/kg DMNQ by Dr. David Dinsdale at the MRC Toxicology Unit. This analysis revealed swelling, a lucent matrix and collapse of the inner membrane in the mitochondria in cardiac tissue (Figure 4.11). The outer mitochondrial membrane remained intact.

In order to directly investigate the cardiac damage resulting from acute treatment with DMNQ (25mg/kg) the ventricular width was measured. Cross sectional sections were cut in a serial step manner and the ventricular width was measured at three separate locations using Axiovision software as described in section 2.13 (Figure 4.12). Increased ventricular width was observed, peaking 10 minutes following DMNQ (25mg/kg) (Figure 4.12C).

This clinical chemistry and physiological data indicated that both acute doxorubicin and DMNQ resulted in cardiotoxicity and electron microscopy implicated the mitochondria as a key target for these compounds.

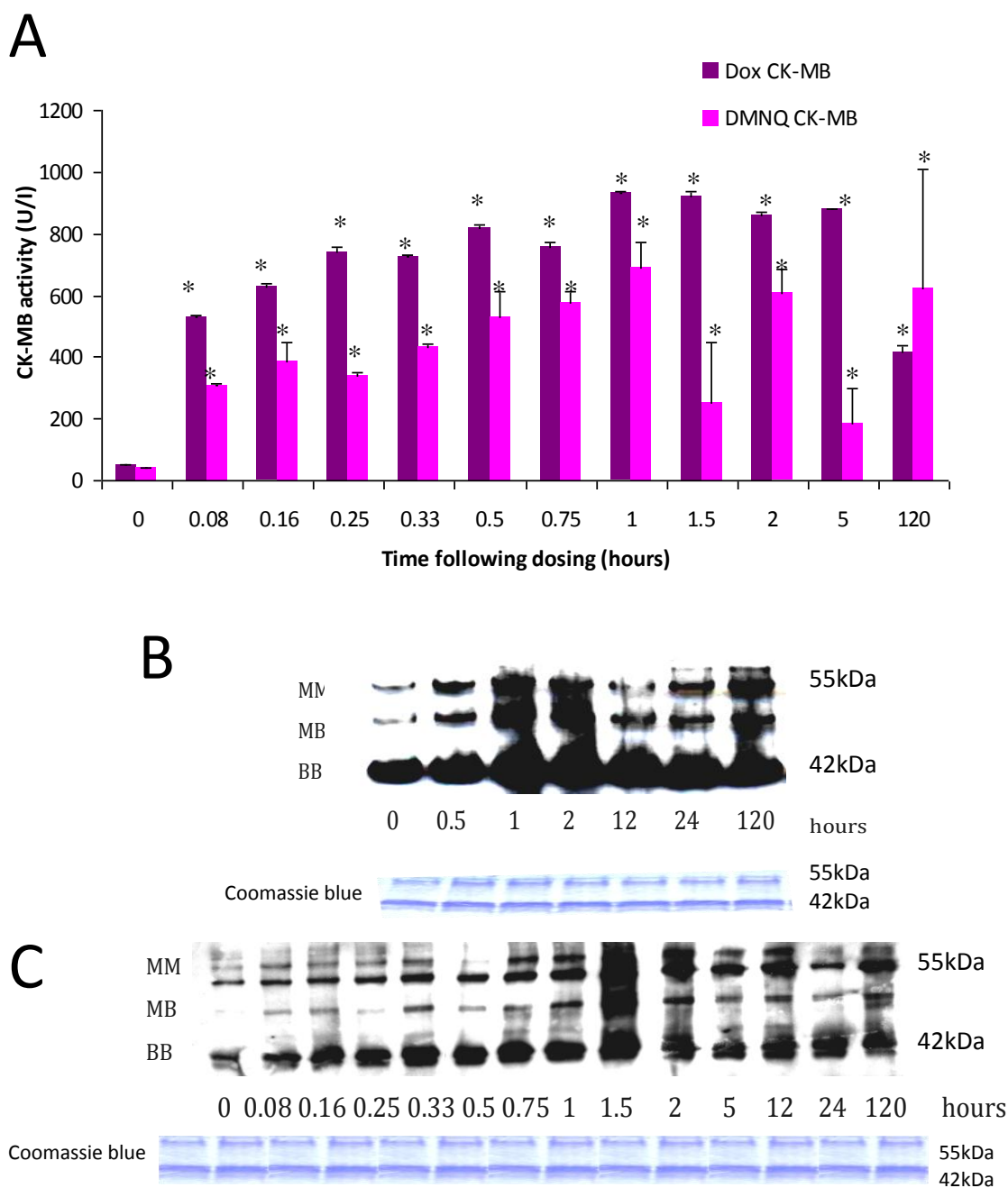


Figure 4.7: Acute creatine kinase measurement. CK-MB activity determined from plasma from treated animals using an antibody inhibition assay of the M form (A), any change reported using this assay could potentially be a result of an increase in the MB or BB form of creatine kinase. Native protein gels following doxorubicin (15mg/kg) (B), or DMNQ (25mg/kg) (C) were probed with an antibody against CK. These were carried out to confirm the assay data, again indicating an increase in CK-MB isoform throughout the time course. Coomassie blue stained gels indicate equal protein loading (n=4 \pm S.D.). One way ANOVA and post-hoc Dunnett's T-test * $p \leq 0.01$ at all time points

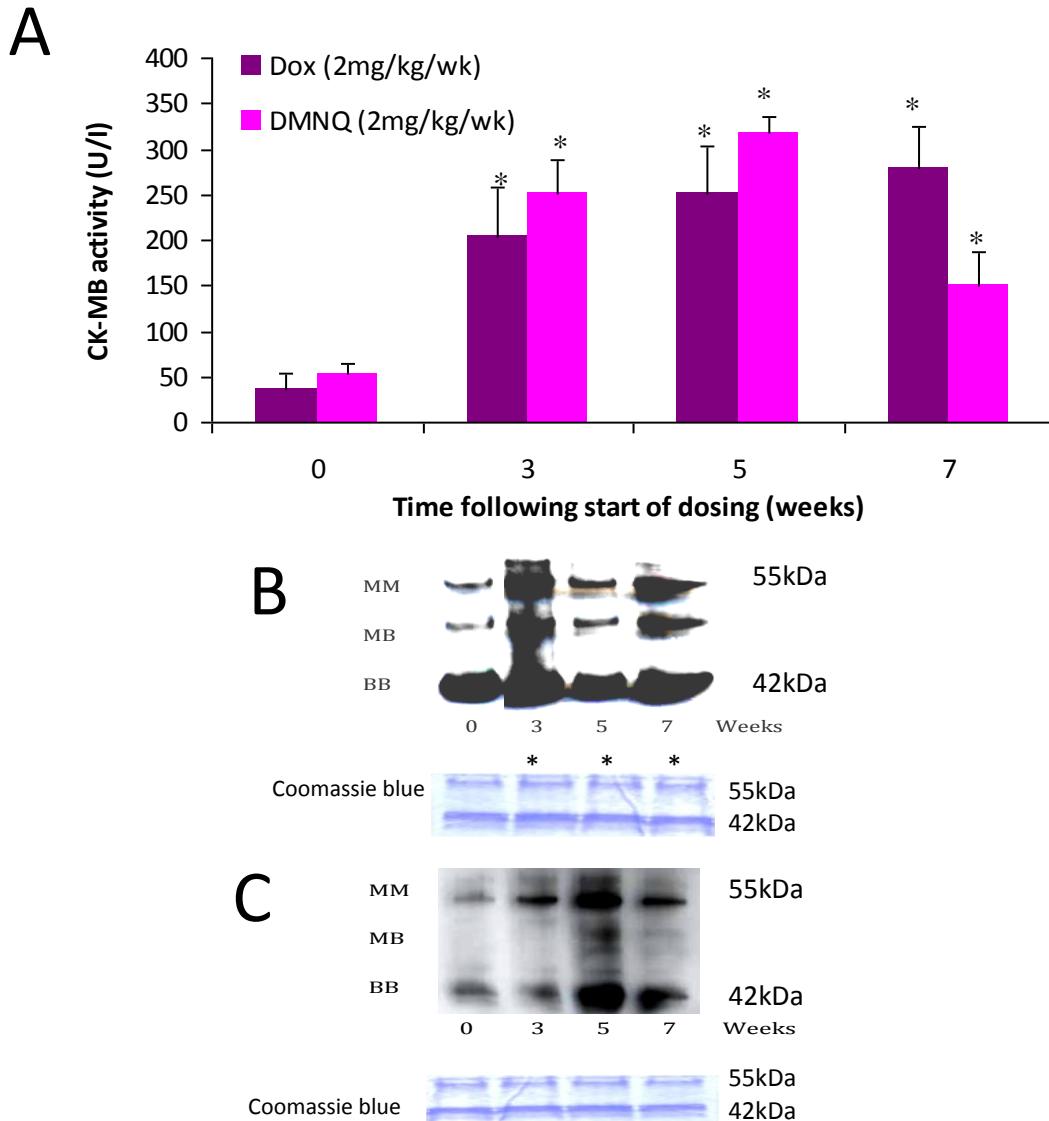


Figure 4.8: Chronic creatine kinase measurement. CK-MB activity determined from plasma from treated animals using an antibody inhibition assay of the M form (A), any change reported using this assay could potentially be a result of an increase in the MB or BB form of creatine kinase. Native protein gels following doxorubicin (2mg/kg/wk) (B), or DMNQ (2mg/kg/wk) (C) were probed with an antibody against CK, to confirm the assay data, again indicating an increase in CK-MB isoform throughout the time course. Coomassie blue stained gels indicate equal protein loading. CK-MB levels increase in a time/cumulative dose manner following chronic doxorubicin dosing. Results are mean values of $n=3$, \pm S.D. One way ANOVA and post-hoc Dunnett's T-test * $p \leq 0.01$.

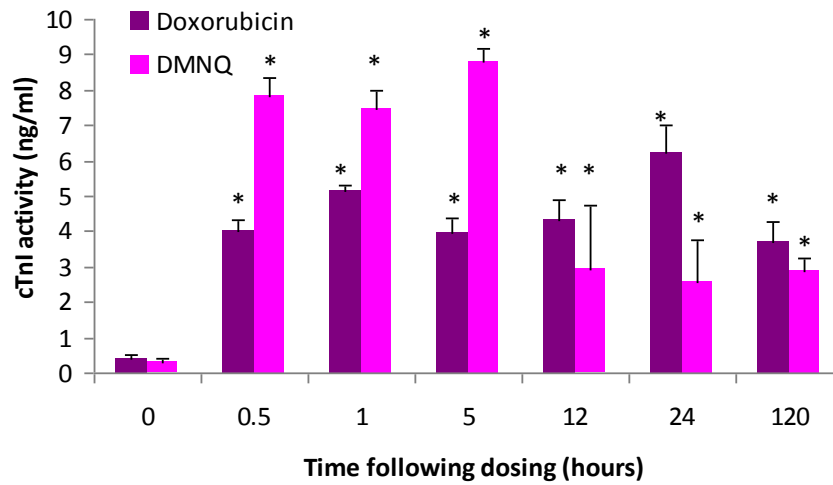
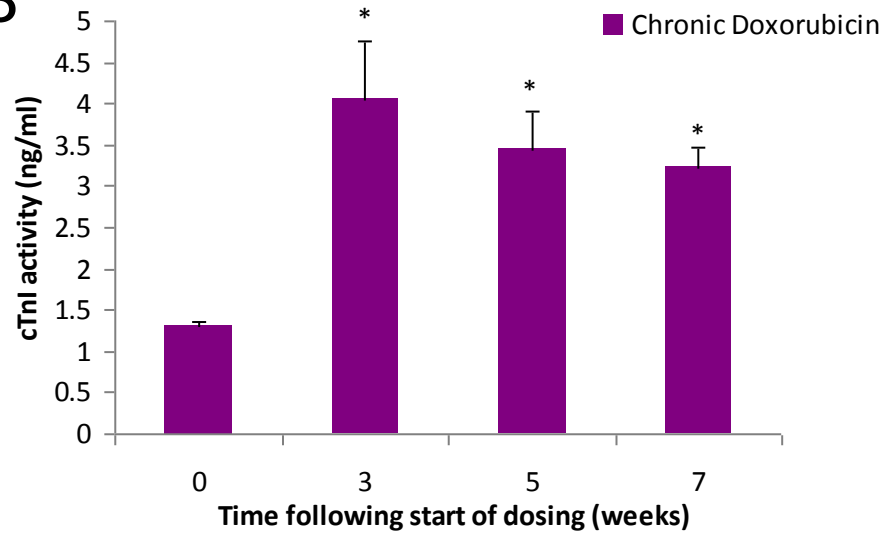
A**B**

Figure 4.9: Troponin I activity, determined from plasma using an ELISA assay kit. Increase observed from 0.5 hours following dosing with DMNQ and doxorubicin in an acute model of toxicity (A) and from week 3 of dosing in a chronic model of doxorubicin toxicity (B). Results are mean values \pm S.D. (0 hours n=7, all other time points n=4). One sample t-test compared to control *p<0.01. Chronic DMNQ time points were not evaluated.

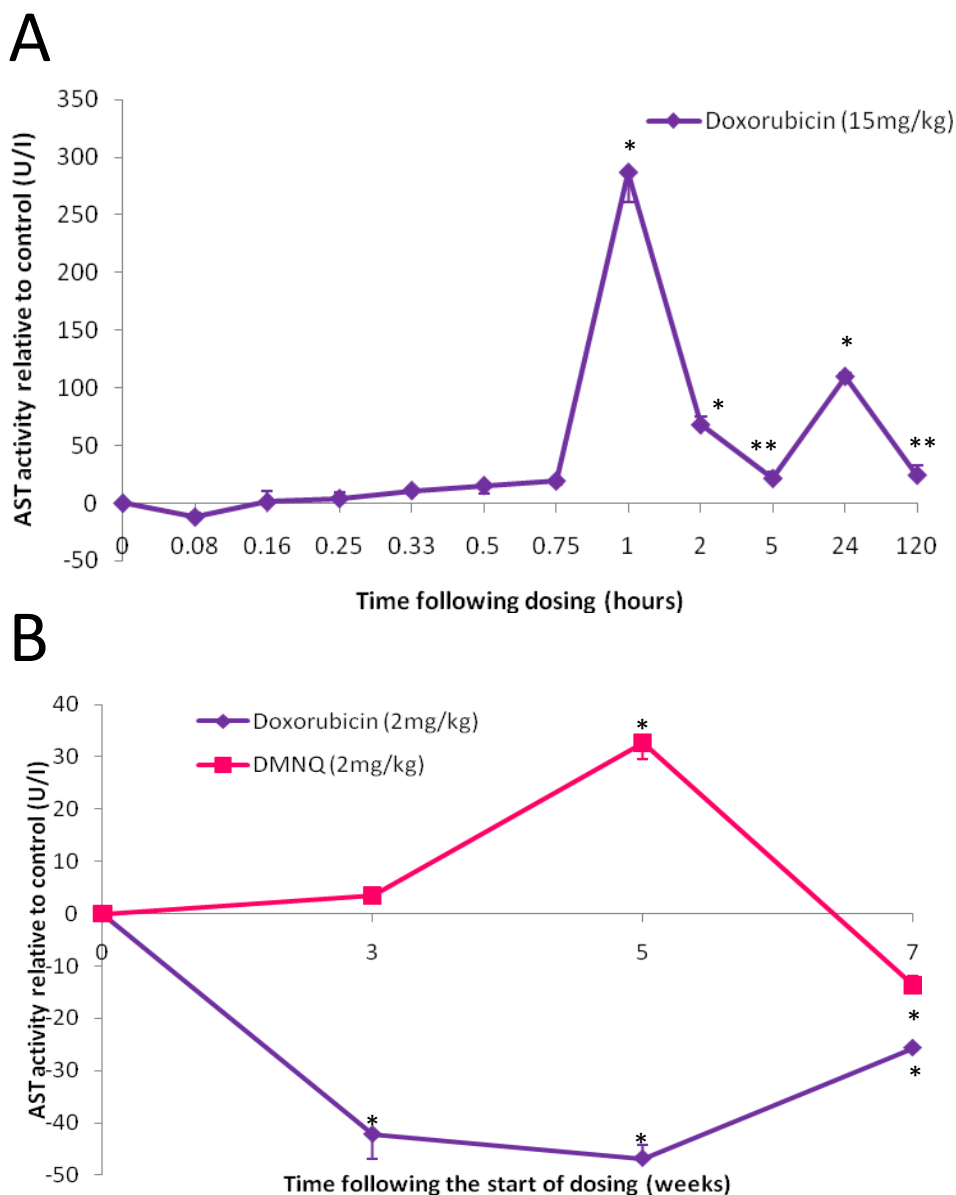


Figure 4.10: AST activity following acute doxorubicin and chronic DMNQ and doxorubicin. AST activity is significantly elevated from 1 hour to 120 hours following a single 15mg/kg dose of doxorubicin (A). Chronic doxorubicin results in a significant decrease in AST activity, chronic DMNQ treatment results in increased AST activity then decreased over the 7 weeks of treatment (B). Results are mean values $n=3 \pm S.D.$ One way ANOVA and post-hoc Dunnett's T-test * $p \leq 0.01$, ** $p \leq 0.05$.

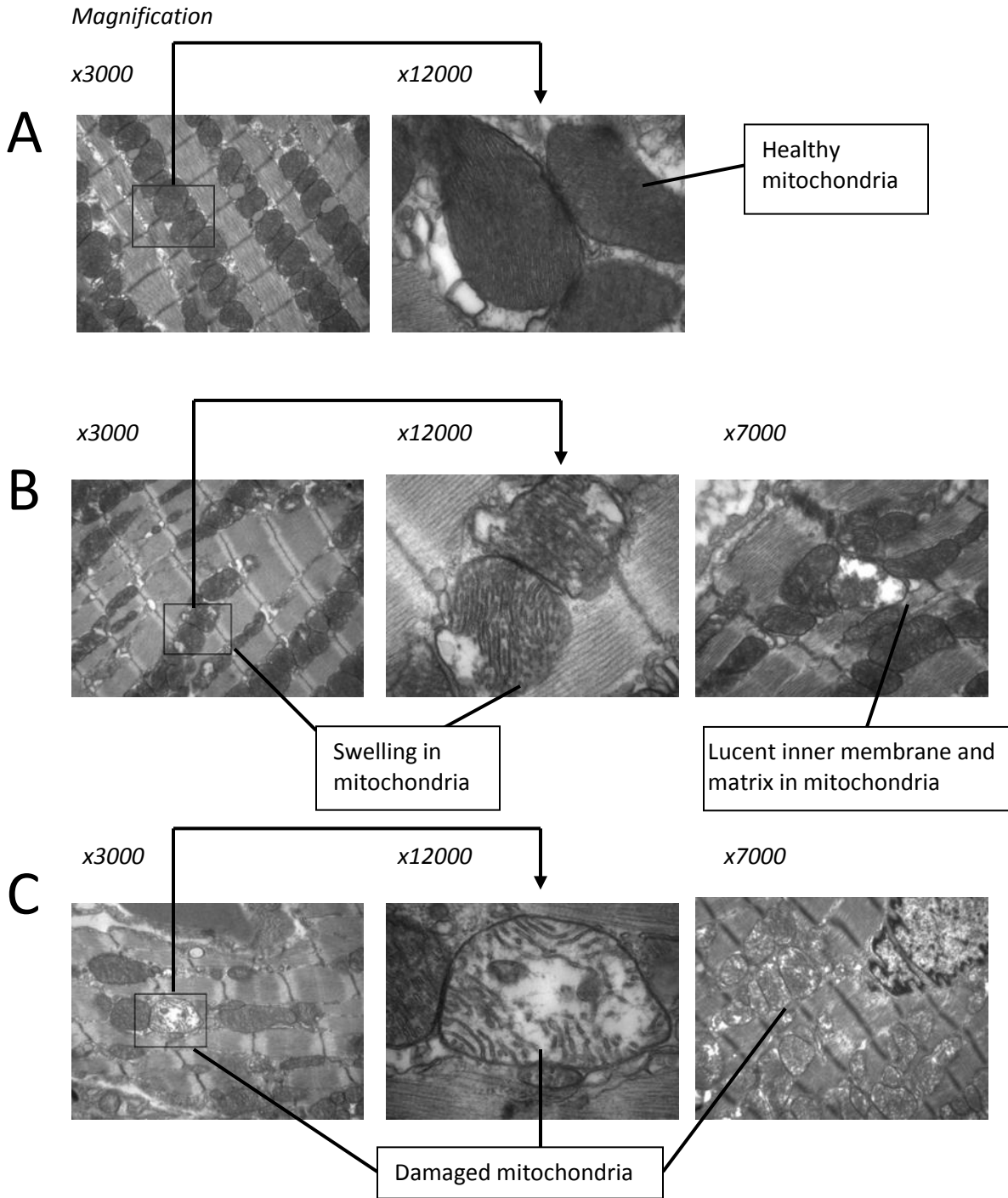


Figure 4.11: Pathophysiological characterisation of cardiac damage. Control (A), doxorubicin (15mg/kg) (B), DMNQ (25mg/kg) (C), n=3. Electron micrographs reveal swelling of the mitochondria and a lucent matrix in the mitochondria of cardiac tissue compared to control.

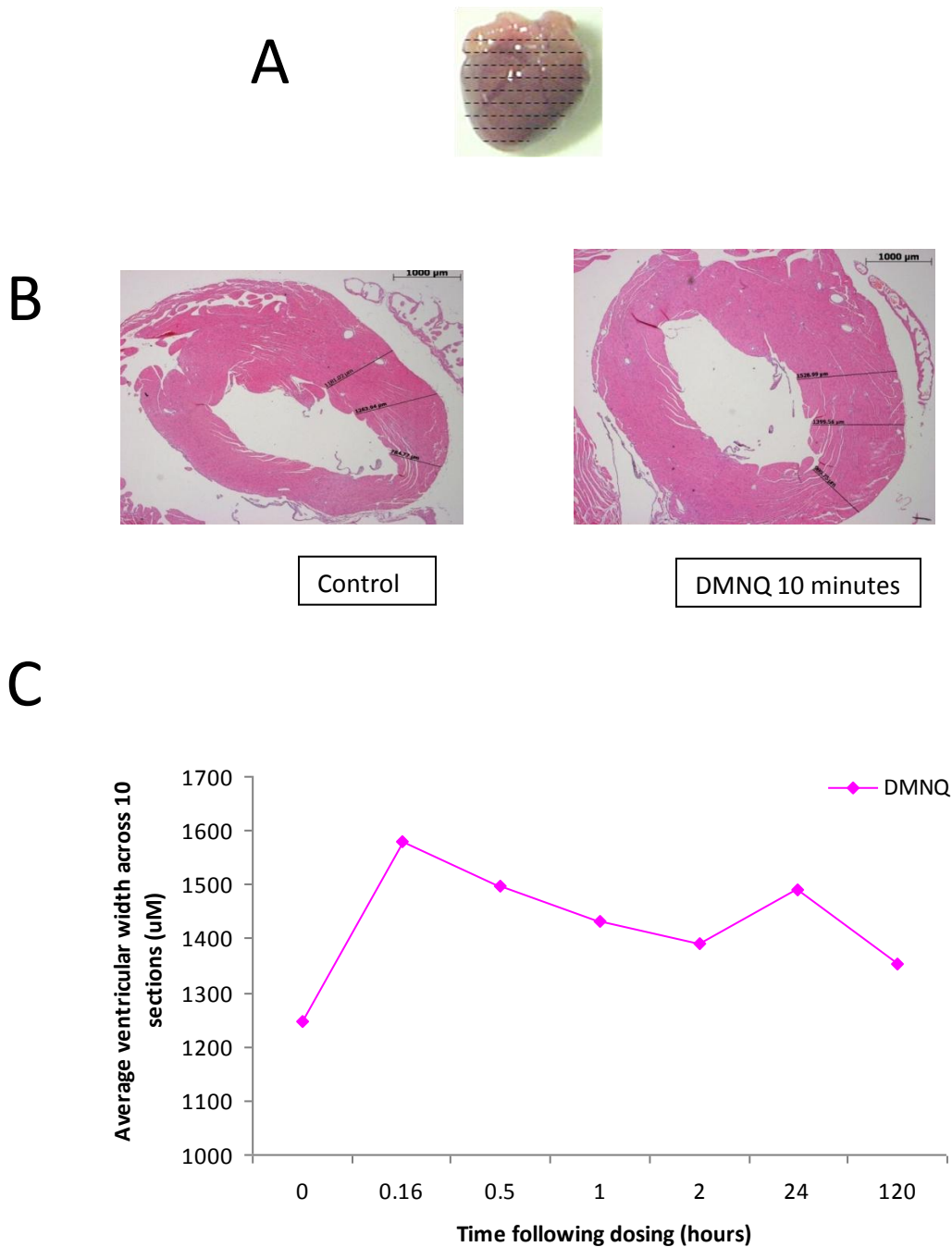


Figure 4.12: Ventricular width, images illustrating how measurements of ventricular wall were obtained. The heart was cut into 10 slices as depicted in (A). Measurements were taken as in (B), and the mean calculated following acute DMNQ treatment (n=1) (C). Peak width of the ventricular wall occurs 10 minutes following 25mg/kg DMNQ, but elevated levels were still apparent 120 hours following dosing.

4.4 DISCUSSION

The overall aim of this chapter was to determine appropriate *in vivo* acute and chronic doses of doxorubicin in C57B6/AJ male mice and characterise the associated cardiac damage at the biochemical level. DMNQ has been extensively used to study the effects of redox stress *in vitro*, exclusively in a hepatic model. No *in vivo* data was available in the public domain for the effects of DMNQ on the heart.

Dose response experiments were conducted to identify concentrations of DMNQ and doxorubicin *in vivo* that led to cardiac damage without the complication of pathophysiological change. This was achieved by measuring organ (liver, heart and kidneys) to body weight ratios and CK-MB activity (Table 4.3). Doses that resulted in liver:body weight percentages below 5% were selected, if they also had significantly elevated CK-MB measurements and cardiac transcriptional gene expression changes, indicating specific cardiotoxicity. Dose levels selected are presented in Table 4.5, above these, toxicity manifested quickly, characterised by withdrawal and a rapid onset of piloerection that did not reduce with time. In addition, during doxorubicin dose selection, clinical relevant concentrations were kept in mind, a total dose of 16mg/kg is known to equate to a cumulative dose of 500mg/m² (Urva et al. 2009). Cardiac cytotoxicity was demonstrated at these selected dose levels, assessed by an increase in CK-MB, cTnI and Heart:Body weight ratios. Cardiac cytotoxic effects on the heart following chronic DMNQ dose administration were not as profound, but the Heart:Body weight ratios were significantly increased, as was CK-MB activity when measured using the inhibition assay (Figure 6A). However further measurement of CK isoforms by native protein gel revealed no significant increase in CK-MB, but increased CK-BB. It has been speculated that increased B isoform expression of CK is a consequence of re-expression of the cardiac 'fetal' gene expression signature. Upon damage it is known that a shift in mRNA expression from one of an adult phenotype to a fetal phenotype occurs. This shift may result as the B isoform has a higher affinity for ADP and phosphocreatine compared to the M isoform of CK possibly allowing more efficient ATP generation (Tokarska-Schlattner et al. 2006). Thus the increase in the B isoform following chronic DMNQ administration may indicate the development of a cardiotoxic phenotype. These

data also demonstrated that DMNQ may not have a cumulative effect at these dose levels unlike doxorubicin (Yi et al. 2006). It maybe that the mechanism responsible for the development of cardiotoxicity is similar for both doxorubicin and DMNQ but the ability of the heart to repair or response to cardiac damage is reduced following doxorubicin but not DMNQ.

Acutely, electron microscopy (Figure 4.11), indicated mitochondria to be a key organelle affected by both compounds. The inner membrane appeared to collapse and the mitochondria swell in size. However, the outer membrane remained unaffected, indicating that the mitochondrial contents were not being continually released at the time points or doses studied. As an acute model of toxicity allows an in depth analysis of the biochemistry and genetics prior to morphological alterations; it maybe that with time the outer mitochondrial membrane is ruptured, due to mitochondrial swelling. Similar ultra structure of mitochondria has been reported by Sardao et al. (2009) following doxorubicin administration *in vitro* in H9C2 cells. In this study it was presumed that the changes in mitochondrial morphology observed were a result of doxorubicin's ability to induce the permeability transition pore. In addition similar mitochondrial abnormalities have been observed in *Epas1* (endothelial PAS domain protein 1) transgenic mice. *Epas1* responds to hypoxia, thus its down-regulation results in cardiac hypertrophy and mitochondrial abnormalities, these alterations are comparable to those observed acutely with doxorubicin and DMNQ (Scortegagna et al. 2003). Thus, indicating partial mitochondrial dysfunction 24 hours following a single dose of doxorubicin or DMNQ. As the functional efficiency of the heart appears to be comprised, and these biochemical changes are normally observed long before any morphological alterations become detectable (Robert 2007), these minor alterations to mitochondria are likely to become more pronounced with time. Additionally following DMNQ the ventricular width increased, no data was obtained following doxorubicin (Figure 4.12). Increased ventricular width is associated with cardiac hypertrophy and cardiac failure due to thickening of cardiac muscle as a consequence of increased workload, or dilation or inflammation of the heart as a result of damage without any change in cell number. As the observed effects occur from 10 minutes following dosing

**Chapter 5: Transcriptional Response of the Heart *In Vivo*
Following Doxorubicin and DMNQ Exposure**

5.1 INTRODUCTION

In the previous chapters the suitability of utilizing DMNQ as a model compound to allow insight into doxorubicin cardiotoxicity was established, along with the associated biochemical and pathophysiological consequences *in vivo* (Chapters 3 and 4). In this chapter the transcriptional genomic response to doxorubicin and DMNQ was assessed using microarray technology. Transcriptional profiling allows the measurement of mRNA levels altered as a result of increased transcription or decreased mRNA degradation in response to stimuli including that following xenobiotic exposure (Gant et al. 2009). The overall objective of this study was to define the transcriptional profiles following dosing with doxorubicin and DMNQ in both an acute and chronic model of toxicity, with the aim of identifying key genes and pathways that could be responsible for the manifestation of the cardiotoxic phenotype characterised in Chapter 4. DMNQ transcriptional profiles allow the cardiotoxic action of doxorubicin to be investigated in greater detail.

5.1.1 PLAN OF INVESTIGATION

The experiments described in Chapter 4 were carried out to identify suitable dose levels for both compounds in an acute and chronic model of toxicity; a summary of the selected dose levels is presented in Table 5.1. At these dose levels specific cardiotoxicity was observed in an acute model allowing mechanistic genetic characterisation to take place without the complication of gross toxicity. A broad range of time points were studied to allow the initial and adaptive response to be investigated. Transcriptional profiles were generated using RNA isolated from acute doxorubicin and DMNQ (n>4) and chronic doxorubicin and DMNQ (n=3) treated hearts and subjected to transcriptional microarray analysis covering the entire mouse genome (Chapter 1 and section 2.16).

Large amounts of data are generated through microarrays, this in itself is problematic. In order to overcome this, bioinformatic tools have been used to filter and apply biological meaning to this data allowing comparisons between both DMNQ and doxorubicin and the acute and chronic models of toxicity (Curtis et al.

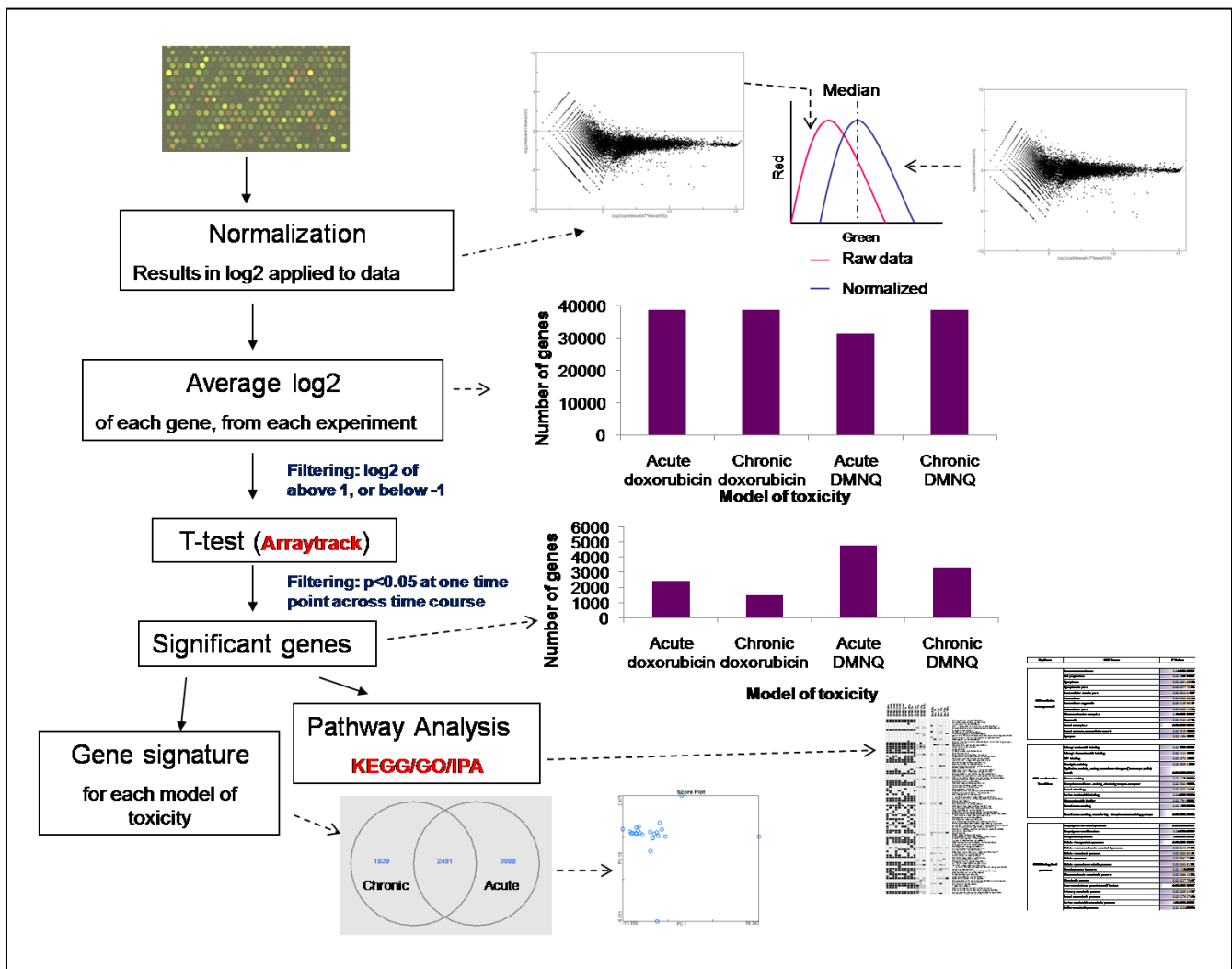
2005). Transcriptional data was analysed as depicted in Figure 5.1, and grouped into functional pathways using the Gene Set Analysis Toolkit (<http://bioinfo.vanderbilt.edu/webgestalt>). In addition a second commercially available application Ingenuity Pathway Analysis (IPA) was used (Section 1.5.7). These two web based applications allow classification into KEGG pathways and biological networks, respectively, applying biological context to the expression profiles. Two programmes have been utilised as software packages classify genes slightly differently each having a different focus (Kamburov et al. 2009). Transcriptional responses in pathways that were expected to be modulated were also examined. As outlined in section 1.4.4 doxorubicin is likely to affect oxidative stress and mitochondrial energy dynamic pathways, possibly through the nuclear response factor 1 (NRF-1) (Section 1.4.4). Genes implicated in NRF-1 targeting, oxidative phosphorylation and oxidative stress response were identified within the transcriptional data sets and their regulation evaluated.

Compound	Model of Toxicity	Dose Level	Time Point of Sacrifice
Doxorubicin	Acute	15mg/kg	0.5, 1, 2, 12, 24 and 120 hours
DMNQ	Acute	25mg/kg	5, 10, 15, 20, 30 minutes and 1, 2, 5, 12, 24, 120 hours
Doxorubicin	Chronic	2mg/kg/week	3, 5 and 7 weeks
DMNQ	Chronic	2mg/kg/week	3, 5 and 7 weeks

Table 5.1: Concentration of compounds used for all transcriptional profiling.

5.1.2 HYPOTHESIS AND AIMS

The overall aim of this study was to define the transcriptional profiles following doxorubicin and DMNQ in an acute and chronic model of toxicity. It was hypothesised that consistent regulation of genes and pathways by both compounds would result in the identification of key mechanisms through which doxorubicin mediates its cardiotoxic effects.



Key:

- ▶ - Direct line of data analysis
- - -▶ - Example of data analysis outputs
- Red** - Packages used in data analysis

Figure 5.1: Summary of the process of transcriptional data analysis. Data normalised using global normalization as illustrated when reverse labelling had been conducted, when not LOWESS normalization was used, MA plots were constructed to assess data quality, if the MA plot revealed distorted data, the microarray was discarded from all further analysis. The average of each gene expression was calculated for each gene followed by a one sample two tailed t-test at each time point and data filtered to remove any genes with a p-value of > 0.05. The resultant gene lists were subjected to pathway analysis and gene signature analysis.

5.2 RESULTS

5.2.1 TRANSCRIPTIONAL PROFILES

Genes were chosen for inclusion for analysis if a gene had one significant time point at $p \leq 0.05$ and a $\text{Log}_2 \leq 1$ or $\text{Log}_2 \geq 1$ within the time course giving a false discovery rate of 5%. In an acute model of toxicity this in total gave 4766 genes for DMNQ and 2438 genes for doxorubicin of which 1171 were affected by both compounds. In a chronic model of toxicity, 1484 and 3342 genes were significantly affected by doxorubicin and DMNQ, respectively, of which 512 were affected by both compounds. In all models both the mitochondrial and nuclear genomes were affected. The overall level of transcription following doxorubicin (acute and chronic models) was reduced to about half that of DMNQ, this is possibly a consequence of doxorubicin's pharmacological activity.

5.2.2 IDENTIFICATION OF MECHANISM SPECIFIC EXPRESSION

Principle component analysis (PCA) was conducted (Chapter 1). PCA of transcriptional profiles in the acute models following both doxorubicin (15mg/kg) and DMNQ (25 mg/kg) indicated clustering of doxorubicin time points (0.5, 1, 2, 12 and 24 hours) and later DMNQ time points (2, 5, 12, 24 and 120 hours), with a separate cluster consisting of early DMNQ time points with both 10 minutes DMNQ and 120 hours doxorubicin being divergent from the two clusters (Figure 5.2A). This clustering also potentially indicates that later time points of DMNQ, model doxorubicin cardiotoxicity. However, PCA of transcriptional profiles following chronic doxorubicin and DMNQ revealed distinct differences between the two compounds (Figure 5.2B). This is in line with the alterations in biochemistry in Chapter 4 further confirming that unlike doxorubicin, DMNQ does not have profound cumulative effects.

In total 37 genes were significantly $p \leq 0.01$ affected at a minimum of two time points in an acute model and one time point in a chronic model following both doxorubicin and DMNQ. A wide range of biologically

diverse genes were present including transcription factors, calcium binding, protein binding, cell-cell signalling and helicase activity genes (Table 5.2).

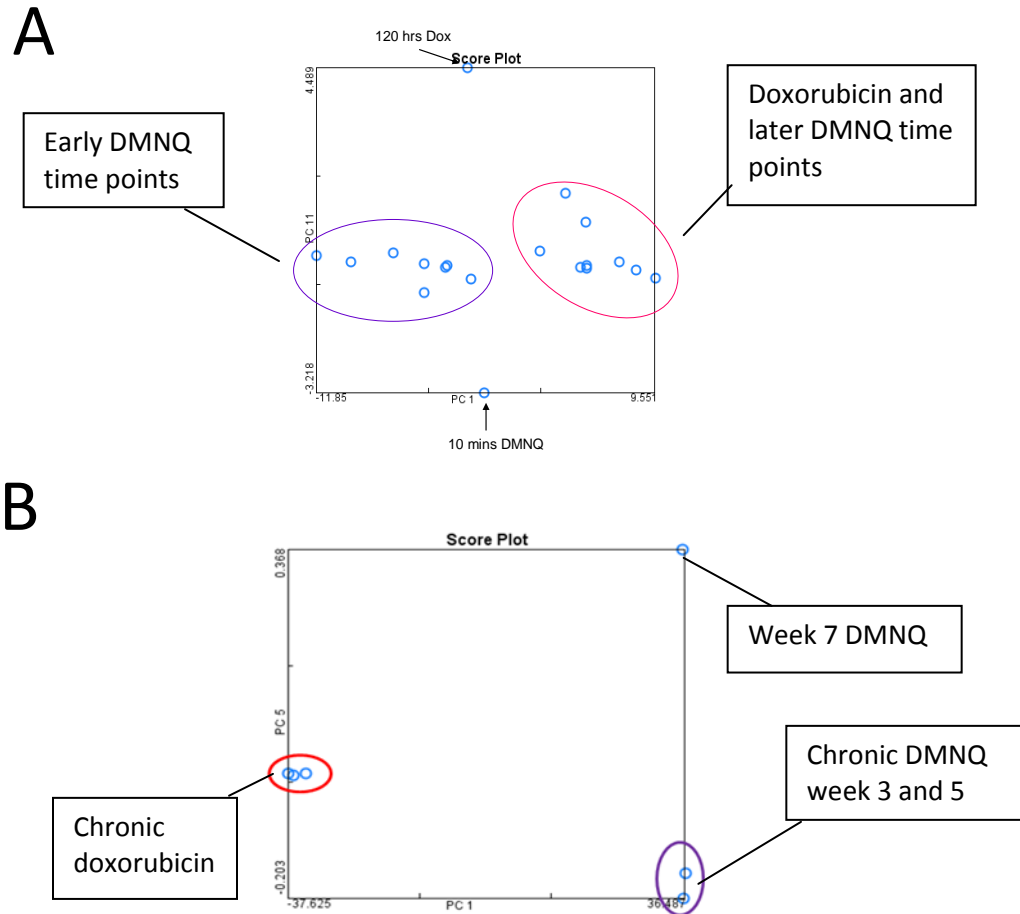


Figure 5.2: PCA of transcriptional data, acute doxorubicin and DMNQ (A) and chronic doxorubicin and DMNQ (B). Results are the mean global normalised values (Acute doxorubicin n=4, acute DMNQ n=5, chronic doxorubicin and DMNQ n=3) subjected to a one sample two tailed t-test at each time point. Genes displaying a p-value of ≤ 0.05 at a minimum of two time point were included in this analysis.

Gene Name	Gene Description	GO Ontology Description	Direction of Change in Expression
Acaa2	Acetyl-Coenzyme A Acyltransferase 2	Acetyl-coenzyme A acyltransferase activity	↑
Pcdh20	Protocadherin20	Calcium ion / protein binding	↓
Gigyf2	GRB10 interacting GYF protein 2	Protein binding	↑
Tnfrsf18	Tumour necrosis factor receptor superfamily member 18	Tumour necrosis factor receptor activity	↓
Hspa12a	Heat shock protein	ATP/nucleotide binding	↑
Impdh1	Inosine monophosphate dehydrogenase 1	Oxidoreductase activity	↑
Gne	Glucosamine (UDP-N-acetyl)-2 epimerase/N-acetylmannosamine kinase	N-acetylmannosamine kinase activity	↓
Cxcl14	Chemokine (Cx-C motif) ligand 14	Cell-cell signaling	↑
Lsamp	Limbic system associated membrane protein	Protein binding	↑
Pax8	Paired box 8	Transcription factor activity	↑
Nkd2	Naked cuticle homolog 2	Calcium ion binding	↑
Igsf8	Immunoglobulin super family member 8	Protein binding	↑
Ddx27	Dead (Asp-Glu-Ala-Asp) box polypeptide 27	Helicase activity	↑
Msh6	Muts homolog 6	ATPase activity	↑
Sirt6	Sirtuin	NAD binding	↑
Phf1	Phd finger protein 1	Metal ion binding	↑
Edaradd	Edar associated death domain	Protein binding / cell death	↑
Sema6c	Sema domain transmembrane domain and cytoplasmic domain	Axon guidance	↑
Myo9b	Myosin IXB	ADP/ATP binding	↑
Bsg	Basigin	Cell surface receptor linked signal transduction	↑
Usp11	Ubiquitin specific peptidase 11	Ubiquitin dependent protein catabolic process	↑
Snx2	Sorting nexin 2	Cell communication	↑
Tyro3	Tyro3 protein tyrosine kinase	Signal transduction	↑
Slc22a12	Solute carrier family 22 member 12	Cellular homeostasis	↑
Abca7	ATP-binding cassette subfamily A member 7	Phagocytosis	↑
Rlms3	Regulating synaptic membrane exocytosis 3	Neurotransmitter transport	↑
Ghrl	Ghrelin/obestatin prepropeptide	Ghrelin receptor binding	↑

Table 5.2: Gene transcriptional signature affected by doxorubicin and DMNQ in an acute and chronic model of toxicity. Genes included are significantly ($p \leq 0.01$) regulated at a $\text{Log}_2 < 1$ or $\text{Log}_2 > 1$ at a minimum of two time points following doxorubicin (acute, 15mg/kg n=4, chronic 2mg/kg, n=3) and DMNQ (acute, 25mg/kg n=5, chronic 2mg/kg, n=3).

5.2.3 PATHWAY ANALYSIS

Pathway analysis allows the identification of more subtle changes in expression than gene lists in isolation and applies biological meaning to the data (Curtis et al. 2005).

5.2.3.1 KEGG PATHWAY ANALYSIS

Each gene that was significantly ($p < 0.05$) affected at a minimum of one time point over the period of study for each compound was classified into KEGG pathways, the number of genes passing this filter are presented in Table 5.3. The gene lists containing Genbank accession numbers were analysed using the KEGG pathway function in the Gene Set Analysis Toolkit. The significance of each KEGG pathway was assessed using a modified Fisher exact test, this generates an enrichment probability score (p value). Any pathway with a p value of > 0.05 at all time points was discarded.

Model of Toxicity	Number of genes subject to pathway analysis
Acute doxorubicin	2438
Chronic doxorubicin	1487
Acute DMNQ	4766
Chronic DMNQ	3342

Table 5.3: Number of transcriptional modulated genes included in subsequent pathway analysis. All genes $p < 0.05$ at a minimum of one time point over the time course.

This analysis indicated a number of significantly altered pathways across the time course following acute doxorubicin (15mg/kg) and DMNQ (25mg/kg) (Figure 5.3). In total 11 KEGG pathways were significantly ($p < 0.01$) affected by both compounds in an acute model, the most prominent was the oxidative phosphorylation pathway (Figure 5.3). This signature of pathways could potentially provide insight into the mechanism of cardiotoxicity. Of interest no redox cycling gene expression signature was apparent indicated by no change in antioxidant response genes including glutathione metabolic and DNA damage pathways. Thus indicating that redox action was not responsible for the toxicity observed, but potentially dysfunction of

the oxidative phosphorylation pathway. 12 hours post dosing a change in pathways affected was observed, this may represent the time point when prior to, any affects were a result of the initial compound insult and after, the activation of an adaptive response.

Chronically seven pathways were affected by both doxorubicin and DMNQ at a minimum of one time point with each compound. Pathways affected included oxidative phosphorylation, regulation of actin cytoskeleton and RNA polymerase. However, the oxidative phosphorylation pathway was the only pathway affected at all time points with both compounds. As DMNQ in a chronic model of toxicity was not as cardiotoxic as doxorubicin (assessed in Chapter 4); any pathways affected may indicate predisposing events (Figure 5.4), thus suggesting the involvement of the oxidative phosphorylation pathway in the development of the cardiotoxicity observed.

Kegg Pathway	Enrichment (P-value) DMNQ												
	5 mins	10 mins	15 mins	20 mins	30 mins	45 mins	1 hr	1.5 hrs	2 hrs	5 hrs	12 hrs	24 hrs	120 hrs
Focal adhesion	1.35E-12	4.03E-15	5.74E-12	3.70E-12	1.14E-14	7.74E-10	8.40E-14	8.85E-14	6.21E-11	9.13E-13			
Regulation of actin cytoskeleton	4.22E-15	6.78E-10	1.30E-13	7.21E-11	4.14E-12	9.40E-10	1.02E-13	3.66E-13	1.01E-13	1.40E-09			
Proteasome	3.51E-05	1.75E-09	1.63E-04	4.68E-06	1.94E-07	2.14E-03	3.15E-06	8.22E-09	7.97E-06	6.25E-05			
Circadian rhythm	2.77E-03						3.10E-03						
Ribosome	1.44E-14	1.18E-16	1.05E-07	9.89E-11	4.27E-10	1.60E-05	5.87E-09	3.67E-13	7.94E-09	2.01E-12		0.00788	
ECM-receptor interaction	2.22E-03	2.47E-04	3.73E-03	1.35E-03	2.38E-03		3.13E-05	1.40E-03		8.85E-04			
Galactose metabolism	7.07E-03							5.50E-03					
Glycolysis / Gluconeogenesis	1.02E-04	3.85E-03	8.28E-04	1.59E-03	1.37E-03			6.97E-04		7.45E-03			
N-Glycan biosynthesis	4.79E-03	3.80E-04	2.46E-05	8.90E-04	8.93E-03	6.78E-04			8.61E-04				
Glycerophospholipid metabolism	2.40E-03		9.35E-03	4.91E-05	4.92E-04	9.92E-04	1.52E-05	4.16E-03	8.02E-04	1.19E-03			
Fatty acid metabolism	8.07E-03	2.30E-03		2.52E-03	2.22E-03			6.74E-04		7.14E-03			
Glycerolipid metabolism	2.65E-03			7.62E-03				5.35E-03		8.83E-03			
T cell receptor signaling pathway							9.46E-03	2.78E-03	7.63E-03	6.40E-03			
Pyruvate metabolism	7.07E-03	6.59E-03		4.66E-03	4.18E-03			5.50E-03		2.91E-03			
Oxidative phosphorylation	8.42E-17	1.42E-22	6.58E-12	4.01E-14	2.87E-16	5.96E-07	1.31E-13	1.74E-20	2.19E-12	1.72E-15	0.0662	0.035	0.0628
Citrate cycle (TCA cycle)	4.22E-05	8.05E-07	7.27E-04	3.63E-05	1.79E-06	5.39E-03	2.72E-04	3.10E-05	5.51E-04	3.24E-04	0.0961		0.052
Apoptosis	1.28E-04	2.09E-03	2.55E-04	1.27E-04	1.01E-04	2.28E-03	3.78E-03	1.89E-04	2.45E-03	1.40E-04	0.243	0.0836	0.144
Purine metabolism	2.15E-05	1.95E-03	1.50E-04	6.85E-06	1.17E-05	3.05E-04	1.98E-03	4.04E-04	2.90E-05	3.91E-04		0.055	
Axon guidance	3.29E-07	5.84E-06	9.27E-04	1.58E-05	6.29E-07	4.11E-05	5.10E-06	6.39E-06	5.56E-06	3.08E-06	0.0468	0.463	0.132
Calcium signaling pathway	1.32E-06	1.64E-02	1.97E-04	1.15E-05	1.63E-05	2.26E-05	5.20E-04	7.91E-05	8.16E-05	1.75E-07	0.0318		0.389

Kegg Pathway	Enrichment (P-value)					
	Dox 0.5 hrs	Dox 1 hr	Dox 2 hrs	Dox 12 hrs	Dox 24 hrs	Dox 120 hrs
Nitrogen metabolism		0.023		0.546		
Androgen and estrogen metabolism	0.0352					
Cyanamino acid metabolism	0.0579			0.0126	0.0243	
Lysine degradation	0.0922				0.0189	
Oxidative phosphorylation		0.00000045	0.00000029	0.0815	0.386	5.26E-13
Citrate cycle (TCA cycle)			0.0775	0.595	0.111	0.00675
Adipocytokine signaling pathway		0.178	0.205	0.0392		
Cell cycle	0.0333	0.108	0.291	0.831	0.0896	0.00192
Purine metabolism	0.0663	0.424		0.0202		
Tryptophan metabolism	0.0374	0.505		0.402		
Bisphenol A degradation	0.184		0.0555	0.472		
PPAR signaling pathway		0.17	0.0207	0.442		0.0456
Neuroactive ligand-receptor interaction	0.369	0.334		0.0313		0.387
Aminosugars metabolism				0.076		0.0085
Bile acid biosynthesis	0.0582					
Axon guidance		0.151		0.0321	0.444	0.46
Pyrimidine metabolism	0.0617	0.211		0.0219		
VEGF signaling pathway		0.538		0.0392	0.285	
Calcium signaling pathway	0.14	0.567		0.00384		
Basal transcription factors	0.293			0.021	0.133	
Regulation of actin cytoskeleton	0.393			0.0403	0.0239	0.0627

KEGG pathway
Purine metabolism
Cell Communication
Axon guidance
Oxidative phosphorylation
Glycerolipid metabolism
Proteasome
Focal adhesion
ECM-receptor interaction
Regulation of actin cytoskeleton
Citrate cycle (TCA cycle)
Calcium signaling pathway

Figure 5.3: Significantly affected KEGG pathways following acute DMNQ (25mg/kg, top) and doxorubicin (15mg/kg, bottom left) with those pathways affected by both compounds separated. Genes included are significantly ($p \leq 0.05$) regulated at a $\text{Log}_2 < 1$ or $\text{Log}_2 > 1$ at a minimum of two time points following doxorubicin (15mg/kg) or DMNQ (25mg/kg). Results are mean values of $n=4$

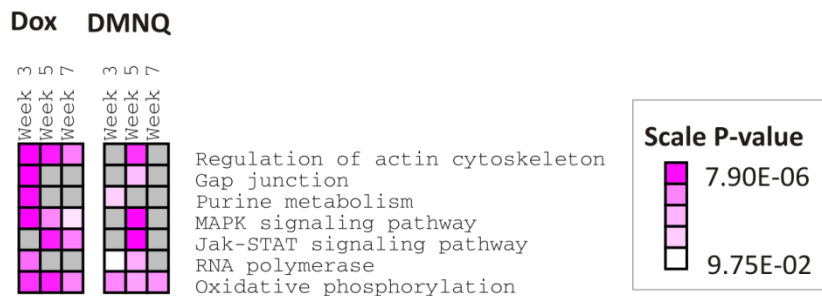


Figure 5.4: Signature of pathways affected by both doxorubicin and DMNQ in a chronic model of toxicity. Genes included are significantly ($p \leq 0.05$) regulated at a $\text{Log}_2 < 1$ or $\text{Log}_2 > 1$ at a minimum of one time point following doxorubicin (2mg/kg/week) or DMNQ (2mg/kg/week). Results are mean values of $n=3$.

5.2.3.2 PATHWAY ANALYSIS: INGENUITY PATHWAY ANALYSIS

As an additional tool to investigate biological function the commercially available software Ingenuity Pathway Analysis (IPA) was used (Section 1.5.7). A more stringent filter was applied to the gene lists selected for IPA. Each gene that was significantly ($p \leq 0.01$) changed in expression at a minimum of all but one time point for each compound was included. All genes were also differentially expressed by both compounds in an acute or chronic model of toxicity. The Genebank accession numbers of each gene meeting the above criteria (Table 5.4) were imported into IPA for both acute and chronic models.

Model of Toxicity	Number of Genes
Acute	556
Chronic	228

Table 5.4: Number of transcriptional modulated genes included in IPA analysis. All genes $p \leq 0.01$ in all but one time point with both doxorubicin and DMNQ.

Both of the gene lists were categorised by IPA into interacting networks dependent on biological function, which were ranked by score. The score was derived using a modified Fisher exact test and then the negative

log of the resultant p value, highlighting the chance of a group of genes being differentially regulated by chance. Any networks giving a score of ≤ 3 were discarded. This equates to a $p \leq 0.001$ cut off. In addition the top functions associated with each network of genes were included. In an acute model of toxicity (Table 5.5) 16 networks were differentially affected by both compounds, genes involved include those concerned with cell assembly, DNA replication and gene expression, molecular transport, cell cycle control, energy production, cardiovascular system development and function and cell death. Chronically (Table 5.6) genes involved in cardiac disease, molecular transport, cell cycle control and cell morphology were differentially expressed.

ID	Genes in Network	Score	Focus	
			Molecules	Top Functions
1	14-3-3,AHcy,AMPK,AP3B2,Caspase,CNNM3,Cytochrome c,DUSP16,EDC3,EFTUD2,FOXO3,GABBR1,GDI1,GIGYF2,GLG1,Jnk,KIAA0999,LMNA,MTCH1,MYCBP2,P2RX1,PFKP,PHF1,PRPF8,PTBP1,RBPMS,SIRT6,TACC2,TNPO1,TXNDC17,UBA1,UBE2K,UCP2,VIM,YWHAZ	48	30	RNA Post-Transcriptional Modification, Cellular Assembly and Organization, Cellular Function and Maintenance
2	14-3-3,AHcy,AMPK,Caspase,CNNM3,Cytochrome c,EDC3,EFTUD2,FOXO3,GABBR1,GDI1,GIGYF2,GLG1,HDAC5,Hsp70,Jnk,KIAA0999,KLC2,LMNA,MTCH1,MYCBP2,P2RX1,PFKP,PHF1,PRPF8,RBPMS,S LAIN2,TACC2,TNPO1,Tubulin,TXNDC17,UBA1,UBE2K,UCP2,YWHAZ	43	28	Cellular Assembly and Organization, Cellular Function and Maintenance, Cardiovascular System Development and Function
3	CACNA1B,CACNB1,CLIP2,EGR3,G protein beta gamma,GNAI1,GNAI2,GNE,GSTP1,HBP1,IRAK4,ITPR,LHB,MADD,MAOB,MAP2K7,MAT2B,Mek,N-type Calcium Channel,NFkB (complex),NR1D1,PECAM1,PELI2,PRKD1,PTGS1,Rap1,Ras,RGS3,RGS8,RS12,RPS6KA5,SP2,TCR,TNFRSF18,TNIP1	41	27	Cellular Development, Reproductive System Disease, Tissue Morphology
4	APC,CBFA2T3,CD226,COPS2,Ctbp,CXCL9,DNMT3A,EFCAB6,EOMES,ERCC5,G6PC2,Hdac,HDAC3,Histone h4,IL7,IL12 (complex),Interferon alpha,LIN9,MHC Class I (complex),MSH5,MXD1,MYB (includes EG:4602),N-cor,OGDH,P38 MAPK,Pias,PIAS1,SENP2,SLC5A1,Smad,SP100,TBL1XR1,TFDP2,TGIF1,Thyroid hormone receptor	34	24	Cell Cycle, Cell Death, Hematological Disease
5	ALP,C4B,CD226,Creb,CXCL9,CXORF15,EFCAB6,ENG,EOMES,ERCC5,FAM3B,G6PC2,Ige,IGFBP4,IL7,IL12 (complex),Interferon alpha,KRT75,LDL,LIN9,MHC Class I (complex),MYB (includes EG:4602),OGDH,P38 MAPK,Pias,PIAS1,PIAS3,POU2F1,SLC5A1,Smad,SP100,TBP,TFDP2,Tgf beta,TGIF1	34	24	Gene Expression, DNA Replication, Recombination, and Repair, Cell Death
6	ADCY,Ap1,BAIAP2,BRAP,CaMKII,CORO1A,DDC,DIAPH1,DTNA,ELAVL4,F Actin,FNBP1,GSS,hCG,IL1,Insulin,Mapk,MAPK14,MYO9B,Pdgf,PDGF BB,PIP5K1C,Pkc(s),PP2A,PPM1J,Rac,Ras homolog,RASA1,Rock,ROCK1,SLC29A1,SNX2,STK19,STRN3,Vegf	24	19	Cell Signaling, Tissue Development, Cell-To-Cell Signaling and Interaction
7	AGRN,Calcineurin A,Calcineurin protein(s),CBFA2T3,COPS2,CSNK1E,CSR3,DNMT3A,ERK,Fcer1,GHRL,Growth hormone,Gsk3,Hdac,HDAC3,HDAC5,Histone h4,MEF2,MSH5,MXD1,N-cor,NAMPT,Nfat (family),NFATC1,NR1I3,OGT (includes EG:8473),POU1F1,Ptk,Rb,RCAN1,RUNX1,Rxr,TBL1XR1,Thyroid hormone receptor,TRAK2	23	20	Cellular Development, Hematological System Development and Function, Hematopoiesis
8	C12ORF52,CAV1,CCDC59,CDK2,CHST9,CITED2,CUL2,DNAJC30,DPH5,F7,FOXRED1,HNF4A,HPN,MED1,MRPS35,MTRF1,NCOA1,NEDD8,NR1I2,NR1I3,PCDH20,POLRMT,PPARGC1A,RNF167,SCAND1,TFB2M,THAP2,UBE2B,UBE2D3,UBE2M,UBE2N,UBE2V1,ZCCHC8,ZSCAN20	17	15	Gene Expression, Molecular Transport, Small Molecule Biochemistry

Table 5.5: IPA networks transcriptionally affected by both DMNQ and doxorubicin in an acute model of toxicity. Table shows the results of IPA for genes significantly ($p \leq 0.01$) affected by both doxorubicin and DMNQ in an acute model of toxicity, giving an overall indication of the gene functions regulated by both compounds.

Table 5.5 continued

ID	Genes in Network	Score	Focus	
			Molecules	Top Functions
9	ADAT1,ALDH8A1,ATG3,BET1,BET1L,DHRS4,DSN1,GABARAPL2 (includes EG:11345),GOLGA2,GOSR1,GOSR2,GTF2H3,HNF4A,IPO13,IRGQ,LRSAM1,MAGOH,MIS12,NSL1,NUF2,ORC3L,PCMT1,PRPF31,RAB33B,RNF44,SCFD1,SEC22A,SPC24,SPC25,STYXL1,TARS,UBA5,USO1,YKT6,ZWINT (includes EG:11130)	17	15	Cellular Assembly and Organization, Cellular Function and Maintenance, Molecular Transport
10	AZIN1,Cdc2,DPF1,EFNA4,EHMT1,EMP1,ENO3,FLG (includes EG:2312),Histone h3,HTT,IKK (complex),INO80,LSAMP,MIR17 (includes EG:406952),MTUS1,NCAPD2,NCAPD3,NCAPG2,NCAPH2,PAF1,POU2F3,PRPF40B,SEC31A,SEPHS1,SLC6A1,SMC2,SMC4,SMOC2,ST8SIA3,ST8SIA5,TP63,TXNDC11,UBE2H (includes EG:7328),WAC,ZMYND8	14	13	Cell Cycle, Cellular Assembly and Organization, DNA Replication, Recombination, and Repair
11	ADA,ADAR,ADARB2,ASB2,BLZF1,C6ORF66,CNOT4,DERL1,DHX30,EIF5A,FAM120C,FIS1,FNG,HM13,LFNG,LRAT,MAPK6,MARCH5,MFNG,NDUFA13,NDUFB7,NDUFV1,NGLY1,NOTCH1,retinoic acid,RFNG,RGR,SEN2,SMC5,SMC6,SUMO1,TOP2B,TRAF7,UBB,XBP1	14	13	Lipid Metabolism, Molecular Transport, Small Molecule Biochemistry
12	ACAA2,ADAM5,ANKRD27,C9ORF7,DUB,ELOVL1,EML4,FAM13A,LRRCS5,MIR124,MIR1 (human),MIR124-1,NARG1,QSER1,SLC22A5,SLC25A30,TEX261,TRIM66,TTC7A,USP11,USP17,USP32,USP35,USP38,USP40,USP41,USP42,USP43,USP45,USP49,USP50,USP27X,USP37 (includes EG:57695),USP51 (includes EG:158880),ZNF790	13	12	Genetic Disorder, Metabolic Disease, Molecular Transport
13	ACTB,ANXA4,CFL2,EIF2C4,HDHC3,HEATR1,HIST3H2A,HMGXB4,IGF2BP1,LIMA1,MDM2,MIRLET7B,MYC,MYRIP,NMI,PELO,PFDN5,PFN,PFN3,RIBIN,PL11,RPS7,RPS18,RPS20,RPS12 (includes EG:6206),SARS,SCAMP5,SSH1,SSH2,SSR4,SUCLG1,Top2,TP53I3,UBR2,VDAC2	12	12	Cancer, Cell Cycle, Skeletal and Muscular Disorders
14	5-HTR3,ADSL,AHCYL1,ATP6V0B,BAI1,Ca2+,CFHR1,CLEC10A,DLG4,ENTPD1,FGF6,FGF7,Fibrinogen,FIGNL1,FKBP1B,GPR177,GRIN2D,HPCAL1,HTR3A,HTR3B,MIRN324,MPP1,POGZ,PQLC3,RIC3 (includes EG:79608),S100A2,SDK2,SH3BGRL2,SIGLEC1,SIPA1L1,SLC24A2,THBS2,TP53,TTF1,ZDHHC3	12	12	Carbohydrate Metabolism, Cell Morphology, Cellular Assembly and Organization
15	ANK2,CANX,CDH15,CER1,CTNNB1,CXCL14,DHH,DKK,FGF2,FOXB1,FRZB,GPSN2,HHAT,HSPA12A,MXRA8,NRCAM,PIGK,PTCH1,RSPO1,SCN7A,SCNN1B,SFRP,SLC2A4,TOB2,WIF1,Wnt,WNT2,WNT6,WNT16,WNT10A,WNT2B,WNT8A,WNT8B,WNT9A,WNT9B	12	12	Cell Signaling, Cell-To-Cell Signaling and Interaction, Cancer
16	ARF5,ATAD4,C6ORF168,CA150,Ck2,CSDC2,CTDP1,CYTH4,EXOC6B (includes EG:23233),FAM13B,GBP3,GTP,HELZ,INTS12,magnesium,MED24,MIR373,MIRLET7D,MSSE,NBPF15,PACIN1,POLR2C,POLR2J2,RAB11FIP4,RBM16, RNA polymerase II,SCN1B,SETD2,SLC9A8,SPT1,TMEM9B,Tubulin,WDR36 (includes EG:134430),ZNF74,ZNF268	11	11	Cell Signaling, Energy Production, Infection Mechanism

Table 5.5: IPA networks transcriptionally affected by both DMNQ and doxorubicin in an acute model of toxicity. Table shows the results of IPA for genes significantly ($P \leq 0.01$) affected by both doxorubicin and DMNQ in an acute model of toxicity, giving an overall indication of the gene functions regulated by both compounds.

ID	Genes in Network	Score	Focus	
			Molecules	Top Functions
1	Akt,Alpha catenin,BSG,CARD10,DDX58,DHX58,F Actin,GAK,GFPT2,GHRL,GNE,IFN Beta,IKK (complex),Insulin,Interferon alpha,Mapk,MAPK8IP2,MARCKSL1,NFkB (complex),PDGF BB,PI3K,Pkc(s),PP2A,PPAP2B,PPM1J,PTPN11,SLAMF6,SLC9A3R2,SLIT2,TNF RSF18,TPD52L1,TYRO3,UBE2N,UPF1,USP6NL	41	22	Small Molecule Biochemistry, Antimicrobial Response, Connective Tissue Development and Function
2	ABCF3,ACAA2,AP2A1,BAI2,C7ORF64,CIAO1,COQ6,DDX27,DNAJA2,FBXO31 (includes EG:79791),FMR1,GLYAT,GTF3C5,HADHA,HADHB,HNF1A,HNF4A,MIR204,MIR211,MIRN330,OPA1,PCDH20,PPARA,RNF44,SLC2A4,SLC35A3,SREBF2,TAPBPL,TGFB1,TLN1,TM9SF4,TOE1,ZNF300,ZNF410	27	16	Lipid Metabolism, Small Molecule Biochemistry, Molecular Transport
3	CAMK1,CN1FR,CYHIP2 (includes EG:26999),DYRK3,ERK,ERK1/2,FDXR,FSH,GLI2,Histone h3,IL17RD,IL1F8,IL22R1-IL10R2,Jnk,Jun-GABP,MAS1,MKNK1,MNK1/2,MPZL1,P38 MAPK,PEBP4 (includes EG:157310),PHF1,PLC,POLR2B,PTPN21,RGS1,RGS12,RP6-213H19.1,RXFP3,SEC31A,SRC,SYN1,TRAF1-TRAF2-TRAF3,TRIB1,ZP3	24	15	Cellular Response to Therapeutics, Lipid Metabolism, Reproductive System Development and Function
5	ABCA2,ABCA7,ADAM23,AGT,ARHGAP8,ATP6V1G1,C11ORF49,cholesterol,DNALI1,FAM98B,FDPS,FRAP1,Frap1-Hd,GIGYF2,GSS,HTT,LANCL1,LSAMP,MPEG1,MRLC2,MYLIP,NUB1,OC90,PPP1R16B,PRR5,PSMA1,PSMD6,RAC1,SGK1,SRGAP1,SRGAP2,SRGAP3,Tsc1-Tsc2,TWISTNB,YWHAZ	21	14	Cell Morphology, Hematological System Development and Function, Humoral Immune Response
6	ABCA7,ADH6,ADH1A,ADH1C (includes EG:54224),ADHFE1,AGT,alcohol dehydrogenase,APP,ARHGAP8,ATN1,BACE2,CD160,cholesterol,CPA1,DBN1,ECM1,FDPS,GALE (includes EG:2582),GCC1,IL6,IMPDH1,MIRN202,MMEL1,MRLC2,MYLIP,OLFM1,PAX3,PCYT2,PHF15,PTGR1,RAC1,RCADH5,SAA4,SC5DL,TWISTNB	20	14	Cardiac Hypertrophy, Cardiovascular Disease, Developmental Disorder
7	AATK,ABCC4,B4GALT6,BPI,CACNG5,CBS (includes EG:875),CCR6,CYP3A1,DHRS3,EIF5A,GCA,GRIP1,KIF3C,melatonin,MYO9B,NR1I3,NRIP2,PAX8,PEX11A,PLA2G7,PLEKHA3,PPFIA3 (includes EG:8541),retinoic acid,RIMS3,ROR,RORB,SERPINB8,SLC5A5,SLCO1A2,SOD3,SYNPO,TMEM49,TNF,ZBTB7A,ZFP36	20	13	Cancer, Cell Cycle, Cellular Growth and Proliferation
8	BCL2L1,BNIPL,Ca2+,CD53,CLEC10A,CSH2,DBN1,FREQ,GALE (includes EG:2582),ICAM2,ICAM3,IGSF8,IL6,ITGB1,LPAR2,LPAR3,MYO10,NKD2,NMU,OLFM1,P2RY4,PAX3,phosphatidylinositol 4,5-diphosphate,PTGER3,RARRES2,SCRIB,SIGLEC1,SLC2A4,STK17B,STX12,SYTL2,TGFA,TPT1 (includes EG:22070),TSPAN3,XPNPEP1	20	13	Cell Signaling, Molecular Transport, Vitamin and Mineral Metabolism
9	ACSM3,ATN1,BACE2,beta-estradiol,C20ORF142,CNN2,DSC2,DSG2,ECM1,GCC1,HSD17B6,HSF2BP,IMPDH1,INSIG2,KDELRL3,KLK11,KRT81 (includes EG:3887),LTBP4,MAOA,MIR373,MIRN202,MSMB,MTMR10,MXD1,MYOF,NELL2,PDZK1IP1,PHF15,PKP2,RRBP1,SLC12A4,SMAD9,SPOCK1,SVEP1,TGFB1	18	12	Cardiovascular Disease, Genetic Disorder, Cellular Function and Maintenance

Table 5.6: IPA networks transcriptionally affected by both DMNQ and doxorubicin in an chronic model of toxicity. Table shows the results of IPA for genes significantly ($P \leq 0.01$) affected by both doxorubicin and DMNQ in an acute model of toxicity, giving an overall indication of the gene functions regulated by both compounds.

Both pathway analysis software packages implicate energy metabolism, oxidative phosphorylation and ATP binding, molecular transport and signalling as key modulators of acute toxicity. In the chronic model of toxicity, gross cytotoxicity following doxorubicin at the transcriptional level appears to be occurring due to the presence of the biological functions involving cellular response to xenobiotics, thus possibly masking the underlying mechanism; however the oxidative phosphorylation pathway was the only pathway differentially affected at all time points. The chronic model of DMNQ exposure resulted in less cardiotoxicity compared to doxorubicin, thus any pathway affected in this model potentially indicates the predisposing events resulting in cardiotoxicity.

5.2.4 TRANSCRIPTIONAL RESPONSES IN OXIDATIVE PHOSPHORYLATION GENES

Oxidative phosphorylation is essential for life and the production of adequate amounts of ATP to conduct cellular processes; this is achieved through the ETC and ATP synthase. Genes known to be involved in the oxidative phosphorylation pathway were identified using the NCBI database. Those that were significantly ($p \leq 0.05$) expressed are presented in Figure 5.5. Within the electron transport chain (ETC) complexes I, III and IV are primarily encoded by the mitochondrial genome, with complex II solely encoded by the nuclear genome implicating both genomes in the mechanism of cardiotoxicity. Initially following acute doxorubicin and DMNQ treatment genes within the oxidative phosphorylation pathway were transcriptionally increased in expression, but this was reversed by 120 hours following a single dose. This down-regulation of the ETC activity is likely to have consequences on all cellular processes within the heart. The greatest response in this pathway was observed following acute DMNQ. Induction of oxidative phosphorylation genes was observed from 5 minutes and 0.5 hours following a single dose of DMNQ (25mg/kg) or doxorubicin (15mg/kg), respectively.

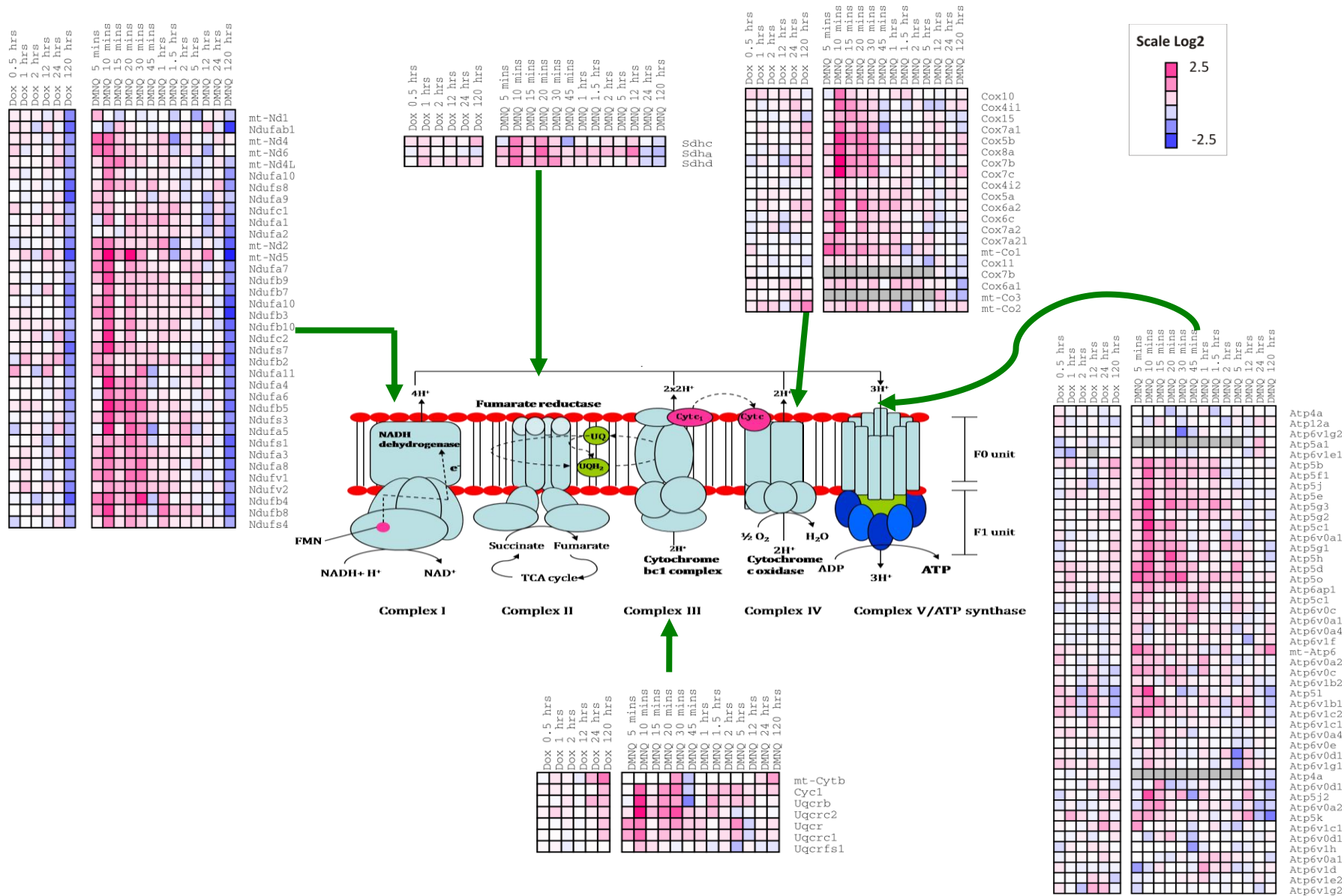


Figure 5.5: HCL of genes encoding the complexes of the ETC involved in oxidative phosphorylation. Genes included were significantly ($p \leq 0.05$) regulated following doxorubicin (15mg/kg, n=4) or DMNQ (25mg/kg, n=5).

5.2.5 TRANSCRIPTION RESPONSE IN NRF-1 TARGET GENES

Genes known to contain NRF-1 binding sites were identified using the NCBI database. In total fifteen genes were a known target of NRF-1 and fifteen were regulated by NRF-1, eight of which were both regulated by and were targets for, NRF-1. Genes transcriptionally differentially expressed at a significance of $p \leq 0.05$ at a minimum of two time points following both compounds were identified, a number of which were increased in expression (Figure 5.6).

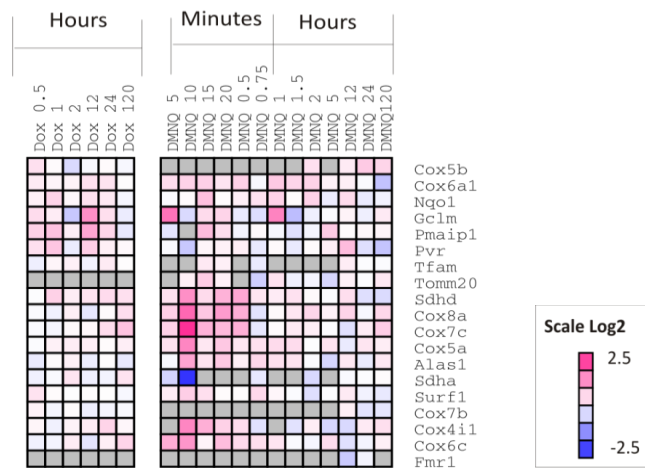


Figure 5.6: HCL of genes that were targeted or regulated by the transcription factor NRF-1. Genes included were significantly ($p \leq 0.05$) regulated following acute doxorubicin (15mg/kg, n=4) or DMNQ (25mg/kg, n=5).

5.2.6 qRT-PCR CONFIRMATION OF MICROARRAY DATA

Regulation of selected differentially expressed genes was verified by qRT-PCR (Chapter 2). Table 5.7 details the time points of study. Transcriptional gene expression data was generated following doxorubicin and DMNQ treatment in an acute and chronic model of toxicity (Figures 5.7, 5.8, 5.9 and 5.10). In general a high level of concordance between qRT-PCR data and microarray data was observed. Overall, the magnitude of change in expression was greater using qRT-PCR.

Model of Toxicity	Time points of study
Acute doxorubicin (15mg/kg)	0, 0.5, 1, 2, 12, 24 and 120 hours
Acute DMNQ (25mg/kg)	0, 0.1, 0.25, 0.5, 1.5, 2, 12, 24, 120 hours
Chronic doxorubicin (2mg/kg/week)	3, 5 and 7 weeks
Chronic DMNQ (2mg/kg/week)	3, 5 and 7 weeks

Table 5.7: Time points used to verify transcriptional microarray data by qRT-PCR.

One gene, *Tcap* (titin-cap), verified by qRT-PCR, demonstrated a maximum fold change of 5 and 48 over control following doxorubicin (15mg/kg) and DMNQ (25mg/kg), respectively. Due to this elevated expression in cardiac tissue, the expression in plasma following doxorubicin and DMNQ was determined. This demonstrated a decrease in *Tcap* expression (Figure 5.11).

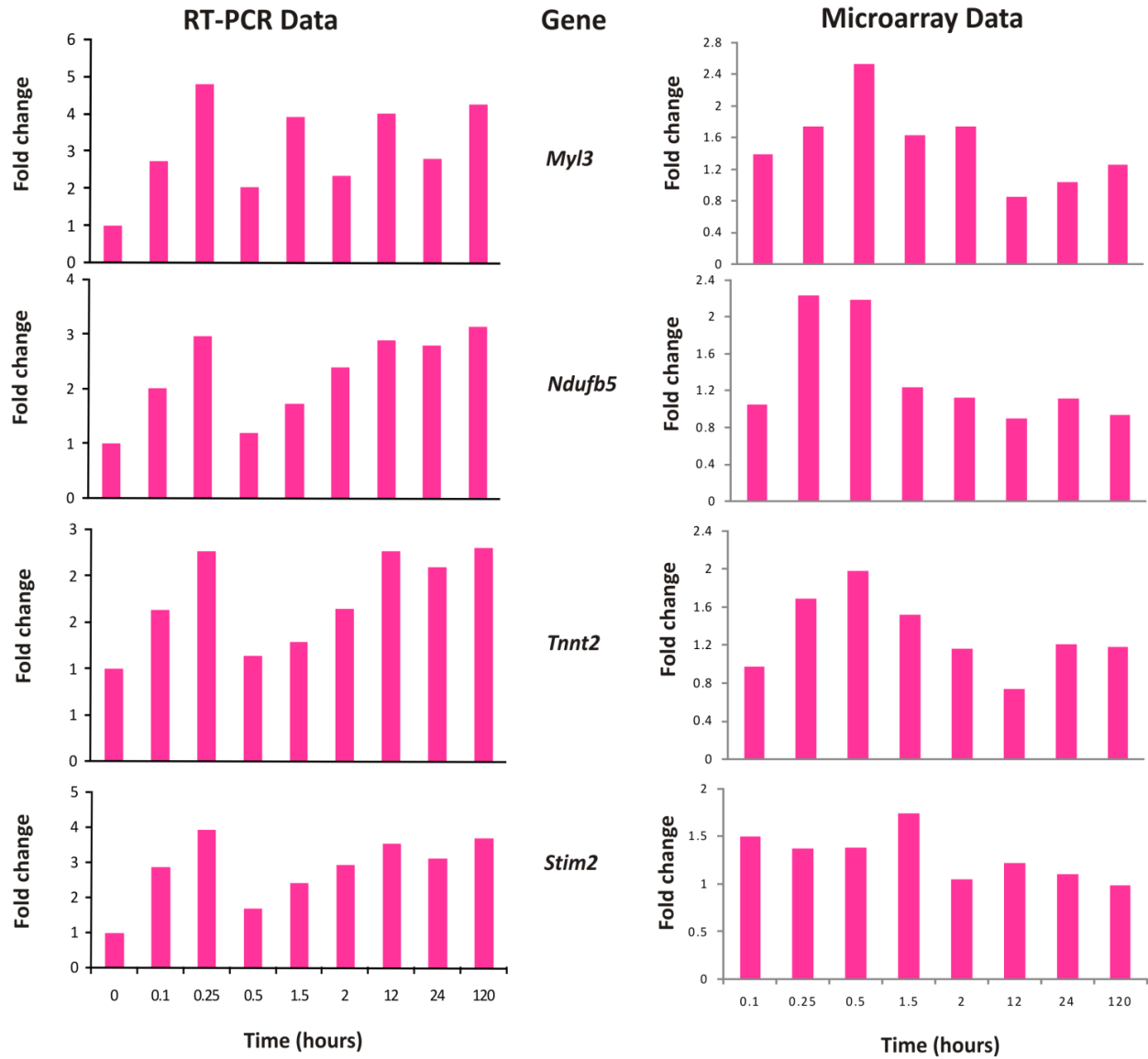


Figure 5.7: Confirmation of selected differentially regulated genes in an acute model of DMNQ toxicity. Results are means of n=5 for microarray data and n=3 for qRT-PCR.

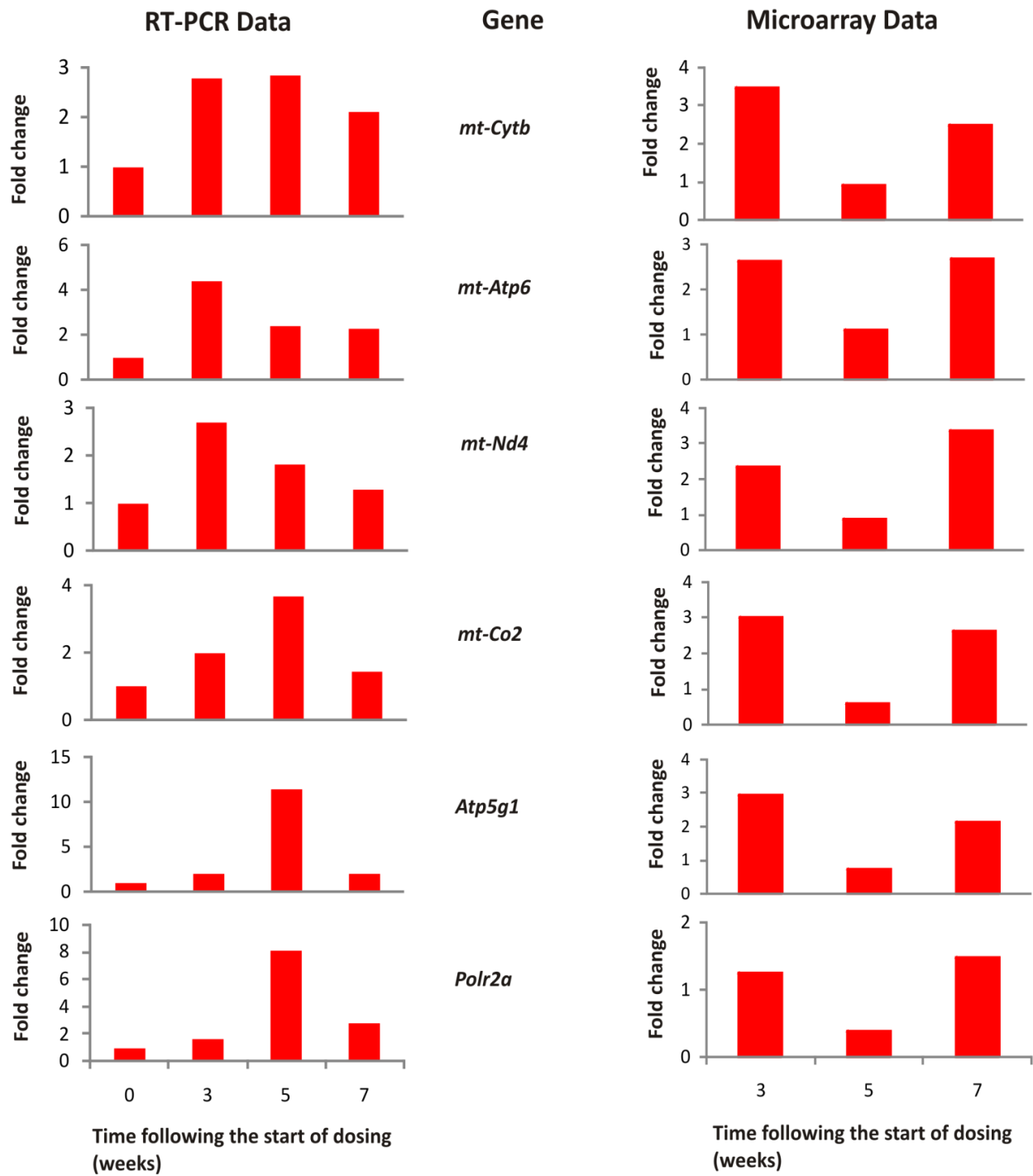


Figure 5.8: Confirmation of selected differentially regulated genes in a chronic model of DMNQ toxicity. Results are means of n=3 for microarray data and n=3 for qRT-PCR.

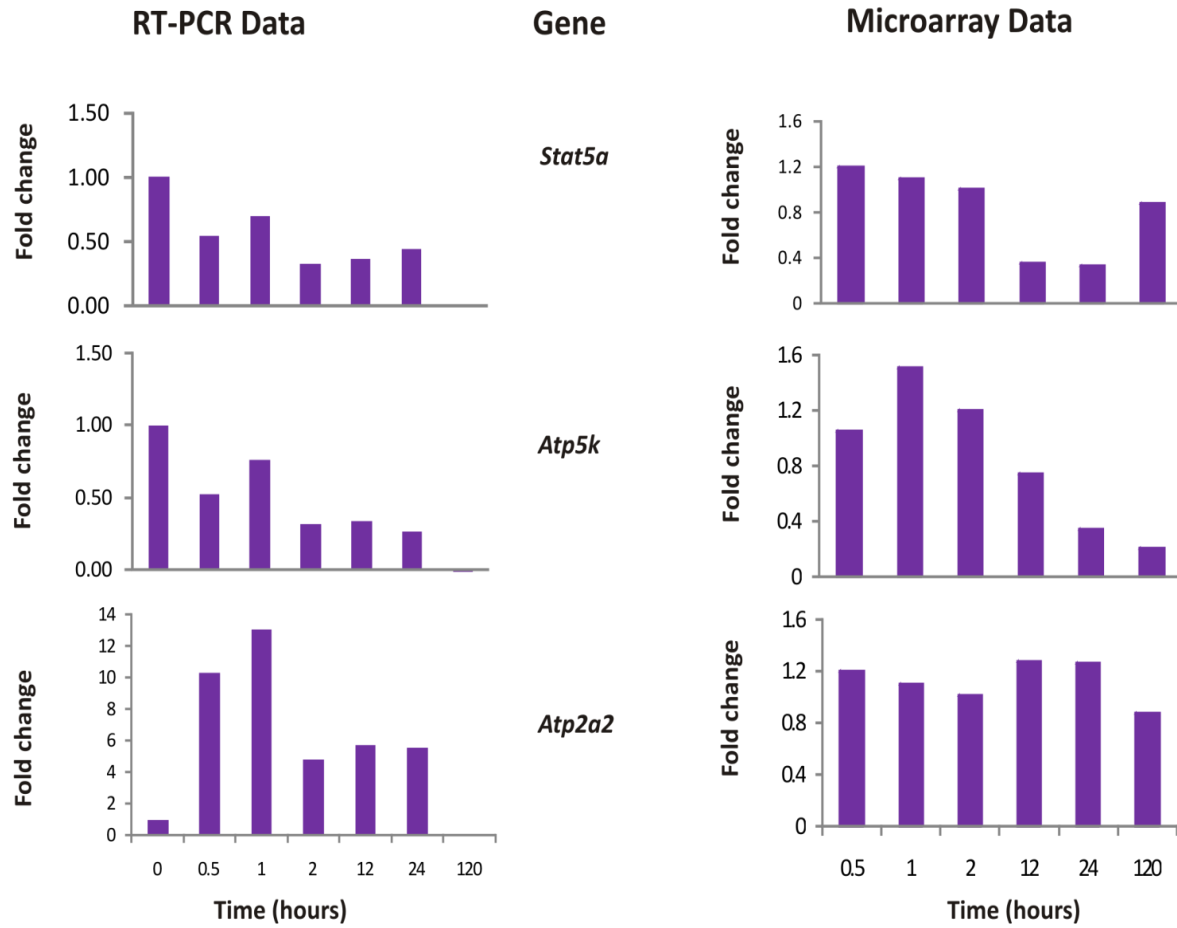


Figure 5.9: Confirmation of selected differentially regulated genes in an acute model of doxorubicin toxicity. Results are means of n=4 for microarray data and n=3 for qRT-PCR.

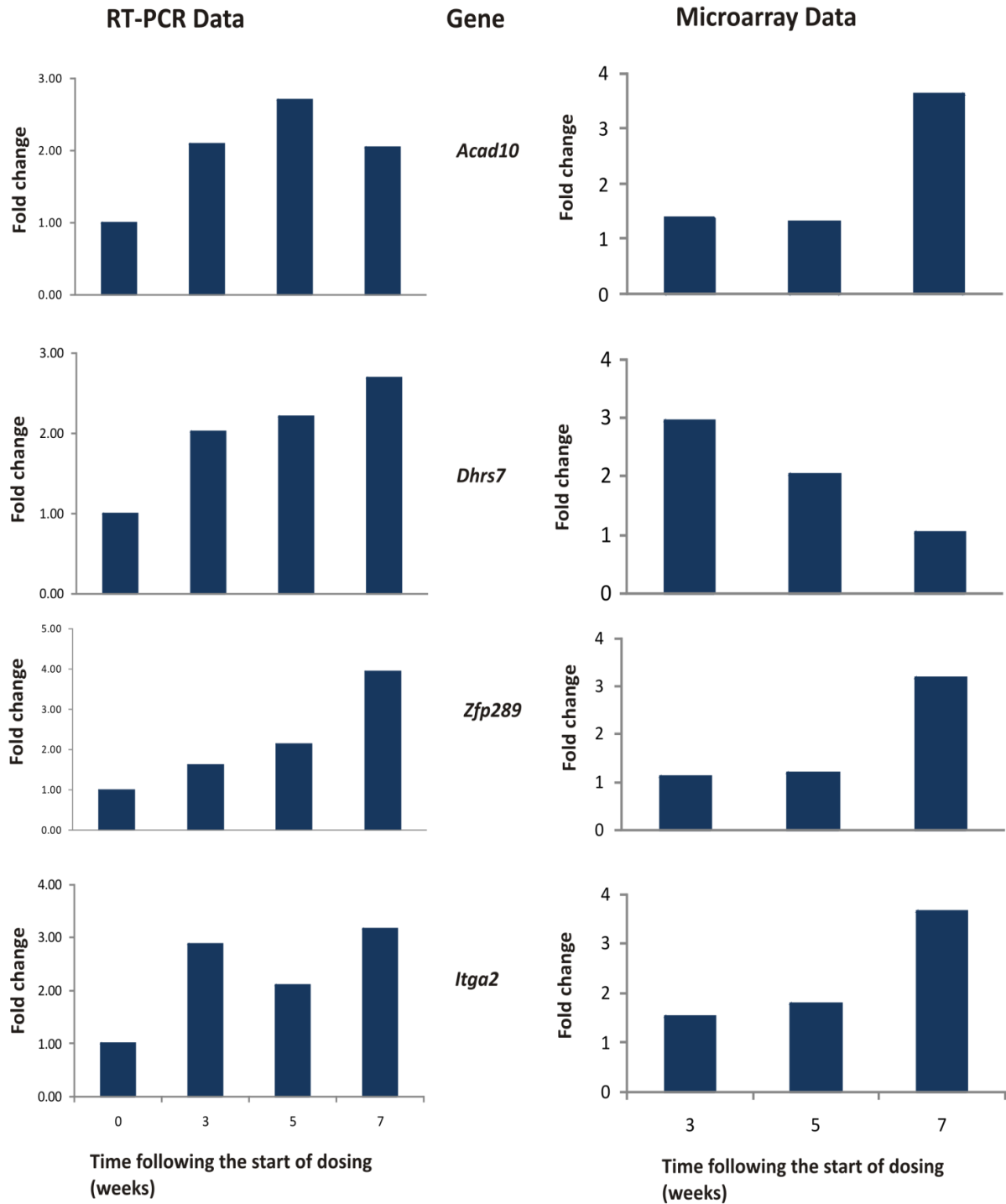
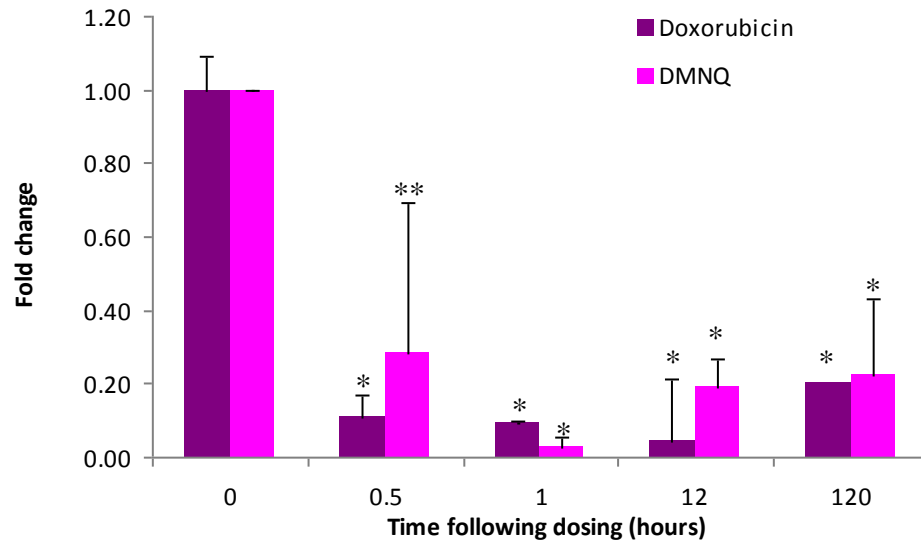


Figure 5.10: Confirmation of selected differentially regulated genes in a chronic model of doxorubicin toxicity. Results are means of n=3 for microarray data and n=3 for qRT-PCR.

A



B

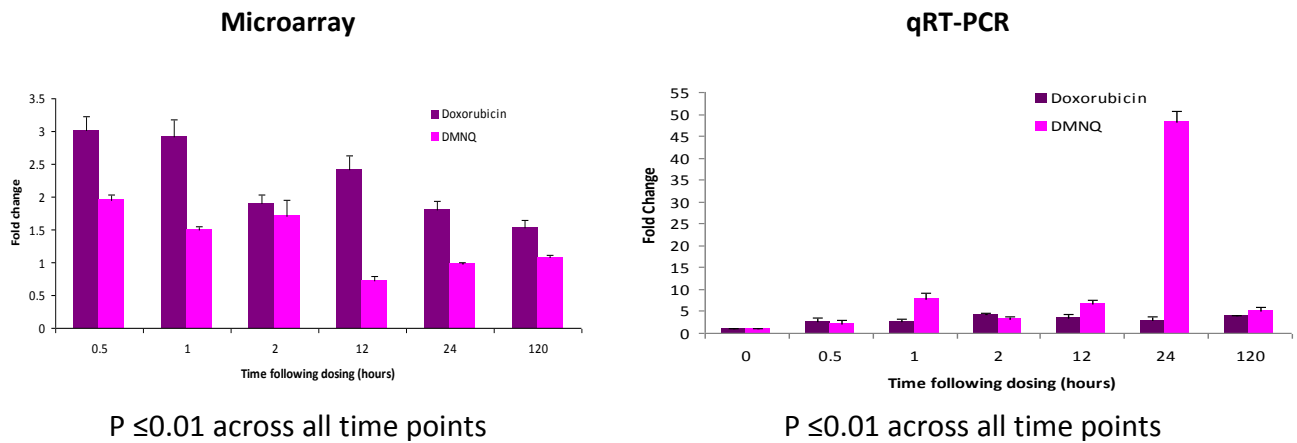


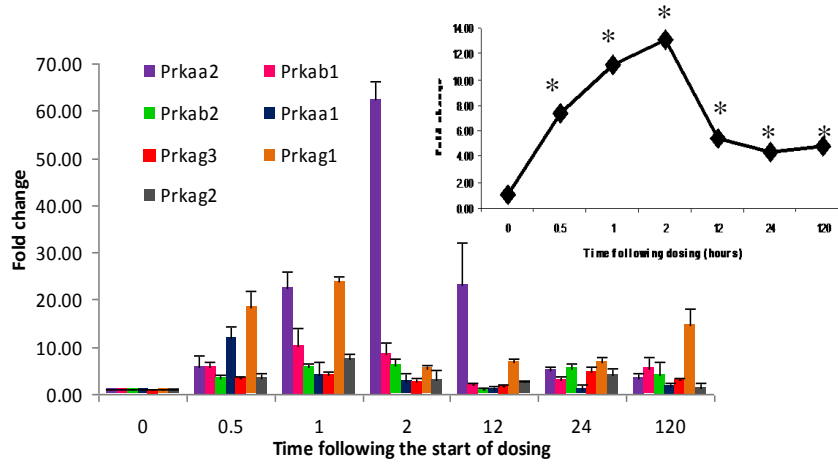
Figure 5.11: *Tcap* gene expression in plasma (A) measured by qRT-PCR (n=3) and cardiac tissue (B) measured by microarray analysis (n=4) and qRT-PCR (n=3). Results are mean values n=3 ±S.D, one way ANOVA and post-hoc Dunnett's T-test * p ≤ 0.01, ** p ≤ 0.03.

5.2.7 GENOMIC CONSEQUENCES OF CARDIAC DAMAGE

5.2.7.1 AMPK ACTIVITY

Following doxorubicin and DMNQ oxidative phosphorylation was the predominant pathway affected along with genes involved in glycolysis and the TCA cycle, suggestive of a change in energy substrate utilization. One protein activated during changes in energy dynamics is AMP-activated protein kinase (AMPK), a heterotrimeric protein kinase. AMPK is encoded by 7 genes (*Prkaa2*, *Prkab1*, *Prkab2*, *Prkaa1*, *Prkag3*, *Prkag1*, *Prkag2*). In situations of increased AMP:ATP ratios AMPK encoding genes will increase in expression characteristic of alterations in energy dynamics. Once activated AMPK inhibits the ATP consuming processes (e.g.: protein synthesis) and activates catabolic pathways resulting in ATP production (e.g.: glycolysis), in an attempt to maintain ATP production. qRT-PCR has been utilised to determine AMPK encoding gene expression (Figure 5.12). This identified an increase in AMPK encoding genes throughout the time course following acute doxorubicin (15mg/kg) and DMNQ (25mg/kg). Peak expression levels occurred 2 and 12 hours following doxorubicin and DMNQ, respectively, indicating a potential change in energy dynamics and substrate utilization. These effects on AMPK indicated a prolonged effect on cardiac muscle sustained following the clearance of both compounds (Chapter 3).

A



B

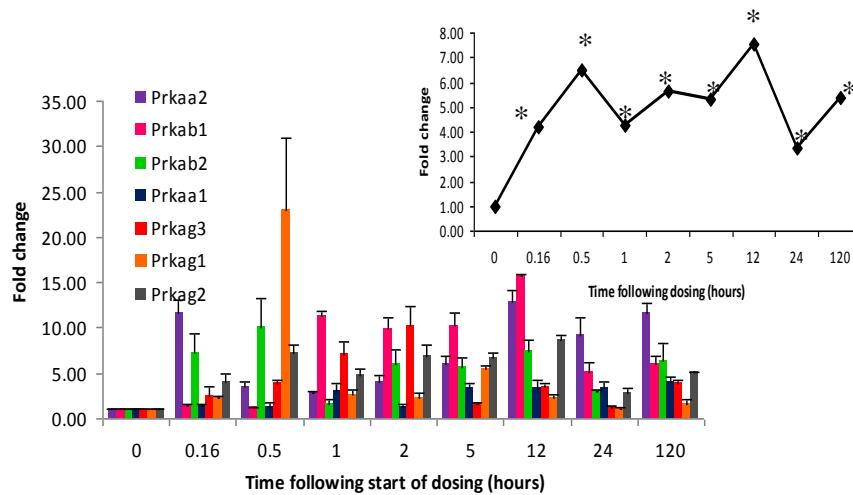


Figure 5.12: Transcription of genes encoding AMPK, following a single dose of doxorubicin (15mg/kg) (A) and DMNQ (25mg/kg) (B) measured using qRT-PCR. Inserts illustrate the average expression of AMPK transcripts at each time point. Results are mean values \pm S.D. (n=3). One way ANOVA and post-hoc Dunnett's T-test * p \leq 0.01.

5.2.7.2 mtDNA COPY NUMBER

Following identification of oxidative phosphorylation as the major pathway affected following DMNQ and doxorubicin, the mitochondrial transcripts appear to be differentially expressed. Mitochondria synthesise their own circular multicopy genome that is approximately 16kbp in size and encodes 13 polypeptides all involved in oxidative phosphorylation. Overall, genes encoded by the mitochondrial genome were upregulated (Figure 5.13). mtDNA copy number in cardiac tissue following either acute doxorubicin or DMNQ treatment was assessed using a quantitative PCR approach (Figure 5.14). mtDNA copy number increased following acute treatment with both compounds, peak levels occurred 1 and 0.16 hours following treatment with doxorubicin and DMNQ, respectively. Increased mitochondrial copy number continued throughout the time course to 120 hours.

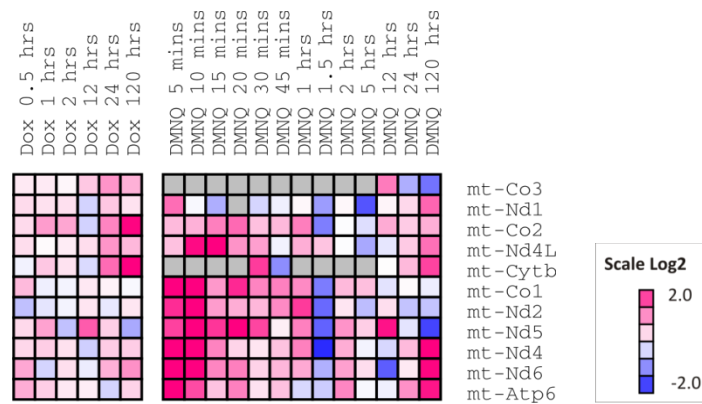
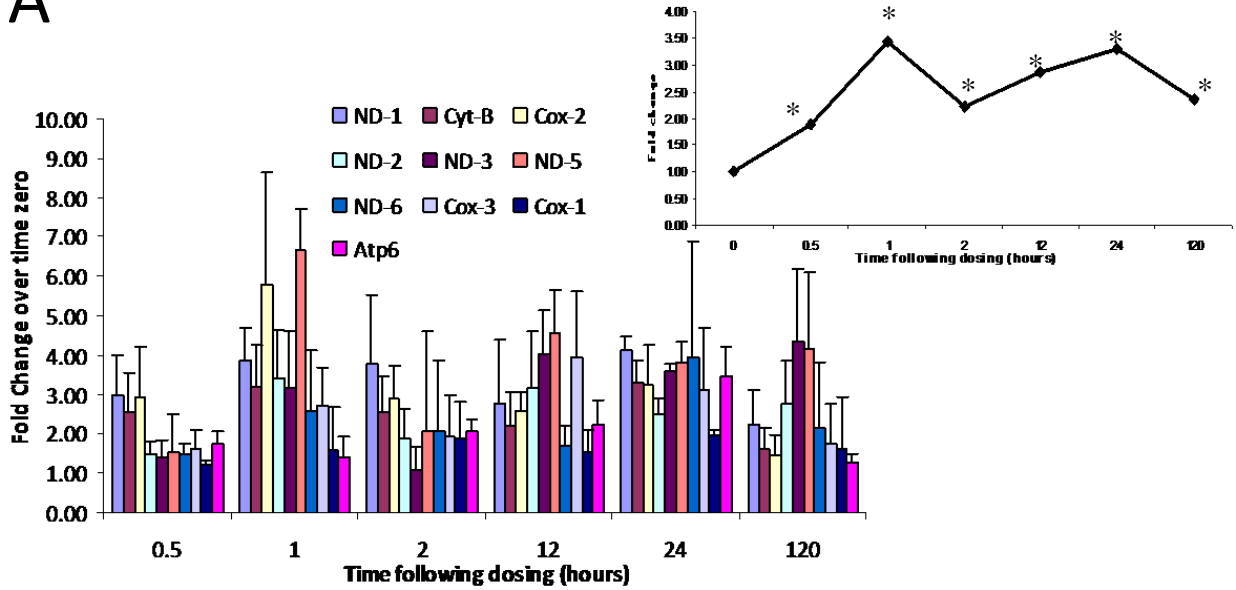


Figure 5.13: HCL of genes that are encoded by the mitochondrial genome. Genes included were significantly ($p \leq 0.05$) regulated following doxorubicin (15mg/kg) or DMNQ (25mg/kg). Results are mean values of $n \geq 4$.

A



B

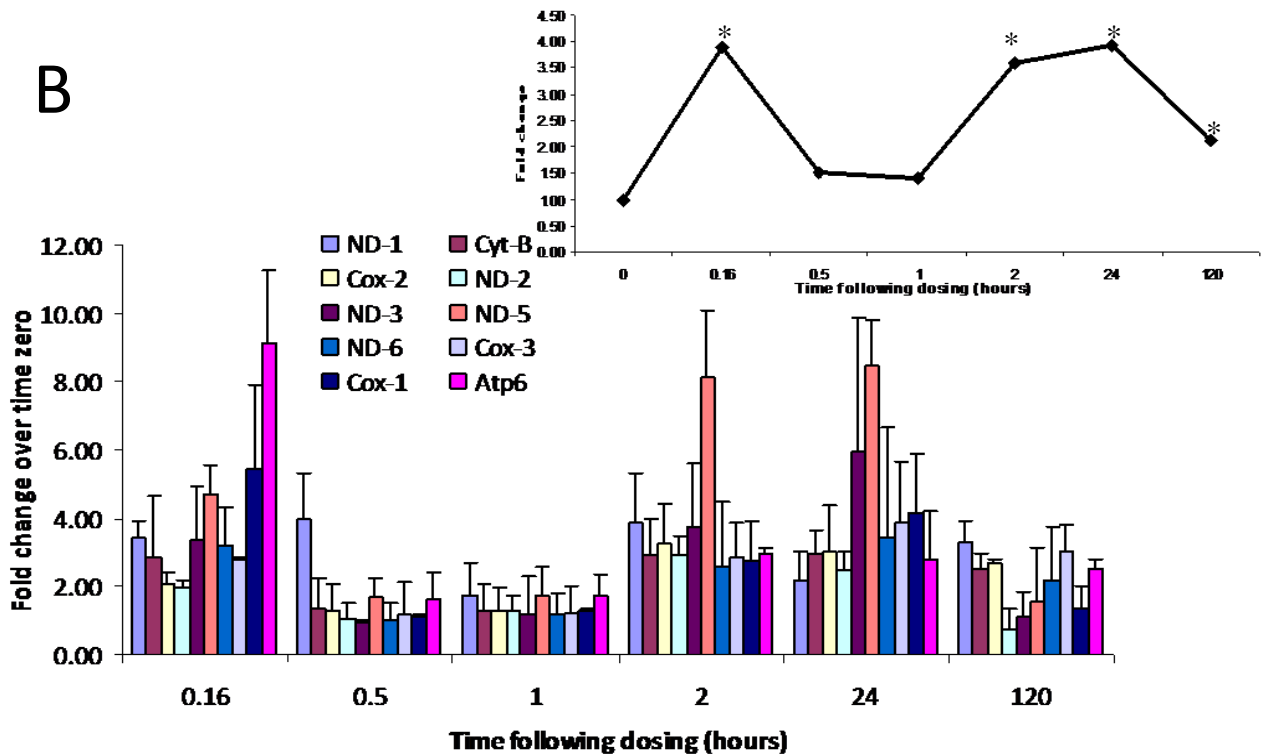


Figure 5.14: mtDNA copy number following acute doxorubicin (15mg/kg) (A) or DMNQ (25mg/kg) (B) treatment. Inserts illustrate the average mtDNA copy number at each time point. Results are mean values \pm S.D. (n=3). One way ANOVA and post-hoc Dunnett's T-test * $p \leq 0.01$.

5.2.8 ACTIVITY OF PROTEOLIPID COMPLEXES ON THE MITOCHONDRIAL MEMBRANE

Transcriptional profiling identified that the oxidative phosphorylation pathway was modulated. It is possible that proteolipid complexes involved in channelling ATP from the mitochondria to the cytosol ensuring efficient export of ATP and import of ADP and may also be affected (Tokarska-Schlattner et al. 2006). These complexes are composed of a number of proteins including adenine nucleotide translocator (ANT) and voltage dependent anion channel (VDAC) on the inner and outer mitochondrial membranes, respectively. The protein expression of both of these transmembrane protein complexes was measured by western blotting to assess the ability of cardiac mitochondria to export ATP to the cytosol. These proteins have also been implicated in the mitochondrial permeability transition pore. The protein expression of ANT and VDAC appear to be decreased following acute doxorubicin and DMNQ, indicating dysfunctional inner and outer mitochondrial membrane transport and function (Figure 5.15), however the effect on ANT was more pronounced.

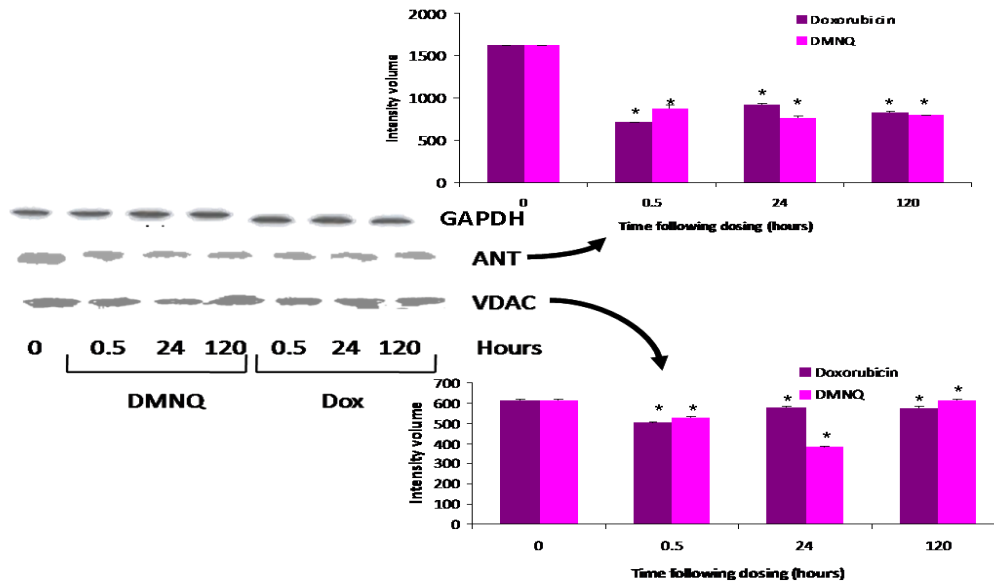


Figure 5.15: Western blots probed for ANT and VDAC following doxorubicin (15mg/kg) and DMNQ (25mg/kg), normalized to GAPDH with the relative intensities of each band plotted. Results are mean values \pm S.D. (n=3). One way ANOVA and post-hoc Dunnett's T-test * $p \leq 0.01$.

5.2.9 INVESTIGATION OF THE RAPID INDUCTION OF TRANSCRIPTION

Transcriptional profiling revealed rapid gene expression changes from 30 and 10 minutes following acute doxorubicin (15mg/kg) and DMNQ (25mg/kg), respectively. The exact mechanism for this rapid transcription was unclear. It may result due to induction of transcription factors promoting the induction of transcription, or through altered biochemistry resulting in a toxic response.

The protein expression of the transcription factor NRF-1 was assessed. NRF-1 is responsible for the transcription of a number of genes involved in oxidative phosphorylation (Figure 5.6). NRF-1 increases in expression from 10 minutes and 0.5 hours following DMNQ and doxorubicin, respectively, indicating a rapid induction of transcription factors (Figure 5.16A). This change in NRF-1 protein expression was prolonged and was still apparent at 120 hours following dosing. In order to assess transcription factor binding, a gel shift assay was conducted, allowing DNA binding to be directly measured (Figure 5.16B). This indicated a rapid increase in binding suggesting that transcription factor recruitment and binding maybe responsible for the rapid and prolonged changes in transcription observed.

In addition to the rapid activation of transcription factors, biochemical alterations may be contributing to the altered transcriptional profiles, particularly at the 10 minute time point following DMNQ. Using PCA, this time point was identified as being significantly different (Figures 5.2). Further clustering did not identify large differences in the genes transcriptionally altered but rather the magnitude of change. In order to further investigate this occurrence, methemoglobin levels were assessed following doxorubicin and DMNQ treatment. Methemoglobin is a form of haemoglobin but the iron in the heme group is ferric iron (Fe^{+3}) rendering the oxygen binding ability of heme dysfunctional. The level of methemoglobin can increase in response to a number of chemicals including quinones. Increases are associated with arrhythmias, palpitations and death if levels continue to rise. Methemoglobin can be converted back to haemoglobin by two methemoglobin reductase pathways, one utilises NADH to

donate an electron through cytochrome b5 resulting in the reduction to haemoglobin. The second pathway is an NADPH methemoglobin reductase pathway that utilises glucose-6-phosphate (this gene is transcriptionally down-regulated). 10 minutes following a single dose of DMNQ a significant elevation in methemoglobin compared to control was present. This is a situation that was reversed by 120 hours following dosing (Figure 5.17). Doxorubicin had no effect. This increase in methemoglobin may account for some of the profound changes in gene expression observed at the 10 minute time point following DMNQ. Overall it is probable that the rapid transcriptional expression changes were a result of quick activation or recruitment of transcription factors leading to perturbation of cellular pathways resulting in the observed effects on oxidative phosphorylation.

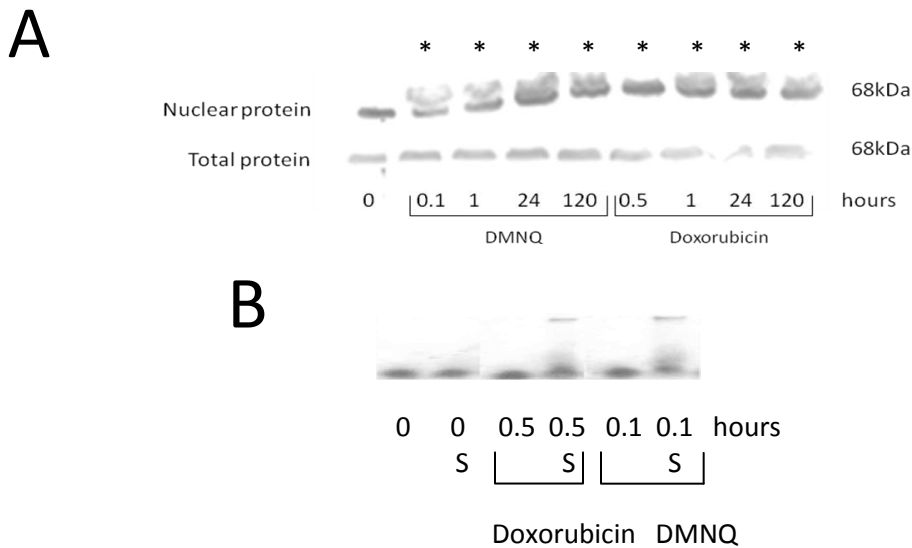


Figure 5.16: NRF-1 activity, protein expression level (A) and DNA binding (B) following a single dose of either DMNQ (25mg/kg) or doxorubicin (15mg/kg) in an acute model of toxicity. Results are n=3, one way ANOVA and post-hoc Dunnett's T-test, * p<0.01. S = supershift, if increased NRF-1 binding is present an extra band is present.

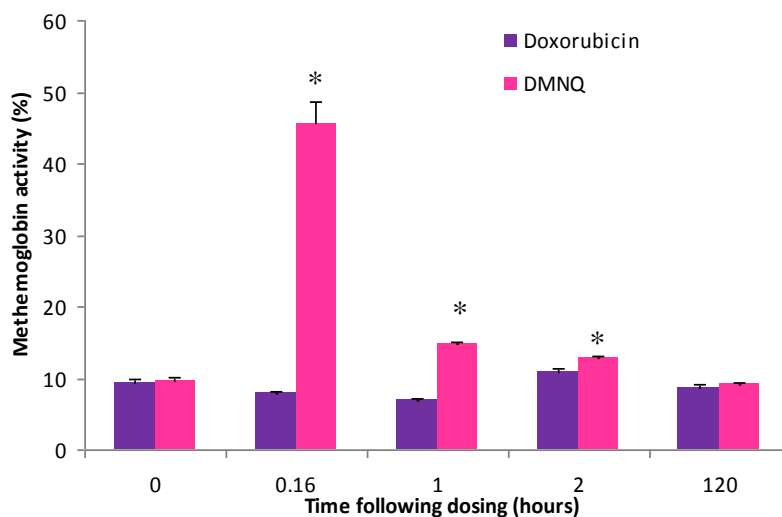


Figure 5.17: Methemoglobin activity following a single dose of doxorubicin (15mg/kg) and DMNQ (25mg/kg). Results are mean values \pm S.D. (n=3), one way ANOVA and post-hoc Dunnett's T-test * $p \leq 0.01$.

In order to further investigate the redox cycling hypothesis following doxorubicin (15mg/kg) GSH and GSSG levels were measured (Figure 5.18). No significant change in either GSH or GSSG was observed throughout the time course. This was in agreement with the lack of transcriptional response to redox stress or the activation of an anti-oxidant response. Similar results were found following DMNQ (Chapter 3).

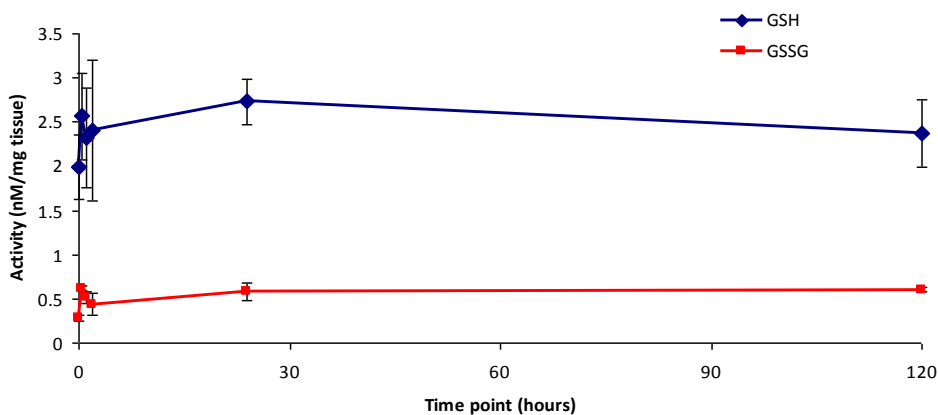


Figure 5.18: GSH and GSSG activity following a single dose of doxorubicin (15mg/kg). Results are mean values \pm S.D. (n=3) one way ANOVA and post-hoc Dunnett's T-test, no significant difference.

5.3 DISCUSSION

The overall aim of this chapter was to identify genes and pathways that were transcriptionally affected by doxorubicin and DMNQ in an acute and chronic model of toxicity. Transcriptional profiles of DMNQ, a pure redox cycling chemical, were generated and compared to those of doxorubicin. As DMNQ can redox cycle more effectively than doxorubicin, comparisons of the transcriptional profiles allow a greater insight into the mechanism of doxorubicin toxicity. Transcription was assessed in an acute and chronic model, allowing the cumulative effects of these compounds to be investigated. Overall, the transcriptional response induced in each model of toxicity was comparable in magnitude to the cardiac biochemical alterations identified in Chapter 4. DMNQ both in an acute and chronic model resulted in a greater number of differentially expressed genes. This, however, is most likely a result of an overall reduction in RNA synthesis following doxorubicin as a consequence of its pharmacological activity leading to inhibition or arrest of the cell cycle in the S phase, thus reducing transcription (Section 3.2.5). In addition greater transcription may have occurred following DMNQ due to the formation of methemoglobin 10 minutes following dosing, possibly inducing hypoxia, however no genomic changes associated with hypoxia e.g. HIF-1 α were observed, or the more ideal redox potential of DMNQ compared to doxorubicin may promote transcription, however no redox activation was apparent.

5.3.1 COMPARISON OF TRANSCRIPTIONAL EXPRESSION PROFILES

Cluster analysis revealed a high level of transcriptional similarity between doxorubicin and DMNQ acute and chronically (Figure 5.2). However, the chronic models were more diverse. This was most likely a consequence of the cumulative properties of doxorubicin and the reduced cardiotoxicity following chronic DMNQ treatment. DMNQ does not appear to have a cumulative affect either biochemically or genomically. This may have arisen due to the selected dose level of 2mg/kg/wk being insufficient to elicit a response, or more likely that DMNQ does not have cumulative properties. The later is probably a reflection of doxorubicin pharmacology, in particular the formation of DNA adducts and inhibition of

DNA synthesis. However, a number of genes were differentially affected following both doxorubicin and DMNQ acute and chronically (Table 5.2). These genes were involved in calcium ion binding, transcription factor activity, ATP binding, acetyl coenzyme A, cell death and NAD binding suggesting a role for increased calcium flux and transcriptional expression changes leading to changes in energy metabolism and substrate utilization.

5.3.2 IDENTIFICATION OF A MECHANISTIC CARDIOTOXIC GENE SIGNATURE

Transcriptional profiling in the acute model allowed the identification of 335 genes differentially expressed ($p \leq 0.01$) at a minimum of two consecutive time points acutely following doxorubicin and DMNQ. Overall this gene signature contained genes implicated in oxidative phosphorylation (Section 5.2.4 and 5.3.5), energy dynamics, ion channels and transcriptional and translational control.

Transcriptional response in the glycolysis pathway

Increased transcription of genes implicated in glycolysis is often observed in conditions of oxidative phosphorylation deregulation in order to attempt to increase ATP levels. The process of glycolysis converts one glucose molecule to two ATP molecules and oxidizes NAD^+ to NADH which is transferred to acetyl-coA in the TCA cycle. Twelve genes involved in the regulation of glycolysis were differentially affected by both doxorubicin and DMNQ, of which nine (*Hk1*, *Gp1*, *Pfhl*, *Aldoa*, *Tpi*, *Eno1*, *Pgk*, *Ldhd* and *Pkm2*) were up-regulated and three (*Gapds*, *Pck1* and *Pgam1*) were down-regulated (Altenberg and Greulich 2004). The key genes in this pathway are *Hk-1*, *PFK-1* and *Pkm2* (Altenberg and Greulich 2004), all of which were increased in expression. During the first step of this pathway *Hk-1* phosphorylates glucose to glucose-6-phosphate, enabling glucose to be used as an energy source. Whereas *PFK-1* catalyzes the irreversible conversion of fructose-6-phosphate to fructose 1, 6-bisphosphate in an ATP consuming reaction. The resulting fructose 1, 6-bisphosphate is required to allow the glycolytic pathway to proceed. The final step in this pathway is catalyzed by the enzyme pyruvate kinase that is encoded by

Pkm2. This process results in the production of ATP and pyruvate, which can enter the TCA cycle and thus drive further ATP generating pathways. Overall glycolysis is transcriptionally up-regulated indicating a change in substrate utilization to one that was more reliant on glucose.

In addition to its role in glycolysis, *Hk-1* has also been implicated in the regulation of cell death. *Hk-1* binds to VDAC on the outer mitochondrial membrane (whose protein expression was decreased following acute doxorubicin and DMNQ) and is thought to be capable of inhibiting the mPTP from opening and thus preventing leakage of the mitochondrial contents into the cytoplasm (Sun et al. 2008). Both mitochondrial binding and glucose phosphorylation need to proceed to result in inhibition of the mitochondrial permeability transition pore by *Hk-1*. Over-expression of *Hk-1* confers protection against cell death. Thus increased transcription of *Hk-1* as observed following doxorubicin and DMNQ may enable glycolysis driven ATP production and act to protect the cell from mitochondrial induced activation of the intrinsic pathway of apoptosis despite reduced VDAC expression.

Maintenance of the TCA cycle

Increased transcription of genes involved in the TCA cycle provides further evidence of effects on energy dynamics. In total nine genes (*CS*, *Aco2*, *Idh2*, *Ogdh*, *Sucla2*, *Sdha*, *FH*, *Mdh1* and *Suclg1*) involved in the TCA cycle were transcriptionally increased. The protein encoded by *CS* is the key enzyme in the TCA cycle that catalyses the synthesis of citrate from oxaloacetate and acetyl coenzyme A to initiate the TCA cycle (Siu et al. 2003). The enzyme encoded by this gene is inhibited in activity and transcription in the presence of high ATP and NADH concentrations, when sufficient ATP and substrates required for cellular processes are present. Thus, it can be assumed that this gene is transcriptionally increased at times of low ATP and NADH concentrations, indicating that the increase in *CS* observed in these models was an adaptive response to decreased oxidative phosphorylation (Section 5.3.5).

Regulation of ion channels

Different ion channels are vital to membrane polarisation and depolarisation during contraction and relaxation of cardiomyocytes (Mishra et al. 2009). Regulation of eight genes (*Tomm40*, *UCP2*, *Kcnh7*, *Kcnq1*, *Kcnn1*, *Kcnh2*, *Cacnb1* and *Cacna1b*) with known roles in the formation and function of ion channels within the cell were observed. Overall transcription of these genes was decreased throughout the time course. *Tomm40* is a channel forming subunit of the translocase of the mitochondrial outer membrane complex (Humphries et al. 2005). This complex is critical for protein import into the mitochondria from the site of synthesis in the cytosol. Increased Tomm40 protein expression is thought to be activated as a consequence of decreased VDAC expression (as observed following acute doxorubicin and DMNQ treatment) on the outer mitochondrial membrane (Kmita et al. 2004). Thus decreased *Tomm40* transcription results in compromised movement into the mitochondria, possibly as a result of compromised VDAC function. The observed decreased VDAC may result in altered membrane transport possibly resulting in dysfunctional ATP and ADP movement. This in turn may impact on energy dynamics or the release of pro-apoptotic factors from the mitochondria as a consequence of lowered membrane function, possibly activating apoptosis.

A number of potassium voltage gated channel genes (*Kcnh7*, *Kcnq1*, *Kcnn1* and *Kcnh2*) were decreased in expression, indicating abnormal repolarisation of the heart. Mutations in these potassium voltage gated channel genes are associated with the congenital heart condition, long QT syndrome, which indicates a role for these genes in cardiac pathology and possibly the development of the cardiotoxic phenotype (Zhang et al. 2006).

Cacnb1 and *Cacna1b* were both down-regulated following doxorubicin and DMNQ, these genes encode calcium channel voltage-dependent ion channels, which are thought to be involved in calcium influx into the cell and thus have a vital role in cell physiology including muscle contractions (Vitko et al. 2008). Knockout of *Cacnb1* in mice is associated with increased blood pressure and heart rate (Ino et al. 2001),

thus the observed down-regulation of these genes may be involved in the progression of the cardiotoxic phenotype. Decreased transcription of calcium voltage-dependent ion channels (as observed in these models) results in increased movement of calcium into the cell due to lack of control of these ion channels. Thus, increasing intracellular calcium concentrations, a known inducer of apoptotic cell death (Gustafsson and Goltlieb 2008). Doxorubicin cardiotoxicity has been previously implicated with impaired calcium channels, leading to cardiac dysfunction. However, this is not likely to be the primary mechanism responsible for the observed toxicity (Takemura and Fujiwara 2007).

5.3.3 EXPRESSION OF TCAP

A number of transcriptionally affected genes were further verified by qRT-PCR. A high concordance between the microarray data and qRT-PCR was apparent. One gene up-regulated was *Tcap*, which is highly expressed in the heart and involved in muscle assembly regulation at the sarcoplasmic disc. Markert et al. (2008) has recently proposed *Tcap* to function as part of a loop that allows signalling between the contractile apparatus and genes involved in muscle development. Both DMNQ and doxorubicin were found to significantly ($p < 0.01$) increase the expression of *Tcap* from 10 and 30 minutes following treatment. *Tcap* encodes the protein titin cap a sarcoplasmic protein. Cultured cardiomyocytes treated with $1\mu\text{M}$ doxorubicin have been found to result in degradation of this protein one hour following the start of treatment (Tokarska-Schlattner et al. 2006). This transcriptional increase in *Tcap* may thus be an adaptive response to overcome the sarcomera disruption. Over-expression of *Tcap* has been reported to result in decreased myostatin and disruption of the normal Z disc assembly and function (Markert et al. 2008). The Z disc is involved in the exchange of proteins during development. Disruption to this structure is likely to result in disruption to myofibril function and maintenance, leading to the development of compromised myocyte function and thus cardiac failure. siRNA experiments to knockout *Tcap* have been shown to result in a marked decrease in IGF-2, a growth factor present in skeletal muscle, and alterations in myofibril maintenance (Markert et al. 2008). In

addition, mutations in *Tcap* have been associated with the occurrence of cardiomyopathy (Hayashi et al. 2004). The rapid induction of increased *Tcap* gene expression following both doxorubicin and DMNQ raises the possibility of this gene being a novel genetic biomarker for cardiotoxicity, both in the pre-clinical and clinical setting. In order to further investigate a role for *Tcap* in cardiotoxicity, mRNA expression was assessed in plasma from doxorubicin and DMNQ treated animals (Figure 5.11). This revealed a decrease in expression of *Tcap* compared to control. *Tcap* is known to bind to titin to maintain sarcomere assembly. Therefore, *Tcap* may be increased in cardiac tissue in an effort to maintain sarcomere structure. Thus, *Tcap* is perhaps binding to titin at a higher frequency or more efficiently than under normal circumstances, which results in decreased expression in circulating plasma.

5.3.4 PATHWAY ANALYSIS

Pathway analysis utilising the Gene Set Analysis Toolkit and IPA was conducted to provide a high level functional overview of the transcriptional response to doxorubicin and DMNQ exposure. All pathway analysis programmes resulted in common pathways and processes being identified conferring a greater degree of confidence of the output. Differential transcription affected a number of cellular pathways predominantly oxidative phosphorylation, but also the TCA cycle, regulation of actin cytoskeleton, glycolysis, RNA polymerase and apoptosis (Figures 5.3, 5.4, Tables 5.5, 5.6). These data illustrate that doxorubicin and DMNQ exposure leads to activation of a signalling cascade, alternative energy generation pathways and transcription factor activation or suppression resulting in cell death and thus highlighting intracellular organs as the target site of action for both compounds. Figure 5.19 depicts a summary of the possible activation of pathways following DMNQ and doxorubicin in an acute model of toxicity. A number of these pathways were affected by both compounds in all models of toxicity. It is likely that this cohort of pathways affected by both compounds is responsible for the cardiotoxic phenotype described in Chapter 4. In a chronic model of toxicity, exposure appeared to lead to changes

in genes involved in small molecule biochemistry, cellular response to xenobiotics and significant changes in cardiovascular function. Changes in oxidation phosphorylation were also apparent but the above functions appear more prominent. This is probably due to the effects of cumulative dosing, which results in pathological changes masking the predisposing mechanism of toxicity following doxorubicin. Oxidative phosphorylation was the only pathway constantly regulated over all time points following chronic DMNQ.

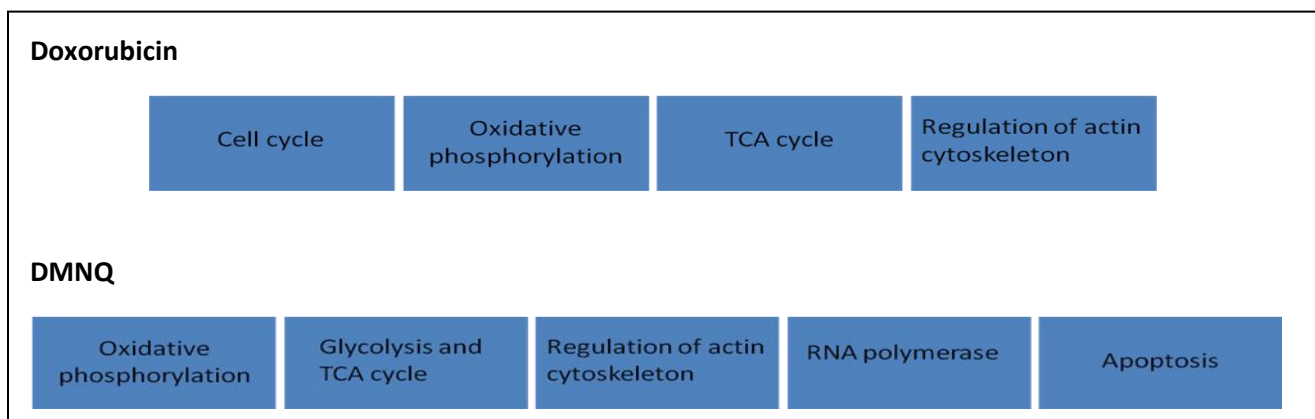


Figure 5.19: Summary of the prominent pathways activated following a single dose of either DMNQ (25mg/kg) or doxorubicin (15mg/kg) in cardiac tissue.

5.3.5 TRANSCRIPTIONAL RESPONSE TO OXIDATIVE PHOSPHORYLATION

Coordinated transcriptional regulation of genes involved in the oxidative phosphorylation pathway was apparent with doxorubicin and DMNQ (Figure 5.5). This effect is likely to be highly dependent on the redox potential and demonstrates how responsive the ETC genes are to disruption of electron flow in the chain. Overall complexes I-III were down-regulated in expression and complexes IV and V were up-regulated. Down-regulation of complex I will affect the formation of the proton gradient formed across the mitochondrial inner membrane that is required to produce ATP. This down-regulation of the oxidative phosphorylation pathway coordinates with the activation of genes encoding AMPK (Figure 5.12). AMPK is activated by a change in cellular energy dynamics (Tokarska-Schlattner et al. 2006). This increase in AMPK plays a key role in the regulation of energy substrate utilization in an attempt to

overcome the energy deficit and increase ATP production. The transcriptional up-regulation of complexes IV and V most probably occurs as a result of electrons bypassing part of the ETC and being received by complex IV or cytochrome c allowing increased electron flow through complexes IV and V. Alternatively, genes encoding complexes IV and V may be up-regulated to compensate for the down-regulation of the other complexes in an attempt to maintain electron flow through the chain. The heart is a highly energy dependent tissue and attempts to counteract this ATP depletion by up-regulation of genes encoding the TCA cycle and the glycolysis pathway. These data suggest the ETC maybe affected but also proteolipid complexes involved in channelling ATP from the mitochondria to the cytosol ensuring efficient export of ATP (Tokarska-Schlattner et al. 2006). These proteolipid complexes are composed of a number of proteins including ANT and VDAC on the inner and outer mitochondrial membrane, respectively. Western blotting revealed a decrease in activity of ANT and VDAC indicating a reduced function of the inner and outer mitochondrial membrane and thus reduced regulation of influx and efflux of molecules from the mitochondria to the cytosol (Figure 5.15).

Despite the fact that both doxorubicin and DMNQ are thought to redox cycle *in vivo*, resulting in the production of ROS and oxidative stress, no gene signature of this was apparent in the heart following either compound in an acute or chronic model of toxicity. This is in concordance with a chronic model of doxorubicin toxicity in the rat receiving the same dose level and similar study design only 8 genes relating to oxidative stress were identified in cardiac tissue (Berthiaume and Wallace 2007a). However this lack of a significant oxidative response does not directly imply a lack of ROS generation in the animal following doxorubicin and DMNQ exposure, but may indicate the inability of the heart to react to this type of damage or the organ not being the target organelle for ROS. The data presented here indicates the predominant mechanism behind the observed cardiotoxicity to be perturbation of the ETC.

Transcriptional profiling revealed differential expression of genes encoded from the mitochondrial genome (Figure 5.14). Mitochondria can have many copies of each gene, but unlike nuclear encoded DNA, mtDNA continues to replicate while DNA repair is being carried out. Consequently it has been hypothesised that mtDNA copy number would be diminished following treatment. However despite the apparent down-regulation of oxidative phosphorylation, mtDNA copy number increased a maximum 7 and 9 fold following acute doxorubicin and DMNQ, respectively (Figure 5.15). In concordance with this finding, several others have reported an increase in mtDNA copy number while mitochondria function is diminished. Similar increases have also been reported following ethidium bromide and benzene exposure (Shen et al. 2008; Chiaratti and Meirelles 2006). In both of these models diminished mitochondrial function was indicated by a decrease in mitochondrial membrane potential, indicating significant mitochondria dysfunction. Exposure to radiation also increases mtDNA copy number as a functional consequence of altered energy dynamics (Malakhova et al. 2005). The ophthalmologic condition leber's hereditary optic neuropathy (LHON) is similarly characterised by a decrease in mitochondrial function and has recently been found to increase mtDNA copy number (Hudson et al. 2007). This discrepancy between decreased mitochondria function and increased mtDNA copy number may be a compensatory mechanism to attempt to overcome the impaired mitochondrial respiration to maintain ATP production and thus correct cellular function and prevent the activation of cell death. Alternatively, animals treated with either doxorubicin or DMNQ may increase mtDNA copy number as a consequence of a feedback mechanism between the nuclear and mitochondrial genome as a possible response to altered energy dynamics. The mitochondrial transcription factor A (TFAM) is essential for mtDNA transcription and a key regulator of mtDNA copy number. However, this transcription factor is encoded by the nuclear genome, hence direct interaction or disruption of the mitochondrial genome may have a limited affect on function, if TFAM continues to function correctly. Microarray transcriptional profiling of TFAM revealed a transient effect on this transcription factor (Figure 5.6).

Thus, it is unlikely that this modulation would result in a significant decrease in mtDNA copy number. Transgenic mice that over-express TFAM demonstrate a marked increase in mtDNA copy number without any observed increase in ETC capacity, thus indicating that mtDNA copy number is separate from the functionality of the ETC (Ekstrand et al. 2004). Recently, Palmeira et al. (2007) found that mtDNA copy number may be regulated by glucose concentrations, suggesting increases in mtDNA copy number may occur as an indirect result of increased glycolysis as observed.

5.3.6 TRANSCRIPTIONAL RESPONSE TO MITOCHONDRIA DAMAGE

As described in section 1.4.4, PGC-1 α , the transcriptional co-activator, modulates a number of transcription factors (NRF-1, NRF-2, ERR α and PPAR α) that regulate the expression of genes involved in energy biogenesis. Transcriptional profiling and western blotting indicated down-regulation of PGC-1 α and increased expression of NRF-1, with the genes NRF-1 regulates also being differentially expressed (Figure 5.6). NRF-1 encodes a phosphorylated nuclear transcription factor regulating the transcription of a number of genes involved in mitochondrial function (Scarpulla 2008; Scarpulla 2006). Elevated NRF-1 DNA binding (as observed) is thought to activate AMPK and thus glycolysis and fatty acid oxidation and regulate cytochrome c. This may suggest that the rapid effects on transcription may result from a rapid induction of transcription factors. DMNQ was a more potent inducer of NRF-1 target genes than doxorubicin in this study. In total eight genes (*Cox6a1*, *Sdh*, *Cox8a*, *Cox7c*, *Cox5a*, *Alas1*, *Surf1* and *Cox6c*) were consistently up-regulated following DMNQ, whereas only four (*Cox6a1*, *Sdh*, *Cox7c* and *Cox5a*) were consistently up-regulated following doxorubicin. Of particular interest *Nqo1*, the gene that encodes the enzyme NQO1, which is involved in the detoxification of quinones, was only slightly transcriptionally increased in expression with both compounds. This increase was reversed to a slight down-regulation at 120 and 24 hours following doxorubicin and DMNQ, respectively. No other genes indicative of redox cycling or oxidative stress were modulated, thus the small change in *Nqo1* may be inconsequential. In addition the down-regulation of PGC-1 α , the co-activation of NRF-1 has previously

been associated with pathological stimuli. It has been proposed that decreased expression of PGC-1 α results in increased glucose utilization (Liang and Ward 2006). This finding in addition to the effects on oxidative phosphorylation, AMPK, glycolysis and the TCA cycle indicates deregulated energy metabolism to be fundamental to the mechanism of toxicity.

Previous studies have shown that doxorubicin has a high binding affinity to cardiolipin. Cardiolipin, present in the inner mitochondrial membrane, is essential to the function and assembly of the ETC proteins (Berthiaume and Wallace 2007a). This binding may initiate the down-regulation of the oxidative phosphorylation pathway and the subsequent cardiac damage observed following doxorubicin (Goormaghtigh et al. 1990; Goormaghtigh et al. 1986). The gene *Mecep2* is responsible for cardiolipin metabolic processes and was transcriptionally decreased following acute doxorubicin and DMNQ. In contrast, the genes *Klc3* and *Taz* (involved in cardiolipin synthase and biosynthetic processes, respectively) were up-regulated in the same models. This suggests that doxorubicin binding to cardiolipin prevents cardiolipin metabolic processes and impact on membrane kinetics. However the expression of genes encoding the ETC were more predominantly influenced. In addition to the identification of cardiolipin doxorubicin binding, both the mitochondria and nuclei membranes have been further identified as key sites of interaction for doxorubicin. The concentration of doxorubicin at these sites is considerably higher than in the surrounding circulating plasma, further confirming the affinity doxorubicin has for the mitochondria (Tokarska-Schlattner et al. 2006). Genes in all complexes within the ETC were affected, including those that are encoded by the mitochondrial genome. This along with decreased ANT and VDAC expression (affecting ATP and ADP influx and efflux and possibly opening of the mPTP), increased mtDNA copy number, rapid activation of transcription factors involved in energy dynamics and activation of AMPK, identifies the mitochondria and mitochondrial energy production as an important target for doxorubicin-induced cellular mitochondrial damage (Chapter 4) and activation of biomarkers of cardiac disease (Figure 5.20). However, this observed mitochondrial

damage appeared to be apparent in a chronic model of toxicity suggesting changes in mitochondrial pathology have a prolonged effect. The maximal oxygen consumption of patient's treated with doxorubicin is reduced in the long term, indicating a long term affect on mitochondria and energy dynamics (Tokarska-Schlattner et al. 2006). This may result from imprinting on cardiac tissue or damage to mtDNA or nDNA transcription, resulting in altered coding sequences for ETC proteins and permanent mitochondrial damage (Berthiaume and Wallace 2007a).

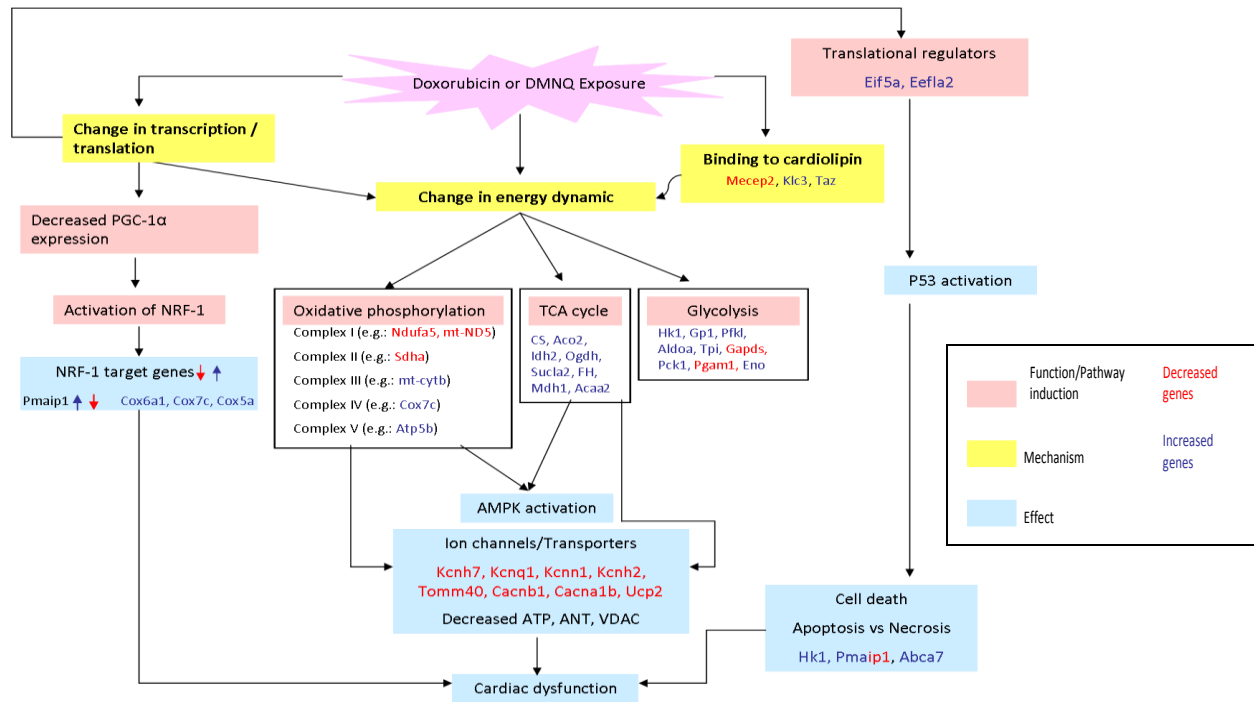


Figure 5.20: Schematic summary of the possible mechanisms of doxorubicin cardiotoxicity with transcriptional modulated genes highlighted.

5.3.7 SUMMARY

The findings of this study indicate genomic alterations to be involved in the cardiotoxic phenotype following doxorubicin and DMNQ. The overall level of transcription following doxorubicin was reduced compared to DMNQ. The oxidative phosphorylation pathway and associated changes in glycolysis, the

TCA cycle, AMPK, mtDNA copy number, ANT and VDAC proteins, and NRF-1 binding appear to be vital to the progression of the cardiotoxic phenotype following doxorubicin and DMNQ in an acute and chronic model of toxicity. Peak genomic changes correlated with the biochemical alterations identified in Chapter 4. However, not all genes that were transcriptionally modulated in expression will result in altered protein synthesis. In order to gain a greater genomic insight into the mechanisms of doxorubicin-induced cardiotoxicity that were identified in this chapter, mRNA translational profiling (Chapter 7) and miRNA expression profiles (Chapter 6) have been investigated.

**Chapter 6: microRNA Response of the Heart *In Vivo*
following Doxorubicin and DMNQ Exposure**

6.1 INTRODUCTION

Over the past 10 years the study of genomics has primarily focused on the analysis of mRNA expression (transcriptomics). Transcriptional investigations were conducted using cardiac tissue from C57B6/AJ male mice treated with doxorubicin or DMNQ in an acute and chronic model of toxicity and established a signature of genes and pathways that were significantly differentially expressed, as described in Chapter 5.

During the process by which protein is synthesised from a gene there are a number of intermediate control points. One post-transcriptional control mechanism is microRNAs (miRNAs) (Sections 1.5.3 and 1.5.4). These small non-coding RNA species are transcribed from the genome, but are not themselves translated into protein. Instead they regulate gene expression post-transcriptionally by affecting the degradation and translation of target mRNAs (Chen et al. 2009; Wang et al 2008). Genomics can be used to analyse miRNA expression, allowing a more complete picture of gene regulation.

miRNAs have been implicated in a range of biological processes (e.g.: cell proliferation and differentiation) and disease states (e.g.: cancer, cardiac dysfunction) (Shivdasani et al. 2006). Over the past four years it has been discovered that miRNAs have a fundamental role in cardiac disease and development (Matkovich et al. 2009; Chien 2007; Thum et al. 2007). It has become increasingly evident that miRNAs are regulated in cardiac dysfunction and possibly have the capacity to create cardiac pathology. A small number of miRNAs have been found to be muscle specific in expression (miR-1, miR-208 and miR-133a), others are significantly modulated in expression during cardiac dysfunction (e.g.: miR-21, miR-29, miR-27b, miR-195 and miR-126) (Figures 1.13 and 1.14). The mechanisms for these tissue specific expression patterns are currently unknown (Thum et al. 2008; Yang et al. 2008; Bruneau 2005). However, they have revealed a novel mechanism by which the proteome is regulated during the dynamic events of cell lineage development and morphogenesis (Zhao and Srivastava 2007).

Due to the importance of miRNAs in cardiac disease, it was hypothesised that miRNA expression in the heart would be modulated in response to xenobiotic challenge and thus be important in cardiotoxicity. To date no data implicating miRNAs in cardiotoxicity are available. However, as miRNAs are transcribed from the genome under the control of RNA polymerase II promoters, which often contain toxicological significant enhancer regions (Taylor and Gant 2008) and are often a target for pharmaceuticals, it was predicted that miRNAs would be involved in toxicology in addition to cardiac biology.

6.1.1 PLAN OF INVESTIGATION

Previous dose levels used in Chapters 4 and 5 were utilised to allow comparison between data sets. miRNA expression profiles were generated utilizing microarray technology. Due to the small size of mature miRNAs (21-23nt) and the lack of a poly A tail, conventional microarray labelling techniques cannot be used. Instead, a form of end labelling was utilised (Gant et al. 2009). For this purpose a poly A tail is attached to the miRNA before ligation to the chosen fluorophore. The small length and base pair similarity between different miRNAs is also problematic when using standard DNA-based microarrays. In this study locked nucleic acid (LNA) probes (miRCURY™ LNA probes, Exiqon) were utilised. These probes contain a locked ribose ring making them high affinity RNA mimics and increasing the thermal stability of the hybridization product, which allows greater specificity and sensitivity (Gant et al. 2009; Castoldi et al. 2006).

6.1.2 HYPOTHESIS AND AIM

The overall aim of this study was to define the miRNA expression profiles following dosing with doxorubicin and DMNQ in both an acute and chronic model of toxicity. It was hypothesised that doxorubicin and DMNQ treatment would result in a signature of differentially affected miRNAs, allowing further unique insight into the key mechanisms through which doxorubicin mediates its cardiotoxic effects and possibly identifying future drug targets.

6.2 RESULTS

6.2.1 miRNA EXPRESSION PROFILES

miRNAs were chosen for inclusion in the analysis if a miRNA had one significant time point at $p \leq 0.05$ (this gave a false positive rate of 75 miRNAs) within the time course. In an acute model of toxicity this in total gave 316 miRNAs for DMNQ and 264 miRNAs for doxorubicin, of which 145 were affected by both compounds. In a chronic model of toxicity 233 miRNAs were significantly affected by DMNQ and 381 by doxorubicin, of which 156 miRNAs were affected by both compounds. Further hierarchical clustering was conducted to visualize the cohort of miRNAs affected by both compounds in an acute (Figure 6.1) and chronic (Figure 6.2) model of toxicity. Only those miRNAs with known names were included. This highlighted a number of miRNAs that have been implicated with cardiac damage previously, including miR-181b, miR-29a, and miR-133a/133b in both models of toxicity and the cardiac specific miR-208 in the chronic model (Wang et al. 2009a). miR-208 is implicated with cardiac contractility, indicating a greater impact on cardiac function following chronic exposure to doxorubicin and DMNQ (van Rooij et al. 2008).

In order to gain further functional information about the miRNA expression profile of the cohort of miRNAs significantly affected by doxorubicin and DMNQ in an acute model, the genomic localization from where each miRNA was transcribed from was determined using publically available databases (<http://143.210.176.81/SystemsToxicology/Home.aspx>). In total the mouse has 19 chromosomes in addition to sex specific X and Y chromosomes. miRNAs were differentially transcribed from all but one of the 19 chromosomes (chromosome 15), with chromosomes 11 and 12 coding for the largest number of differentially expressed miRNAs (representing 8.95% and 17.91% of miRNAs, respectively) (Figure 6.1). Further principle component analysis (PCA) was conducted to directly assess the profiles of miRNAs affected in both acute and chronic models of toxicity following both doxorubicin and DMNQ (Figure 6.3A). PCA indicated three main clusters. The first cluster contained acute DMNQ <0.75 hour

time points. The second cluster contained acute doxorubicin, acute DMNQ >0.75 hours and selected chronic doxorubicin (week 3) time points. The final cluster contained chronic DMNQ time points. Chronic doxorubicin time points week 5 and 7 were both divergent from the main clusters, indicating distinct miRNA expression profiles, maybe due to the development of cumulative toxicity throughout the time course. This may result in a gradual accumulation of pathological change, the effects of which may be masking the predisposing biochemistry following doxorubicin and the modulation of miRNA expression.

In order to compare the acute models of toxicity following doxorubicin and DMNQ in isolation, further PCA was conducted to compare the expression profiles (Figure 6.3B). This analysis revealed a distinct difference between the two models of toxicity, which may be a result of doxorubicin's pharmacological action. A number of miRNAs including miR-22, miR-222, miR-195, miR-15a and miR-18a all involved in cell cycle regulation or tumour suppression were modulated in expression following acute doxorubicin treatment but not DMNQ exposure (Bandi et al. 2009; Tsang and Kwok 2009; Xu et al. 2009; Chivukula and Mendell 2008). This clustering, however, indicated that modulation of miRNA expression is a vital event following xenobiotic exposure. In total 38 miRNAs were affected by both doxorubicin and DMNQ in an acute and chronic model of toxicity (Figure 6.4).

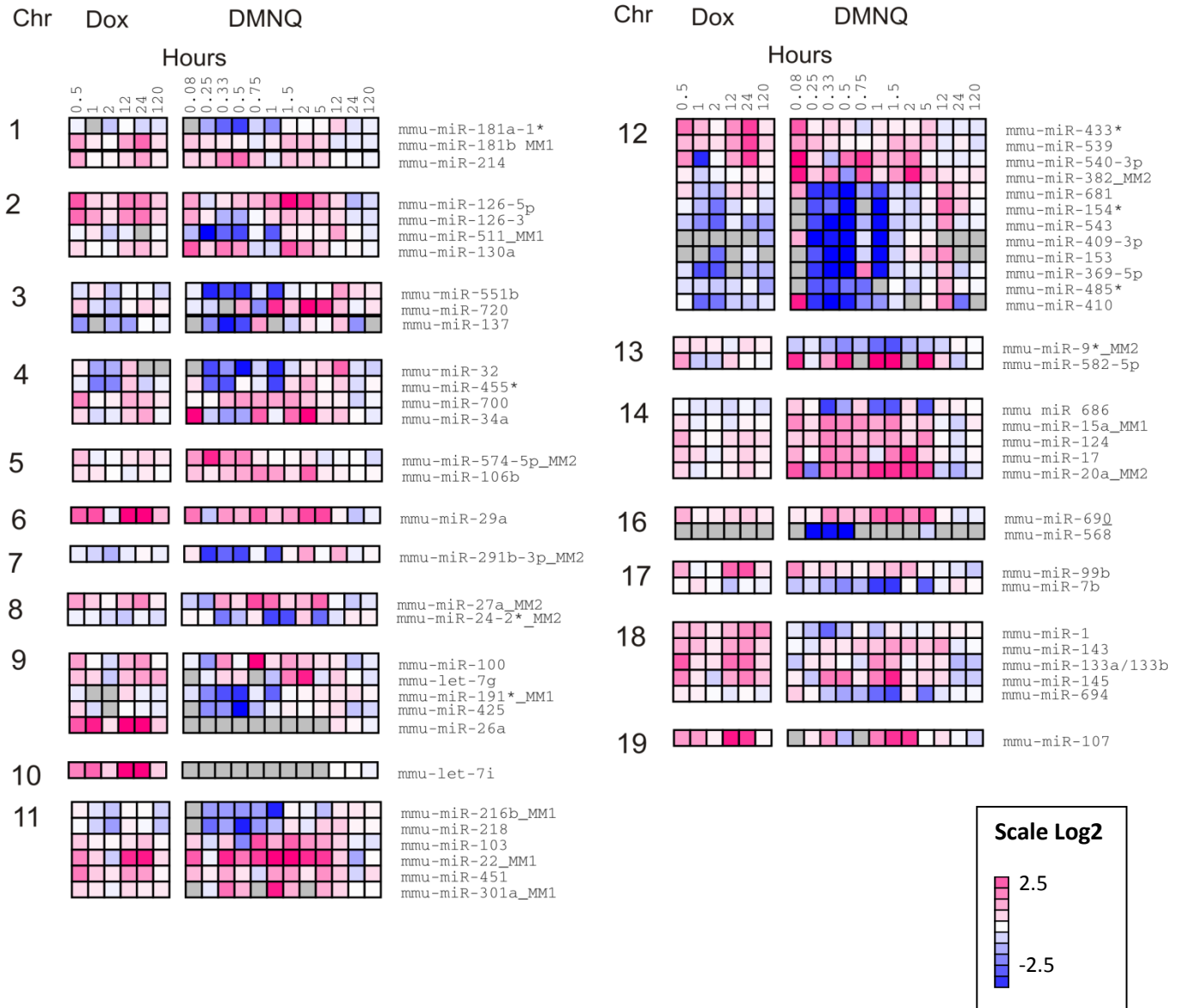


Figure 6.1: Clustering of miRNAs significantly affected in an acute model of doxorubicin and DMNQ toxicity. miRNAs included were significantly ($p \leq 0.05$, one sample two tailed t-test) regulated at $\text{Log}_2 < 1$ or $\text{Log}_2 > 1$ at a minimum of two time points following either acute doxorubicin (15mg/kg, $n=4$) or DMNQ (25mg/kg, $n=5$), chromosome (Chr).

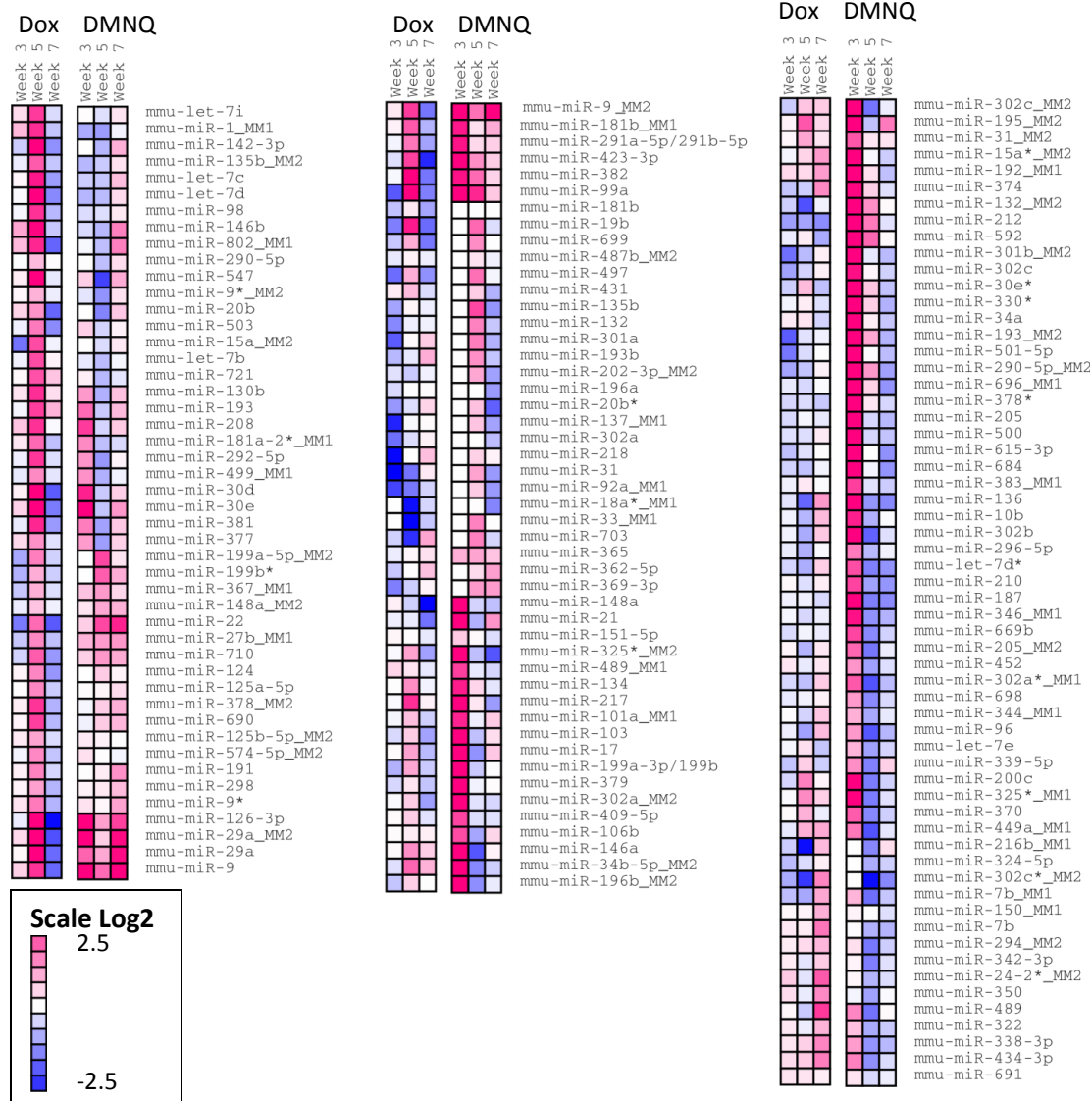


Figure 6.2: Clustering of miRNAs significantly affected in a chronic model of doxorubicin and DMNQ toxicity. miRNAs included were significantly ($p \leq 0.05$, one sample two tailed t-test) regulated at $\text{Log}_2 < 1$ or $\text{Log}_2 > 1$ at all time points following either doxorubicin (2mg/kg/week) or DMNQ (2mg/kg/week), $n=3$.

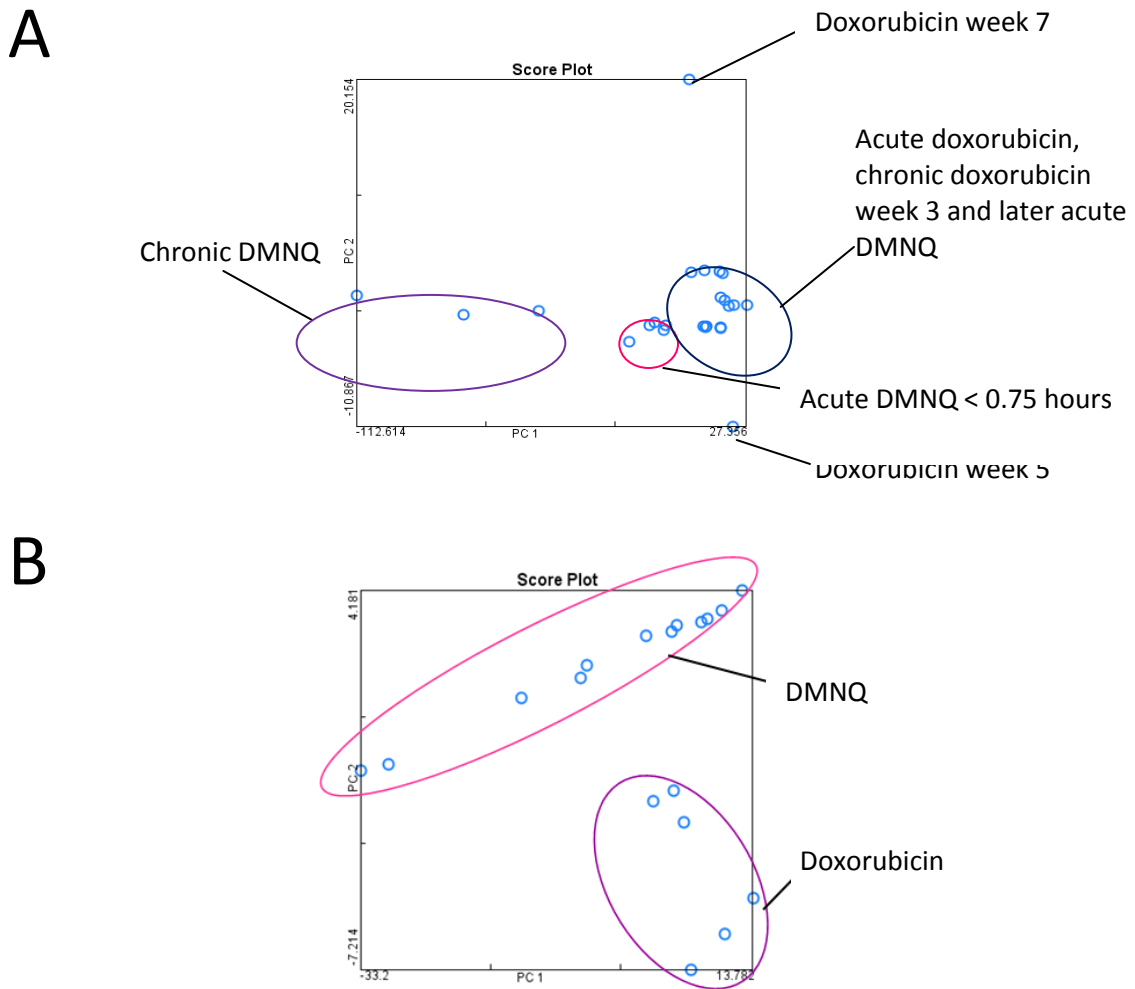


Figure 6.3: Clustering of miRNAs significantly affected by doxorubicin and DMNQ. PCA carried out using miRNA profiles following all models of toxicity (doxorubicin and DMNQ administration acute and chronically) (A), and those affected following acute exposure to doxorubicin and DMNQ (B). miRNAs included are the mean results of $n > 3$ and significantly ($p \leq 0.05$, one sample two tailed t-test) regulated at $\text{Log}_2 < 1$ or $\text{Log}_2 > 1$ at a minimum of one time point following either doxorubicin (15mg/kg or 2mg/kg/week) or DMNQ (25mg/kg or 2mg/kg/week).

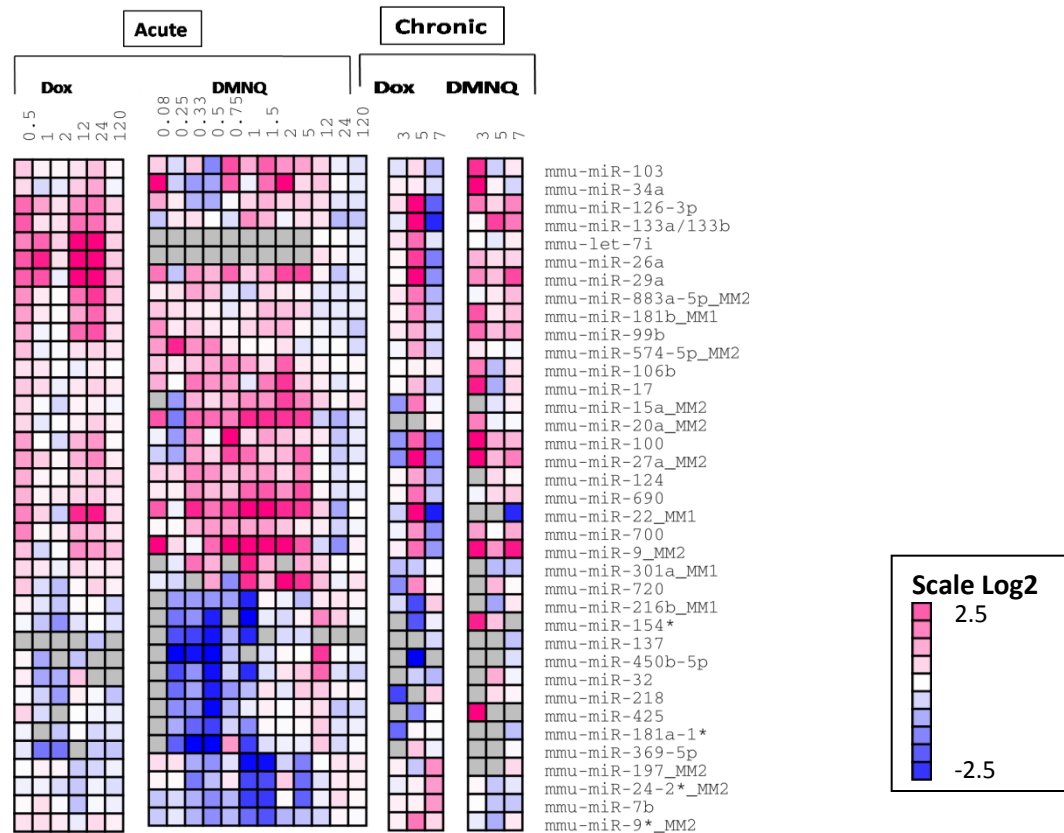


Figure 6.4: Clustering of miRNAs significantly affected in all models of toxicity. HCL carried out using miRNAs modulated in expression at a minimum of one time point in all models of toxicity. miRNAs included are the mean results of $n > 3$ and significantly ($p \leq 0.05$, one sample two tailed t-test) regulated at $\text{Log}_2 < 1$ or $\text{Log}_2 > 1$ at a minimum of one time point following either doxorubicin (15mg/kg or 2mg/kg/week) or DMNQ (25mg/kg or 2mg/kg/week).

6.2.2 GENOMIC LOCALIZATION OF miRNA CODING SEQUENCES

Many miRNAs are coded from localized areas of the genome called polycistronic regions where their expression is co-ordinated (Figure 6.1). The exact location within each chromosome was determined to investigate if any miRNAs were derived from common precursor transcripts (bicistronic clusters) (Figure 6.5). For the acute model this analysis identified five clusters within the genome that encode more than one miRNA within a 500bp sequence. In addition, the previously identified miR-133a and miR-1 cluster was present (Section 1.5.4). Three of these clusters present on chromosomes 1, 8 and 14 were affected by both acute and chronic doxorubicin and DMNQ treatment (Figure 6.6).

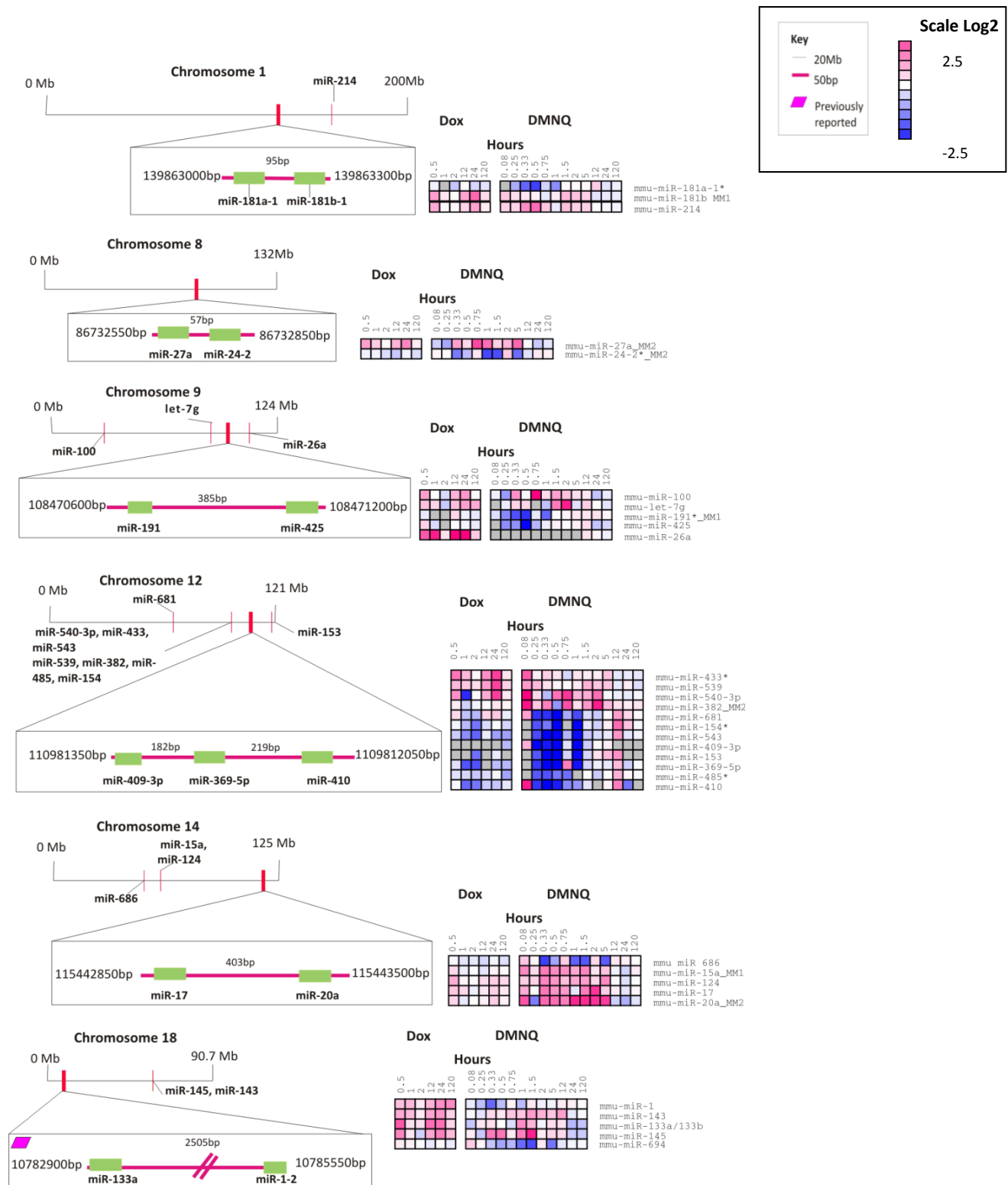


Figure 6.5: Representation of the relative location from where significantly expressed miRNAs are encoded from in an acute model of toxicity. miRNAs included are the mean results of $n > 3$ and significantly ($p < 0.05$) regulated at $\text{Log}_2 < 1$ or $\text{Log}_2 > 1$ at a minimum of one time point in an acute model following doxorubicin and DMNQ and encoded from within 500bp of another miRNA with the exception of miR-133a and miR-1.

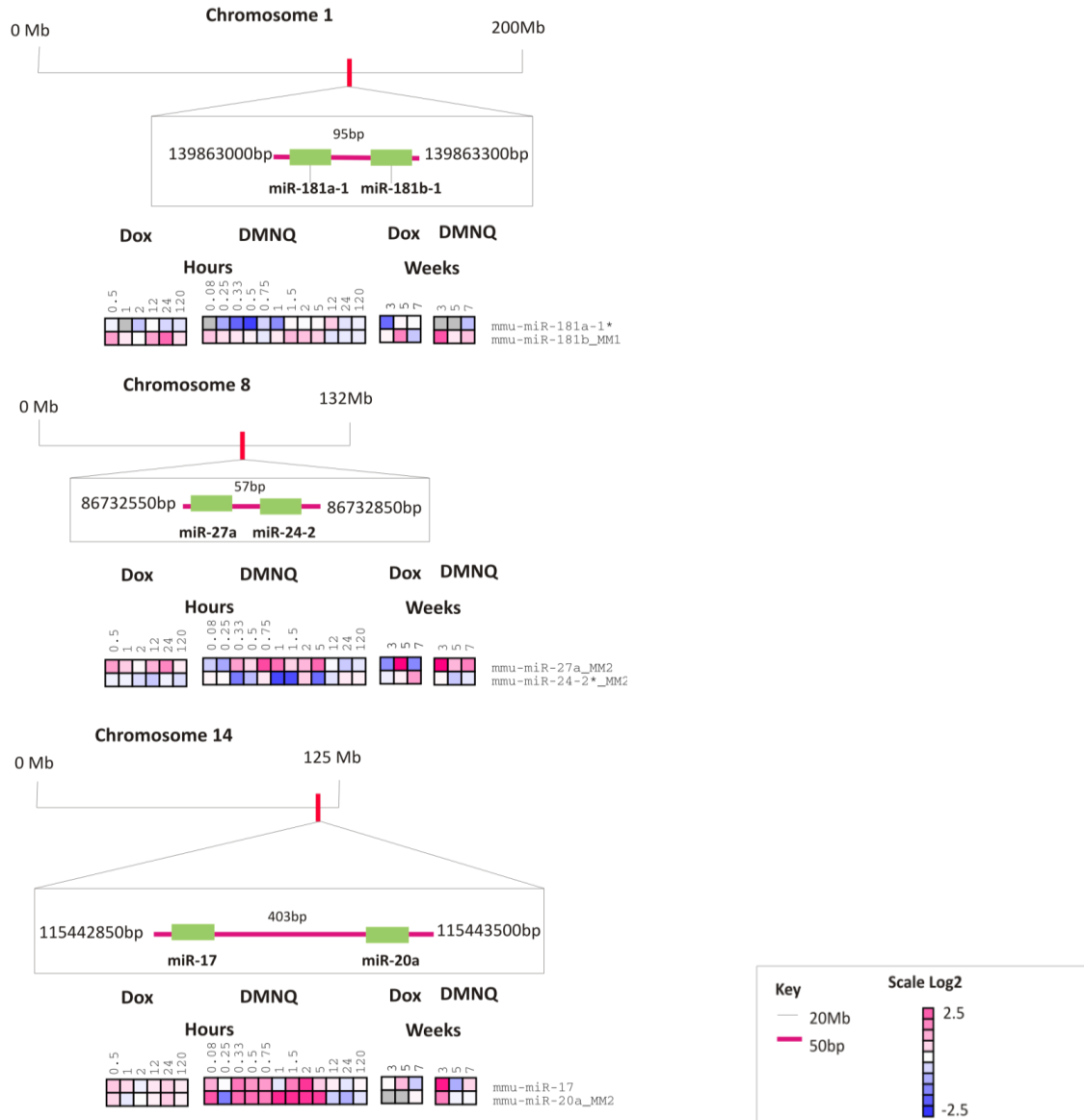


Figure 6.6: Representation of the relative location from where significantly expressed miRNAs are encoded in the genome that are differentially expressed in all models of toxicity (doxorubicin and DMNQ acute and chronic) miRNAs included were the mean results of $n \geq 3$ and significantly ($p \leq 0.05$) regulated at $\text{Log}_2 < -1$ or $\text{Log}_2 > 1$ at a minimum of one time point in all models and encoded from within 500bp of another miRNA.

6.2.3 qRT-PCR and Northern Blot Confirmation of Microarray Data

Regulation of selected differentially expressed miRNAs was verified by northern blotting and qRT-PCR as outlined in Chapter 2. Northern blotting was conducted as it allows both the pre and mature form of the miRNA to be identified (Section 1.5.2). A high level of concordance between qRT-PCR, northern

blotting and microarray data was observed (Figures 6.7-6.10). miRNA expression was confirmed for all miRNAs verified apart from one. miRNA expression of miR-210 in an acute model of doxorubicin toxicity was not confirmed by qRT-PCR.

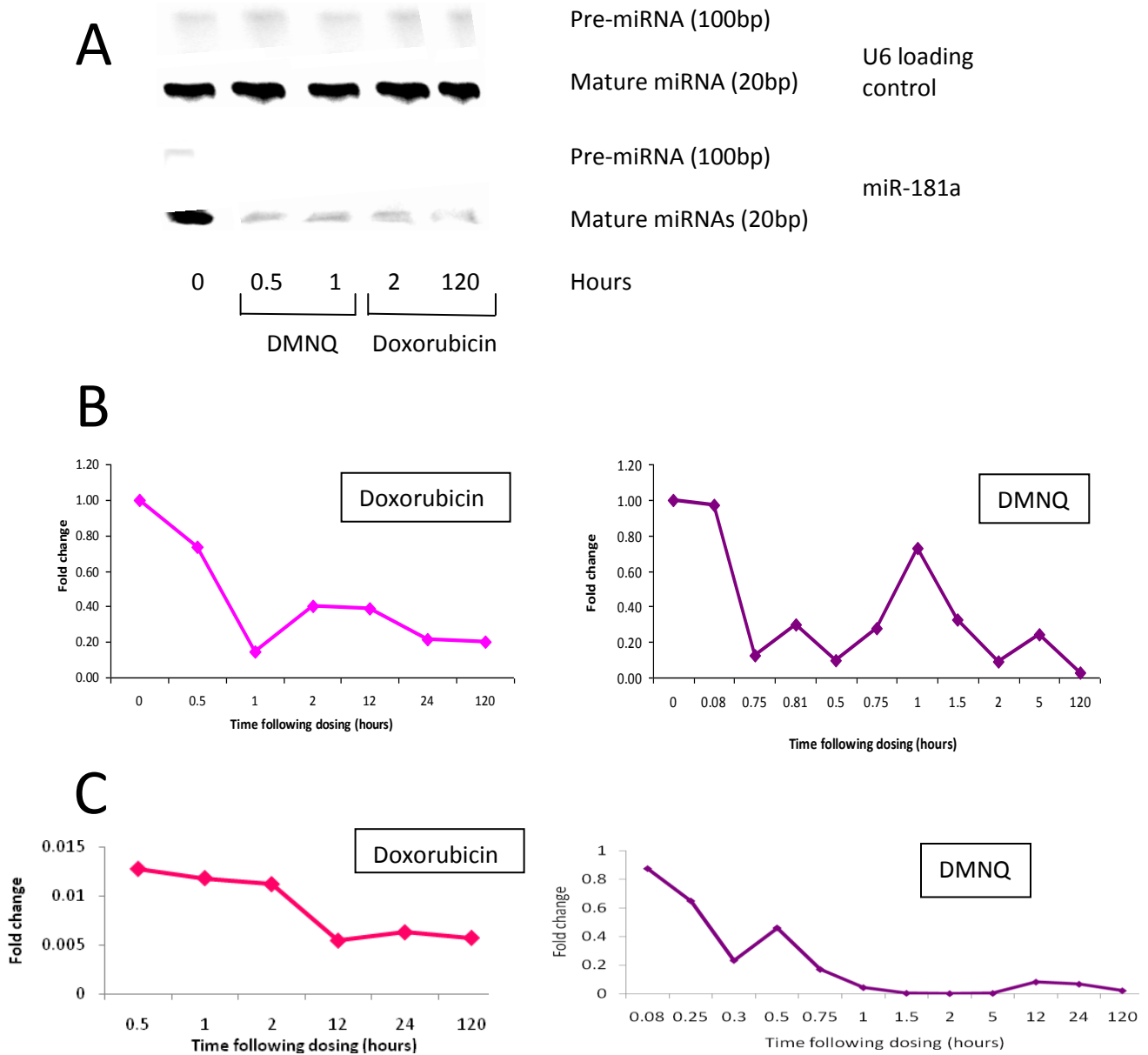


Figure 6.7: Confirmation of down-regulated miR-181a in cardiac tissue, by northern blotting (n=3) (A) and qRT-PCR (n=3) (B) compared to microarray expression data (C) (n=4) in an acute model of toxicity following doxorubicin (15mg/kg) and DMNQ (25mg/kg).

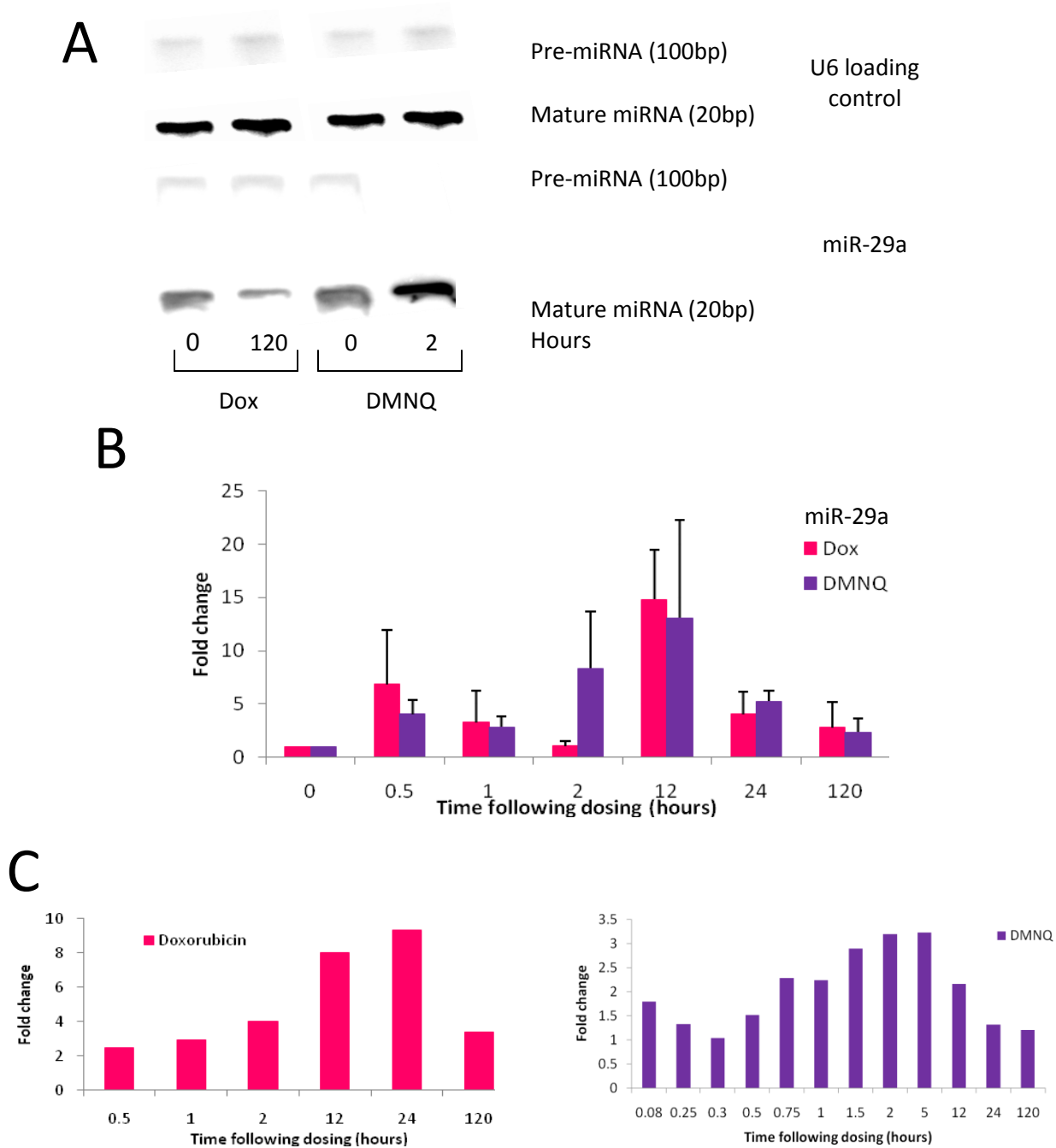
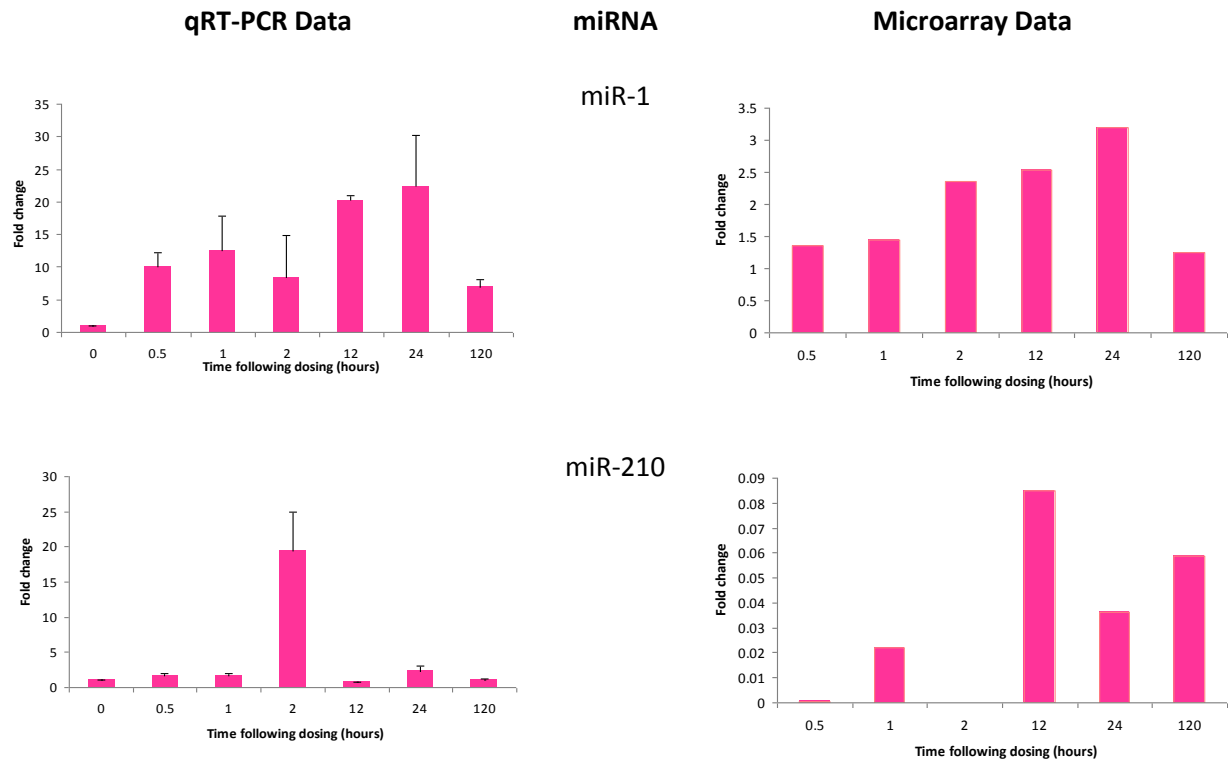


Figure 6.8: Confirmation of up regulated miR-29a, by northern blotting (n=3) (A) and qRT-PCR (n=3) (B) compared to microarray expression data (n=4) (C) in an acute model of toxicity following doxorubicin (15mg/kg) and DMNQ (25mg/kg).

A



B

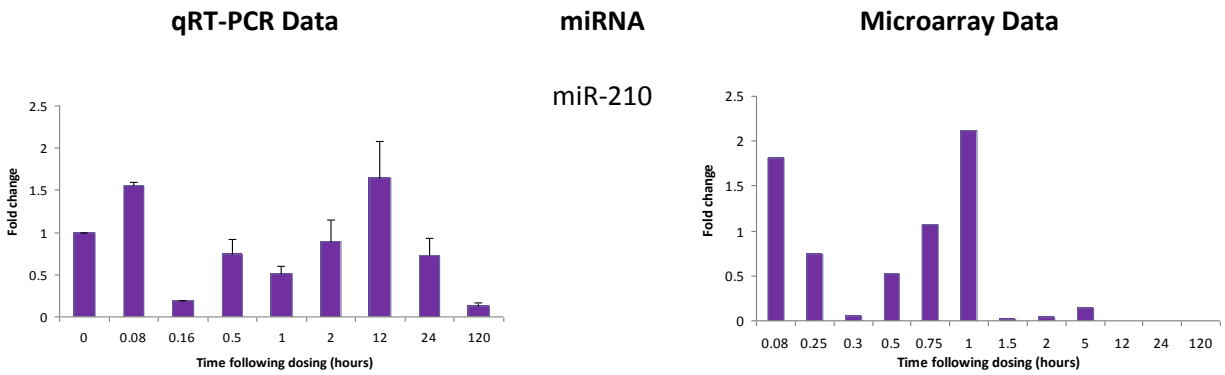
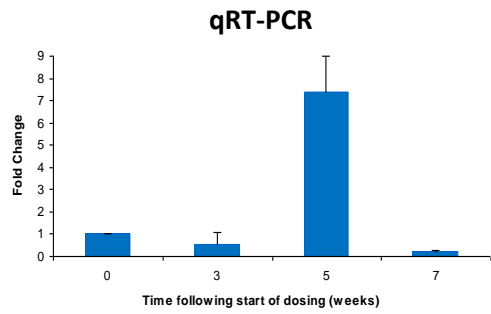
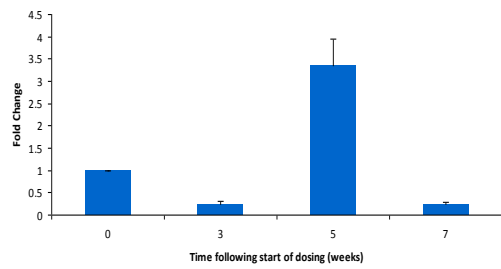
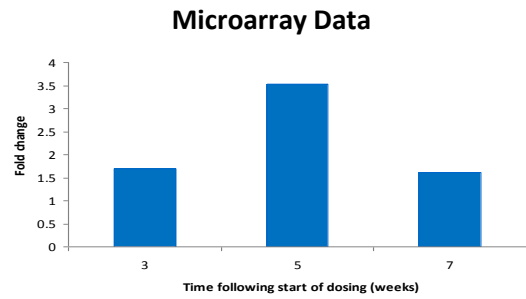


Figure 6.9: Further qRT-PCR confirmation of selected differentially regulated miRNAs in an acute model, of doxorubicin (15mg/kg) (A) and DMNQ (25mg/kg) (B) toxicity. Results are means of n=4 for microarray data and n=3 for qRT-PCR.

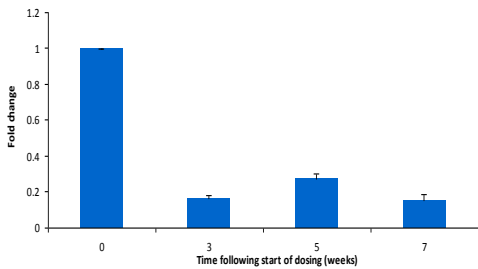
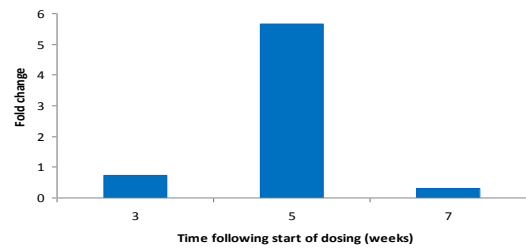
A



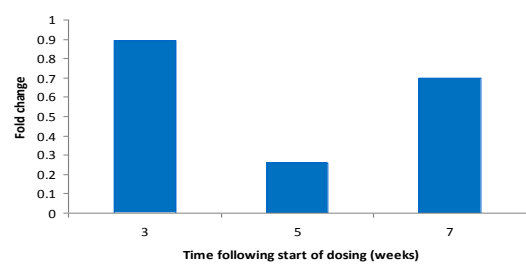
miRNA
miR-1



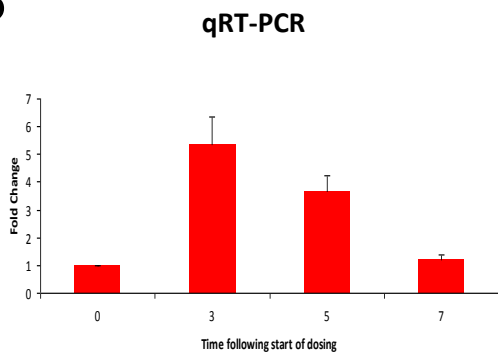
miR-24



miR-27b



B



miRNA

miR-9

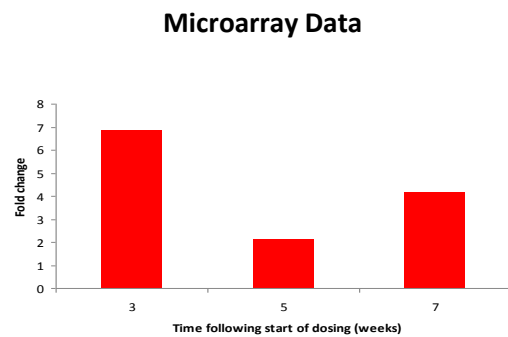
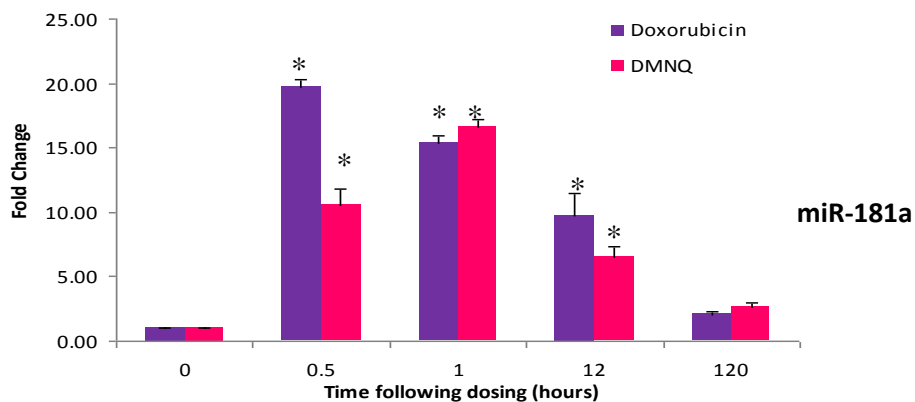


Figure 6.10: qRT-PCR confirmation of selected differentially regulated miRNAs in a chronic model, of doxorubicin (2mg/kg/week) (A) and DMNQ (2mg/kg/week) (B) toxicity. Results are means of n=4 for microarray data and n=3 for qRT-PCR.

6.2.4 PLASMA EXPRESSION OF miRNAS

To investigate the role of miRNAs in cardiac dysfunction further, the expression of two miRNAs, miR-181a (down-regulated in cardiac tissue, Figure 6.7) and miR-29a (up-regulated in cardiac tissue, Figure 6.8) in plasma was determined following doxorubicin (15mg/kg) and DMNQ (25mg/kg) treatment (Figure 6.11). miR-181a expression in plasma was up-regulated throughout the time course from 0.5-120 hours following both doxorubicin and DMNQ. A maximum fold change was observed 0.5 and 1 hour following a single dose of doxorubicin or DMNQ, respectively. Plasma expression of miR-29a was also up-regulated from 0.5-24 hours following both doxorubicin and DMNQ in an acute model of toxicity. 120 hours following a single dose of either compound, plasma expression returned to near baseline levels.

A



B

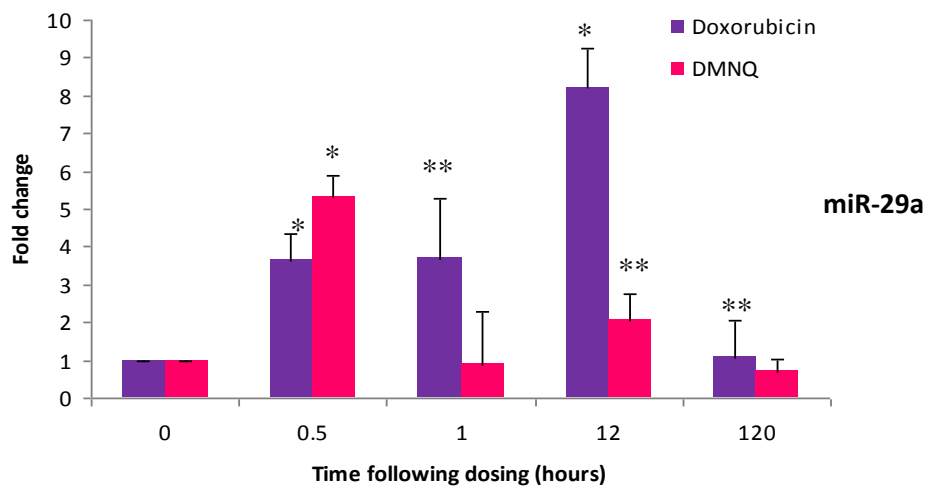


Figure 6.11: Plasma expression of miR-181a (A) and miR-29a (B) in a model of acute doxorubicin (15mg/kg) and DMNQ (25mg/kg) toxicity. Results are mean values \pm S.D. (n=3), one way ANOVA and post-hoc Dunnett's T-test * $p \leq 0.01$, ** $p \leq 0.05$.

6.3 DISCUSSION

The overall aim of this chapter was to identify miRNAs that were significantly affected by doxorubicin and DMNQ in an acute and chronic model of toxicity. The role of miRNAs in cardiotoxicity has not been previously reported. Cluster analysis identified a number of miRNAs that were significantly affected by both doxorubicin and DMNQ in an acute and chronic model of toxicity (Figures 6.2-6.5). Further investigation into miRNAs affected by doxorubicin but not DMNQ revealed the differential expression of a number of miRNAs involved in cell cycle regulation, in particular the G1 to S phase transition, and tumour suppression. The differential expression of these miRNAs was suggestive of doxorubicin's pharmacological action. Despite the apparent difference in biochemistry following chronic doxorubicin and DMNQ (Figure 6.3), a number of miRNAs implicated with cardiac function were differentially expressed, including miR-181b, miR-124, miR-21 and miR-208. Of interest these miRNAs were up-regulated at week 3, but by weeks 5 and 7 this was reversed to down-regulation, suggesting a role for etiologic factors in the expression of miRNAs as different pathology develops. This finding also supports the hypothesis that chronic models of toxicity mask the predisposing mechanisms. This occurrence of miRNAs associated with cardiac dysfunction in a chronic model of DMNQ, in which only minor changes in cardiac biochemistry occurred (Chapter 4), suggests miRNAs are differentially expressed prior to either the occurrence of changes in biochemistry or morphological alterations. This highlights miRNAs as key modulators in disease progression. Despite this finding it is currently unknown if miRNAs are activated as a protective or toxic mechanism following doxorubicin and DMNQ exposure. A number of miRNAs were significantly ($p < 0.05$) affected by both doxorubicin and DMNQ acute and chronically (Figure 6.4) including miR-133a/133b, miR-26a, miR-29a, miR-34, miR-181a-1 and miR-181b all previously associated with cardiac dysfunction suggesting a role for miRNAs in cardiotoxicity (Figure 6.12).

Both miR-181a and miR-26a are implicated in myogenesis, their over-expression repressing the genes *HoxA11* and *Ezh2*, respectively, preventing muscle differentiation (Wong and Tellam 2008; Naguibneva et al. 2006). Both miR-181a and 26a were down-regulated following doxorubicin and DMNQ acute and chronically, potentially leading to a change in myogenesis and pathological changes characteristic of cardiac damage.

miR-133a is a muscle specific miRNA that is present predominantly in cardiac tissue, and principally over-expressed both acute and chronically following doxorubicin and DMNQ (Figure 6.4). Gain and loss of function transgenic mouse models have demonstrated that miR-133a regulates ventricular development by reducing cardiomyocyte proliferation, with over-expression resulting in hypoplastic hearts and septal defects (Barringhaus and Zamore 2009; Latronico and Condorelli 2009; Meder et al. 2008). Over-expression of this miRNA also decreases the expression of the HERG protein, a voltage-activated potassium channel encoded by the *Kcnh2* gene, which is essential for cardiac contractility (Xiao et al. 2007). Decreased expression of *Knch2* is associated with the congenital long QT syndrome, leading to a decline in cardiac function. These data suggest a role for miR-133a in the progression of cardiac dysfunction and toxicity. Decreased transcriptional expression of *Knch2* was observed following acute doxorubicin and DMNQ treatment (Chapter 5), illustrating a possible miRNA-mRNA interaction affecting cardiac function. In addition, miR-133 family members have been found to be anti-apoptotic, with over expression (as observed) leading to repression of caspase 9, a vital caspase in the intrinsic pathway of apoptosis (Xu et al. 2007). These results suggest that one miRNA has a variety of functions both protective and prognostic. Thus, the distinction of miRNAs that are differentially expressed as a result of toxic insult cannot be separated into those that progress or protect against it.

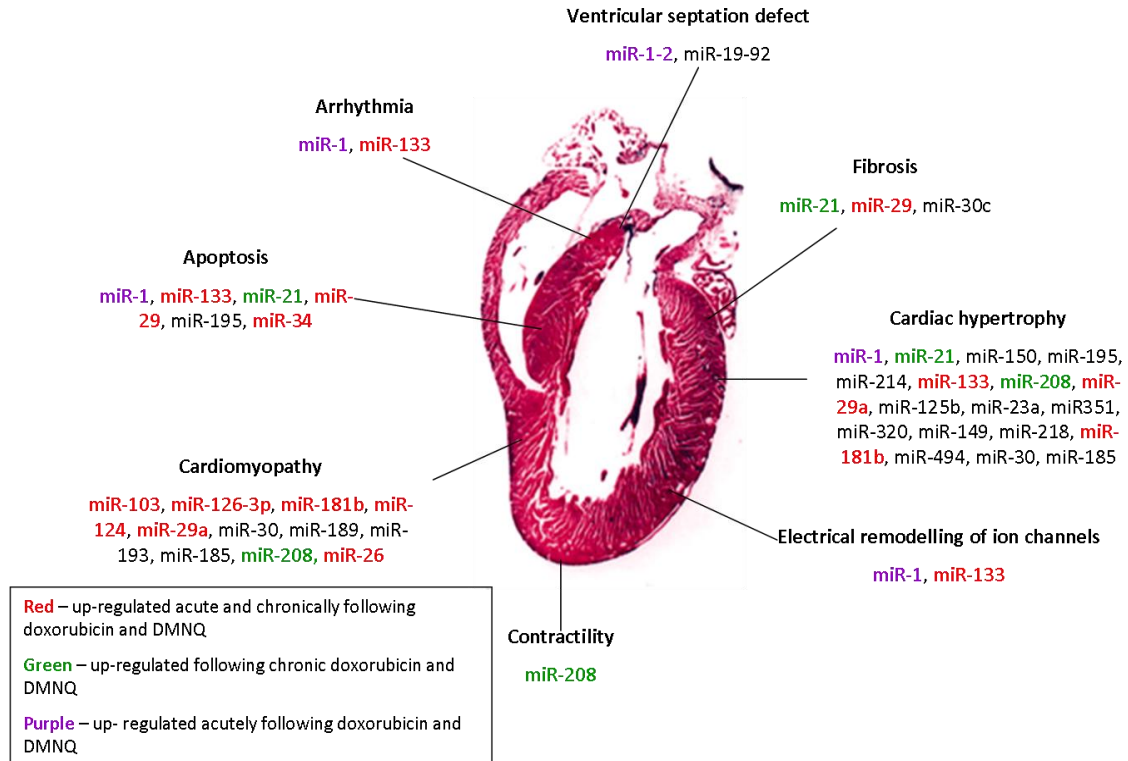


Figure 6.12: Summary of the role of miRNAs in cardiac function with those affected in these studies highlighted (Latronico and Condorelli 2009; Callis and Wang 2008; Latronico et al. 2008; Scalbert and Bril 2008; van Rooij et al 2008;).

Another miRNA affected by both doxorubicin and DMNQ acutely and chronically is miR-29a. miR-29a was found to be up-regulated and has been implicated in cardiac hypertrophy, myocardial infarction and fibrosis. Over-expression and knockdown experiments implicate miR-29a as a regulator of cardiac fibrosis. Decreased miR-29a expression leads to greater collagen deposition through increased translation, the converse has also been shown (Latronico and Condorelli 2009; Wang et al. 2009a; van Rooij et al. 2008). Thus illustrating that the increased miR-29a observed in this study may reduce collagen deposition, and structurally alter cardiac muscle, probably contributing to the development of the cardiotoxic phenotype. Park et al. (2009) have also experimentally verified a role for miR-29a and p53, the tumour suppressant and activator of apoptosis (Figure 6.13). Thus over-expression of miR-29

as observed following doxorubicin and DMNQ treatment in an acute and chronic model may render cells more susceptible to p53 dependent damage, inducing the activation of apoptosis. In addition miR-34 is also differentially regulated in all models of toxicity and is directly induced by p53 (He et al. 2007). These findings suggest miR-29a mediated induction of p53 induces miR-34, resulting in activation of the intrinsic pathway of apoptosis and cell death following acute and chronic doxorubicin and DMNQ treatment (Figure 6.13).

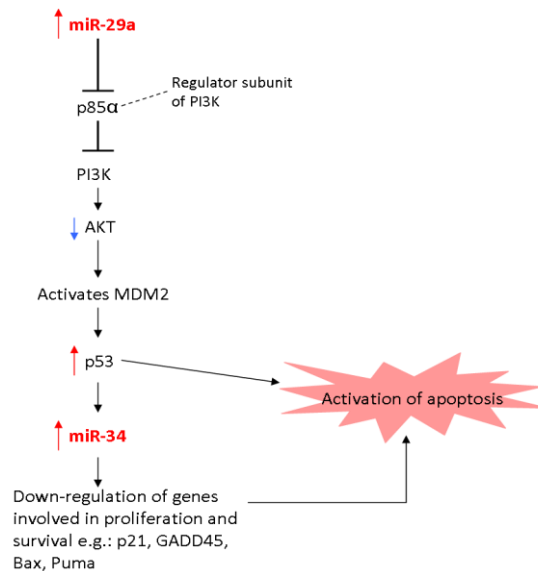


Figure 6.13: Role of miR-29a and miR-34 in the activation of p53 induced apoptosis. miRNAs in red were increased in expression following doxorubicin and DMNQ both acutely and chronically.

6.3.1 GENOMIC LOCALIZATION OF miRNAs

Many miRNAs are coded from localised areas of the genome called polycistronic regions where their expression is co-ordinated (Figure 6.1). The exact location within each chromosome from where each miRNA was transcribed was determined to identify any miRNAs derived from common precursor transcripts (bicistronic clusters) (Figures 6.7 and 6.8). This analysis revealed six clusters of miRNAs differentially expressed in an acute model of toxicity following doxorubicin and DMNQ treatment, of

which three were also affected in a chronic model of toxicity (Figures 6.7 and 6.8). This suggests a similar function for each miRNA in each cluster, identifying possible genomic regions affected by cardio toxins. Only one of these clusters has been previously identified, miR-1-2 and miR-133a (Barrinhaus and Zamore 2009). Both miR-133a and miR-1-2 are transcribed by the same transcription factor, the serum response factor, suggesting a similar function for these miRNAs. miR-1 or miR-133a transgenic or knockout mice have been utilised to confirm a role for these two miRNAs in cardiac biology. The direction of modulation of these two miRNAs appears to be different depending on the type of cardiac damage occurring, thus suggesting a role for etiological factors in miRNA expression. However, both over and under expression of miR-1 and miR-133a appear to result in cardiac dysfunction (Barrinhaus and Zamore 2009; Latronico and Condorelli 2009).

One novel cluster identified was that of miR-181b-1 and miR-181a-1 (Figure 6.6). miR-181a-1 was found to be down-regulated following doxorubicin and DMNQ, whereas miR-181b-1 was up-regulated. Thus, close genomic location within an intronic region did not appear to result in co-regulation. This may be a result of etiologic factors. In a state of cardiac hypertrophy miR-181b-1 has been found to be down-regulated (Yang et al. 2008). Following myocardial infarction, however, the same miRNA was shown to be up-regulated (Yang et al. 2008), thus co-ordinated expression of miRNAs from bicistronic clusters may not always occur.

Another novel cluster of miRNAs up-regulated in an acute and chronic model of toxicity following doxorubicin and DMNQ treatment was miR-17 and miR-20a (Figure 6.6). In addition, these two miRNAs are transcribed by the same transcription factor, c-Myc (Pickering et al. 2009). c-Myc is involved in a wide array of biological functions including cell cycle progression and apoptosis through the inhibition of Bcl-2 (Russo et al. 2003). Increased c-Myc directly increases miR-17 and miR-20a expression, thus implicating a role for both these miRNAs in cell proliferation and apoptosis (Pajic et al. 2000). As both

miR-17 and miR-20 were up-regulated following doxorubicin and DMNQ exposure, it could be postulated that c-Myc activity is also increased. Thus the increased expression of these miRNAs may be promoting cell proliferation and possibly providing a protective response to toxic insult.

The final cluster of miRNAs differentially expressed in all models of toxicity was miR-27a and miR-24-2 (Figure 6.6). miR-27a was up-regulated, whereas miR-24-2 was down-regulated. Little functional information regarding either of these miRNAs is in the public domain. All of the clusters of miRNAs affected following doxorubicin and DMNQ exposure potentially highlight vital areas of the genome that are preferentially affected during cardiotoxicity.

6.3.2 miRNA EXPRESSION IN PLASMA

These results suggest that miRNA species have important roles in cardiotoxicity and pathophysiology. The identification of the cardiac specific miRNAs miR-1 and miR-133a along with a number of miRNAs previously associated with cardiac dysfunction highlight miRNA expression as tissue and disease specific (Figure 6.12). A number of identified miRNAs are potential biomarkers of doxorubicin induced cardiotoxicity. However, as obtaining cardiac tissue biopsies in the clinical setting is an invasive procedure, miRNA profiles in body fluids e.g. plasma would be more convenient. Recently, miRNAs have been found to be stable in plasma (protected from endogenous RNase activity), thus allowing blood based detection of miRNAs (Lodes et al. 2009; Mitchell et al. 2008). miRNA profiling of plasma has identified specific differences between patients with and without prostate cancer and B-cell lymphoma (Lawrie et al. 2008; Mitchell et al. 2008). The expression of two miRNAs, miR-181a and miR-29a were determined in plasma from acutely treated doxorubicin and DMNQ animals. Both these miRNAs were up-regulated following both doxorubicin and DMNQ (Figure 6.11), despite miR-181a being down-regulated and miR-29a being up-regulated in cardiac tissue in the same animals. Similar discrepancies have been observed between tumour cells and circulating plasma in a range of cancers (Lodes et al.

2009). These differences in expression between cardiac tissue and plasma may result from cell lysis. Thus cellular contents are released into circulating plasma, a product of active transport possibly involving the formation of exosomes or release into plasma due to other cellular sources. Exosomes are produced by a range of cell types including intestinal epithelial, microglia, T cell, B cells and activated platelets (Valadi et al. 2007; Savina et al. 2003). They are formed through fusion of multivesicular bodies with the plasma membrane, resulting in the release of contents into circulating plasma. The exact stimuli activating release is unclear, but increases in calcium concentrations possibly through the activation of $\text{Na}^+/\text{Ca}^{2+}$ exchanger have been proposed (Savina et al. 2003). Calcium concentration is involved in the formation of an action potential enabling cardiac contractions and increases in calcium are associated with cardiac damage. It is therefore possible that cardiomyocytes are able to produce exosomes. Alternatively, exosomes of cardiac origins maybe released from activated platelets, which are recruited to sites of vascular injury (Savina et al. 2003). Once released, exosomes are involved in intracellular communication and transfer of RNA and protein between cells (Lodes et al. 2009; Valadi et al. 2007). 121 miRNAs have been found to be carried in exosomes, thus possibly allowing release of some miRNAs from damaged tissue into circulating plasma (Valadi et al. 2007). A number of miRNAs have been identified as being at higher concentrations in exosomes than in tissue. One identified miRNA is miR-181a (Valadi et al. 2007). This interaction of miR-181a with exosomes likely explains the higher level of expression in plasma compared to cardiac tissue following acute doxorubicin and DMNQ treatment (Figures 6.9 and 6.13A). Also, since not all miRNAs are thought to be carried in exosomes, these vesicles are also likely to explain why some miRNAs are released into plasma but not all e.g.: the up-regulation of miR-29a in cardiac tissue and plasma following acute doxorubicin and DMNQ treatment (Figures 6.10 and 6.13B). Alternatively miR-29a up-regulation in both plasma and tissue may occur due to the suggested involvement of miR-29a in p53 mediated cellular damage, suggesting widespread induction of p53 mediated apoptosis. This profiling in plasma has identified two miRNAs that are

modulated in expression in both cardiac tissue and plasma following chemical insult. These results highlight the importance of miRNAs in cardiac biology and toxicology. The difference in expression of miR-181a between cardiac tissue and plasma highlights the need for miRNA expression profiling to be conducted in plasma following chemical insult (Latronico and Condorelli 2009).

6.3.3 miRNA TARGET PREDICTION

miRNA profiles are fairly simple to generate but are of only real value when their expression is correlated with mRNA translation. However, as miRNAs can regulate multiple mRNAs involved in many biological processes, a single miRNA can have both advantageous and pathogenic effects. In order to transfer miRNA biology into viable treatment further research is required to gain detailed insight into the mRNA targets of miRNA. This will allow specific treatment to be developed (van Rooij et al. 2008). Binding of a single miRNA to an mRNA target may not alone be sufficient to affect translation, raising the question that several miRNAs or clusters may need to bind to facilitate an effect (Latronico et al. 2007). Not only is there a large number of mRNAs that are potentially affected by one miRNA, but different bioinformatic packages identify different miRNA-mRNA interactions resulting in a high false positive rate (Parker and Wen et al. 2009; Latronico et al. 2007). In order to provide functional insight into miRNAs, miRNA-mRNA interactions need to be experimentally determined. One method to identify miRNA-mRNA interactions is to assess the global translational profiles (Chapter 7).

6.3.4 SUMMARY

The findings of this study indicate a role for differential miRNA expression in toxicology. miRNAs may be modulated in expression as a direct result of xenobiotic insult or during the progression of toxicity. The presence of miRNAs in plasma provides a novel approach to diagnose cardiac dysfunction in the clinical setting. Before miRNAs can be successfully used as either pharmaceutical targets or agents further research is required into the effects of miRNAs on mRNAs.

**Chapter 7: Translational Response of the Heart *In Vivo*
following Doxorubicin and DMNQ Exposure**

7.1 INTRODUCTION

The overall objective of this study was to develop a high throughput method to assess translational changes following doxorubicin and DMNQ, allowing identification of putative miRNA-mRNA interactions.

As doxorubicin appeared to reduce the level of transcription, compared to DMNQ, (Chapter 5), it was hypothesised that doxorubicin may modify gene expression primarily at the level of translation.

Translational profiles obtained, were compared to those generated following administration of the known redox cycling compound DMNQ (Gant et al. 1988). Any common features provide a novel insight into the mechanism responsible for doxorubicin's associated cardiotoxicity.

Both transcriptional (Chapter 5) and translational profiling were conducted following doxorubicin and DMNQ acutely and chronically. Transcriptional profiling allows the measurement of total mRNA, whereas translational profiling measures the suppression of all mRNAs. This analysis allows the off-target effects of miRNA modulation to be identified as miRNAs regulate translation by suppressing mRNA expression.

Gene expression and subsequent protein synthesis is dependent not only on transcriptional activity (Chapter 5), but on a variety of post-transcriptional events resulting in mRNA translation (Lü et al. 2006). Translation is initiated in a cap dependent manner or via internal ribosome entry, both resulting in the binding of the 40S ribosomal subunit to the mRNA strand prior to binding of the 60S ribosomal subunit, allowing translation to proceed (van der Beucken et al. 2006; Pickering and Willis 2005; Stoneley and Willis 2004). Translational control on gene expression was originally proposed to be a fundamental process in development (Blais et al. 2004). However, over recent years it has been proven vital in a wide array of physiological processes e.g.: growth stimulation, cellular stress, tumourgenesis (Lü et al. 2006; Provenzani et al. 2006; Blais et al. 2004). Translational control of gene expression is not directly linked to transcription and is thought to occur rapidly, resulting in changes in translational and protein expression

(Lü et al. 2006; Blais et al. 2004). This rapid induction of translation and subsequent protein synthesis may account for the discrepancies between transcription and protein expression following cellular stress (Lü et al. 2006). One post-transcriptional regulatory mechanism that is thought to control initiation of translation is the activity of miRNAs (Chapter 6). The differentially expressed miRNAs identified in Chapter 6, thus highlight a potential role of differential translation in the mechanism of doxorubicin induced cardiotoxicity.

Increased translational mRNA expression has also been observed in models of reduced transcriptional activity, as observed following doxorubicin. A cellular model of colorectal cancer found a two fold increase in mRNA translation compared to transcriptional expression (Provenzani et al. 2006). In addition the number of genes whose translational activity was modulated following radiotherapy treatment was ten fold higher than the corresponding transcriptional activity (Lü et al. 2006). These data highlight an important role for translation, in particularly in models of cellular stress and inhibited transcription. This suggests that mRNA translational profiles will be differentially affected to a greater degree than transcriptional profiles following doxorubicin.

mRNA translational profiling conducted as described here, allows high throughput genomic identification of mRNA translation that can be combined with miRNA profiling (Chapter 6) to identify putative miRNA-mRNA interactions. This approach has been widely utilised (over 50 publications) to generate mRNA translational profiles *in vitro* (Melamed and Arava 2007; Blais et al. 2004) but only a single *in vivo* study is publically available (Iguchi et al. 2006). In addition a number of *in vitro* methods have been developed to either over or under express miRNAs combined with both microarray and proteomic analysis (Baek et al. 2008; Selbach et al. 2008). However, transfer of such methods to the *in vivo* setting is problematic and only one miRNA can be investigated at one time. Thus translational

profiling as described here may allow a further insight into the role of mRNA-miRNA interactions involved in doxorubicin cardiotoxicity *in vivo* in a high throughput manner.

7.1.1 PLAN OF INVESTIGATION

C57B6/AJ mice were dosed at 25mg/kg DMNQ or 15mg/kg doxorubicin to represent an acute model and 2mg/kg/wk DMNQ or doxorubicin to represent a chronic model. The number of time points studied in an acute model of DMNQ was reduced, as earlier data indicated that time points 0.5 hours after dosing mimicked the toxicity observed following doxorubicin at the miRNA level. As miRNAs regulate mRNA translation, it was hypothesised that changes in miRNA expression would result in altered mRNA translational expression; Table 7.1 depicts the time points of study.

Compound	Model of Toxicity	Time Point of Sacrifice
Doxorubicin	Acute	0.5, 1, 2, 12, 24 and 120 hours
DMNQ	Acute	0.5, 1, 2, 12, 24 and 120 hours
Doxorubicin	Chronic	3, 5 and 7 weeks
DMNQ	Chronic	3, 5 and 7 weeks

Table 7.1: Table stating the time points of sacrifice for translational profiling experiments

Global translational expression profiles were generated using RNA separation techniques followed by expression microarrays. In order to assess global translation, total RNA was first separated by sucrose density gradient centrifugation followed by fractionation into actively translated mRNA species (polysomes) and non-actively translated mRNA species (monosomes). Polysomal mRNAs have a larger number of ribosomes attached and are denser compared to monosomal mRNAs which have few if any ribosomes attached. A block in translational initiation would result in a reduced number of ribosomes attached to mRNA thus these mRNAs would be present in the lighter fractions, whereas a block in elongation would result in less ribosome release (Clancy et al. 2007). Following centrifugation each gradient was fractionated while monitoring UV absorbance at 254nm to obtain a gradient profile to ensure correct separation of RNA species. This profile was used to identify the monosomal ribosomal subunits, 40S and 60S. Correct separation was further confirmed by the addition of EDTA and northern

blotting. Due to the nature of separated mRNA species, experimental design of microarray experiments is crucial to prevent the mistaken identification of transcription instead of translation. The experimental design used here is illustrated in Figure 7.1. The principle behind this design is discussed in Chapter 1. Comparison with miRNA gene expression profiles (Chapter 6) was conducted in order to identify putative mRNA-miRNA interactions using TargetScan 5.0 (www.targetscan.org). This correlation in data allows a novel insight into the affects of doxorubicin and DMNQ on the heart.

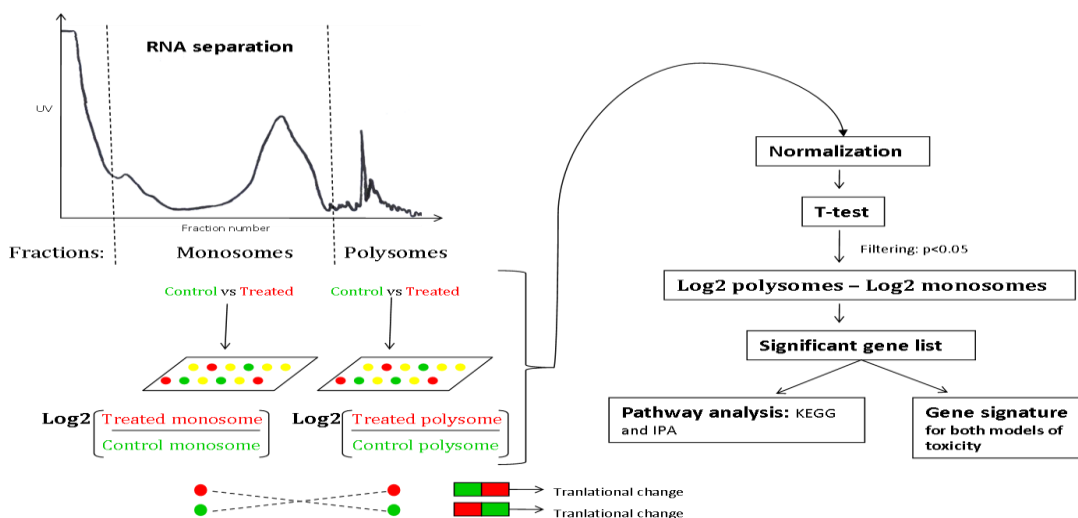


Figure 7.1: Representation of the experimental design employed to carry out translational microarray analysis. RNA was separated into monosomes and polysome species by sucrose gradient centrifugation, followed by microarray analysis to determine the translational profiles following doxorubicin and DMNQ in an acute and chronic model of toxicity. Significant gene lists were subjected to pathway analysis and cluster analysis to allow comparison between samples and models of toxicity.

7.1.2 HYPOTHESIS AND AIM

The overall aim of this study was to examine the mRNA translation on a global scale to identify translational changes induced by doxorubicin and DMNQ. It was hypothesised that consistent regulation of genes and pathways by both compounds translationally would result in the identification of key mechanisms through which doxorubicin mediates its cardiotoxic effects. Such profiles were probed for miRNA binding sites to enable the identification of putative miRNA-mRNA interactions.

7.2 RESULTS

C57B6/AJ male mice were dosed i.p. with doxorubicin (15mg/kg), DMNQ (25mg/kg) or the respective vehicle control in an acute model or 2mg/kg/wk doxorubicin or DMNQ in a chronic model (Section 2.1). Animals were sacrificed as detailed in Table 7.1 and total RNA from heart tissue was subjected to sucrose density centrifugation and subsequent microarray translational profiling (Figure 7.1).

7.2.1 mRNA TRANSLATIONAL PROFILING

Total RNA from heart tissue treated with doxorubicin or DMNQ in an acute or chronic model of toxicity and HL-1 cells were fractionated following sucrose density centrifugation (Section 2.22). This method is well established for cell lines, but has not been widely used to separate RNA from tissue samples, thus the HL-1 cardiac cell line was subjected to separation as a positive control (Figure 7.2). The A_{254} profiles demonstrate the presence of the 40S and 60S ribosomal subunits and polysomal fractions. Separation of mRNA from cardiac tissue resulted in an additional large peak; this appeared to be predominately due to a tissue contaminant that co-sedimented with RNA (Figure 7.2C). Further verification of separated RNA was conducted by gel electrophoresis and northern blotting (β -actin), confirming correct separation of monosome and polysome fractions. β -actin is considered to be actively translated in most biological materials, thus acts as a marker of the polysomal region. The monosomal fractions were identified by the addition of EDTA, which dissociates ribosomes, and the presence of the 40S and 60S peaks on the A_{254} profile (Figure 7.2B). These peaks were less defined in profiles obtained from *in vivo* samples compared to *in vitro* samples.

Microarrays were conducted in the manner outlined in section 2.23, using the experimental design and data analysis methods described in section 7.1.1. In total this analysis revealed 5119 genes that were differentially translated following DMNQ, and 11673 genes following doxorubicin in an acute model, of which 669 genes were affected by both compounds (Figure 7.3). A chronic model of toxicity resulted in

1468 and 2898 genes affected by doxorubicin and DMNQ, respectively, of which 170 were affected following both compounds. The overall level of translation following acute doxorubicin was greater than with DMNQ, with the majority of mRNAs being more efficiently translated (Table 7.2). PCA clustering was carried out to further identify shared mechanisms of action between the two compounds in both acute and chronic models of toxicity (Figure 7.3). This revealed a similarity between the two acute models of toxicity, with all samples clustering together apart from doxorubicin 0.5 hours that clustered with chronic DMNQ time points. A distinct difference between each of the chronic doxorubicin time points was apparent; potentially the result of cumulative translational damage masking the predisposing toxic mechanisms.

Treatment	Time point (hours)	Number of mRNAs differentially translated	% total more efficiently translated	% total less efficiently translated
Doxorubicin (15mg/kg)	0.5	3997	89	11
	1	766	88	12
	2	2402	63	37
	12	1970	52	48
	24	1757	17	83
	120	781	92	8
DMNQ (25mg/kg)	0.5	158	13	87
	1	371	74	26
	2	59	32	68
	12	2780	72	28
	24	280	57	43
	120	1471	51	49

Table 7.2: Doxorubicin and DMNQ translationally modulated genes in an acute model. Results are mean LOWESS normalised values (n=3) subjected to a one sample two tailed t-test at each time point followed by subtraction of monosome expression from polysome expression. Genes displaying a p-value of ≤ 0.05 at a minimum of two time points and a $\text{Log}_2 < 2$ or $\text{Log}_2 > 2$ were included.

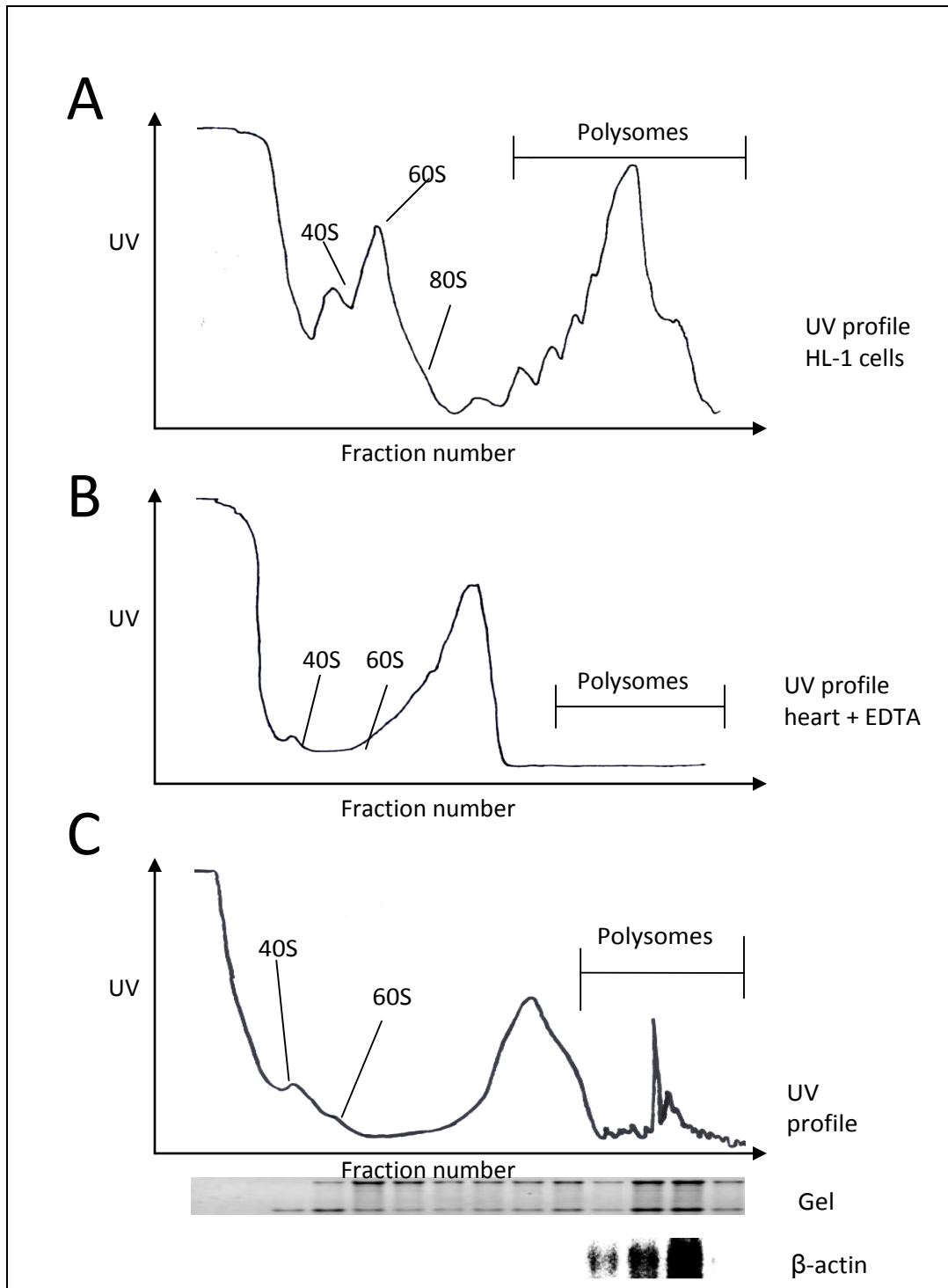


Figure 7.2: RNA fractionation profiles, from HL-1 cells (A), cardiac tissue + EDTA (B) and cardiac tissue (C). In order to separate RNA species into monosome and polysome fractions, RNA was subjected to density fractionation on a sucrose gradient. Fractions were collected while continually monitoring absorbance, A_{254} . The RNA within each fraction was purified and equal volumes of each used for further analysis. Denaturing gels confirmed successful separation and β -actin northern blots identified polysomal fractions (C). The presence of monosomal mRNA within the early fractions from the tissues was also confirmed by treating total RNA with EDTA. EDTA disaggregates polysomes, leaving free mRNA; this clearly identified the monosomal fractions.

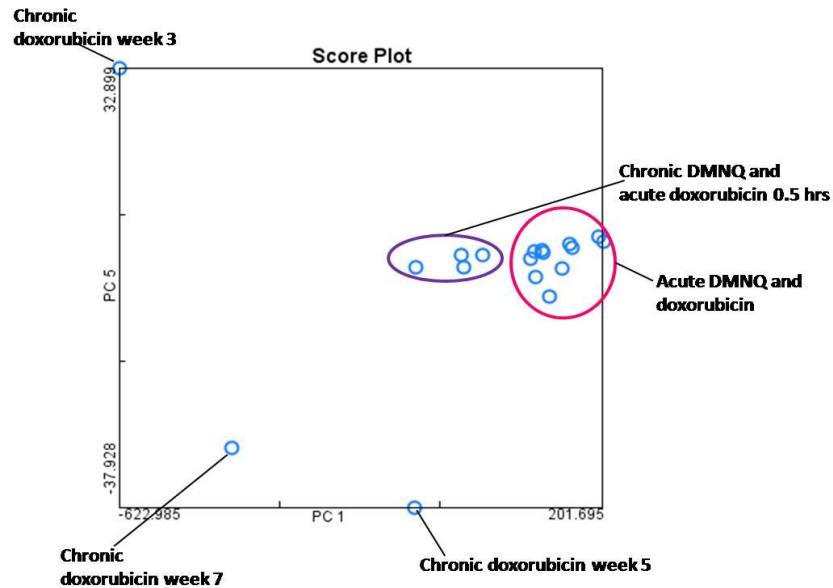


Figure 7.3: PCA of doxorubicin and DMNQ translational profiles in an acute and chronic model of toxicity. Results are mean LOWESS normalised values (n=3) subjected to a one sample two tailed t-test at each time point followed by subtraction of monosome expression from polysome expression. Genes displaying a p-value of ≤ 0.05 at a minimum of two time points were included in this analysis.

7.2.2 PATHWAY ANALYSIS

Due to the high level of concordance between different pathway analysis packages in Chapter 5, only one application, the Gene Set Analysis Toolkit was used. Each gene that was significantly regulated at one or more time points over the period of study for each compound was classified into KEGG pathways. The significance of each KEGG pathway was assessed using a modified Fisher exact test, this generates an enrichment probability score (p value). Only pathways with a p value of ≤ 0.05 at a minimum of two time points were included.

This analysis indicated a number of significantly altered pathways (Figure 7.4). In total 19 KEGG pathways were significantly ($p \leq 0.05$) affected, in particular oxidative phosphorylation, TCA cycle, axon guidance and cell communication were all modulated at all time points following both doxorubicin and DMNQ in an acute model (Figure 7.4A). Constant with the transcriptional profiling no changes in

glutathione metabolism, an antioxidant response and DNA damage pathways were affected. A number of pathways were affected by doxorubicin, but not DMNQ, including apoptosis and Jak-STAT signalling pathways (Figure 7.4A).

In the chronic model of toxicity only five pathways were affected by both doxorubicin and DMNQ at a minimum of one time point with each compound (Figure 7.4B). The only pathways affected at all time points was oxidative phosphorylation and the regulation of actin cytoskeleton. These changes in gene expression may indicate predisposing pathways responsible for the development of the cardiotoxic phenotype.

7.2.3 TRANSLATIONAL RESPONSE IN OXIDATIVE PHOSPHORYLATION GENES

Oxidative phosphorylation functions to synthesise ATP through the utilisation of the electron transport chain (ETC) (Section 1.4). Genes in all five enzyme complexes were translationally modulated (Figure 7.5), a number of which were more or less efficiently translated within each complex. This suggests disruption to the dynamics of the ETC and energy production in the heart, sustained 120 hours following a single dose of either doxorubicin or DMNQ. However, it appears that subsets of genes in each complex were more or less efficiently translated. As a result it is difficult to predict the overall direction of expression. However these modulations in gene expression, suggest that overall complexes of the ETC were not functioning optimally.

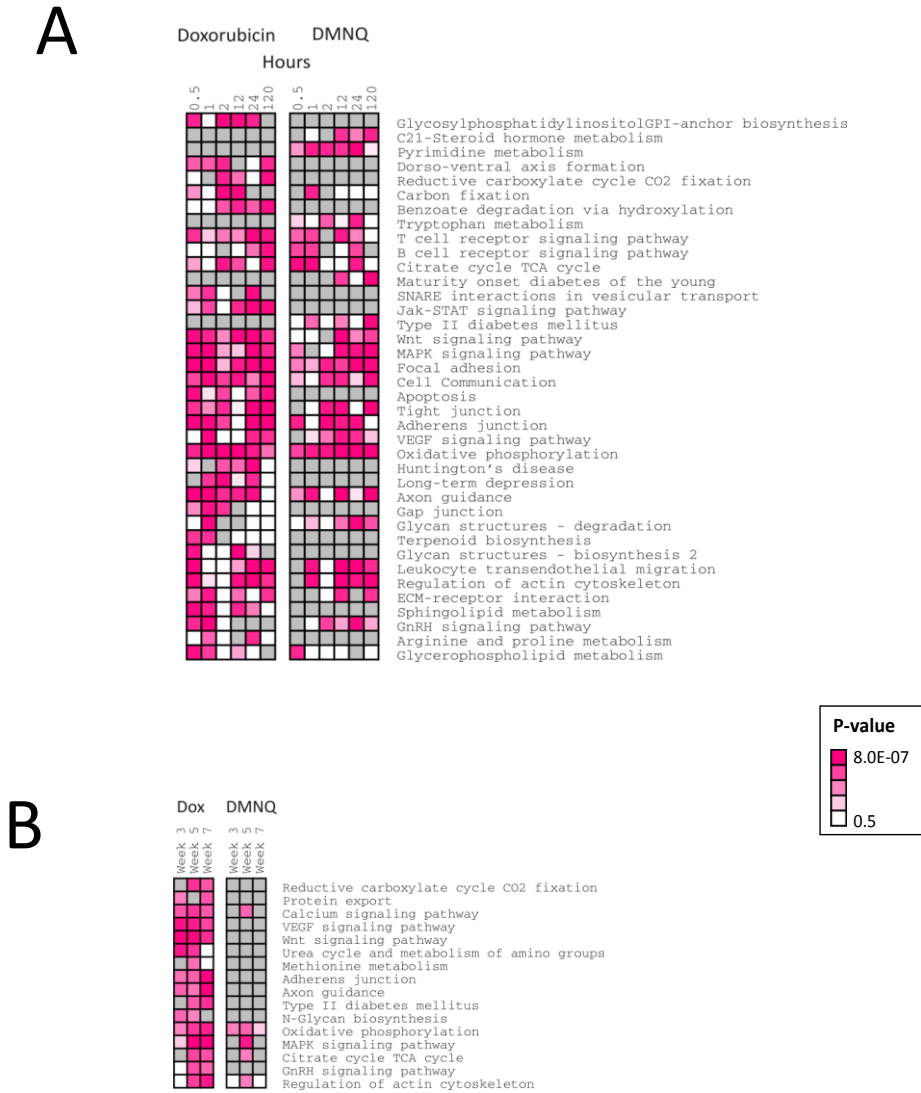


Figure 7.4: Significantly affected translational KEGG pathways, following acute doxorubicin (15mg/kg) or DMNQ (25mg/kg) (A), and chronic doxorubicin or DMNQ (2mg/kg/week) (B). Genes included are significantly ($p \leq 0.05$) regulated at a $\text{Log}_2 < 1$ or $\text{Log}_2 > 1$ at a minimum of two time points (acute model) or a minimum of one time point (chronic model). Results are mean values of $n=3$.

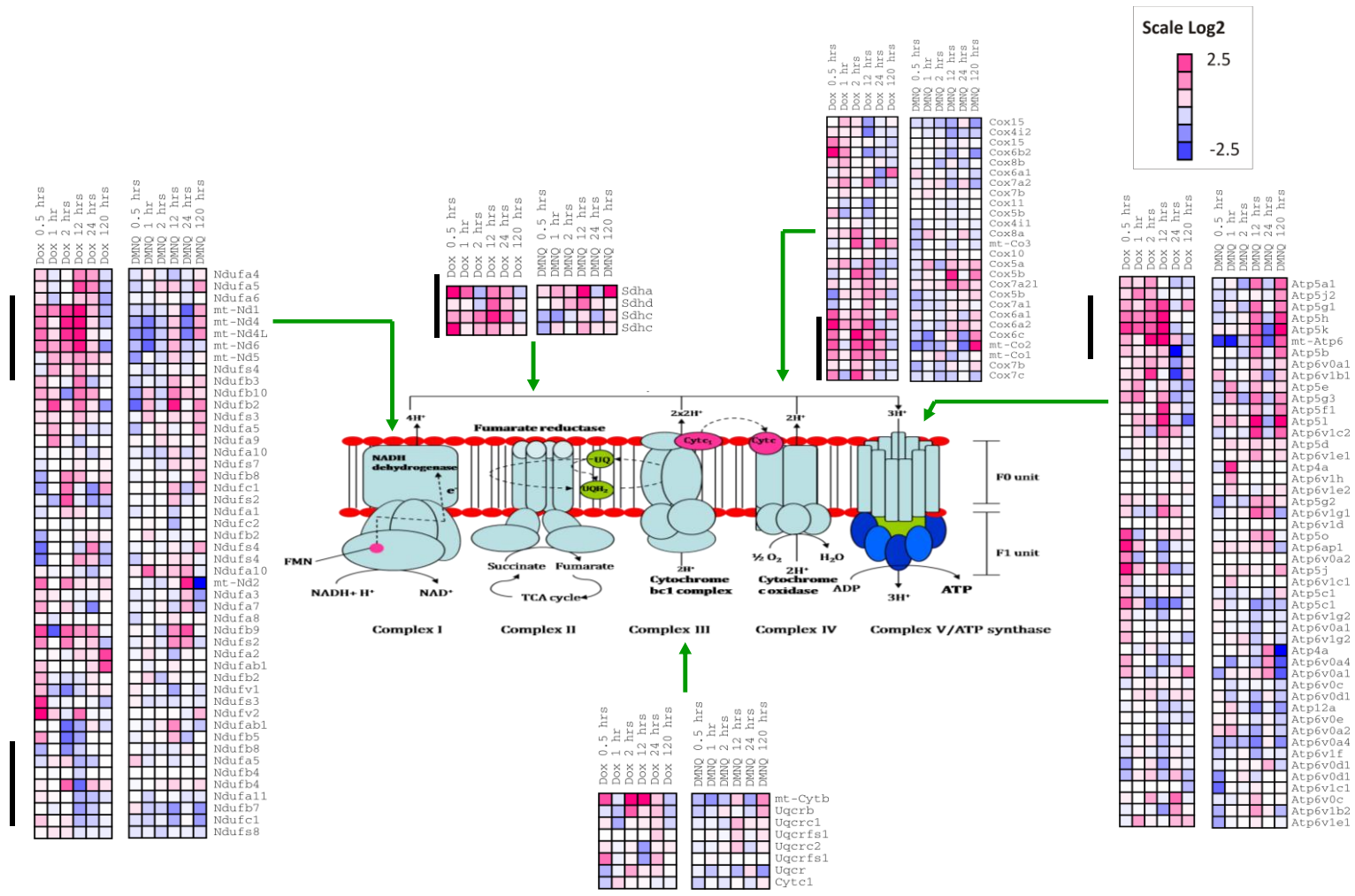


Figure 7.5: HCL of translationally affected genes encoding the complexes of the ETC. Genes included were significantly ($p \leq 0.05$) translationally modulated following doxorubicin (15mg/kg) and DMNQ (25mg/kg). Results are mean values of $n=3$.

7.2.4 qRT-PCR CONFIRMATION OF MICROARRAY DATA

qRT-PCR was used to verify translational microarray changes (Section 2.22). Table 7.3 details the time points of study. qRT-PCR allows the relative abundance of a particular mRNA in each fraction to be determined allowing the identification of mRNAs more and less effectively translated. In general, a high level of concordance between qRT-PCR data and microarray data was observed. Examples of mRNAs more efficiently translated are presented in Figure 7.6 and those less efficiently translated in Figure 7.7. Whilst the majority of mRNAs in Figure 7.6 from the hearts of control animals were present in the polysomal region, i.e. being actively translated, some were present in the monosomal region, i.e. not being actively translated. However, following acute doxorubicin or DMNQ administration a greater proportion of each mRNA moved into the polysomal region, thus confirming these mRNAs were being more efficiently translated following doxorubicin or DMNQ (Figure 7.6). Less effectively translated mRNAs were identified by qRT-PCR by movement of mRNAs into lighter polysome and monosome regions (Figure 7.7).

Model of Toxicity	Time points of study
Acute doxorubicin (15mg/kg)	0, 0.5, 1, 2, 12, 24 and 120 hours
Acute DMNQ (25mg/kg)	0, 0.5, 1, 2, 12, 24, 120 hours

Table 7.3: Time points used to verify translational microarray data by qRT-PCR.

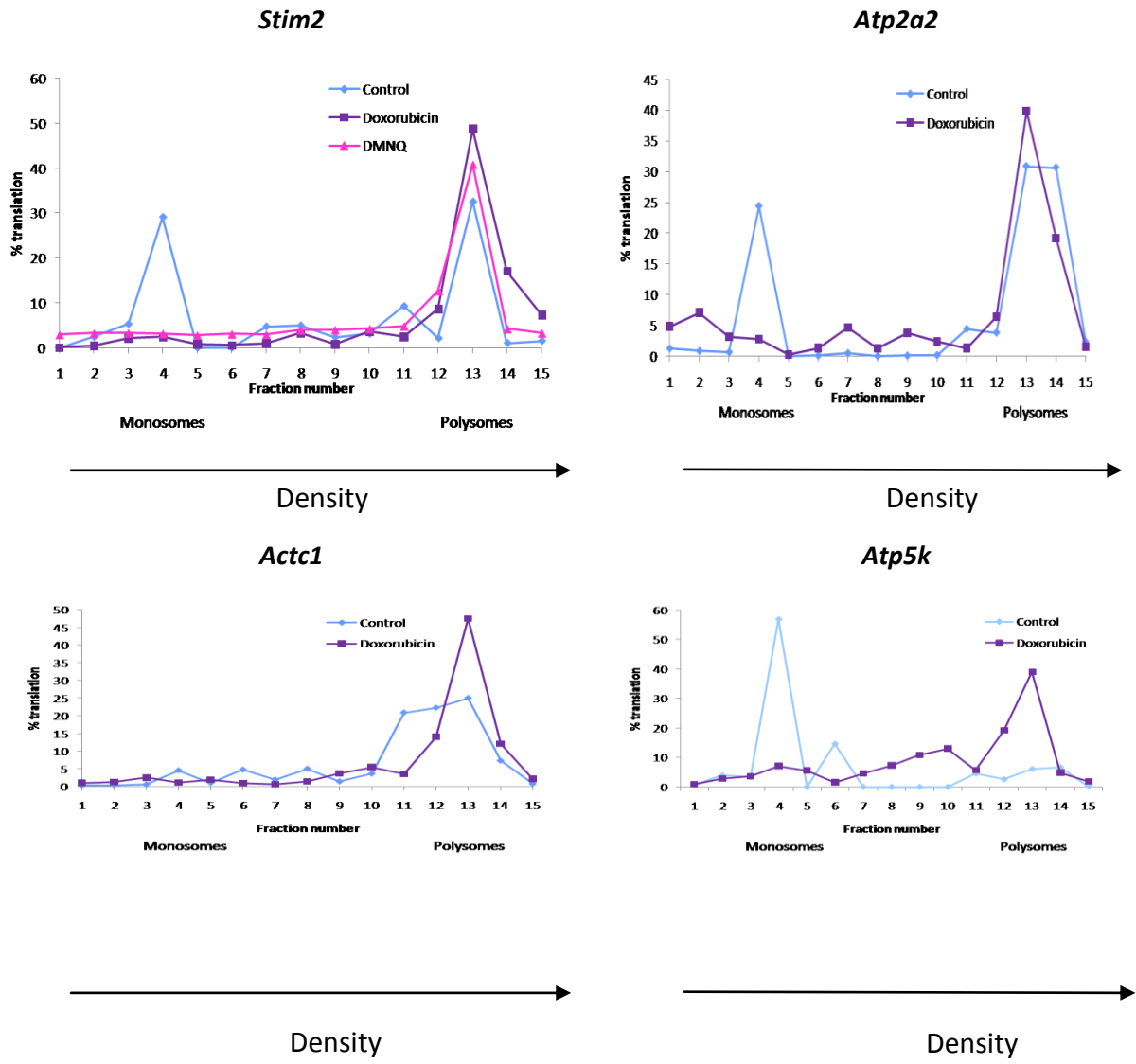
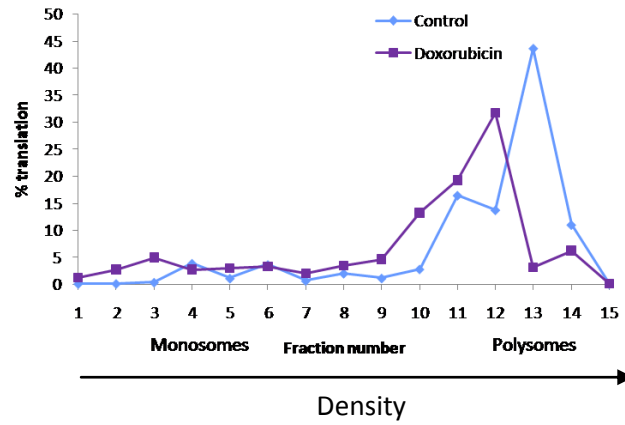
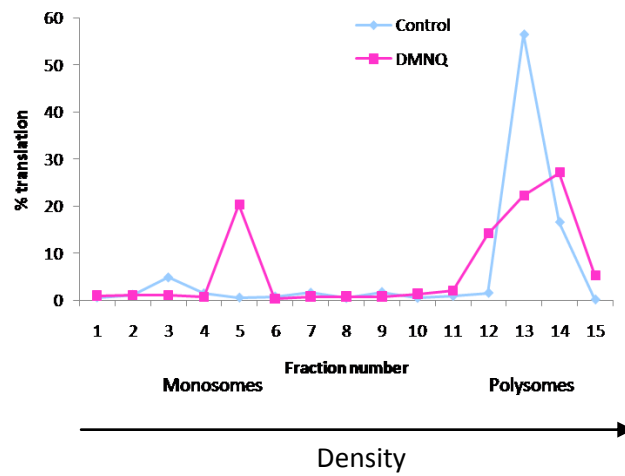


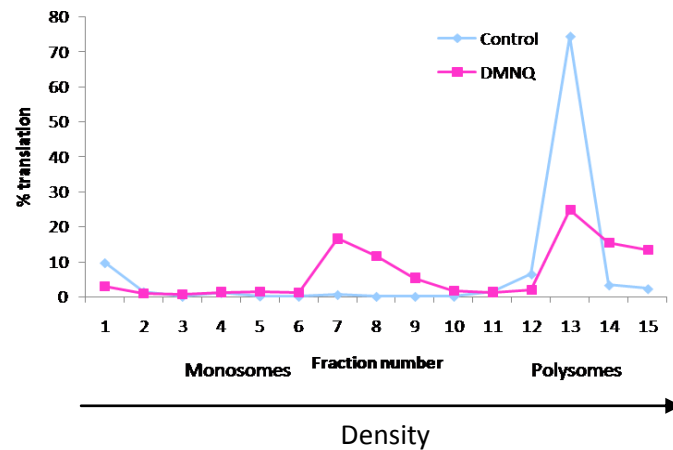
Figure 7.6: Verification of more efficiently translated mRNAs, by qRT-PCR in an acute model of doxorubicin and DMNQ treatment. Results are the mean expression in each fraction across the time course (n=3).



Gata4



Myh9



Acaa2

Figure 7.7: Verification of less efficiently translated mRNAs, by qRT-PCR in an acute model of doxorubicin and DMNQ treatment. Results are the mean expression in each fraction across the time course (n=3).

7.2.5 CORRELATION OF mRNA TRANSLATIONAL PROFILES WITH miRNA EXPRESSION PROFILES

miRNA expression profiles generated in Chapter 6 are only of real value when correlated with actual global mRNA translational changes generated in this chapter. Each miRNA is thought to have hundreds of predicted mRNA targets. Correlations between mRNA and miRNA profiles were identified to allow possible functional interactions to be highlighted. TargetScan 5.0 was used to identify those differentially translated mRNAs containing a binding site for miRNAs that demonstrated a correlating change. For example the gene *Stim2* was more efficiently translated following both doxorubicin and DMNQ in an acute model. *Stim2*, was predicted to contain a binding site for the down-regulated miR-181a (Figure 7.8A). Conversely the gene *Atp1b2* was less efficiently translated following both doxorubicin and DMNQ in an acute model. *Atp1b2* was predicted to contain a binding site for the up-regulated miR-29a (Figure 7.8B). Examples of further possible mRNA-miRNA interactions are shown in Figure 7.9, particularly those involved in the ETC.

During miRNA profiling in Chapter 6 a number of miRNAs identified following doxorubicin administration, but not DMNQ, had been previously associated with cell cycle regulation and DNA damage. Translational profiling following acute doxorubicin exposure also identified a number of genes (E.g.: *Bbc3*, *Nfix*, *Niban*, *Egfl6*, *Btrc*) associated with cell cycle regulation. Correlation between these mRNA and miRNA profiles identified a number of possible interactions (Figure 7.9). These novel correlations enable the identification of possible functionally important mechanisms involved in the cardiotoxic phenotype.

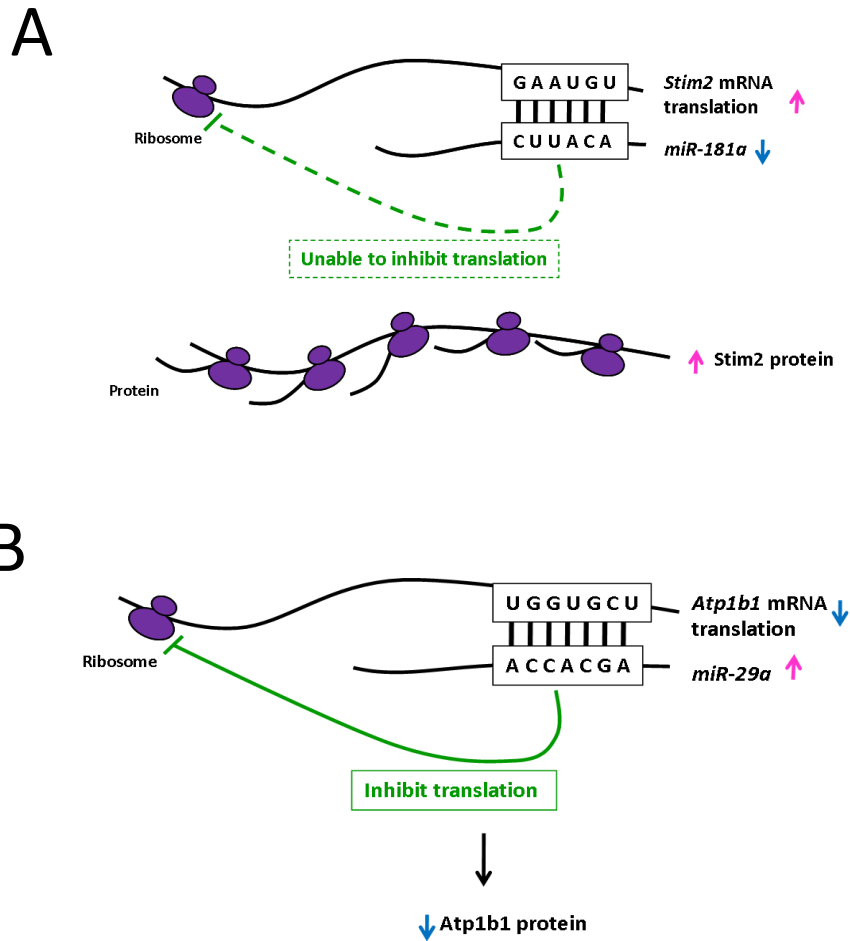


Figure 7.8: Correlation of mRNA-miRNA interactions following acute doxorubicin (15mg/kg) and DMNQ (25mg/kg) treatment. TargetScan 5.0 was used to identify differentially translated mRNAs containing binding sites for miRNAs that demonstrated a corresponding change. mRNAs less efficiently translated following treatment were likely to be targets of miRNAs that were up-regulated, and vice versa. *Stim2* was more efficiently translated and was predicted to contain a binding site for the down-regulated miR-181a (A). Decreased levels of miR-181a resulted in lowered repression of *Stim2* mRNA translation, thus increasing Stim2 protein. The converse was also true (B). *Atp1b1* was apparently translationally less efficiently translated following acute doxorubicin and DMNQ. This gene was predicted to contain a miR-29a binding site, whose expression was up-regulated. Increased miR-29a resulted in increased repression of *Atp1b1* mRNA translation thus reduced *Atp1b1* protein.



Figure 7.9: Correlation of mRNA translational profiles and miRNA expression profiles. mRNAs translationally modulated following acute doxorubicin (15mg/kg, n=3) two hours following dosing and DMNQ (25mg/kg, n=3) one hour following dosing were correlated with miRNAs containing relevant binding sites. TargetScan 5.0 was used to identify such putative interactions. mRNAs less efficiently translated following treatment were likely to be targets of miRNAs that were up-regulated, and vice versa.

7.3 DISCUSSION

The overall aim of this Chapter was to develop a method to allow identification of genes and pathways translationally modulated by either doxorubicin or DMNQ in an acute and chronic model of toxicity. It was hypothesised that, since doxorubicin did not affect transcription as extensively as DMNQ (Chapter5), there may be significant regulatory control at the level of translation. Translational profiles of DMNQ, a pure redox cycling chemical (Gant et al. 1988), were also generated and compared to those of doxorubicin allowing separation of doxorubicin's pharmacological and toxicological activities. Translational profiling firstly requires the separation of RNA into those mRNAs actively undergoing translation, termed polysomes, and those not being actively translated termed monosomes (Figure 7.2), followed by microarray analysis (Figure 7.1).

This analysis indicated the majority of mRNAs to be more efficiently translated following doxorubicin treatment, whereas following DMNQ, an overall equal proportion of mRNAs were more or less efficiently translated. However, the number of transcripts affected was reduced following DMNQ compared to doxorubicin (Table 7.2). The opposite occurred transcriptionally. This was probably a reflection of the inhibition of DNA transcription that is an intrinsic property of doxorubicin. Similar increases in translation have been observed following exposure to radiation, a known inhibitor of transcription (Lü et al. 2006). These data indicate that doxorubicin modifies gene expression primarily at the level of translation, whereas DMNQ primarily regulates gene expression transcriptionally. Changes in translational control therefore appear critical in the regulation of gene expression following doxorubicin and DMNQ treatment. Translational control has been found to be a vital cellular response to hypoxic stress and during oncogenesis (Spence et al. 2006; Blais et al. 2004). During hypoxia and tumour progression a specific subset of mRNA transcripts are translated more efficiently, in particular those involved in cell viability and cellular adaptations. However, during hypoxia a global reduction in translation has been observed. The increase in translation of a specific group of genes is thought to occur through the recruitment of ribosomes from internal ribosome entry sites, thus suggesting that the two mechanisms to initiate translation, internal ribosome entry sites and CAP binding may respond to cellular stimuli in opposing manners, allowing cell survival and adaptations to occur (Blais et al. 2004). These mechanisms may explain the reduction in translational gene expression compared to transcriptional gene expression following DMNQ treatment. It is possible that DMNQ treatment inhibits one mechanism of translational initiation. This inhibition, however, may be overcome by recruitment of ribosomes to mRNA via an alternative method, thus allowing cellular damage to be repaired.

7.3.1 PATHWAY ANALYSIS

Pathway analysis utilising the Gene Set Analysis Toolkit was conducted. Following an acute dose of either doxorubicin or DMNQ a number of pathways were significantly modulated including oxidative phosphorylation, the TCA cycle, axon guidance and cell communication (Figure 7.5A). Both oxidative phosphorylation and the TCA cycle were also significantly modulated at the transcriptional level (Chapter 5). A number of other pathways including the Jak-Stat pathway were significantly affected following acute doxorubicin. As these pathways were only differentially affected by doxorubicin, the occurrence was most likely to be a result of doxorubicin's pharmaceutical activity including its ability to inhibit DNA synthesis and develop resistance. The induction of the Jak-Stat pathway is known to be transcriptionally modulated in breast tumours following doxorubicin treatment (Lee et al. 2009), thus indicating modulation of this pathway in tissues that are the pharmacological target of doxorubicin. Chronically, only oxidative phosphorylation and regulation of the actin cytoskeleton pathway were translationally modulated following both doxorubicin and DMNQ (Figure 7.5B). This lack of concordance between chronic models of toxicity was also apparent at the transcriptional level (Chapter 5). This similar response translationally most likely occurs due to the development of cumulative morphological changes in the heart following doxorubicin but not DMNQ. This lack of cumulative effects following DMNQ administration provides evidence that DMNQ causes cardiotoxicity. However, cardiac tissue exposed was in part able to compensate for, or repair damage, whereas the continued inhibition of gene transcription most likely reduces the ability of the heart to overcome damage following doxorubicin exposure, thus cumulative damage arises.

7.3.2 VERIFICATION OF TRANSLATIONAL MODULATION

Translational changes identified through microarray analysis (Figure 7.5) were verified by qRT-PCR. In general a high level of concordance between the two platforms was observed (Figures 7.7 and 7.8). qRT-PCR using separated RNA allows the movement of each gene

through the gradient to be identified, distinguishing between gross shifts from the monosome to the polysome fractions and vice a verse (E.g.: *Stim2*, *Atp2a2*, *Myh9*, *Atp5k*) from more discrete shifts from the heavy polysome fractions to the lighter polysome fractions and vice a verse (E.g.: *Actc1*, *Gata4*, *Acaa2*), thus identifying different mechanisms responsible for the initiation, elongation and termination of translation (Figures 7.7 and 7.8) (Pillai et al. 2007). A translational block at the initiation stage would most likely result in a shift from the polysome fractions to the monosomal fractions as observed with the gene *Myh9* following acute DMNQ treatment (Figure 7.7). *Myh9* was down-regulated following treatment compared to control and is a member of the myosin heavy chain family responsible for maintaining cell morphology. The inhibition of a translational block at the initiation stage would result in the opposite, i.e.: movement of the gene from the monosome fractions to the polysome fraction. An example of this was *Stim2* (Figure 7.6). *Stim2* is a member of the stromal interaction molecule (STIM) family encoding a transmembrane protein that moved to the lighter fractions of the gradient. A discrete shift from the heavy polysomal region to the lighter polysomal region or vice a verse may result due to disturbances in the elongation or termination stages of translation. As a number of ribosomes remain attached to the mRNA thus a gross translocation to the monosome fractions does not occur or the converse (Pillai et al. 2007). A number of genes verified by qRT-PCR demonstrated such a shift (Figures 7.6 and 7.7). One example was *Gata4*, indicating this gene to be less efficiently translated (Figure 7.7). Transcriptional down-regulation of *Gata4*, a transcription factor, has been previously observed following doxorubicin treatment (Kim et al. 2003). *Gata4* is a survival factor for cardiomyocytes and an upstream regulator of *Bcl-X*, an anti-apoptotic gene (Aries et al. 2004). Consequently down-regulation of *Gata4* could possibly result in the induction of cardiomyocyte apoptosis, manifesting as cardiac failure. Thus the identification of *Gata4* being less efficiently translated provides further evidence of the modulation of gene and protein expression

contributing to the development of the cardiotoxic phenotype. Another example of a discrete shift between fractions was the more efficient translation of *Actc1* (Figure 7.6). *Actc1* encodes an alpha actin filament present in cardiac muscle. These alpha actin filaments are vital to the contractility of cardiac muscle (Matsson et al. 2008). Defects have been associated with dilated cardiomyopathy (Matsson et al. 2008). Similar such discrete changes in gene movement have been reported (Pillai et al. 2007; Petersen et al. 2006). These data thus indicate that translational control is vital to the functionality of the heart following doxorubicin exposure.

7.3.3 miRNA-mRNA PREDICTED INTERACTIONS

Translation is regulated by miRNAs. They appear to be involved in the cellular response to doxorubicin and DMNQ in acute and chronic models of toxicity (Chapter 6). miRNAs modulate translation by binding to partially complementary 8bp recognition sites located in the 3' UTR of target mRNA, and repressing translation or guiding processes for mRNA degradation (Meister 2007; Pillai et al. 2007). The specific biochemical mechanism underlying miRNA induced gene expression remains to be elucidated. However, miRNAs are thought to repress translation initiation by preventing the binding of the 60S ribosomal subunit to the target mRNA (Wang et al. 2008), thus preventing mRNA translation. However, due to the recent identification of miRNAs in polysome fractions, a role for these small non-coding RNA species in elongation has been proposed (Meister 2007).

miRNA expression profiles are only of any value when correlated with mRNA translational profiles, hence identifying specific miRNA-mRNA interactions. A number of *in vitro* methods for identifying such interactions have been developed. They rely on the knockdown of specific miRNAs followed by genomic and proteomic analysis (Baek et al. 2008; Selbach et al. 2008). Of most importance these methods depend on the assumption that a change in transcription leads to a change in translation. This however does not always hold true as

shown by decreased translational change compared to transcriptional gene expression following DMNQ treatment and vice a versa following doxorubicin.

Genome wide profiling of translational changes as conducted in this chapter allows correlation with altered miRNA expression profiles (Chapter 6) in a high throughput manner. However the identification of miRNA-mRNA interactions does rely upon current bioinformatic packages that can generate hundreds of possible mRNA targets that are variable between packages. This variability likely arises due to inaccuracies in the underlying algorithms. However, this method does allow a more focused analysis of such putative interactions following doxorubicin and DMNQ treatment. A number of possible putative miRNA-mRNA interactions have also been identified following acute doxorubicin and DMNQ treatment (Figure 7.9). A number of these interactions implicate genes involved in the ETC.

7.3.4 SUMMARY

The findings of this study indicate that this combined genomic and bioinformatic approach can be successfully utilised to generate translational profiles coupled with the identification of putative miRNA-mRNA interactions. The increased translational gene expression compared to transcriptional gene expression (Chapter 5) suggests doxorubicin modifies gene expression primarily at the level of translation, whereas DMNQ modified gene expression primarily at the level of transcription. Translational profiling combined with pathway analysis identified the oxidative phosphorylation pathway to be predominantly differentially translated following both doxorubicin and DMNQ in an acute and chronic model of toxicity. Further experiments are required to determine the exact influence of doxorubicin and DMNQ on each complex of the ETC (Chapter 8). miRNA-mRNA interactions were identified that possibly contribute or protect against the associated cardiotoxicity. Further in-depth functional analysis of these miRNAs is required to determine the importance of each.

**Chapter 8: Effect of Doxorubicin and DMNQ on
Mitochondria and the Utilisation of *In Vitro*
Models to Investigate microRNA Function**

8.1 INTRODUCTION

Two objectives were investigated in this study both derived from previous chapters implicating differential transcription and translation of the oxidative phosphorylation pathway and the identification of miRNAs in the modulation of toxicity. miRNA knockdown was conducted in an *in vitro* model, followed by doxorubicin and DMNQ exposure, to evaluate the function of specific miRNAs in models of cardiotoxicity.

Genes involved in energy dynamics were found to be differentially expressed following both doxorubicin and DMNQ in an acute and chronic model of toxicity. Oxidative phosphorylation is the metabolic process that couples the oxidation of reduced NADH and FADH₂ to the phosphorylation of ADP to ATP, by utilizing the ETC in the inner mitochondria membrane (Muravchick and Levy 2006). The oxidoreductive activity of the ETC is converted to the high-energy phosphate bond of ATP through a series of five enzyme complexes (Wallace and Starkov 2000). Further in-depth functional investigations were conducted to determine the activity of each of the five enzyme complexes to assess mitochondrial energy dynamics. No data of this nature is currently available. Mitochondrial function and mass and ATP synthesis was further assessed by the measurement of citrate synthase, GLDH levels and ATP levels within cardiac tissue. GLDH is located within the mitochondrial matrix and catalyzes the conversion of glutamate to 2-oxoglutarate. GLDH is released from mitochondria upon damage, thus measurement of this enzyme allows measurement of mitochondrial function. Citrate synthase is involved in the first step of the TCA cycle and allows determination of mitochondrial mass.

8.1.2 PLAN OF INVESTIGATION

The overall objective of this study was to assess the activity of the five complexes of the ETC both *in vivo* (Chapter 4) and *in vitro*, in HL-1 cells. In addition, the *in vitro* model allowed the knockdown of specific miRNAs, identified as modulated in the cardiotoxic state (Chapter 6). After the modulation of miRNA expression, cells were treated with doxorubicin and DMNQ,

to assess the role of specific miRNAs in cardiotoxicity. The phenotypic consequences of miRNA knockdown were measured by LDH and creatine kinase muscle/brain (CK-MB) release. This allowed the hypothesis that miRNAs are important in regulating the cardiomyocyte response to doxorubicin and DMNQ to be tested. Knockdown of specific miRNAs was achieved using locked nucleic acid (LNA) miRNA probes that allowed antisense inhibition of miRNAs. These probes were transfected into cells by chemical transfection using a lipid carrier.

Previous *in vivo* dose levels and exposure times defined in Chapter 4 were utilised. Prior to the establishment of suitable *in vitro* models of toxicity, two *in vitro* models were compared, the HL-1 cell line and primary cardiomyocytes. HL-1 cells were used in all further *in vitro* models as transcriptional profiling revealed a high level of similarity.

In vitro models of doxorubicin and DMNQ toxicity were established. Dose response experiments were conducted over a range of 0.1-10 μ M for 24 hours. These dose levels and length of exposure were derived from available literature. Suitable sub-cytotoxic dose levels were selected using an MTS assay to assess cell viability. Subsequently transcriptional and miRNA expression profiling was conducted. This allowed assessment of the suitability of *in vitro* models for use in cardiotoxic screening.

8.1.3 HYPOTHESIS AND AIM

The overall aim of this study was to investigate two hypotheses derived from previous data. The first aim was to evaluate the activity of the ETC and assess mitochondrial function *in vivo* and *in vitro*. It was hypothesised that altered transcription and translation of genes encoding the enzymes of the ETC would affect the activity of each complex and possibly result in altered mitochondria function and decreased ATP synthesis. The second aim was to knockdown specific miRNAs. It was hypothesised that the knockdown of miRNAs that were differentially expressed in Chapter 6 would affect the resulting toxicity.

8.2 RESULTS

8.2.1 COMPARISON OF CARDIAC *IN VITRO* AND *IN VIVO* MODELS

For assessment of the role of miRNA species, an *in vitro* model was required. Two models were considered, primary cardiomyocytes and a cardiac cell line (HL-1). HL-1 cells were obtained as a gift from Dr. W. Claycomb and cultured as outlined in section 2.2. Primary cardiomyocytes were also prepared and cultured as described in section 2.3. Microarray transcriptional profiling was conducted to compare the transcriptional profiles of HL-1 cells and primary cardiomyocytes versus cardiac tissue from untreated animals. This allowed the comparison between *in vivo* and *in vitro* models. Genes were included in the analysis if they were differentially expressed at a $\text{Log}_2 < 1.5$ or $\text{Log}_2 > 1.5$ with a p-value of < 0.05 . This revealed 529 and 900 genes that were differentially regulated in HL-1 cells and primary cardiomyocytes respectively, compared to cardiac tissue (Figure 8.1). As the gene expression profiles of HL-1 cells resulted in fewer gene changes, these cells were used as the *in vitro* cardiomyocyte model in all future experiments.

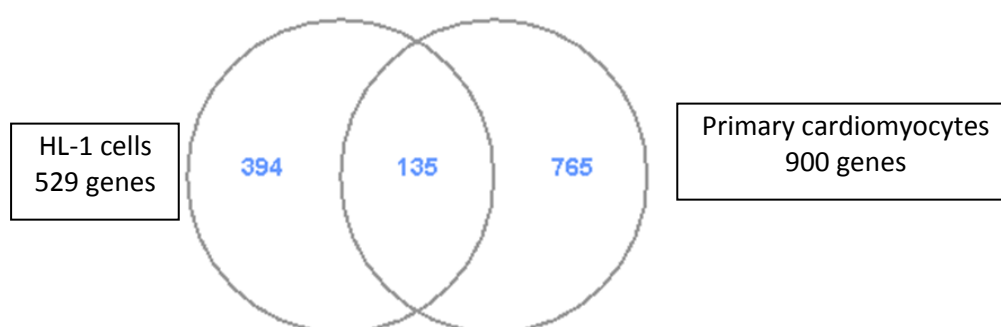


Figure 8.1: Venn diagrams of HL-1 and primary cardiomyocyte gene expression changes compared to cardiac *in vivo* gene expression profiles. Results are the mean of LOWESS normalised values (n=3) subjected to a one sample two tailed t-test.

8.2.1.1 IN VITRO DOSE SELECTION

Dose ranging experiments were conducted in HL-1 cells treated with doxorubicin and DMNQ in 1% DMSO (Section 2.2). Cell viability was assessed by an MTS assay (Section 2.5). The concentrations evaluated for each compound are detailed in Table 8.1.

Compound	Concentration (μM)	Exposure Time (hours)
Doxorubicin	0, 0.25, 0.5, 0.75, 1, 5, 10	24
DMNQ	0, 0.25, 0.5, 0.75, 1, 5, 10	24

Table 8.1: Concentration range of doxorubicin and DMNQ tested in dose selection experiments *in vitro*.

The MTS assay revealed the threshold of cytotoxicity following 24 hours exposure in HL-1 cells was $1\mu\text{M}$ for doxorubicin and $5\mu\text{M}$ for DMNQ (Figure 8.2). These concentrations were used for all further *in vitro* experiments.

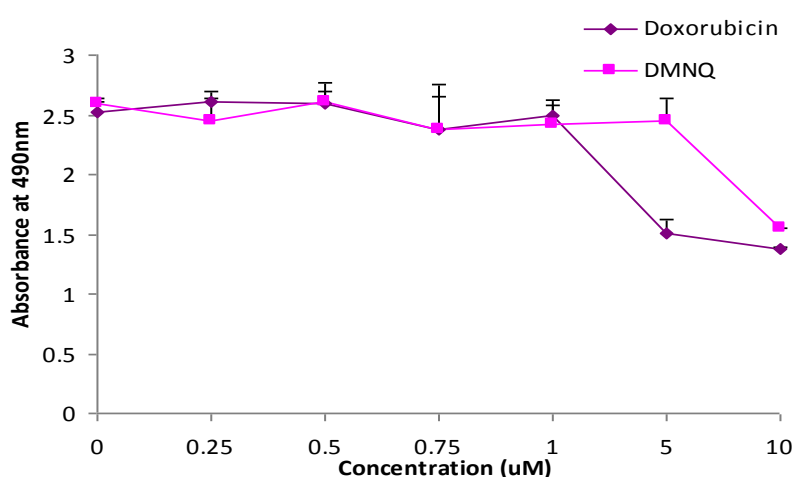


Figure 8.2: Cell viability following 24 hours exposure of doxorubicin or DMNQ. Cell viability was measured by an MTS assay; the absorbance at 490nm is directly proportional to the number of viable cells. Results are mean values of $n=3 \pm \text{S.D.}$ A $1\mu\text{M}$ and $5\mu\text{M}$ dose of doxorubicin and DMNQ, respectively, were the sub-cytotoxic doses, identified as the dose level at which after there is a sharp decrease in absorbance indicative of increased cell death (Chapter 2).

8.2.1.2 TRANSCRIPTIONAL AND miRNA PROFILING IN VITRO

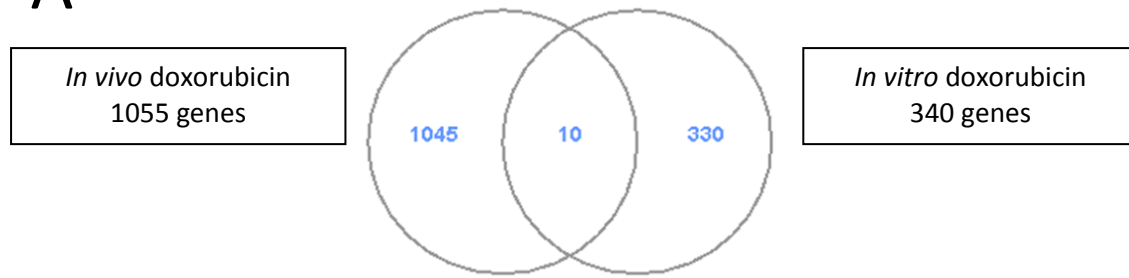
Following establishment of a suitable *in vitro* model and dosing regime, transcriptional and miRNA expression profiles were conducted to identify miRNAs and genes differentially

regulated following doxorubicin and DMNQ exposure *in vitro*. This allowed a genomic comparison between *in vivo* and *in vitro* models and identified miRNAs for functional analysis.

Transcriptional *in vitro* profiling

Total RNA was isolated from triplicate cultures exposed to vehicle control, 1 μ M doxorubicin or 5 μ M DMNQ for 24 hours (Section 2.2). Microarray analysis was conducted using MEEBO microarrays printed in-house, followed by LOWESS normalization and a one sample two tailed t-test as outlined in section 1.5.7. Genes were included in the analysis if a gene was significant at $p \leq 0.05$ and had a $\text{Log}_2 < 1$ or $\text{Log}_2 > 1$. This resulted in 340 and 219 genes differentially expressed following doxorubicin and DMNQ treatment, respectively, of which 14 were affected by both compounds. In order to compare the *in vitro* and *in vivo* models, venn diagrams were constructed (Figure 8.3). This identified limited similarity between the response to either doxorubicin or DMNQ *in vivo* and *in vitro*, thus highlighting the necessity to investigate cardiotoxicity *in vivo* and the need for improved *in vitro* cardiomyocyte models to reduce the reliance on animals. In order to apply biological meaning to the *in vitro* gene expression profiles pathway analysis was conducted using the Gene Set Analysis Toolkit to classify genes into KEGG pathways (Table 8.2). This identified cell communication to be the predominantly affected pathway following doxorubicin and bile acid biosynthesis following DMNQ, this highlights distinct differences compared to the *in vivo* transcriptional profiles. However glycolysis and oxidative phosphorylation were modulated by doxorubicin and the TCA cycle and glycolysis following DMNQ exposure, suggesting a role for altered energy dynamics *in vitro*, but it was not the dominant mechanism. This was most likely to be a result of altered metabolism and oxygen tension *in vitro*.

A



B

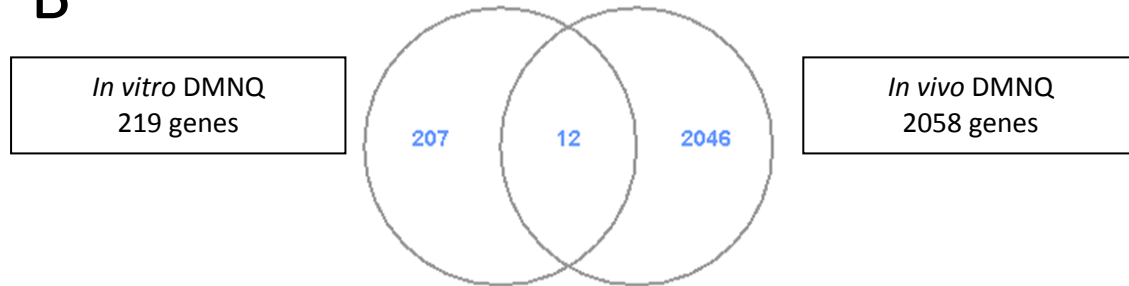


Figure 8.3: Venn diagrams of *in vitro* and *in vivo* gene transcriptional expression changes following doxorubicin (A) or DMNQ (B). *In vivo* expression profiles were generated by calculating the mean expression at each time point including all modes of toxicity. Results are the mean of LOWESS normalised values (n=3) subjected to a one sample two-tailed t-test. Genes displaying a p-value of ≤ 0.05 were included in this analysis.

Doxorubicin		DMNQ	
KEGG pathway	Enrichment (P value)	KEGG pathway	Enrichment (P value)
Cell Communication	7.87E-04	Bile acid biosynthesis	2.78E-04
PPAR signaling pathway	1.95E-03	Antigen processing and presentation	3.82E-03
Focal adhesion	3.33E-03	Fatty acid metabolism	5.42E-03
Glyoxylate and dicarboxylate metabolism	9.17E-03	Glycerolipid metabolism	6.75E-03
Regulation of actin cytoskeleton	1.47E-02	Type I diabetes mellitus	8.79E-03
Glycolysis / Gluconeogenesis	2.68E-02	Glycolysis / Gluconeogenesis	1.12E-02
Carbon fixation	3.21E-02	1- and 2-Methylnaphthalene degradation	1.28E-02
gamma-Hexachlorocyclohexane degradation	3.80E-02	Metabolism of xenobiotics by cytochrome P450	1.32E-02
Tight junction	4.35E-02	Citrate cycle (TCA cycle)	2.23E-02
Oxidative phosphorylation	4.49E-02	Pyruvate metabolism	3.81E-02
Cell cycle	4.91E-02		

Table 8.2: Significantly affected KEGG pathways following doxorubicin (1 μ M) and DMNQ (5 μ M) in HL-1 cells for 24 hours. Genes included are significantly ($p \leq 0.05$) regulated at $\text{Log}_2 < 1.5$ or $\text{Log}_2 > 1.5$, n=3. The enrichment score was calculated using a modified Fisher exact test. Any pathway with a p value of > 0.05 were discarded.

miRNA *in vitro* profiling

Total RNA was isolated from triplicate cultures exposed to vehicle control, 1 μ M doxorubicin or 5 μ M DMNQ for 24 hours (Section 2.2). Microarray analysis was conducted (Section 2.19).

miRNAs were included in analysis if a miRNA was significant at $p \leq 0.05$ and a $\text{Log}_2 < 1.5$ or $\text{Log}_2 > 1.5$ in the *in vitro* model. *In vivo* expression profiles from Chapter 6 were generated by calculating the mean expression at each time point including all models of toxicity. This analysis identified miRNAs affected in an *in vitro* model following doxorubicin ($1\mu\text{M}$) and DMNQ ($5\mu\text{M}$) exposure (Figure 8.4). In order to compare the *in vitro* and *in vivo* models, venn diagrams were constructed (Figure 8.5). This identified limited similarity between the response to either doxorubicin or DMNQ *in vivo* and *in vitro*. Despite this limited similarity in response following both doxorubicin and DMNQ *in vitro* and *in vivo*, a number of miRNAs differentially expressed *in vivo* were also differentially expressed in a comparable manner *in vitro*. One such miRNA was miR-181a (down-regulated); the function of this miRNA was further investigated by knockdown experiments.

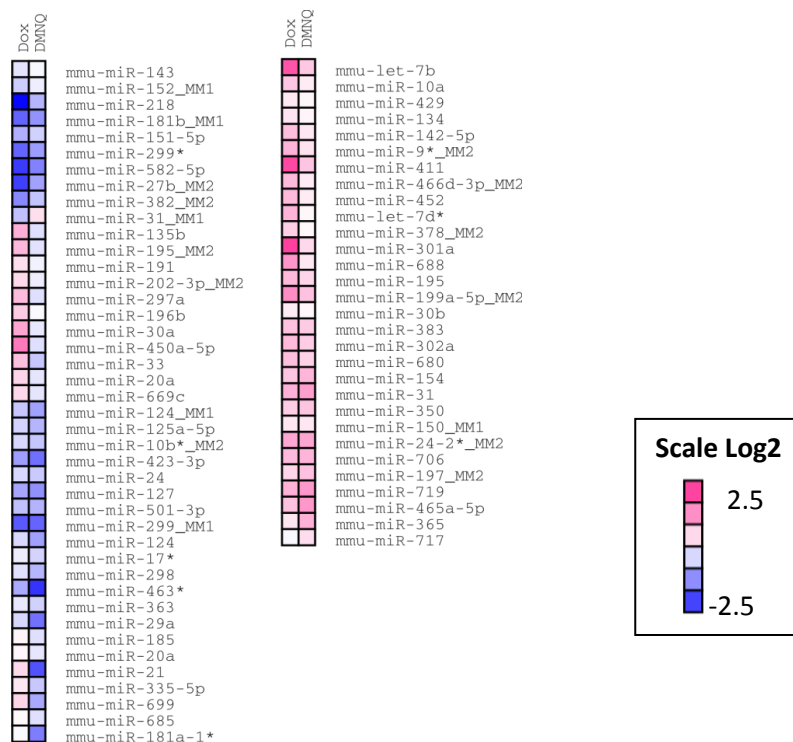


Figure 8.4: Signature of miRNAs affected *in vitro*, by both doxorubicin ($1\mu\text{M}$) and DMNQ ($5\mu\text{M}$). miRNAs included are significantly ($p \leq 0.05$, one sample two-tailed t-test) regulated at a $\text{Log}_2 < 1$ or $\text{Log}_2 > 1$ following $1\mu\text{M}$ doxorubicin or $5\mu\text{M}$ DMNQ for 24 hours ($n=3$).

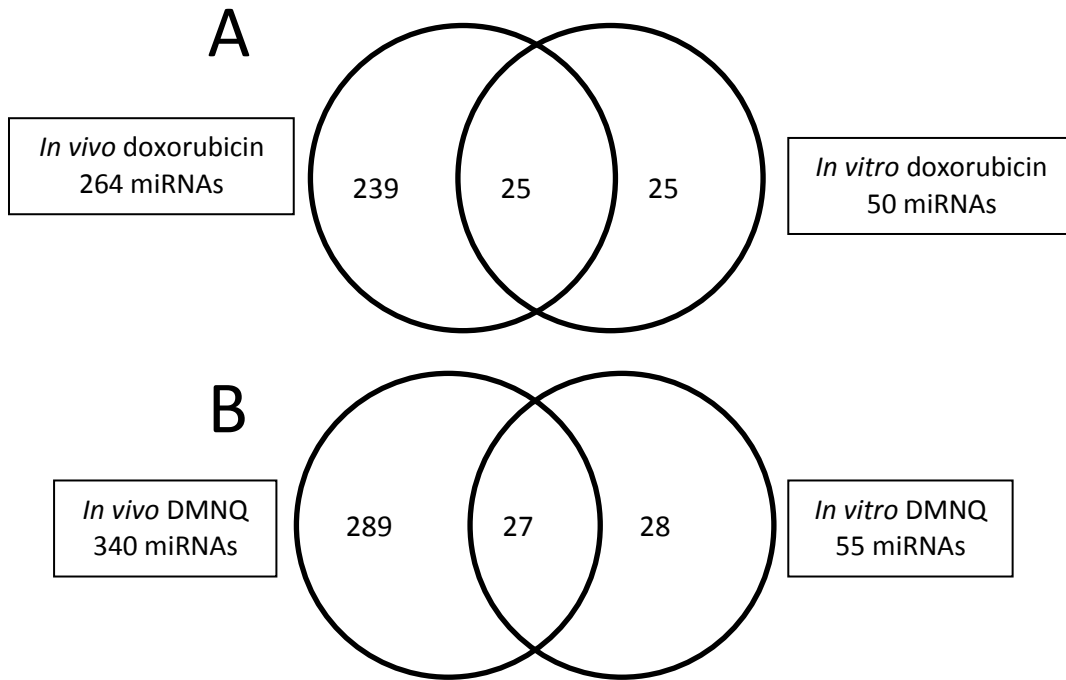


Figure 8.5: Venn diagrams of *in vitro* and *in vivo* miRNA expression changes following doxorubicin (A) or DMNQ (B). *In vivo* expression profiles were generated by calculating the mean expression at each time point including all models of toxicity. Results are mean LOWESS normalised values (n=3) subjected to a one sample two tailed t-test at each time point. Genes displaying a p-value of ≤ 0.05 were included in this analysis.

8.2.2 miRNA KNOCKDOWN

HL-1 cells were incubated with transfection media containing 20nM locked nucleic acid miR-181a antisense probe (Section 2.2.1) for 48 hours to allow miR-181a knockdown to occur.

Following the 48 hour transfection incubation, HL-1 cells were exposed to 1 μ M doxorubicin or 5 μ M DMNQ and incubated for a further 24 hours (Section 2.2). Cells were observed by light microscopy at regular intervals to check cell viability compared to endogenous control and treated HL-1 cells. No gross morphological differences were observed. Following 24 hours exposure to doxorubicin or DMNQ, miR-181a expression, LDH leakage and CK-MB activity was assessed.

To determine the level of target miRNA knockdown, qRT-PCR was used to assess miR-181a expression. 72 hours following initial exposure to transfection complexes, miR-181a expression was reduced by 80%, thus efficient knockdown was achieved (Figure 8.6). LDH

release into culture media was assessed to observe the effects on cell viability. Following 24 hours exposure of doxorubicin or DMNQ in HL-1 cells or HL-1 miR-181a knockdown cells, LDH leakage in cell culture media was increased compared to vehicle control knockdown and endogenous cultures. No change in LDH release was observed in control endogenous and control knockdown cells, indicating the presence of miR-181a knockdown did not affect cell viability prior to chemical exposure (Figure 8.6).

miR-181a knockdown resulted in no change in CK-MB levels (Chapter 1) in culture media following 72 hours of knockdown (Figure 8.6). However increased CK-MB release was observed in knockdown cells following 24 hours exposure to doxorubicin or DMNQ compared to treatment in endogenous cells or vehicle treated controls (Figure 8.6). There also appeared to be a slight change in mobility of CK-MB in knockdown cells following doxorubicin (Figure 8.6).

8.2.3 ELECTRON TRANSPORT CHAIN COMPLEX ACTIVITY

C57B6/AJ male mice were dosed i.p. with doxorubicin (15mg/kg), DMNQ (25mg/kg) or the respective vehicle control in the acute model, or 2mg/kg/wk doxorubicin or DMNQ in a chronic model (Section 2.1). Animals were sacrificed at the time points detailed in Table 8.3. The *in vitro* model established in section 8.2.1 was also used. The primary reason for the use of an *in vitro* model was to enable method development of each enzyme assay, as a number of publications (Nowak et al. 2008; Chinta and Andersen 2006; Law et al. 1995) report measurement of ETC enzyme complexes *in vitro* but not *in vivo*. *In vitro* systems were therefore employed to act as positive control and allow optimisation and validation of each method. In order to investigate the activity of each of the five enzyme complexes that constitute the oxidative phosphorylation pathway, kinetic based assays were developed (Section 2.25). Each assay was optimised and validated by omitting electron donors or acceptors.

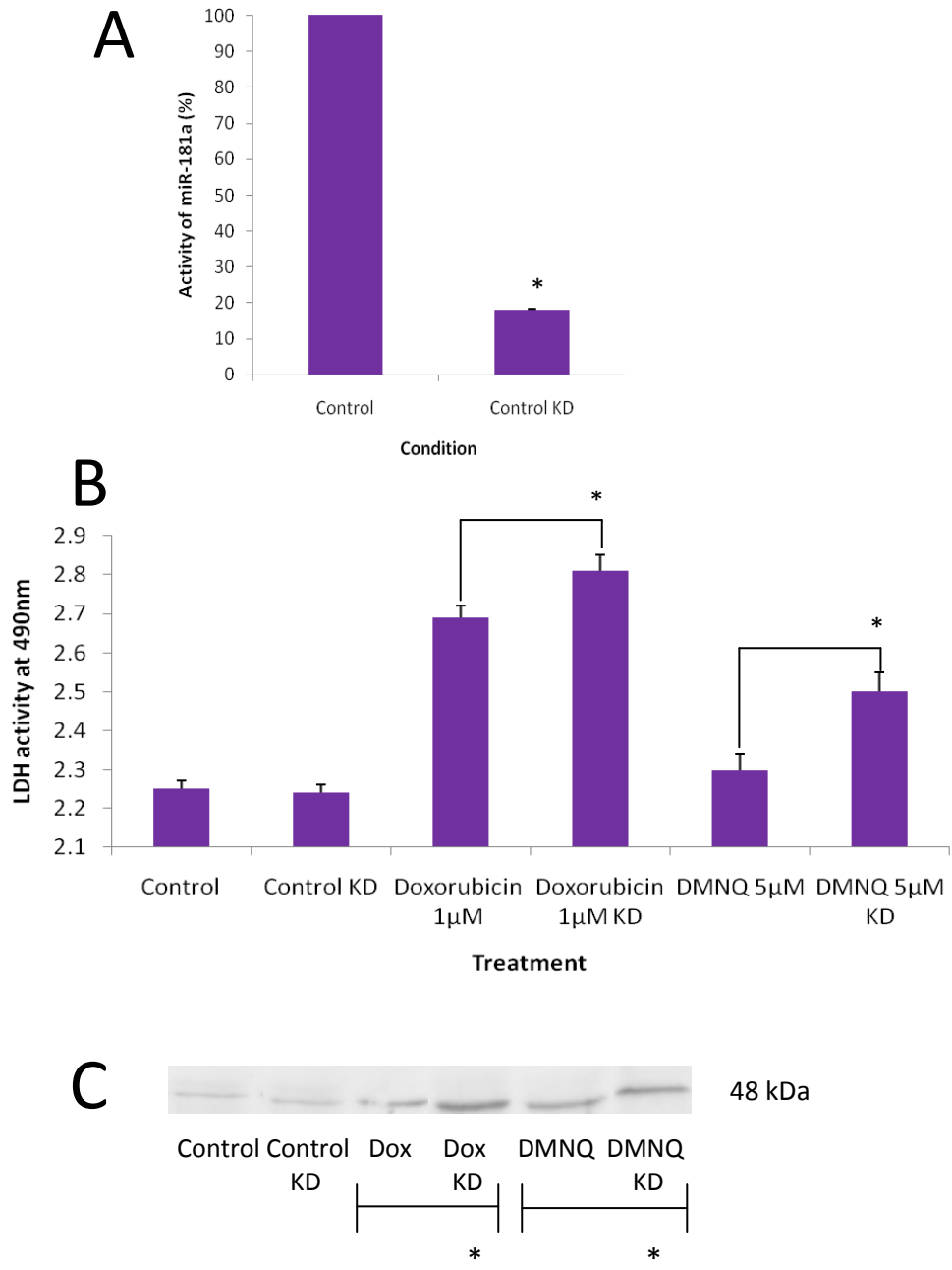


Figure 8.6: miR-181a expression (A), LDH release (B) and CK-MB release (C) in HL-1 cells exposed to doxorubicin or DMNQ exposure following miR-181a knockdown. miR-181a expression was assessed prior to exposure to doxorubicin and DMNQ to ensure miR-181a expression was reduced. LDH leakage and CK-MB release was assessed 24 hours following doxorubicin and DMNQ in culture media. Results are mean values of triplicate cultures \pm S.D. and one way ANOVA and post-hoc Dunnett's T-test * $p \leq 0.01$. Results are mean values of $n=3$, \pm S.D.

Compound	Model of Toxicity	Time Point of Sacrifice
Doxorubicin	Acute	0.5, 1, 2, 12, 24 and 120 hours
DMNQ	Acute	0.16, 0.5, 1, 2, 12, 24 and 120 hours
Doxorubicin	Chronic	3, 5 and 7 weeks
DMNQ	Chronic	3, 5 and 7 weeks

Table 8.3: Table stating the time points of sacrifice for mitochondrial enzyme activity assays *in vivo*.

Complex I of the ETC receives electrons in the form of NADH formed in the TCA cycle. This enzyme transfers electrons from NADH to ubiquinone (an electron acceptor), resulting in the oxidation of NADH to NAD⁺. Complex I activity was measured by a rotenone sensitive oxidation of NADH. Rotenone is a known inhibitor of complex I and binds to the ubiquinone binding site on the enzyme complex, thus preventing the oxidation of NADH. The amount of NADH is directly proportional to absorption at 340nm. Complex I activity was reduced in all models of toxicity (Figure 8.7). *In vivo* in an acute model, doxorubicin treatment resulted in a gradual decrease in complex I activity from 0.5 to 2 hours following dosing. From 12 to 120 hours a gradual increase in activity was observed, however levels were still reduced compared to control. Lowest activity was observed 2 hours following a single dose of doxorubicin (Figure 8.7A). Acute DMNQ treatment also resulted in a gradual decrease in activity from 0.5 to 12 hours, from which point a gradual increase was present. However, activity was still reduced in comparison to control levels. Lowest activity was observed 12 hours following a single dose of DMNQ (Figure 8.7A). A similar reduction was also present *in vivo* following chronic administration of both doxorubicin and DMNQ, with the lowest activity being observed 3 weeks following the start of dosing. Activity was still reduced at 7 weeks following the start of dosing (Figure 8.7 B). An *in vitro* model also resulted in a decrease in complex I activity. However, the magnitude of reduction was reduced compared to the *in vivo* data (Figure 8.7C).

The activities of complexes II and III were measured in conjunction. Complex II oxidises succinate to fumarate in the TCA cycle and transfers electrons to ubiquinone, which is

subsequently reduced to ubiquinol by complex III. Complex III then transfers electrons from ubiquinol to cytochrome c. Complex II activity was measured by a succinate-dependent TFA sensitive reduction of cytochrome c at 550 nm. Complex III activity was measured by a succinate-dependent antimycin-A sensitive reduction of cytochrome c at 550 nm (Figures 8.8). *In vivo* in an acute model of doxorubicin and DMNQ toxicity an overall significant ($p \leq 0.05$) decrease in complex II activity was observed. Lowest activity was present 120 and 12 hours following a single dose of doxorubicin and DMNQ, respectively (Figure 8.8A). Chronically a significant ($p \leq 0.05$) decrease in complex II activity was also present, with lowest activity occurring 3 and 7 weeks following the start of doxorubicin and DMNQ dosing, respectively (Figure 8.8B). *In vitro*, however, no significant reduction in complex II activity occurred (Figure 8.8C).

Complex III activity was also reduced in all models of toxicity (Figure 8.9). In the acute *in vivo* model, lowest activity was observed 1 and 12 hours following doxorubicin and DMNQ, respectively. Chronically a decrease in activity was also observed, with lowest activity occurring 5 weeks following the start of dosing with both compounds. *In vitro* a decrease was also present.

Complex IV is the terminal member of the ETC, coupling the transfer of electrons from cytochrome c to oxygen. Complex IV activity was measured by a sodium azide sensitive oxidation of cytochrome c. Sodium azide is a known competitive inhibitor of complex IV. *In vivo* in an acute model of doxorubicin and DMNQ toxicity a gradual increase in complex IV activity occurred with peak activity occurring 120 and 12 hours following doxorubicin and DMNQ, respectively (Figure 8.10A). Chronically, increased complex IV activity was also present. However, doxorubicin treatment resulted in a maximum 4 fold change 5 weeks following the start of dosing, whereas DMNQ treatment resulted in only a maximum fold change of 1.5, 3 weeks following the start of dosing (Figure 8.10B). A similar result was found in the *in vitro* model of toxicity (Figure 8.10C).

Complex V is the final enzyme complex in the oxidative phosphorylation pathway. It catalyzes the formation of ATP using a proton gradient generated by the movement of protons across the inner mitochondrial membrane by the previous enzyme complexes. Complex V activity was measured by an oligomycin sensitive oxidation of NADH via two enzymatically catalysed reactions. *In vivo*, in both models of toxicity, a significant ($p \leq 0.05$) increase in activity was present following both doxorubicin and DMNQ (Figure 8.11). *In vitro*, complex V activity was also increased following both doxorubicin and DMNQ (Figure 8.11C). In summary, the activity of complex I, II and III were decreased while the activity of complex IV and V were increased following doxorubicin and DMNQ both *in vivo* (acute and chronic) and *in vitro* (Figure 8.12).

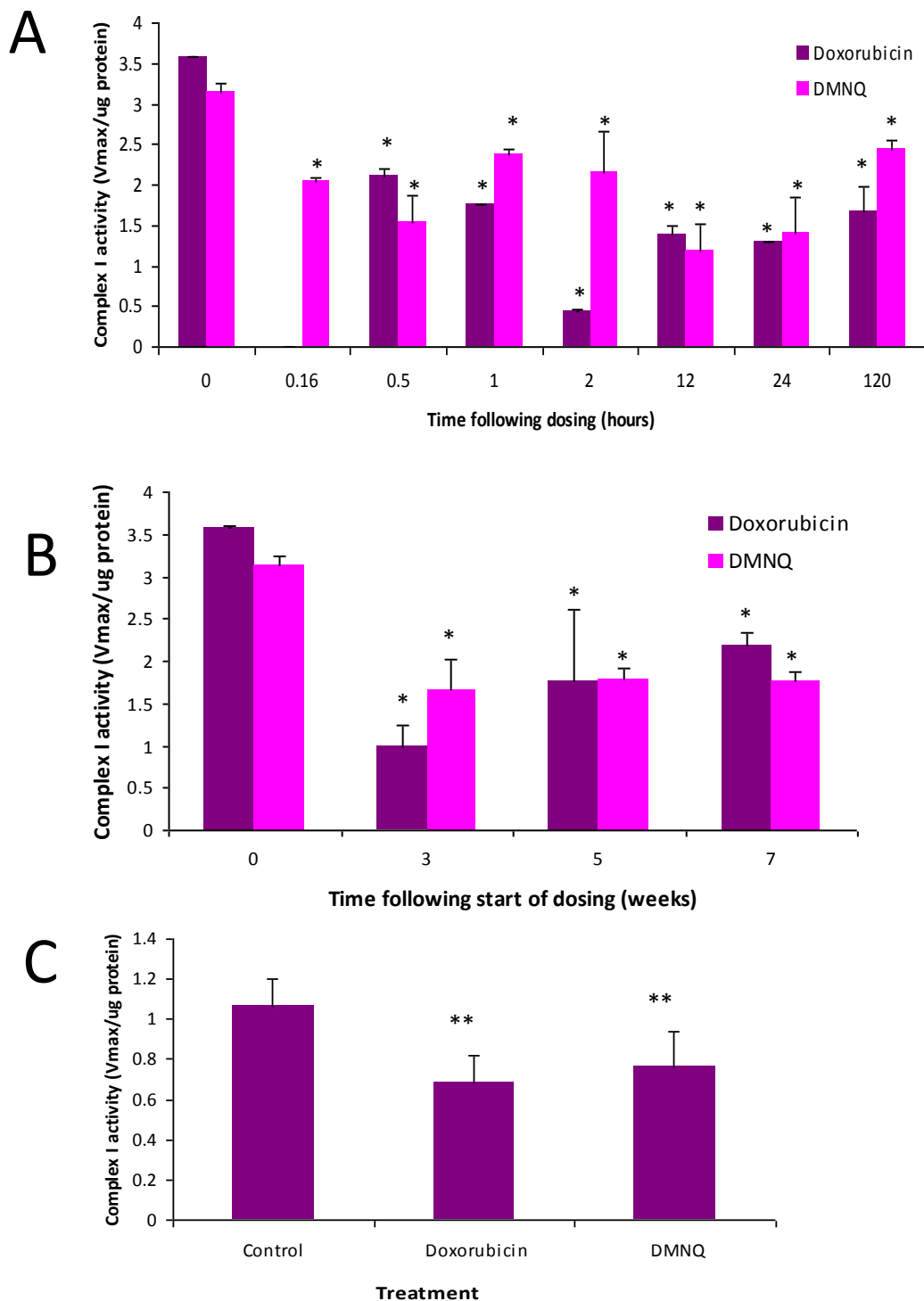


Figure 8.7: Complex I activity *in vivo* in an acute (A) and chronic (B) model of toxicity following doxorubicin DMNQ. The activity in HL-1 cells following both compounds was also determined (C). A significant decrease in complex I activity was recorded in all models. The magnitude of change was lower in HL-1 cells. Results are mean $n=3 \pm$ S.D., one way ANOVA and post-hoc Dunnett's T-test * $p \leq 0.01$, ** $p \leq 0.05$.

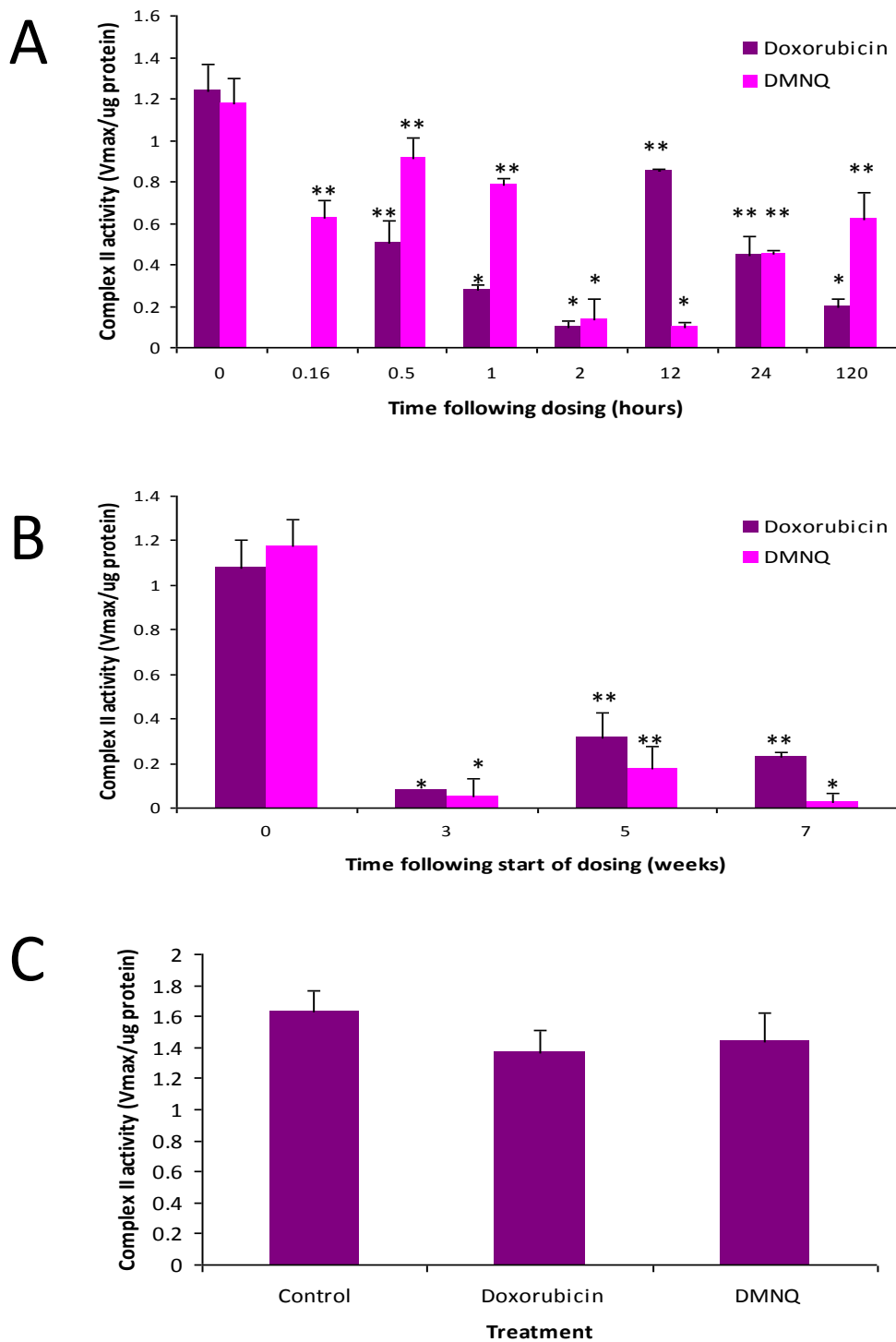


Figure 8.8: Complex II activity *in vivo* in an acute (A) and chronic (B) model of toxicity following doxorubicin DMNQ. The activity in HL-1 cells following both compounds was also determined (C). A significant decrease in complex II activity was recorded *in vivo* but not *in vitro*. Results are mean $n=3 \pm$ S.D., one way ANOVA and post-hoc Dunnett's T-test * $p \leq 0.01$, ** $p \leq 0.05$.

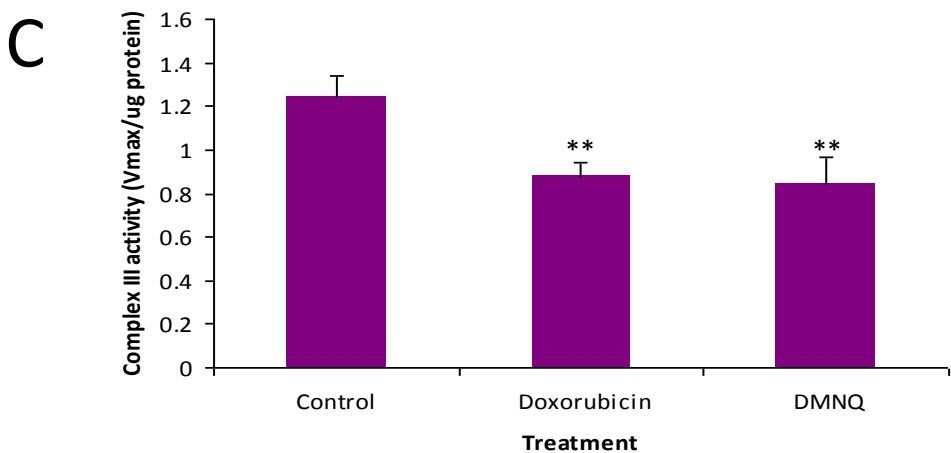
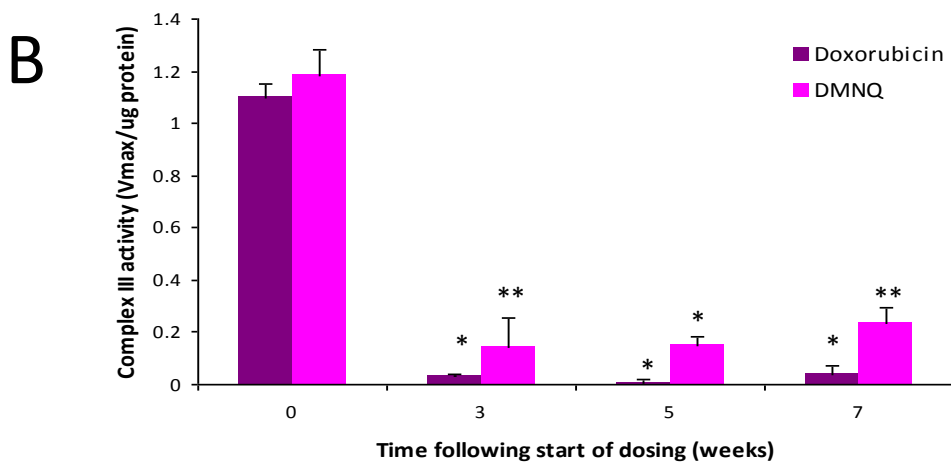
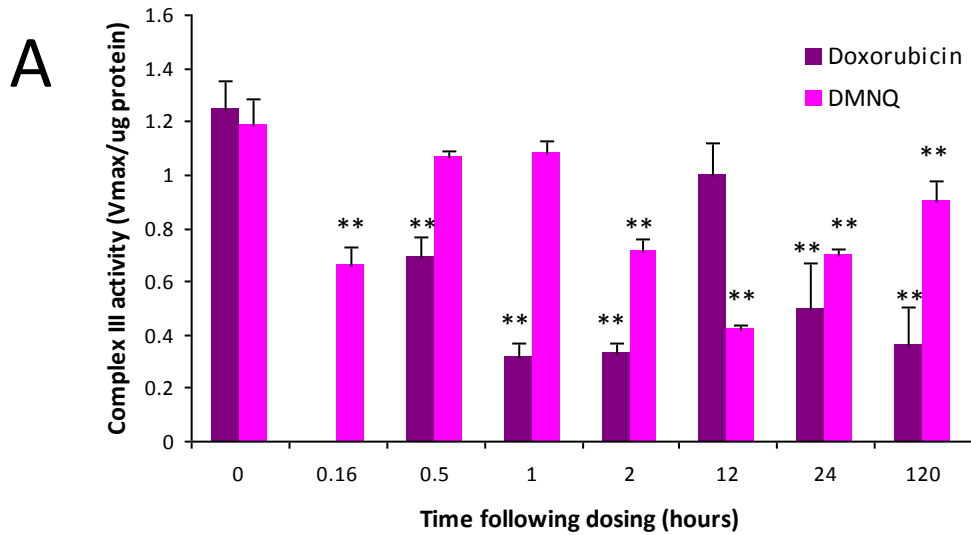


Figure 8.9: Complex III activity *in vivo* in an acute (A) and chronic (B) model of toxicity following doxorubicin DMNQ. The activity in HL-1 cells following both compounds was also determined (C). A significant decrease in complex III activity was recorded in all models. Results are mean $n=3 \pm$ S.D., one way ANOVA and post-hoc Dunnett's T-test * $p \leq 0.01$, ** $p \leq 0.05$.

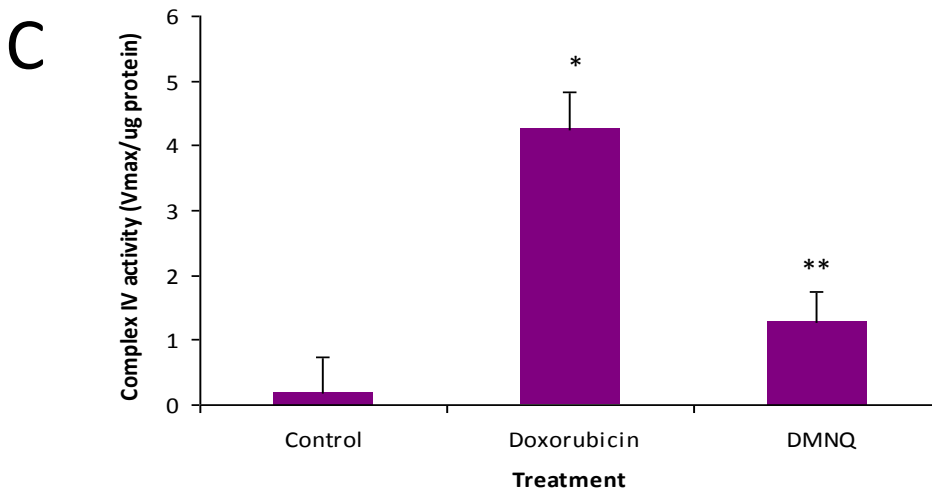
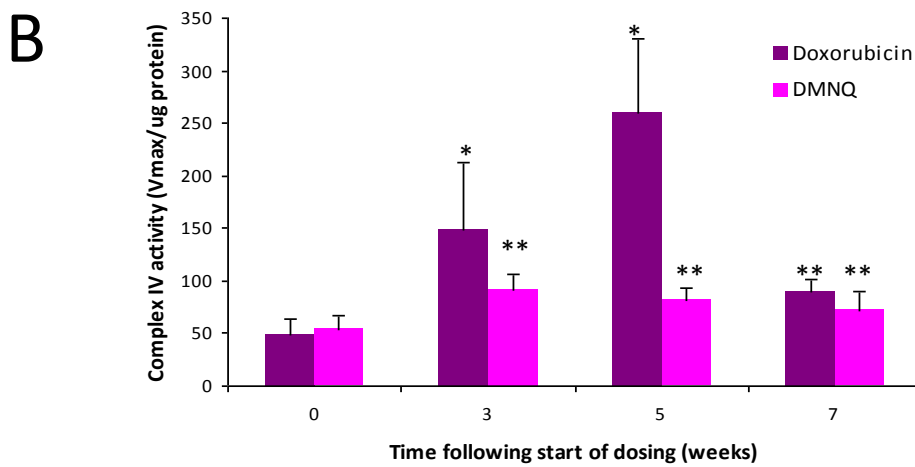
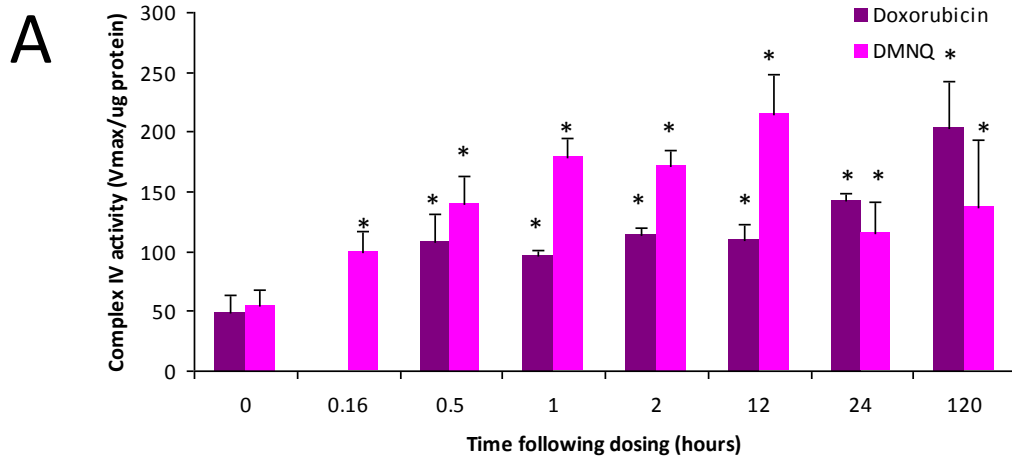


Figure 8.10: Complex IV activity *in vivo* in an acute (A) and chronic (B) model of toxicity following doxorubicin DMNQ. The activity in HL-1 cells following both compounds was also determined (C). A significant increase in complex IV activity was recorded in all models. The magnitude of change was lower in HL-1 cells. Results are mean $n=3 \pm$ S.D., one way ANOVA and post-hoc Dunnett's T-test * $p \leq 0.01$, ** $p \leq 0.05$.

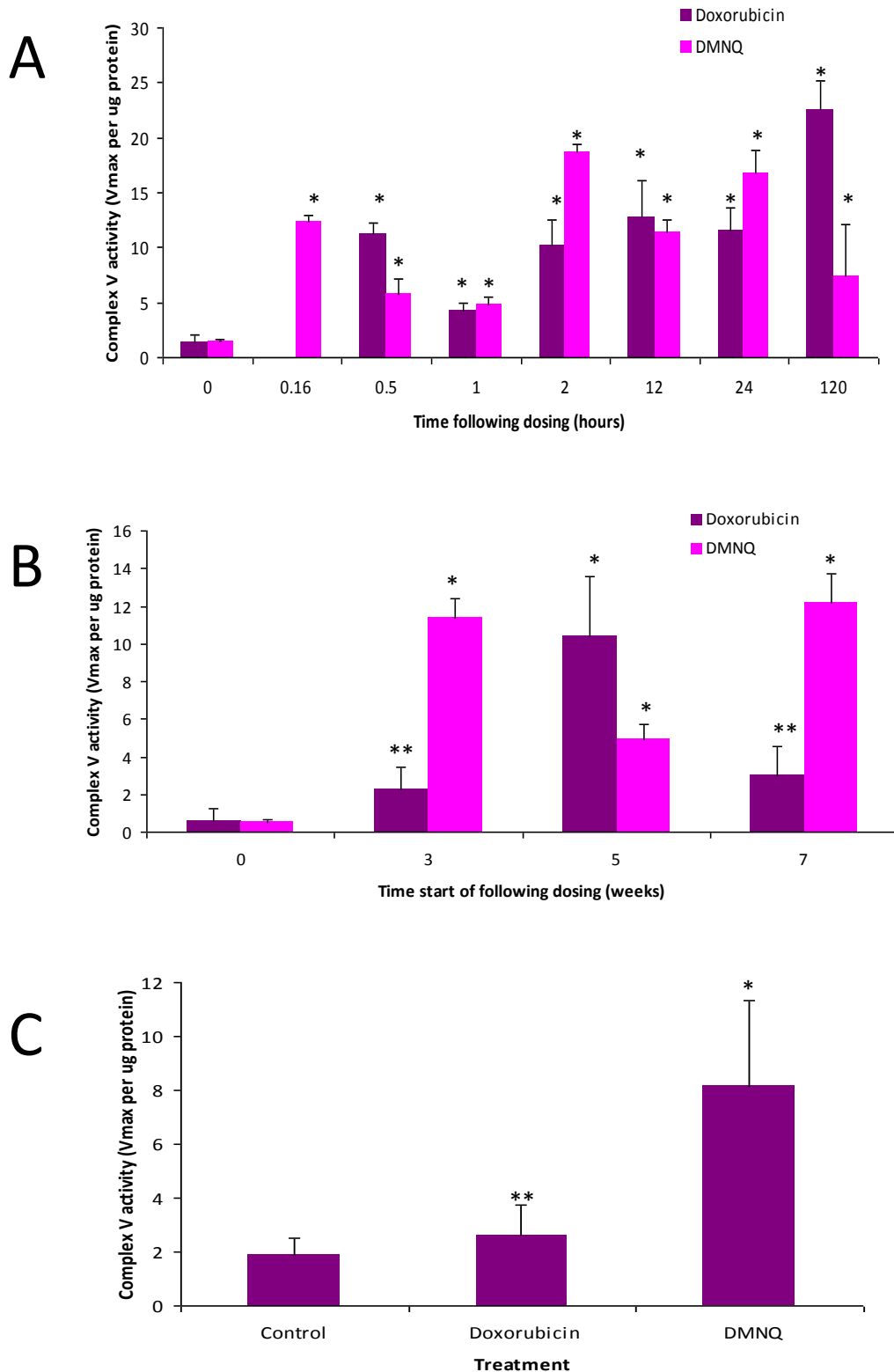


Figure 8.11: Complex V activity *in vivo* in an acute (A) and chronic (B) model of toxicity following doxorubicin DMNQ. The activity in HL-1 cells following both compounds was also determined (C). A significant increase in complex IV activity was recorded in all models. Results are mean $n=3 \pm$ S.D., one way ANOVA and post-hoc Dunnett's T-test * $p \leq 0.01$, ** $p \leq 0.05$.

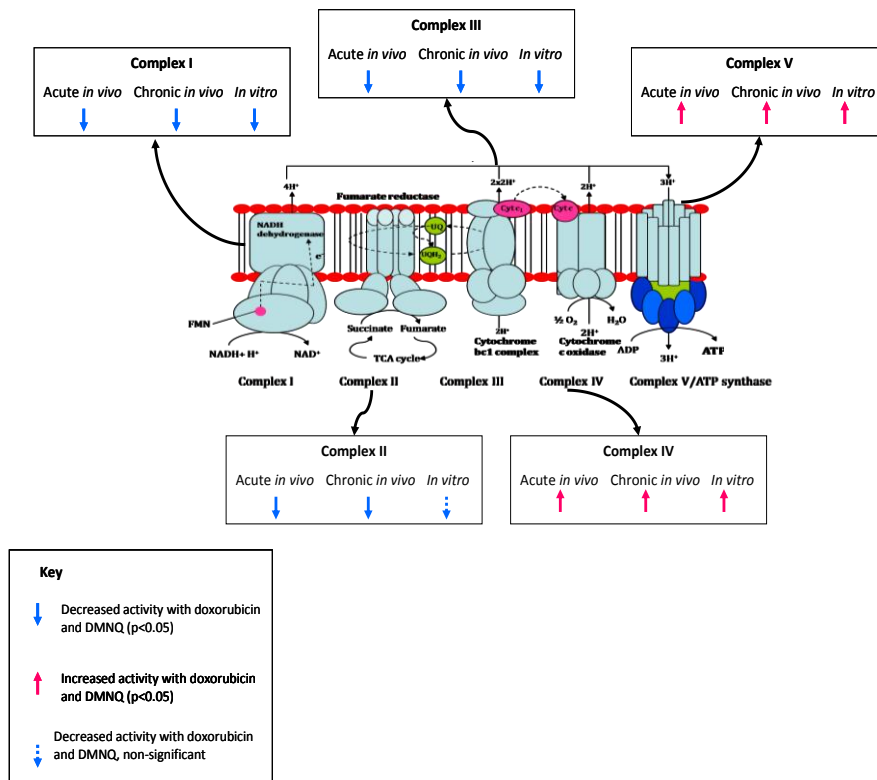


Figure 8.12: Summary of the activity of each complex of the oxidative phosphorylation pathway.

8.2.4 ASSESSING MITOCHONDRIA INTEGRITY

In order to further investigate the effects on mitochondria following doxorubicin and DMNQ, citrate synthase and GLDH were measured. Citrate synthase is the enzyme involved in the first step of the TCA cycle. It catalyses the reaction of acetyl-coA and oxaloacetate to citrate allowing the formation of NADH and FADH₂, both of which donate electrons to complex I and II of the ETC, respectively. This enzyme is synthesised in the cytoplasm and transported into the mitochondrial matrix. Due to its association with the mitochondrial matrix, the activity of this enzyme is commonly used as a measurement of mitochondrial mass. Citrate synthase was assessed *in vivo* both acutely and chronically in cardiac tissue and *in vitro*. In an acute model of toxicity (Figure 8.13A) an increase in citrate synthase activity was observed. Doxorubicin treatment resulted in a gradual increase in activity with a maximum 4 fold increase at 120 hours following a single dose. DMNQ did not affect citrate synthase activity as dramatically as doxorubicin, a maximum 2 fold change was present 2 hours

following dosing. Activity was still elevated above control 120 hours following a single dose. In a chronic model of toxicity (Figure 8.13B), again doxorubicin resulted in a larger increase in activity compared to DMNQ. Following doxorubicin a significant increase ($p \leq 0.01$) was observed throughout the time course with activity peaking 3 weeks after the start of dosing. An increase was still apparent 7 weeks after the commencement of dosing. DMNQ significantly ($p \leq 0.02$) increased citrate synthase activity up to 3 weeks after the start of dosing, time points after which were not significantly changed. The response of citrate synthase *in vitro* was comparable between the two compounds (Figure 8.13C). Both doxorubicin and DMNQ resulted in ~2 fold increase in activity following 24 hours exposure to both compounds. GLDH activity was assessed in cardiac tissue in an acute and chronic model of toxicity treated with both doxorubicin and DMNQ and in the *in vitro* model of toxicity. GLDH activity *in vivo* in an acute model of toxicity decreased up to 2 hours following dosing, a situation that was reversed to one of increase at the 12 and 24 hour time points. However, this increase in activity was transient. 120 hours following a single dose of both compounds GLDH levels were reduced to about half of control levels (Figure 8.14). Chronically, GLDH was decreased in activity throughout the time course following doxorubicin administration. Chronic DMNQ exposure resulted in decreased GLDH up to 5 weeks following the start of dosing, however at 7 weeks GLDH activity was elevated (Figure 8.14). *In vitro* GLDH activity in cell lysate was reduced by ~80% compared to control (Figure 8.14). This reduced activity of GLDH in cardiac tissue and cells indicates dysfunctional mitochondria.

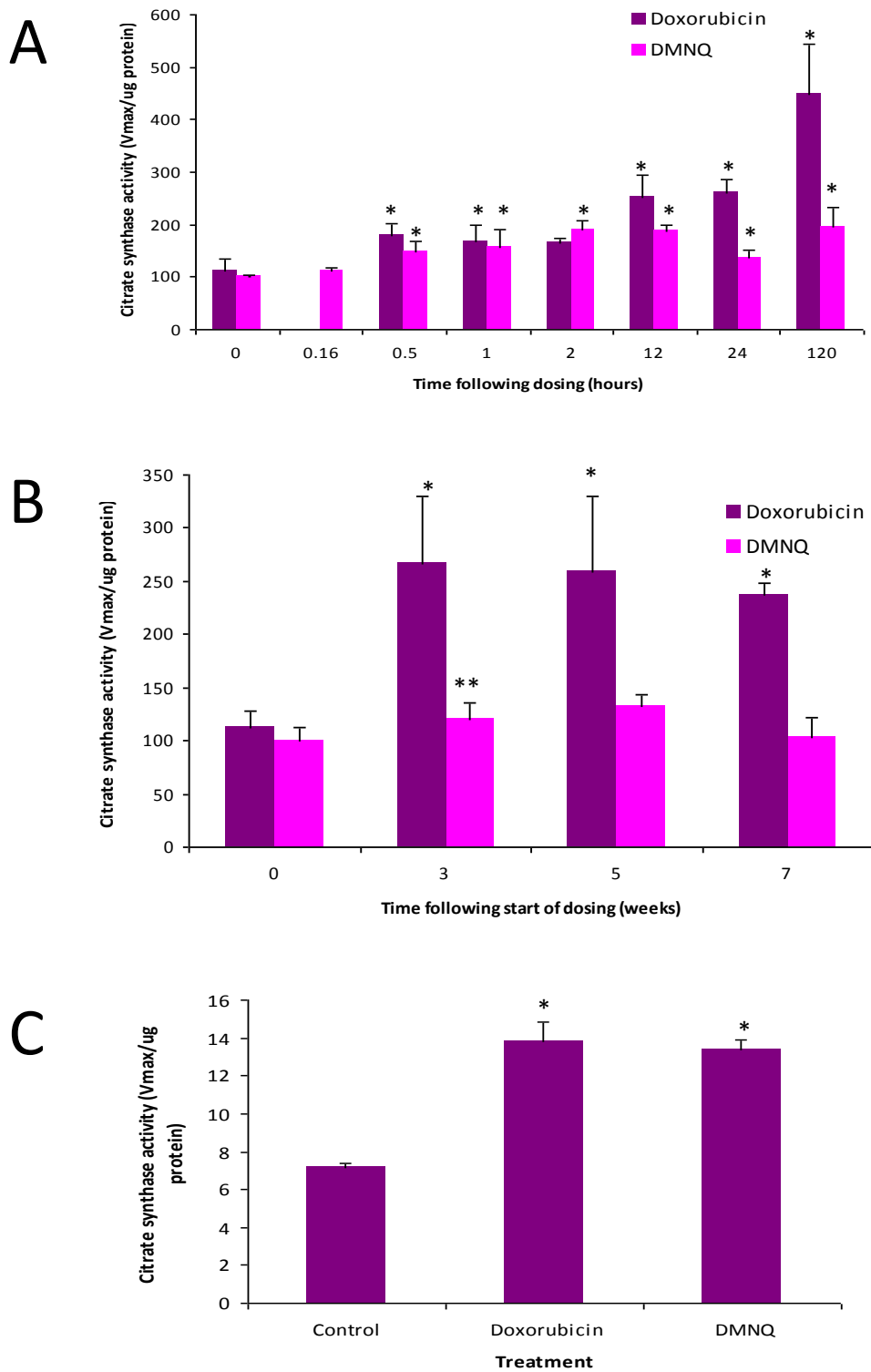


Figure 8.13: Citrate synthase activity *in vivo* in an acute (A) and chronic (B) model of toxicity following doxorubicin and DMNQ. The activity in HL-1 cells following both compounds was also determined (C). Results are mean $n=3 \pm$ S.D., one way ANOVA and post-hoc Dunnett's T-test * $p \leq 0.01$, ** $p \leq 0.02$.

GLDH

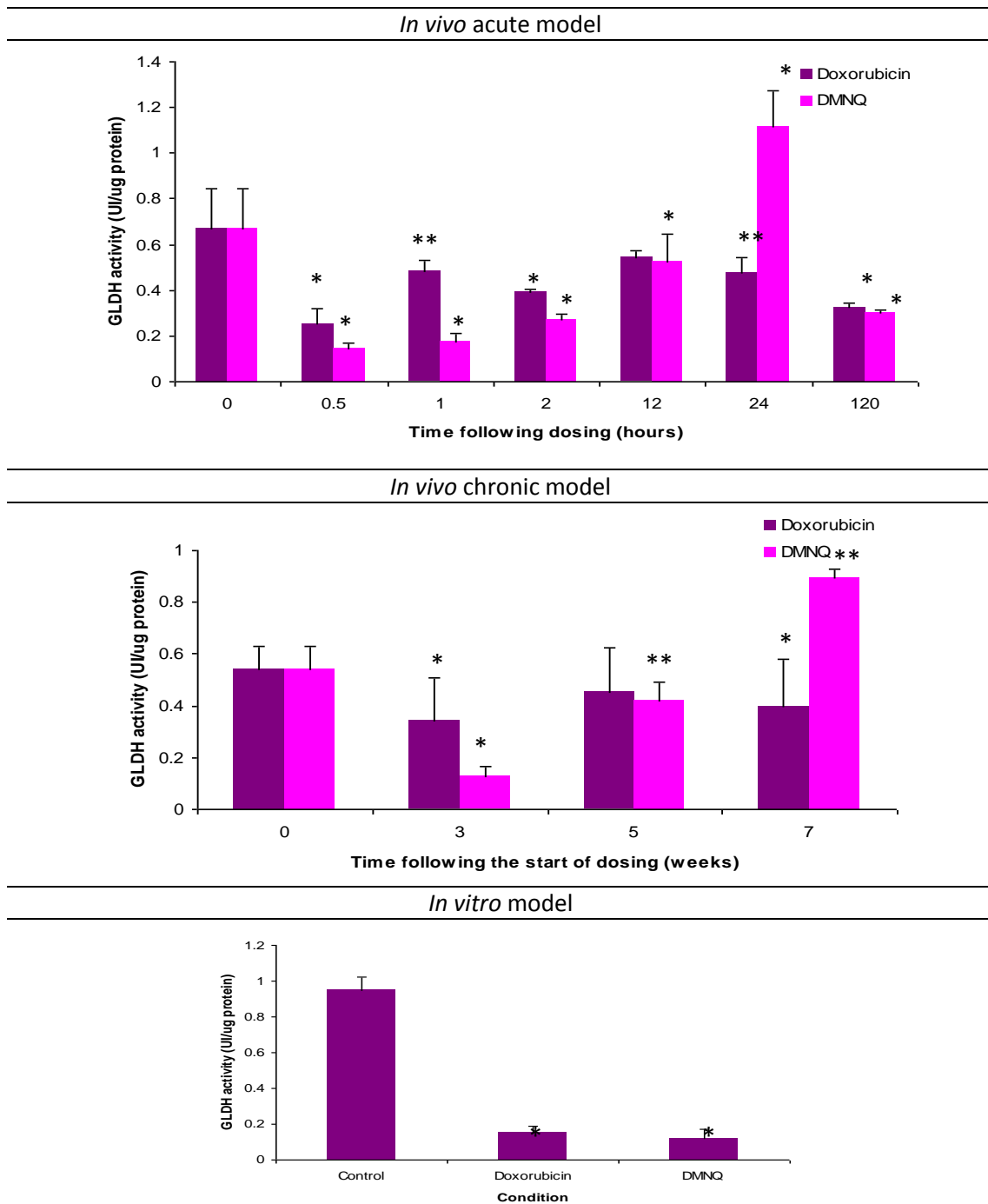


Figure 8.14: GLDH activity in cardiac tissue from an acute and chronic model of toxicity and from an *in vitro* model of toxicity. Results are mean $n=3 \pm$ S.D., one way ANOVA and post-hoc Dunnett's T-test * $p < 0.01$, ** $p < 0.05$.

8.2.5 MECHANISTIC CONSEQUENCES OF MITOCHONDRIAL DAMAGE

ATP, AMP and ADP were measured in cardiac tissue following doxorubicin (15mg/kg) and DMNQ (25mg/kg) administration by HPLC allowing simultaneous measurement (Section 2.12). ATP is produced through the ETC. A 10 μ M solution of ATP, ADP and AMP was spiked into cardiac tissue prior to extraction to assess extraction efficiency (Figure 8.15). A significant decrease ($p\leq 0.01$) of about 5 fold in ATP was present 0.5 hours following both doxorubicin (15mg/kg) and DMNQ (25mg/kg) compared to control, this decrease was still significant ($p\leq 0.05$) at 120 hours following dosing. An initial decrease of four fold in ADP was also present at 0.5 hours following a single dose of doxorubicin (15mg/kg) and DMNQ (25mg/kg). However, this reversed to a significant ($p\leq 0.05$) increase starting at 2 and 12 hours following DMNQ (25mg/kg) and doxorubicin (15mg/kg), respectively. In contrast to ATP and ADP, the level of AMP was significantly ($p\leq 0.01$) increased following both doxorubicin (15mg/kg) and DMNQ (25mg/kg) from 2 hours. This affect, however, was more pronounced following DMNQ (25mg/kg) (Figure 8.16). In order to observe if any shift in ATP, ADP, or AMP had occurred the ratios of ATP:ADP and AMP:ATP were calculated (Table 8.4). A decrease in ATP:ADP ratio was present, while the AMP:ATP ratio increased.

As mitochondrial function appears to be compromised, caspase 3 activity was measured using a colorimetric assay and western blotting to investigate the activation of apoptosis. Both demonstrated a significant ($p\leq 0.03$) increase in activated caspase 3 in cardiac tissue following acute doxorubicin (15mg/kg) or DMNQ (25mg/kg) from 0.5 to 120 hours following dosing (Figure 8.17). Increases up to 15% following DMNQ and up to 49% following doxorubicin over control levels were recorded. The amount of caspase 3 activity did reduce with time but remained significantly elevated above control throughout the time course.

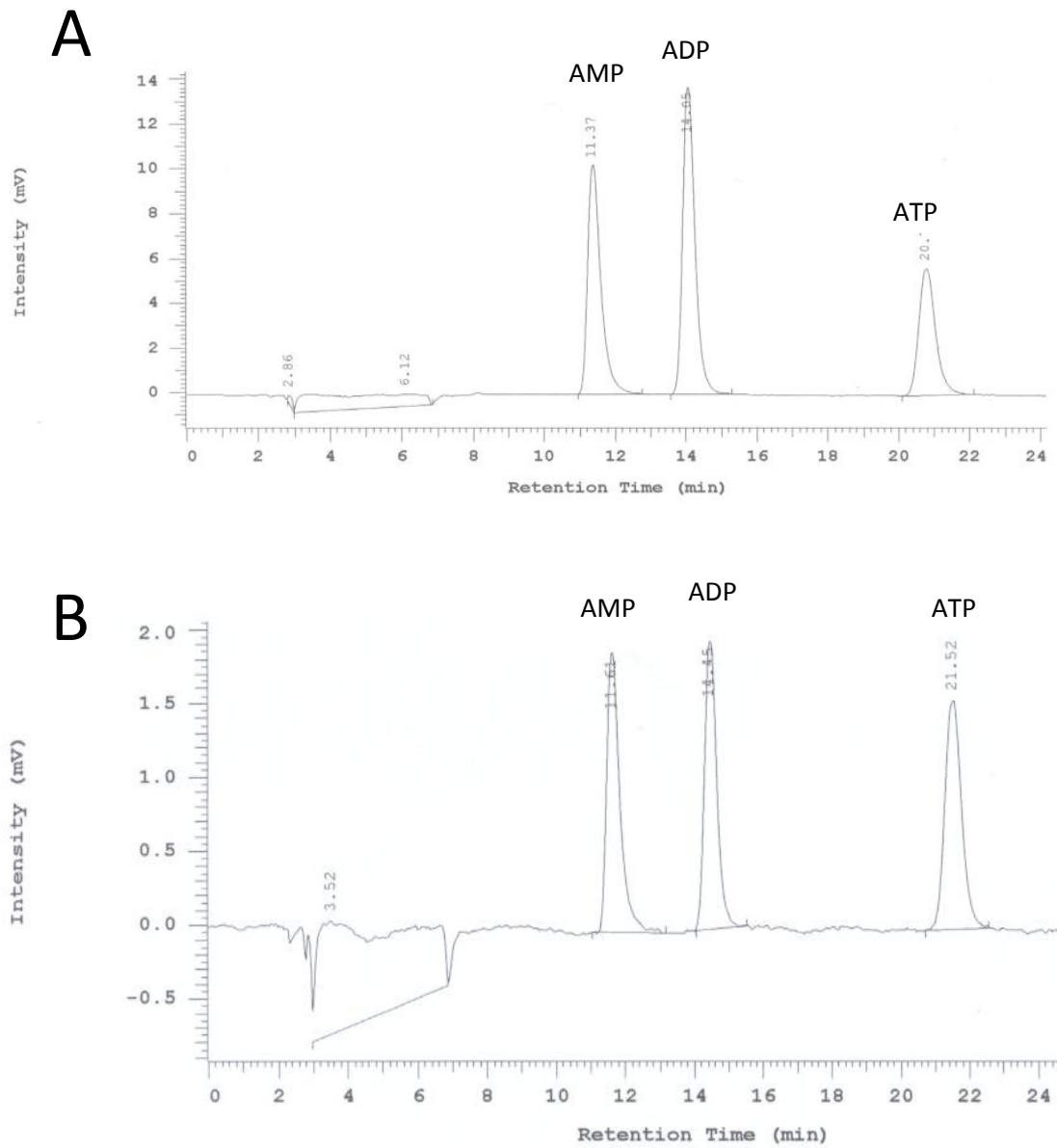


Figure 8.15: ATP/ADP/AMP HPLC spectra (B) and spiked cardiac sample with 10uM ATP/ADP/AMP to ensure efficient extraction (A).

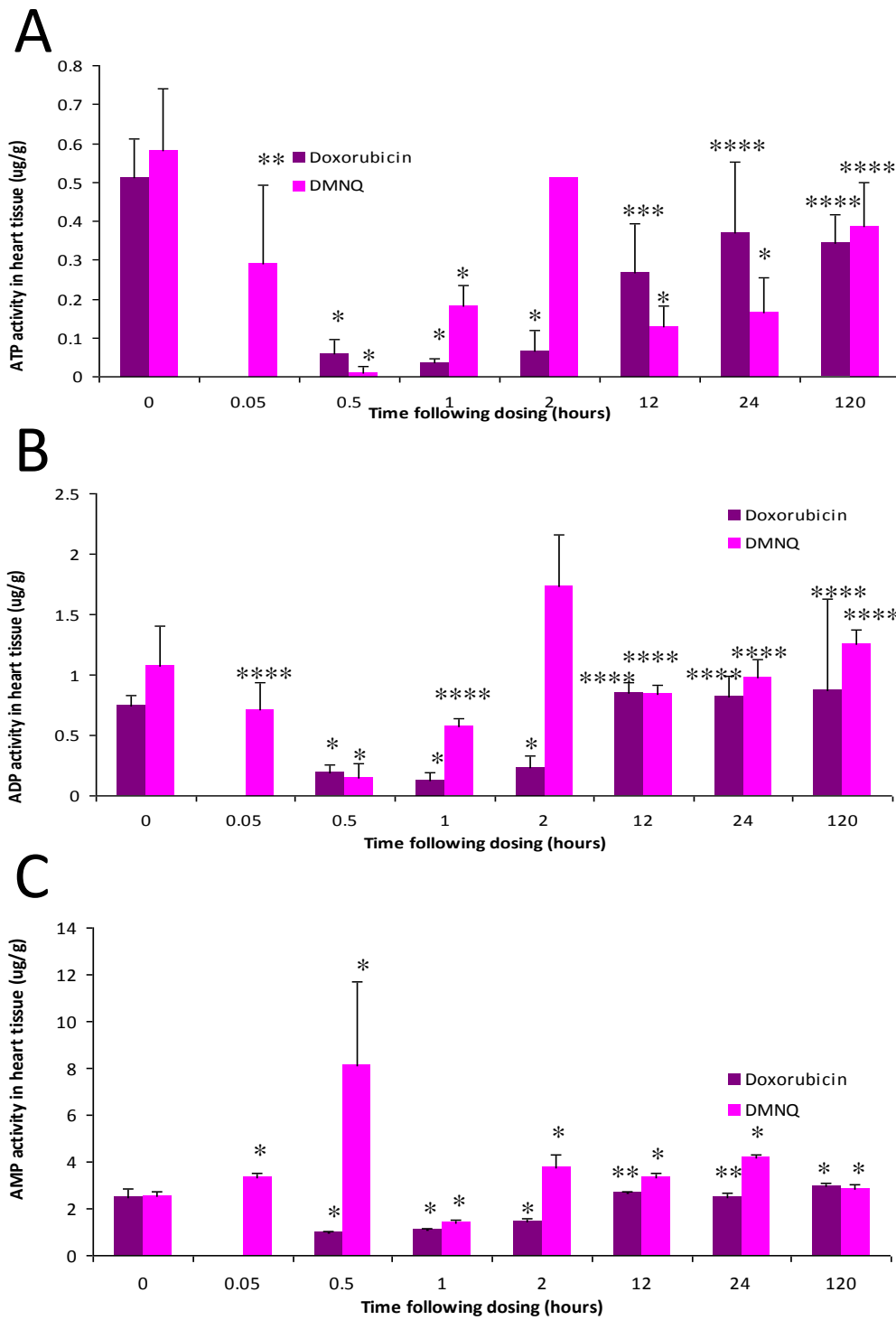


Figure 8.16: ATP (A), ADP (B), AMP (C) measurement following doxorubicin (15mg/kg) or DMNQ (25mg/kg) in an acute model of toxicity. A significant decrease in ATP and ADP was recorded and an increase in AMP. Results are mean $n=3 \pm$ S.D., one way ANOVA and post-hoc Dunnett's T-test * $p \leq 0.01$, ** $p \leq 0.02$, *** $p \leq 0.03$, **** $p \leq 0.05$.

Time point	ATP:ADP ratio		Time point	AMP:ATP ratio	
	Doxorubicin (15mg/kg)	DMNQ (25mg/kg)		Doxorubicin (15mg/kg)	DMNQ (25mg/kg)
0	0.62	0.54	0	4.89	4.41
0.05		0.41	0.05		11.53
0.5	0.3	0.06	0.5	16.06	949.7
1	0.26	0.32	1	31.41	7.51
2	0.29	0.32	2	22.28	6.81
12	0.32	0.15	12	9.85	25.88
24	0.45	0.17	24	6.72	25.09
120	0.39	0.31	120	8.65	7.32

Table 8.4: ATP/ADP and AMP/ATP ratios following a single dose of doxorubicin (15mg/kg) or DMNQ (25mg/kg) in an acute model of toxicity. A decrease in ATP:ADP ratio occurs and an increase in AMP:ATP ratio. Results are the mean n=3 at each time point for each treatment.

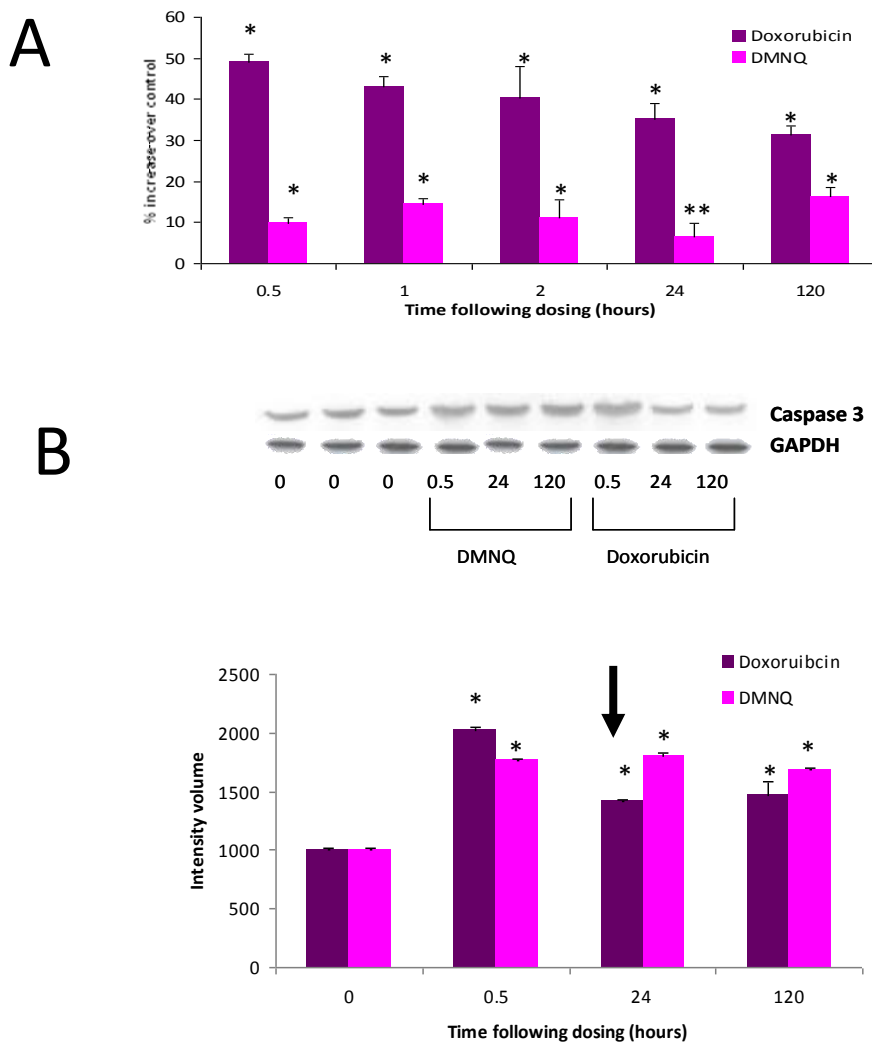


Figure 8.17: Caspase 3 activity, following a single dose of doxorubicin (15mg/kg) or DMNQ (25mg/kg). Caspase 3 activity measured using a colorimetric assay (A) and western blotting, an increase observed from 0.5 hours through to 120 hours. Results are mean values (n=> 3 ±S.D.). One way ANOVA and post-hoc Dunnett's T-test *p≤0.01, **p≤0.03.

8.3 DISCUSSION

The overall aim of this chapter was to investigate two hypotheses derived from previous chapters. Firstly differential transcription and translation of genes involved in the oxidative phosphorylation pathway was demonstrated (Chapters 5 and 7). This pathway contains the ETC that facilitates ATP generation through the utilization of enzyme complexes within the ETC. The activity of each enzyme complex was determined. Secondly decreased transcription of the miRNA, miR-181a *in vivo* exposed to acute and chronic doxorubicin and DMNQ was consistently demonstrated (Chapter 6). Little functional knowledge was available concerning miR-181a or the consequences of reduced levels. Previous studies have shown an association between miR-181a and promotion of myogenesis (Naguibneva et al. 2006) and T cell development (Li et al. 2007). To investigate the function of miR-181a further, reduced miR-181a was induced *in vitro* prior to treatment with either doxorubicin or DMNQ.

8.3.1 ESTABLISHING A CARDIAC *IN VITRO* MODEL SYSTEM

Before the aims of this chapter could be investigated, *in vitro* models of doxorubicin and DMNQ toxicity were required. All commercially available cardiac cell lines are derived from rat origins, thus preventing direct comparison with the *in vivo* data previously generated. A number of mouse cardiac cell lines have been developed, including AT-2, MCM1 and HL-1 cells. Both AT-2 and MCM1 cells lose their cardiac phenotype after several passages thus limiting long term use (Claycomb et al. 1998). HL-1 cells retain cardiac morphology, biochemistry, electrophysiological and genomic characteristics of adult cardiomyocytes, (White et al. 2004). A comparison between cardiac *in vitro* models was conducted to identify if primary cardiomyocytes or the cell line HL-1 transcriptionally mimic the *in vivo* transcriptional profiles. This analysis revealed differences between both *in vitro* models and cardiac tissue. However the HL-1 cell line, resulted in fewer significant ($p < 0.05$) gene changes indicating a greater similarity to the *in vivo* situation compared to primary

cardiomyocytes (Figure 8.1). This was an unexpected finding, it was postulated that primary cardiomyocytes would mimic the *in vivo* transcriptional expression better. This discrepancy may have arisen due to a lack of a fine network of collagen fibres surrounding cardiomyocytes *in vitro* (van Rooij and Olson 2007). These fibres are known to be involved in cardiac dysfunction thus possibly affecting contractility and cardiac function that is not affected *in vitro*. In addition neonatal cardiomyocytes were studied. During cardiac development there is a shift in gene expression, from a fetal to an adult phenotype, one that is thought to reverse following damage. Thus genomic identification using these models is intrinsically problematic. In addition, a number of studies have reported variability between different cardiomyocyte isolations and the culture conditions used. The expression of the cardiac troponin genes (e.g. Tnnt2) and cardiomyocyte electrophysiology have been found to change as a consequence of different coatings being applied to culture vessels (Miskon et al. 2009). These results highlight the importance of animal studies and the need for the development of improved *in vitro* systems. The *in vitro* models compared here cannot be relied upon in isolation due to the large discrepancy between the transcriptional profiles *in vivo* before exposure to any xenobiotics. Improved cardiac *in vitro* models involving cardiomyocyte derived pluripotent stem cells are currently providing promise to bridge this divide (Tanaka et al. 2009).

Dose ranging experiments were conducted in HL-1 cells to identify concentrations of doxorubicin and DMNQ *in vitro* that were on the threshold of cytotoxicity. This was achieved by determining the relative cytotoxicity of both doxorubicin and DMNQ using an MTS assay, thus assessing cell viability. The length of exposure of 24 hours was chosen following consultation of the literature describing the use of doxorubicin in the rat cardiomyocyte cell line H9c2. In H9c2 cells a 24 hour exposure induced dose dependent cytotoxicity, including morphological and biochemical alterations (Sardao et al. 2009). Concentration-dependent cytotoxicity was observed following both compounds and

revealed doxorubicin to be more cytotoxic than DMNQ in a cardiomyocyte cell line. A 24 hour exposure was sufficient to elicit a cytotoxic response (Figure 8.2). No data is currently available in the public domain regarding the use of DMNQ in an *in vitro* cardiomyocyte model, thus this finding was unknown but it is in line with the relative toxicity observed *in vivo* (Chapter 4).

Transcriptional and miRNA profiling following a 24 hour exposure to 1 μ M doxorubicin and 5 μ M DMNQ was conducted and compared to *in vivo* data (Figures 8.3-8.5 and Table 8.2). Only limited similarity in the response of the two models was observed. Pathway analysis did identify effects on energy generation pathways following both doxorubicin and DMNQ. However, these were not the predominant mechanism. These data indicate distinct differences in the response to xenobiotics *in vivo* and *in vitro*. These discrepancies may have arisen as cells in culture are at a higher oxygen tension than those in tissues so the kinetics of redox reactions *in vitro* do not mirror those that might occur *in vivo* at physiological oxygen tensions (Corrêa et al. 2008; Hirabayashi et al. 1987). The metabolism of each compound may vary between *in vivo* and *in vitro* models, thus affecting genomic expression. In addition the development of cardiac hypertrophy and heart failure affect the whole heart. Disease progression occurs within a dynamic biochemical and neuroendocrine milieu, that is not present *in vitro* (Molkentin and Robbins 2009). Thus, *in vitro* models may not develop cardiotoxicity in the same manner as *in vivo*, maybe accounting for the difference in gene and miRNA expression observed.

8.3.2 DOXORUBICIN AND DMNQ CHALLENGE OF HL-1 CELLS WITH SUPPRESSED miR-181A EXPRESSION

miR-181a expression was decreased following both acute and chronic exposure to doxorubicin and DMNQ *in vivo* (Chapter 6) and *in vitro* (Figure 8.4). miR-181a knockdown resulted in increased cytotoxicity, assessed by LDH release and CK-MB activity following doxorubicin and DMNQ treatment (Figure 8.6). miR-181a knockdown resulted in greater

sensitivity to doxorubicin than DMNQ, however, this maybe a result of the relative increased cytotoxicity of doxorubicin. These results indicate the importance of miR-181a in the response to cytotoxicity resulting from doxorubicin and DMNQ exposure. Knockdown of miR-181a combined with doxorubicin or DMNQ treatment resulted in increased cardiac damage. miR-181a appears to aid progression to the cardiotoxic state, validating the hypothesis that miRNAs are modulated in expression as a consequence of toxic insult and in the progression of toxicity. This was the first time knockdown of miR-181a has been conducted in cardiomyocytes. Knockdown or over-expression of miR-133, miR-208, miR-195 and miR-1-2 have been previously associated with cardiac dysfunction (Thum et al. 2008; van Rooij and Olson 2007; Zhao and Srivastava 2007). Thus decreased miR-181a expression may contribute to the observed cardiotoxicity. The mechanism by which miR-181a enhances the toxicity following doxorubicin and DMNQ remains to be elucidated. However, miR-181a maybe a negative regulator of cell growth or a regulator of pro-survival pathways, thus down-regulation may predispose cardiac tissue to damage.

8.3.3 EFFECTS ON MITOCHONDRIA AND ENERGY DYNAMICS

Doxorubicin and DMNQ treatment *in vivo* resulted in transcriptional and translational changes in the regulation of genes that encode enzymes within the oxidative phosphorylation pathway (Chapters 5 and 7). Methods to measure the activities of the five enzymes that compose the ETC present in the oxidative phosphorylation pathway were developed *in vivo* and *in vitro* (Diwakar et al. 2008; Luo et al. 2008; Gellerich et al. 2004; Barrientos 2002). The activity of complexes I, II and III were decreased in all models of toxicity (Figures 8.7-8.9) in contrast the activity of complexes IV and V were increased (Figures 8.10-8.11). The net affect of these changes in activity was a decrease in ATP production (Figure 8.16), with an associated decrease in ATP:ADP ratio and an increase in AMP:ATP ratio. Decreased ATP production has previously been reported following doxorubicin treatment *in vivo* (Kawasaki et al. 1996). Complexes I-IV pass protons across the

inner mitochondrial membrane to create an electrochemical gradient, this gradient drives the flow of protons through complex V allowing the phosphorylation of ADP (Muravchick and Levy 2006). The inhibition of complexes I, II and III appears to be sufficient to prevent the formation of an adequate electrochemical gradient, thus ATP production is decreased regardless of the activity of complexes IV and V. The increased activity of complex IV may occur as a compensatory mechanism in an effort to create a proton gradient and allow protons to flow through complex V to drive ATP synthesis. However, this increase in activity is unable to overcome the inhibition of the upstream complexes (Figure 8.12). Alternatively, doxorubicin and DMNQ may act as an electron shuttle (Wallace and Starkov 2000). They may accept electrons from complex I of the ETC and feed them back into the chain further upstream, possibly complex IV. This would result in large portions of the ETC being bypassed, thus resulting in decreased complex I activity due to diversion of electrons from this enzyme complex to the compound. This diversion of electrons would result in decreased complex I, II and III activity due to a lack of electrons flowing through these complexes and possibly increased complex IV and V activity. This increased activity may result due to electrons being accepted by cytochrome c thus providing electrons to these complexes (Figure 8.18). The naphthoquinone menadione (MNQ) is known to act as an electron shuttler. Electrons are accepted by MNQ from complex I of the ETC. MNQ then feeds these electrons back to complex IV of the chain, thus bypassing a number of enzyme complexes (de Groot et al. 1985). Doxorubicin has previously been reported to directly interact with complex I (Berthiaume and Wallace 2007a). Complex I is thought to provide a supply of electrons to doxorubicin to facilitate its redox cycling, thus diverting electrons away from the ETC. The same may occur following DMNQ administration. This interaction may result in reduced complex I activity and a lack of electron flow through the chain, consequently preventing the establishment of an electrochemical gradient required to drive ATP synthesis (Berthiaume and Wallace 2007a; Wallace 2003; Wallace and Starkov 2000).

Pre-clinical and clinical studies have both reported a decrease in complex I activity following doxorubicin. Of interest, alterations in complex I activity were observed prior to the onset of clinical symptoms of cardiomyopathy in patients treated with doxorubicin (Berthiaume and Wallace 2007a; Tokarska-Schlattner et al. 2006). Another pharmaceutical agent metformin, an anti-diabetic drug also inhibits complex I of the ETC and induces a p53-and AMPK-dependent increase in glycolysis, both AMPK and glycolysis were activated in these models (Chapter 5) (Toogood 2008). Complexes II, III and IV have also been reported to be inhibited following doxorubicin *in vivo*, but the concentration of doxorubicin administered exceeded those used clinically (Tokarska-Schlattner et al. 2006). However at the clinically relevant concentrations used in this study complexes II and III were inhibited (Figures 8.8 and 8.9). Hiraumi et al. (2009) recently reported that each complex of the ETC helps maintain the assembly and stability of other complexes in the chain. Previous findings support this notion. Genetic alterations resulting in inhibition of complex III lead to a secondary loss of complex I (Schagger et al. 2004). As doxorubicin has previously been found to interact with complex I, it could be that the reverse occurs, i.e. the inhibition of complex I results in a secondary loss of complex III activity. In addition, inhibition of complex III is thought to block all energy production in the mitochondria, thus increased activity of complexes IV and V as observed in these studies would have little effect on ATP synthesis (Figure 8.12) (Wallace and Starkov 2000).

Despite the decrease or increase in activity of each complex, the mechanism by which each complex is inhibited or enhanced is still unknown. Further functional experiments are required to determine the area of each enzyme responsible for differential activity. By inhibiting electron transport these agents inhibit both substrate oxidation and oxygen consumption (Wallace 2008). Thus, the effects of doxorubicin and DMNQ on mitochondrial energy dynamics may result in reduced mitochondrial function and increased reliance on alternative ATP generating pathways.

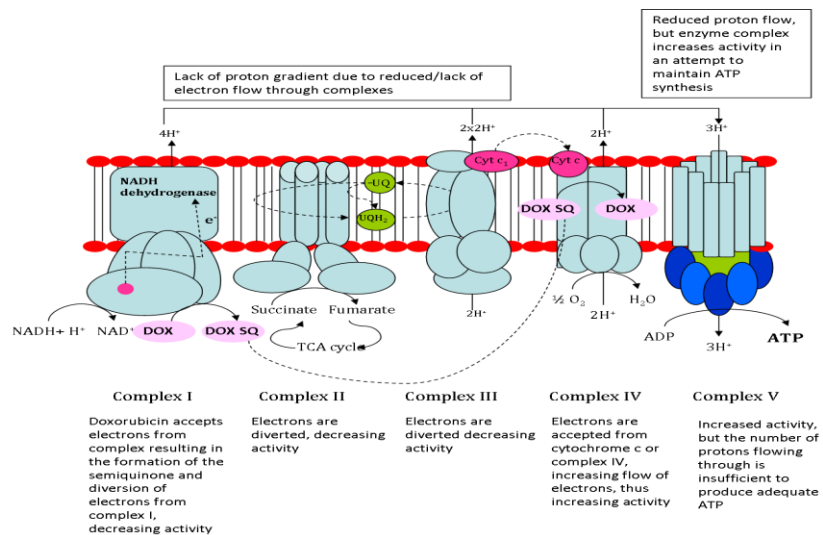


Figure 8.18: Overview of the possible diversion of electrons from the ETC. Electrons from complex I of the ETC may be accepted from doxorubicin or DMNQ resulting in the formation of the semiquinone, which passes electrons to either cytochrome c or directly to complex IV of the ETC enabling oxidation back to the parent compound, thus bypassing complexes I-III.

Citrate synthase activity was assessed as a marker of mitochondrial mass *in vivo* and *in vitro*.

Overall citrate synthase activity was increased indicating an increase in the number of mitochondria (Figure 8.13). However, this increase in mitochondrial mass is proportionally less than the increase in complex IV activity, thus this increase in citrate synthase is unable to fully explain the increase in activity of complexes IV and V. The increase in mitochondrial mass most likely arises due to an increase in the amount and occurrence of fusion and fission, thus increasing the number of mitochondria. Mitochondrial fusion and fission occurs every 2 minutes (Hom and Sheu 2009). Hence, it is not surprising that these effects on mitochondria occur as quickly as 30 minutes following dosing. The activity of citrate synthase was greater following doxorubicin than DMNQ. This possibly reflects the increased mitochondrial sensitivity following doxorubicin exposure and the inability of mitochondria to repair successfully following doxorubicin insult. The ability of cardiac tissue to repair itself following doxorubicin was thought to be compromised compared to DMNQ treatment in Chapter 4. This hypothesis is likely to be true. Citrate synthase activity was increased at a consistent level acutely and chronically up to week 5 following the start of dosing, after

which point DMNQ had no significant effect. This finding is indicative of DMNQ partially repairing the cardiac tissue damage. GLDH activity in cardiac tissue reveals mitochondrial damage, in all models of toxicity. However, 7 weeks following the start of chronic DMNQ administration *in vivo* an increase in GLDH activity in cardiac tissue occurred (Figure 8.14). This is again indicative of cardiac tissue repair.

Due to the presence of dysfunctional mitochondria caspase 3 activation was assessed. DMNQ and doxorubicin increased caspase 3 activity (Figure 8.17). This increase in caspase 3 activation, and the mitochondrial effects identified using electron microscopy (Chapter 4) and enzyme activity assays, could indicate the activation of the intrinsic pathway of apoptosis. A number of studies *in vivo* have implicated the activation of the intrinsic pathway of apoptosis following doxorubicin through the measurement of cytochrome c release and caspase 3 activation (Reeve et al. 2007; Childs et al. 2002). As apoptosis is an ATP dependent process, it is possible that apoptosis is the initial form of cell death, but as ATP synthesis decreases cells may remain in a 'suspended' state of apoptosis or a transition to a necrotic form of cell death may occur. Necrosis does not require ATP, which is low following doxorubicin and DMNQ. This transition from apoptosis to necrosis may explain why there is a decline in caspase 3 over the time course following a single dose of both doxorubicin and DMNQ, while ATP remains depleted.

8.3.4 SUMMARY

The findings of these studies indicate the differences between *in vivo* and *in vitro* models of toxicity and highlight that miR-181a knockdown sensitises cardiac HL-1 cells to doxorubicin and DMNQ, demonstrating the importance of miRNAs in progression of the cardiotoxic phenotype. Measurement of the activity of each complex of the ETC indicated complexes I, II and III to be decreased in activity, whereas complexes IV and V were increased, coupled with decreased ATP synthesis indicates dysfunctional mitochondrial energy dynamics.

Chapter 9: Thesis Discussion

The overall aim of this project was to further elucidate the mechanism of doxorubicin cardiotoxicity at clinically relevant concentrations using novel genomic methods *in vivo* and *in vitro*. Due to the complex chemistry of doxorubicin, a simpler naphthoquinone, DMNQ, which is able to redox cycle was also investigated, to allow greater insight into the toxicological properties (Figure 4.1). For the first time the utility of DMNQ *in vivo* was investigated through the establishment of its pharmacokinetic properties and its ability to cause cardiotoxicity (Chapter 3). The overall cardiac acute toxicity of DMNQ was lower than that of doxorubicin *in vivo*. However, increased dose levels of DMNQ (equivalent to 11.5 μ M) resulted in comparable cardiotoxicity to that following doxorubicin (2.59 μ M) in an acute model (Chapter 4). Thus suggesting that the pharmacological and toxicological properties of doxorubicin are distinct and that the quinone moiety is the segment of doxorubicin most likely to be responsible for the observed cardiotoxicity.

Repeat dosing of doxorubicin is widely associated with cumulative toxicity clinically (Tokarska-Schlattner et al. 2006), a phenomenon apparent in the chronic model (Chapter 4). DMNQ, however, did not appear to have cumulative properties (Chapter 4). Chronically DMNQ did not significantly alter cardiac biomarkers (Chapter 4). Despite this, the underlying mechanism of toxicity appeared similar in all models. Suggesting that cardiac tissue following DMNQ administration has a greater capacity to protect against further damage or was better able to repair damaged tissue.

The cumulative effects of doxorubicin thus may arise from its pharmacological action. Doxorubicin unlike DMNQ intercalates and binds to nuclear DNA between base pairs, resulting in the formation of DNA strand breaks and the formation of DNA adducts (Takemura and Fujiwara 2007; Wallace 2003; Cutts et al. 1996). This interaction with nuclear DNA may result in imprinting of doxorubicin induced damage, thus maintaining a dysfunctional phenotype months or years after the cessation of treatment as observed clinically (Takemura and Fujiwara 2007). More significantly Ashley and Poulton (2009)

recently reported intercalation of doxorubicin into mitochondrial DNA (mtDNA). mtDNA differs from nuclear DNA in the manner in which replication and repair occurs. mtDNA only has a limited capacity to conduct DNA repair, thus replication continues prior to the repair of damaged DNA, thus any defects are maintained within the mitochondrial genome, possibly resulting in affected gene expression that can be maintained months to years after the cessation of treatment (Berthiaume and Wallace 2007b; Scatena et al. 2007; Lebrecht et al. 2003). Importantly the mitochondrial genome encodes transcripts that have important functions in complexes I, III, IV and V of the ETC. Any changes in mtDNA may impact on the function of the ETC and thus influence the rate of ATP synthesis. With both acute and chronic dosing, genes encoded from the mitochondrial genome were found to be differentially expressed following both doxorubicin and DMNQ (Chapter 5 and 7). This coupled with the increase in mtDNA copy number observed in an acute model (Chapter 5), indicated a prolonged insult to the mitochondrial genome sustained after the elimination of both compounds.

This project identified genes, biological pathways and genomic relationships transcriptionally (mRNA and miRNA) (Chapters 5 and 6) and translationally (Chapter 7) modulated. Overall the results indicate differential transcription (mRNA and miRNA) and translation from 5 and 30 minutes following DMNQ and doxorubicin treatment, respectively. At the systems level this genomic analysis implicated the oxidative phosphorylation pathway to be predominantly affected following doxorubicin and DMNQ administration in an acute and chronic model of toxicity. However, chronically, the two compounds affected this pathway in a different manner. Chronic doxorubicin resulted in a dose dependent influence, whereas DMNQ appeared to affect this pathway constantly throughout the time course. This discrepancy appears to be a reflection of doxorubicin's cumulative properties or possibly, resulting from the reported binding to cardiolipin, a phospholipid in the inner mitochondrial membrane (Goormaghtigh et al. 1987). This may potentially result in an accumulation of

doxorubicin in mitochondria. These data suggest that the impact on cardiac function is directly related to the total dose received. This is supported by clinical observations that the overall dose level and not the Cmax, is responsible for the observed toxicity (Minotti et al. 2004; Lipshultz et al. 2002).

In vitro, energy generating pathways were also affected, but to a lesser extent. Possibly, arising as cells in culture have a limited capacity to use mitochondria to generate ATP, thus any impact on mitochondrial derived ATP may have a reduced cellular impact *in vitro*. In addition cells may metabolise doxorubicin and DMNQ differentially in culture compared to *in vivo*. Furthermore cardiac dysfunction is a whole organ phenomenon, thus *in vitro* models maybe unable to re-create the correct cellular dynamics (Molkentin and Robbins 2009).

As a consequence cardiotoxicity *in vitro* may manifest differently than *in vivo*, maybe accounting for the difference in transcriptional, translational and miRNA expression observed (Chapters 5, 6 and 7). The involvement of oxidative phosphorylation was further established and confirmed by ETC complex activity assays (Chapter 8). This novel in-depth genomic and biochemical analysis highlights the role of mRNA transcription, miRNAs and mRNA translation in the development of a cardiotoxic phenotype.

9.1 STUDY DESIGN AND DATA ANALYSIS

One of the main aims of this project was to employ the power of transcriptomics to identify the mechanism responsible for the manifestation of doxorubicin's associated cardiotoxicity. Through the use of DMNQ, a redox cycling chemical (Gant et al. 1988) a greater insight into the toxicological action of doxorubicin can be identified. Thus any genes transcriptionally and translationally differentially expressed by both compounds, contributes to the development of the cardiotoxic phenotype. The only pathway constantly regulated both transcriptionally and translationally in all models of toxicity at all time points was oxidative phosphorylation as described in section 9.0 (Chapter 5 and 7). This genomic investigation also revealed key differences between the two compounds consistent with doxorubicin's

pharmacological activity. The data presented here indicates the advantage of using a compound with simple chemistry to model aspects of a complex compound allowing specific mechanistic insight without the confounding chemical properties. The inclusion of such compounds may allow identification of mechanisms of toxicity earlier in the drug development process, possibly during lead optimization thus reducing developmental costs. A difference in biological pathways influenced transcriptionally and translationally following both compounds was observed (Chapters 5 and 7). These differences highlight the need for translational profiling, to aid improved genomic investigations allowing the generation of more robust data sets. Transcriptional profiling is quicker, easier and does provide an overview of differentially expressed genes. However, it needs to be remembered that not all mRNA transcriptional changes will result in translation and associated protein change. This is particularly relevant when studying compounds such as doxorubicin that inhibit DNA synthesis. In order to validate such a system translational and transcriptional profiles following a compound that inhibits DNA synthesis in isolation is required. One compound that could be utilised would be etoposide. Etoposide inhibits topoisomerase II, thus inhibiting DNA synthesis without the potential redox effects (Choi et al. 2009). The use of etoposide would enable differences between transcription and translation to be investigated in isolation. The use of etoposide has been previously utilised to model doxorubicin's DNA inhibition activity in tumour cells (Reymann and Borlak 2008). However, a thorough genomic study following etoposide treatment has to date not been conducted in cardiac tissue. Similar findings on DNA synthesis following etoposide and doxorubicin have been reported using immunoblotting and reporter assays (Wang et al. 2009b). Hence it is possible that etoposide treatment or that of other topoisomerase II inhibitors teniposide (Gordaliza et al. 2000), HU-331 (Kogan et al. 2007) or fostriecin (de Jong et al. 1999) could be utilised with genomic analysis to investigate the complex chemistry and toxicity involving

topoisomerase II inhibition e.g.: doxorubicin. In addition, this would validate the importance of conducting translational profiling routinely when conducting genomic investigations. The broad range of time points studied in this project from 5 minutes to 120 hours following a single dose in an acute model, has allowed a thorough analysis of the initial and adaptive response following chemical insult. Perturbation of genomic pathways occurred from 30 and 10 minutes following dosing with doxorubicin and DMNQ, respectively. Previous genomic studies have not investigated such early time points, thus these results were novel and raise the question that assessment of genomic studies aimed routinely at later time points are perhaps highlighting adaptive responses to xenobiotics rather than the initial insult. Therefore the predisposing mechanisms maybe masked. An adaptive response to doxorubicin and DMNQ was apparent 12 hours following a single dose in both acute models and throughout the chronic time course following doxorubicin. This change was apparent transcriptionally (mRNA and miRNA, Chapters 5 and 6), translationally (Chapter 7) and through biochemical assessment of mitochondrial enzymes (Chapter 8) and clinical chemistry cardiac biomarkers (Chapter 4).

9.2 MECHANISMS OF TOXICITY

Redox cycling

Despite over 30 years of research the mechanisms involved in the development of doxorubicin cardiotoxicity have not been fully described. This study aimed to identify the molecular mechanisms responsible through the use of genomics *in vivo* using clinically relevant concentrations. The majority of previous hypotheses involve an element of redox cycling and the development of oxidative stress (Arola et al. 2000). As discussed in section 9.0, DMNQ was also utilised. DMNQ has been widely employed as a redox cycling compound in hepatocyte models *in vitro* (Ishihara et al. 2006; Gant et al. 1988). However, no indication of redox cycling was apparent transcriptionally (Chapter 5), translationally (Chapter 7), or biochemically through the measurement of GSH and GSSG (Chapters 3 and 5)

either acutely or chronically following administration of both doxorubicin and DMNQ in the heart, thus discounting the redox cycling hypothesis. These results may have occurred as clinically relevant concentrations of doxorubicin were utilised. This has not been the case in many of the studies implicating redox cycling (Tokarska-Schlattner et al. 2006). In addition studies were conducted *in vivo*, whereas those implicating redox cycling have mainly been conducted *in vitro*. Cells in culture are at a higher oxygen tension than that achieved physiologically (Corrêa et al. 2008; Hirabayashi et al. 1987), thus questioning the transferability of results across models (Bernuzzi et al. 2009; Menna et al. 2007).

Oxidative phosphorylation

The predominant pathway affected both acutely and chronically *in vivo* and to a lesser extent *in vitro* was oxidative phosphorylation. This was identified through both mRNA transcriptional and translational profiling (Chapters 5 and 7) and was further confirmed through the measurement of the activity of enzyme complexes involved in the ETC (Chapter 8). Overall complexes I, II and III of the ETC were found to be reduced in activity, while complexes IV and V were increased in activity. These changes in the activity of complexes of the ETC were accompanied by decreased ATP synthesis with an increase in AMP:ATP ratio and a decrease in the ATP:ADP ratio (Chapter 8), increased AMPK activation (Chapter 5), an increase in mtDNA copy number (Chapter 5) and activation of caspase 3 (Chapter 8). Increases in caspase 3 have been previously reported *in vivo* in acute and chronic models of doxorubicin toxicity, suggesting activation of the intrinsic pathway of apoptosis in cardiac tissue (Childs et al. 2002; Arola et al. 2000). These changes were accompanied by a parallel increase in citrate synthase activity, a marker of mitochondrial mass. This indicates that the increases in complex IV and V activity and mtDNA copy number could result from an increase in mitochondrial mass. However, the increase in complex IV activity exceeded the increase in citrate synthase, suggesting that while an increase in mitochondrial mass was part of the response it was not totally responsible for the increases observed. Increased

complex IV protein expression has been previously associated with increased muscle activity (Bengtsson et al. 2001). Therefore increased translation and transcription of complex IV encoding genes (as observed) may occur as a consequence of increased contractility of the heart. Increased contractility most likely occurs during the development of the cardiotoxic phenotype, increased heart rate is a clinical symptom of cardiac disease. Decreased complex I transcription and activity has been previously reported during Parkinson's disease, HIV infection and following ischemic injury and reperfusion (Chinta and Andersen 2006; Ladha et al. 2005; Panov et al. 2005; Paradies et al. 2004). Decreased transcriptional activity of the gene *Ndufa6*, which encodes one subunit of complex I is thought to directly induce apoptosis, highlighting the importance of regulation of the ETC in maintaining correct cellular dynamics (Ladha et al. 2005). The central nervous system stimulant, methamphetamine a cardiotoxin also interferes with the ETC. The cardiotoxicity appears to be manifested as tachycardia, hypertension, hypertrophy and dilated cardiomyopathy (Kaye et al. 2007; Maeno et al. 2000). Methamphetamine inhibits complex II and III of the ETC (Brown et al. 2005). Further investigations into these effects on the ETC revealed, methamphetamine selectively targets and alters specific sites on the enzyme complexes that compose the ETC. This raises the question that differential expression of genes encoding each complex of the ETC may result as doxorubicin and DMNQ may interfere with select components of each enzyme complex, resulting in effects on the entire complex function but not necessarily each individual gene that encodes part of each enzyme. Differential effects on genes encoding the same enzyme complex were observed translationally (Figure 7.5). This highlights the changes in activity of each complex of the ETC may result as a consequence of modulation of a select number of genes encoding each complex. The tendency of doxorubicin and DMNQ to inhibit complexes I-III and increase activity of complexes IV and V may depend on the intricate structure of these enzymes making them susceptible to xenobiotic induced damage (Scatena et al. 2007). In support of this

Fernández-Vizarra et al. (2009) reported that distinct subsets of genes encoding each complex have different functions. For example in complex I *Ndufv2* and *Ndufv1* are responsible for the oxidation of NADH to NAD⁺, whereas *Ndufs7*, *Ndufs8*, *Ndufs3* and *Ndufs2* are all involved in the transfer of electrons to ubiquinone. In addition the mitochondrial encoded genes within complex I are thought to be responsible for the formation of the proton gradient across the inner membrane. Genes within each of these groups appear to be expressed in a similar manner following doxorubicin and DMNQ. Translationally genes involved in the oxidation of NADH to NAD⁺, were overall less effectively translated whereas those involved in the transfer of electrons to ubiquinone were overall more effectively translated. These data indicates that different sub-sets of genes within each complex are probably regulated in a different manner.

Direct effects on mitochondria

Doxorubicin has been previously reported to interact with complex I of the ETC (Wallace 2003). The reduction in activity of complexes I-III was perhaps a consequence of doxorubicin and DMNQ acting as an electron shuttle within the ETC (Wallace and Starkov 2000). In this scenario doxorubicin may accept electrons from complex I of the ETC then release them back into the chain further upstream, possibly complex IV or cytochrome c. This would result in two ATP generating sites of the ETC being bypassed, due to diversion of electrons from these enzyme complexes to the compound and then to cytochrome c or complex IV (Figure 9.1). This diversion of electrons would result in decreased complex I, II and III activity due to a lack of electrons flowing through these complexes, while avoiding the production of ROS species (Figure 9.1).

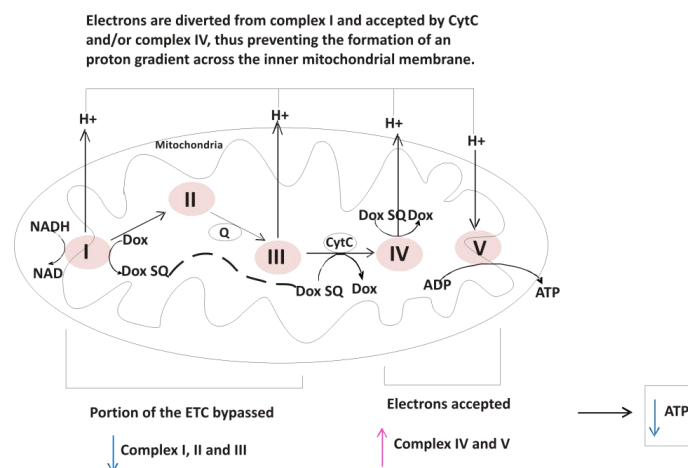


Figure 9.1: Overview of the possible shuttling effect of electrons following doxorubicin and DMNQ. Electrons from complex I of the ETC may be accepted from doxorubicin or DMNQ, resulting in the reduction of these compounds to the semiquinone, which passes electrons to either cytochrome c or directly to complex IV of the ETC enabling oxidation back to the parent compound. Other electron acceptors within mitochondria e.g.: heme proteins, glutathione or oxygen, may accept electrons from doxorubicin or DMNQ. However, no evidence for this was apparent through measurement of GSH and GSSG. In addition increased complex IV activity above the increase in mitochondrial mass is suggestive of flow of electrons through this complex of the ETC.

The impact of chemical redox potential

These influences on the ETC are however, dependent on the redox potential of doxorubicin.

Epirubicin, a doxorubicin analog with structural modifications, has a cardiotoxic to pharmacological activity ratio similar to doxorubicin in addition both these compounds have a redox potential of -328mV (Wallace and Starkov 2000). Thus indicating that the redox potential of a compound and the incident of cardiotoxicity appears to be intrinsically linked despite the lack of evidence of redox cycling in the heart (Figure 9.2). Also another analog of doxorubicin, mitoxantrone a substituted aglyconic anthraquinone (Minotti et al. 2004) has been found to be less cardiotoxic than doxorubicin, however, lower pharmacological activity has also been reported (Figure 9.2) (Minotti et al. 2004). Mitoxantrone has a redox potential of -450mV that is more negative than doxorubicin (Vile and Winterbourn 1989). These differences in cardiotoxicity and redox potential highlight the possibility of altering the structure of doxorubicin by the addition of side groups, reducing the redox potential to an extent that the molecule is itself much more difficult to be reduced by complex I of the ETC

thus modulating the cardiotoxic consequences. This hypothesis is supported by the redox potential of mitoxantrone which renders this compound less able to be reduced by complex I of the ETC, thus reducing the cardiotoxic consequences. Another quinone with anticancer properties is HU-331 derived from cannabidiol (Kogan et al. 2007). HU-331 has been proposed to have greater potency than doxorubicin and lacks any cardiotoxic effects. The structure of HU-331 suggests the potential of this compound to have a lower redox potential, due to the presence of long carbon side chains and hydroxyl groups. This highlights the importance of the redox potential of compounds to the perturbation of the oxidative phosphorylation pathway thus resulting in cardiotoxicity (Figure 9.2) (Kogan et al. 2007). A lower redox potential would prevent the acceptance of electrons from complex I of the ETC thus preventing the downstream consequences on the mitochondria and energy dynamics. Another quinone, 2-Hydroxy-1,4-naphoquinone (henna), used as a commercial dye has a redox potential of -415mV and no associated cardiotoxicity (Figure 9.2). Again illustrating that lowering the redox potential of doxorubicin may reduce the associated cardiotoxicity. This hypothesis suggests that the cardiotoxicity could be eliminated by reducing the redox potential. This hypothesis is supported by an *in vivo* study with lapachol which has a redox potential of -349mV (Rau and Stolz 2003). Lapachol was found to have no effect on CK-MB activity a marker of cardiac function and no significant cardiac transcriptional changes despite good distribution to the heart (Figure 9.3). These results provide possible strategies for the modulation of doxorubicin cardiotoxicity.

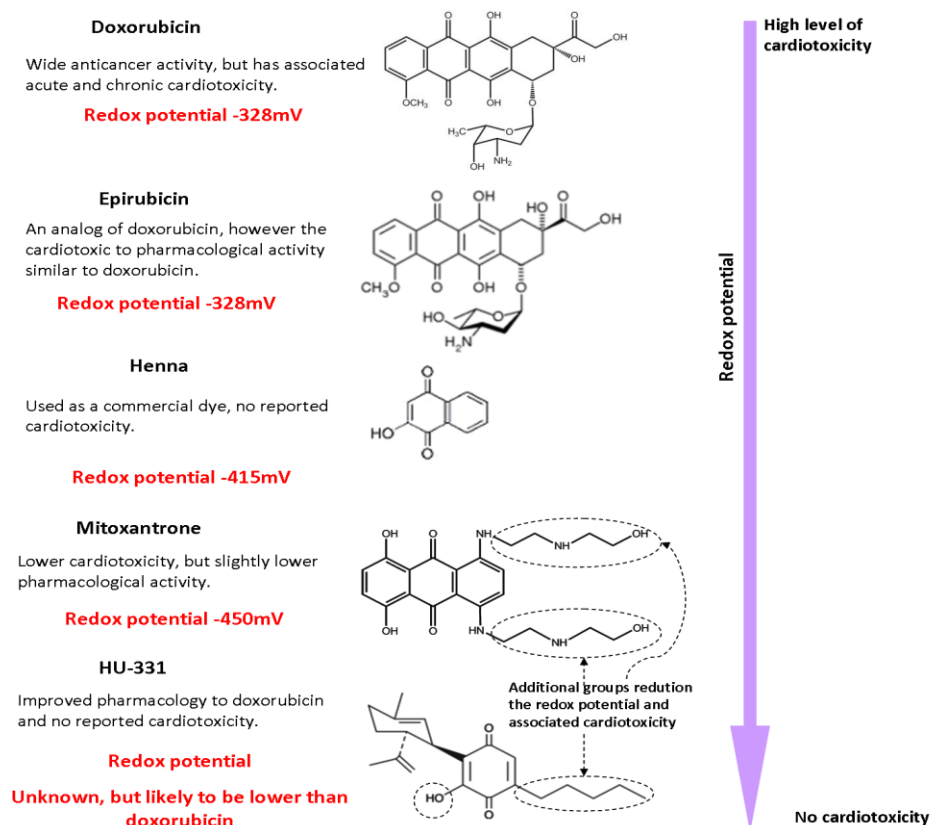


Figure 9.2: Illustration of the relationship between cardiotoxicity and redox potential. Doxorubicin and epirubicin both have the same pharmacological to toxicological ratio in addition they have the same redox potential. However, mitoxantrone has a greater pharmacological to toxicological ratio and in addition has a lower redox potential most likely a result of the addition of extra groups on the molecule, also the anti-cancer agent HU-331 has no associated cardiotoxicity and most likely a lower redox potential. Thus highlighting a link between cardiotoxicity of anti-cancer agents and redox potentials. In support of this the commercial dye, henna has a redox potential of -415mV and no associated cardiotoxicity. All redox potentials are versus the normal hydrogen electrode.

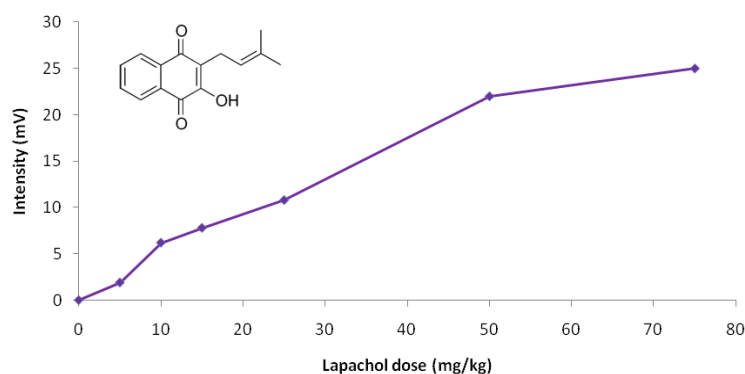


Figure 9.3: Cardiac distribution *in vivo* and structure of the quinone lapachol. HPLC analysis of cardiac tissue from male C57BL/AJ mice administrated with increasing doses of the quinone lapachol, distribution to the heart, with a dose dependent increase in cardiac retention occurring. This quinone was found to lack any cardiotoxic effects, possibly as a result of the lowered redox potential and side groups.

Altered transcription factors

I hypothesised that; the consequences on gene expression may arise as a consequence of altered transcription factor activation. One important mitochondrial transcription factor increased in activity was NRF-1 (Chapter 5). NRF-1 encodes a phosphorylated nuclear protein that functions as a transcription factor regulating the transcription of a number of genes that encode the oxidative phosphorylation pathway, mtDNA transcription and replication, heme biosynthesis, protein import and mitochondrial translation therefore implicating this transcription factor as a key mediator between nuclear and mitochondrial functions (Scarpulla 2008; Scarpulla 2006). Elevated NRF-1 DNA binding is thought to activate AMPK (as observed in Chapter 5) and thus glycolysis (as observed in Chapter 5) and fatty acid oxidation and regulate cytochrome c, required for the passage of electrons through the ETC. Transgenic mice with a *NRF-1* knockout do not survive past 3.5 to 6.5 days during the embryonic stage of development, indicating a critical role for this transcription factor in cell development and growth (Scarpulla 2006). LeMoine et al. (2006) reported a marked increase in *NRF-1* transcription in aged rats with cardiac impairment, suggesting a link between *NRF-1* status and cardiac dysfunction. NRF-1 may though be modulated as a result of cellular damage rather than as a consequence of a primary chemical insult. Western blotting of NRF-1 levels indicated a rapid increase in protein expression (Chapter 5), suggesting that the rapid genomic effects were partially due to the chemical insult, rather than downstream pathophysiology.

Another transcription factor down-regulated transcriptionally and translationally following doxorubicin was GATA-4 (Chapters 5 and 7). *GATA-4* transcriptional down-regulation has been previously associated with doxorubicin cardiotoxicity (Kim et al. 2003). GATA-4 is a vital regulator of cardiac development involved in the transcriptional regulation of genes involved in cardiac function, in particular sarcomeric proteins including the myosin heavy chain gene family and troponin I genes (Takemura and Fujiwara 2007). Thus differential

regulation of this transcription factor impairs cardiac energy production and contractility, thus impacting on cardiac function. Furthermore GATA-4 is an upstream regulator of Bcl-X, an anti-apoptotic gene (Aries et al. 2004). Therefore down-regulation could possibly activate the intrinsic pathway of apoptosis ultimately leading to activation of caspase 3 (observed in Chapter 8) and loss of cardiomyocytes resulting in the manifestation of a cardiotoxic phenotype. This modulation in transcription factors could be a direct result of doxorubicin or a secondary mechanism to overcome the toxic insult or a combination of both.

The role of cardiolipin

Doxorubicin is known to accumulate in the mitochondria in cardiac tissue (Tokarska-Schlattner et al. 2006) due to binding to cardiolipin a phospholipid found in the inner mitochondrial membrane (Goormaghtigh et al. 1987). Doxorubicin-cardiolipin binding is thought to directly affect the function of membrane bound enzymes and protein complexes including complex III and IV of the ETC (Sparagna and Lesnefsky 2009). Transcriptional profiling identified increased expression of genes involved in cardiolipin synthesis and biosynthetic processes and decreased expression of genes involved in cardiolipin metabolic processes. This differential gene expression may indicate altered activity as a result of doxorubicin-cardiolipin binding; however, further experiments are required to explore this mechanism as the genomic consequences on the ETC were greater than those on cardiolipin. In addition activity of complexes III and IV of the ETC have been found to be cardiolipin dependent. Thus, accumulation of doxorubicin in the mitochondrial inner membrane binding to cardiolipin may affect the function of complexes III and IV of the ETC. However, as the activity of complex III was decreased and that of complex IV increased the impact of cardiolipin on these complexes is likely to be insignificant in these models.

The role of mitochondrial mediated cell death

The dysfunctional ETC chain, mtDNA, AMPK and caspase 3 activation were accompanied by decreased protein expression of ANT and VDAC following acute doxorubicin and DMNQ.

Both of these proteins are present on the inner and outer mitochondrial membrane, respectively and are involved in the influx and efflux of ATP and ADP from the mitochondria to the cytosol and vice versa (Tokarska-Schlattner et al. 2006). ANT is also a vital protein in the mitochondrial permeability transition pore (mPTP) (Chapter 1). A decrease of ANT protein expression has been previously implicated with doxorubicin treatment (Jeyaseelan et al. 1997), during cold acclimation (Roussel et al. 2000) and left ventricular remodeling (Ning et al. 2000). A key route through which quinones cause cell death is via opening of the mPTP (Henry et al. 1995). An opened mPTP would be characterized by mitochondrial swelling (Chapter 4) and loss of mitochondrial membrane potential, leading to release of cytochrome c activating the intrinsic pathway of apoptosis (Chapter 1). If this opening is prolonged uncoupling of oxidative phosphorylation results, reducing ATP synthesis and leading to a switch, to a necrotic cell death due to insufficient ATP to drive apoptosis (Halestrap et al. 2000). Doxorubicin has been previously reported to decrease ANT protein expression as identified in Chapter 5 and induce opening of the mPTP (Oliveira and Wallace 2006) possibly as a result of calcium overload (Kowaltowski et al. 2001). Deregulation of calcium signaling pathways was observed transcriptionally but not translationally. However, calcium may be released from intracellular stores e.g.: the endoplasmic reticulum (Deniaud et al. 2008), thus opening of the mPTP. Recent evidence has suggested that VDAC, a protein on the outer mitochondrial membrane is not essential for opening of the mPTP; instead it is thought to have a protective role allowing removal of toxins through the outer membrane (Baines 2009). Therefore decreased protein expression as observed following acute doxorubicin and DMNQ may be indicative of removal of cellular protective mechanisms thus indicating release of pro-apoptotic factors from the mitochondria. The function of VDAC has been proposed to be regulated by the actin-binding protein gelsolin, promoting VDAC closure through an actin regulatory mechanism (Gourlay and Ayscough 2005). This mechanism of VDAC regulation highlights the interaction between dysfunctional

mitochondria and activation of the actin cytoskeleton pathway as observed in Chapter 5. However, the amount of apoptotic cell death as a result of opening of the mPTP is questionable due to the requirement of ATP to drive the cleavage of caspases in the intrinsic pathway of apoptosis. It is likely that cell death results due to a combined apoptotic and necrotic mechanism.

Alternatively apoptosis may be activated via mechanisms not mediated by the mPTP. The intrinsic pathway of apoptosis is regulated by the *Bcl-2* family of genes (Chapter 1.4.5). Down-regulation of the gene *Bcl-xl*, has been previously associated with inducing mitochondrial dysfunction and reduced ATP synthesis followed by subsequent cell death (Azim et al. 2009). Reduction in *Bcl-xl* gene expression was identified through transcriptional profiling following both doxorubicin and DMNQ. This therefore suggests that the resultant activation of caspase 3 (Chapter 8) may result from none mPTP mechanisms that were able to proceed with reduced ATP synthesis as observed in Chapter 8.

Activation of transcripts encoding the heterotrimeric enzyme AMPK were also observed following both doxorubicin and DMNQ (Chapter 5). Activation of AMPK is an important protective response against dysfunctional oxidative phosphorylation (Azim et al. 2009), supported by the increased occurrence of ischemia in mice containing an AMPK knockout (Arad et al. 2007). AMPK is activated by a decrease in the amount of ATP synthesis and the increase in AMP:ATP ratio combined with a decrease in the ATP:ADP ratio, all of which were observed following acute doxorubicin and DMNQ (Chapter 8) (Arad et al. 2007). Increased AMP concentration enables binding of AMP to the γ subunit of AMPK enabling activation (Arad et al. 2007). AMPK reduces the activity of ATP consuming processes while simultaneously increasing ATP production processes e.g.: glycolysis, thus maintaining ATP supply and preventing the induction of apoptosis. Activation of AMPK may explain why ATP synthesis improves over the time course following an initial drop (Figure 9.4). The initial drop in ATP (Figure 4.15) may trigger the activation of AMPK thus increasing ATP synthesis to

maintain adequate cardiac function. Lapatinib, an anti-cancer agent associated with minimal cardiotoxicity is a known activator of AMPK. These data thus support the notion that AMPK activation prevents the induction of apoptosis. This hypothesis would also account for the lower levels of caspase 3 activation at the later time points throughout the period of study. These data following doxorubicin and DMNQ is suggestive of effects on the mitochondria and consequently decreased ATP synthesis, which activates both AMPK and initially caspase 3 either through modulation of *Bcl-xl* or transient opening of the mPTP as a result of reduced ANT expression. AMPK activation increases transcription of genes involved in glycolysis (Chapter 5). This maintains a supply of ATP while reducing ATP consuming processes, resulting in a net increase in ATP available to the heart. As AMPK activation increases ATP synthesis allowing cellular processes to occur, the rate of caspase 3 activation and subsequently apoptosis declines (Figure 9.4).

All these data suggest that the major impact of doxorubicin in the cell is on mitochondria, with subsequent activation of pathways a consequence of dysfunctional mitochondria and energy dynamics (Figure 9.5).

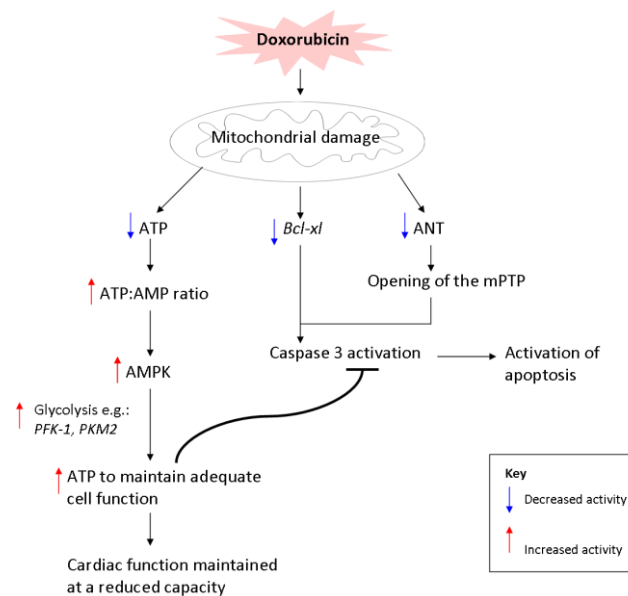


Figure 9.4: Summary of the influence of AMPK on doxorubicin induced cardiotoxicity.

Direct DNA damage

Another mechanism of doxorubicin cardiotoxicity previously reported is direct DNA damage (Arola et al. 2000). However, no evidence for this mechanism was identified through genomic profiling. To date evidence for direct DNA damage in cardiomyocytes has not been reported *in vivo*; despite activation of p53 and partial DNA repair *in vitro* (L'Ecuyer et al. 2006). However, it is possible that doxorubicin cumulative damage develops as a result of the inhibition of transcription.

9.3 SPECIFICITY OF DOXORUBICIN AS A CARDIOTOXIN

Figure 9.5 summarizes the proposed mechanisms of doxorubicin induced cardiotoxicity arising from inhibition of ATP synthesis from the ETC. These effects on mitochondria and ATP synthesis may also help explain why doxorubicin results in specific cardiotoxicity despite a wide bioavailability *in vivo* (Al-Abd et al. 2009; Urva et al. 2009). The heart is the most energy demanding tissue; it meets these demands by cells containing ~35% more mitochondria compared to other tissues (Gustafsson and Gottlieb 2008; Tokarska-Schlattner et al. 2005; Lebrecht et al. 2003). 90% of the ATP utilised by cardiomyocytes is produced through the ETC, thus any alterations in enzyme function within the ETC is likely to result in cellular damage more pronounced than in other tissues (Tokarska-Schlattner et al. 2006). These effects on mitochondria function in particular on the ETC were accompanied by transcriptional and translational changes in genes encoding the TCA cycle, glycolysis pathway and the AMPK protein. Under normal physiological conditions the heart generates acetyl-coA to enter the TCA cycle to provide electrons to complex I or II of the ETC. Acetyl-coA is produced as a result of the metabolism of mainly fatty acids through the utilization of oxaloacetate and also the oxidation of pyruvate through glycolysis. Upon damage to cardiac tissue there is an increased reliance on glycolysis to generate pyruvate that is oxidized to produce acetyl-coA, as observed following transcriptional and translational profiling.

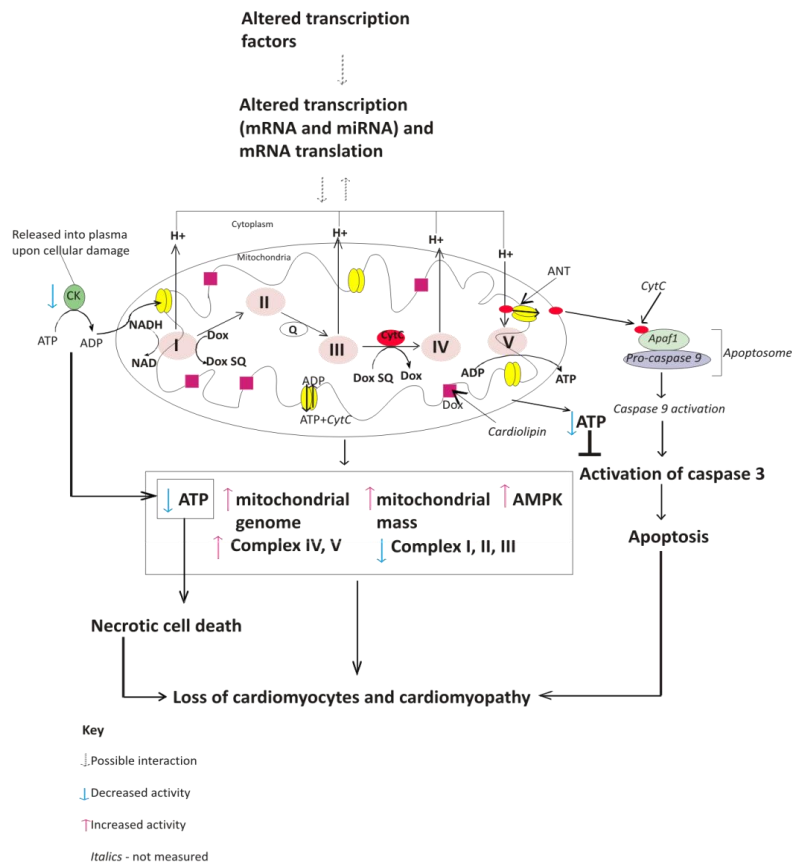


Figure 9.5: Schematic of the proposed mechanism of doxorubicin toxicity resulting from inhibition of ATP production from the ETC.

9.4 THE POTENTIAL ROLE OF miRNAs

miRNAs have a fundamental role in controlling translation as outlined in Chapter 1 (Kim and Nam 2006). Over the past 4 years the role of these small RNA molecules in cardiac dysfunction has been determined (Wang et al. 2008). To date no data exists in the public domain implicating miRNAs in cardiotoxicity. miRNAs are likely to contribute to the cardiotoxic phenotype as some are transcribed from the genome under the control of RNA polymerase II promoters. Some of these promoters contain toxicologically significant enhancer regions a target for many pharmaceutical agents (Taylor and Gant 2008). miRNA profiling (Chapter 6) identified a number of miRNAs differentially expressed that have previously been associated with cardiac dysfunction, thus suggesting that miRNAs were modulated in expression following both doxorubicin and DMNQ. The reason for differential

expression could be to promote the development of cardiotoxicity or as a protective mechanism to prevent the development of the cardiotoxic phenotype. From my profiling of miRNAs differential expression was apparent. In order to investigate a possible function for one miRNA in cardiotoxicity knockdown experiments were conducted *in vitro*. miR-181a was found to be down-regulated in expression both *in vivo* and *in vitro* following doxorubicin and DMNQ treatment. Modelling this *in vitro* by knockdown of miR-181a followed by treatment with doxorubicin and DMNQ demonstrated an increase in cardiotoxicity. In a similar manner further knockdown of individual miRNAs would allow a greater insight into miRNA biology and the function of these RNA species in toxicology.

The correlation of differential miRNA and mRNA translational changes (Chapter 7) can permit putative bioinformatic predictions to be made. For example, the more efficiently translated gene *Stim2* contains a binding site for the down-regulated miR-181a, hence identifying a possible interaction that mediates the cellular response to acute doxorubicin and DMNQ treatment (Figure 7.8A). As discussed in section 7.3.2, the exact function of *Stim2* is currently unknown, but this gene is possibly involved in calcium transport (Brandman et al. 2007). miR-181a has been previously implicated in myogenesis (Naguibneva et al. 2006). This interaction could possibly be important in the development of the cardiotoxic phenotype following both doxorubicin and DMNQ. Calcium signalling and transport are known to play an essential role in cardiac physiology and have also been implicated with cardiac development thus intrinsically linking this putative interaction between miR-181a and *Stim2*. Another putative miRNA-mRNA interaction identified was between the less efficiently translated gene *Atp1b1* and miR-29a (Figure 7.8B). *Atp1b1* encodes a Na⁺/K⁺ ATPases involved in the establishment and maintenance of an electrochemical gradient of sodium and potassium ions across the plasma membrane involved in muscle contractility. The miRNA, miR-29a is associated with cardiac fibrosis and apoptosis (Latronico and Condorelli 2009; Park et al. 2009; Wang et al. 2009a; van Rooij et

al. 2008). Decreased contractility may result as a consequence of fibrosis and apoptosis, thus possibly highlighting another important interaction. This work highlights miRNAs that may provide a novel therapeutic treatment or target to modulate cardiotoxicity in the future.

9.5 POSSIBLE STRATEGIES TO MODULATE DOXORUBICIN CARDIOTOXICITY

The studies contained within this project demonstrate that the pharmacological and toxicological activities of doxorubicin are distinguishable. The results indicate the major influence of doxorubicin in the cell was with the mitochondria; however, the redox potential of the molecule may be essential to allow this to occur. An approach to overcome this would be to modify the side groups that allow retention of the pharmacological properties while making the one-electron redox potential more negative possibly reducing the cardiotoxicity, but retaining the anti-cancer properties of the molecule. Other ways to reduce the cardiotoxicity would involve co-administration of compounds known to prevent the mPTP opening or those that increase the activity of complexes I-III of the ETC. A known inhibitor of the mPTP is the immunosuppressant cyclosporin A (Sardao et al. 2009).

Cyclosporin A is thought to bind to cyclophilin-D preventing its binding to other pore proteins such as ANT, thus preventing the functioning of the pore. Co-administration of cyclosporin A with doxorubicin has previously been reported to reduce the associated cardiotoxicity (Zhou et al. 2001). In addition Faustin et al. (2004) reported an increase in ANT protein expression on the inner mitochondrial membrane following co-administration of doxorubicin and cyclosporin A, hence suggesting that the decreased protein expression of ANT identified in Chapter 5 contributes to the cardiotoxic phenotype, maybe through the promotion of apoptosis. These data further highlight mitochondria to be key organelles involved in doxorubicin cardiotoxicity and provide a possible mechanism for co-administration of compounds to counteract any toxic consequences. Pharmacological activation of pyruvate dehydrogenase has previously resulted in improved left ventricular

function during heart failure (Stanley and Hoppel 2000). Increased pyruvate dehydrogenase activity is thought to stabilize ion homeostasis thus allowing more efficient use of ATP for contractile function through the myosin and calcium ATPase in the heart. Pyruvate dehydrogenase can be chemically increased by the use of partial fatty acid oxidation inhibitors e.g.: trimetazidine and ranalazine thus possibly providing a novel approach to reduce to toxicity associated with doxorubicin (Stanley and Hoppel 2000; Stanley et al. 1997). Another potential novel approach would be to increase the activity of complex I on the ETC through co-administration of doxorubicin with desferrioxamine. Desferrioxamine, is an iron chelator known to competitively activate NADH dehydrogenase (complex I) and protect complex I activity from inhibition, thus potentially maintaining the flow of electrons through the ETC thus allowing ATP synthesis to occur (Glinka et al. 1998). These influences on the ETC are thought to be distinct from the iron chelating properties of this agent. Desferrioxamine has been used in the treatment of Parkinson's disease by increasing ETC complex I activity, thus highlighting the therapeutic potential of this compound (Glinka et al. 1996).

9.6 OTHER CARDIOTOXIC ANTI-CANCER AGENTS

Cardiotoxicity is not unique to the anthracyclines, many pharmaceutical agents have been found to be cardiotoxic including non-steroidal anti-inflammatory drugs (e.g.: celecoxib and oxaprozin), anti-diabetics (e.g.: rosiglitazone), antiarrhythmics (e.g.: amiodarone), statins and other anti-cancer agents (e.g.: trastuzumab) (Force and Kerkelä 2008; Sirvent et al. 2008; Dykens and Will 2007). The cardiotoxicity of a number of these agents is thought to implicate the mitochondria. To date, a number of new anti-cancer agents have been developed to attempt to reduce the frequency of doxorubicin's use. However, a number of these agents e.g.: epirubicin have both reduced pharmacology and toxicology, thus the therapeutic index of these compounds is comparable to that of doxorubicin. Over recent years a novel approach to the development of anti-cancer agents has been developed, using

monoclonal antibodies and small molecule inhibitors (Force and Kerkelä 2008). Two such agents are trastuzumab and lapatinib, a monoclonal antibody and tyrosine kinase inhibitor, respectively. Both these biological agents target the tyrosine kinase HER2 and inhibit its activity (Popat and Smith 2008). HER2 is over-expressed in a number of cancers in particular breast carcinoma thus inhibition results in cancer cell death, reducing tumour size, thus the development of such agents has the potential to revolutionise the treatment of cancer (Force and Kerkelä 2008). However, HER2 is also important in cardiogenesis and protection from cardiomyocyte apoptosis (Azim et al. 2009). HER2 knockout mice die prior to birth as a result of poorly developed cardiac trabeculae, highlighting the importance of HER2 during development (Popat and Smith 2008). In addition selective knockout of HER2 in ventricular cardiomyocytes leads to severe dilated cardiomyopathy two months after birth (Meyer et al. 1995). These knockout studies in mice indicate the importance of HER2 in cardiac development and function, thus reduction in activity following xenobiotic exposure is likely to have an influence on cardiac function and survival (Ozcelik et al. 2002). Trastuzumab has a cardiotoxic incidence of 4-7% in man which is increased to 27% following doxorubicin treatment, the mechanism responsible for the increased sensitivity of cardiomyocytes to trastuzumab following doxorubicin treatment remain elusive (Force and Kerkelä 2008; Popat and Smith 2008; Seidman et al. 2002). However, the increased sensitivity may arise due to the occurrence of previous cardiomyocyte damage induced by doxorubicin being maintained at sub-clinical levels thus further insult results in increased cardiac damage. The utilisation of knockout mice further illustrates the development of cardiotoxicity during HER2 suppression characterised as dilated cardiomyopathy. The resultant cardiotoxicity appears to arise due to direct targeting and inhibition of the HER2 receptor, not as a consequence of an immune response (Azim et al. 2009; Popat and Smith 2008). This was investigated though the assessment of the number of mononuclear cells present in cardiac biopsies, no significant difference was observed, discounting an immune response as the causative

mechanism responsible for the observed cardiotoxicity (Azim et al. 2009). It is currently thought that trastuzumab affects mitochondrial integrity affecting the mitochondrial membrane, decreasing ATP synthesis and contractility (Azim et al. 2009). However, lapatinib has been found to be less cardiotoxic despite targeting HER2, however, the inhibitory effect on HER2 is less potent, thus suggesting the importance of HER2 in the development of a cardiotoxic phenotype (Azim et al. 2009; Force and Kerkelä 2008). HER2 was found to be less efficiently translationally expressed following acute doxorubicin and DMNQ. This thus indicates the importance of HER2 in cardiotoxicity, and the importance of maintaining mitochondrial function. It also raises the question, do all cardiotoxic compounds modulate mitochondrial function in some way. Increasing HER2 expression may provide a novel mechanism to reduce the development of cardiotoxicity following a broad range of compounds.

9.7 FUTURE WORK

Knockout experiments confirmed a role for miR-181a in increasing the degree of cardiotoxicity following doxorubicin and DMNQ. Additional knockout and over-expression experiments are required combined with translational profiling to confirm the importance of miRNAs in the development of cardiotoxicity. In addition reporter assays are required to confirm the putative bioinformatic correlations between miRNA and mRNA translational profiles. This would allow conformation of novel biological relationships in this model system.

9.8 CONCLUSIONS

Throughout this study I have sought to use genomic and biochemical techniques to elucidate the mechanism of doxorubicin induced cardiotoxicity. A novel naphthoquinone compound, DMNQ was utilised to allow the complex chemistries of doxorubicin to be separated. An *in vivo* model demonstrated that a single acute dose of doxorubicin and DMNQ results in an increase in cardiac clinical chemistry biomarkers, without profound morphological

alterations thus allowing the predisposing mechanisms to be identified. Chronic models of toxicity *in vivo* demonstrated the cumulative properties of doxorubicin; however, DMNQ did not appear to result in profound cumulative toxicity. Transcriptional and translational gene perturbation occurred from 30 and 5 minutes following doxorubicin and DMNQ, illustrating major effects on oxidative phosphorylation (Figures 5.6 and 7.6). No changes associated with redox cycling or an antioxidant response were apparent either in the genome or biochemically. The rapid genomic alterations indicated how responsive cardiomyocytes are to chemical stress *in vivo*, and should serve as a caution to the long time periods that are often employed in similar studies. Profiling of miRNA and mRNA translation indicated altered translation of mRNA control by miRNAs following toxic exposure and the contribution of miR-181a to the progression of the cardiotoxic phenotype (Chapter 6 and Figure 8.6). The overall mechanism of doxorubicin cardiotoxicity appears in part to be due to the disruption of the ETC in particular decreased activity of complexes I-III and increased activity of complex IV and V (Figures 8.7-8.12), with associated changes in mtDNA (Figure 5.14), AMPK activation (Figure 5.12), glycolysis, citrate synthase activity (Figure 8.13) and caspase 3 activation (Figure 4.13). This demonstrates how responsive the ETC genes are to disruption of electron flow in the chain and the importance of mitochondria. The findings of this study provide a novel insight into doxorubicin cardiotoxicity, possible ways in which the toxicity could be modulated and illustrates the utilisation of genomics in the identification of toxicity.

REFERENCES

- Al-Abd, A.M., Kim, N.H., Song, S.C., Lee, S.J. & Kuh, H.J. 2009, "A simple HPLC method for doxorubicin in plasma and tissues of nude mice", *Archives of Pharmacal Research*, vol. 32, no. 4, pp. 605-611.
- Alderton, P.M., Gross, J. & Green, M.D. 1992, "Comparative study of doxorubicin, mitoxantrone, and epirubicin in combination with ICRF-187 (ADR-529) in a chronic cardiotoxicity animal model", *Cancer research*, vol. 52, no. 1, pp. 194-201.
- Al-Nasser, I.A. 1998, "In vivo prevention of adriamycin cardiotoxicity by cyclosporin A or FK506", *Toxicology*, vol. 131, no. 2-3, pp. 175-181.
- Altenberg, B. & Greulich, K.O. 2004, "Genes of glycolysis are ubiquitously overexpressed in 24 cancer classes", *Genomics*, vol. 84, no. 6, pp. 1014-1020.
- Anders, J.C. & Chung, H. 1984, "Deficiencies and improvement of methemoglobin assay", *Journal of analytical toxicology*, vol. 8, no. 6, pp. 260-262.
- Anderson, M.E. & Mohler, P.J. 2007, "MicroRNA may have macro effect on sudden death", *Nature medicine*, vol. 13, no. 4, pp. 410-411.
- Arad, M., Seidman, C.E. & Seidman, J.G. 2007, "AMP-activated protein kinase in the heart: role during health and disease", *Circulation research*, vol. 100, no. 4, pp. 474-488.
- Aries, A., Paradis, P., Lefebvre, C., Schwartz, R.J. & Nemer, M. 2004, "Essential role of GATA-4 in cell survival and drug-induced cardiotoxicity", *Proceedings of the National Academy of Sciences of the United States of America*, vol. 101, no. 18, pp. 6975-6980.
- Armstrong, J.S. 2007, "Mitochondrial medicine: pharmacological targeting of mitochondria in disease", *British journal of pharmacology*, vol. 151, no. 8, pp. 1154-1165.
- Arola, O.J., Saraste, A., Pulkki, K., Kallajoki, M., Parvinen, M. & Voipio-Pulkki, L.M. 2000, "Acute doxorubicin cardiotoxicity involves cardiomyocyte apoptosis", *Cancer research*, vol. 60, no. 7, pp. 1789-1792.
- Ashley, N. & Poulton, J. 2009, "Mitochondrial DNA is a direct target of anti-cancer anthracycline drugs", *Biochemical and biophysical research communications*, vol. 378, no. 3, pp. 450-455.
- Azim, H., Azim, H.A., Jr & Escudier, B. 2009, "Trastuzumab versus lapatinib: The cardiac side of the story", *Cancer treatment reviews*, .
- Baek, D., Villén, J., Shin, C., Camargo, F.D., Gygi, S.P., Bartel, D.P. 2008, "The impact of microRNAs on protein output", *Nature*, vol. 455, pp. 64-71.
- Baetz, A.L. & Mengeling, W.L. 1971, "Blood constituent changes in fasted swine", *American Journal of Veterinary Research*, vol. 32, no. 10, pp. 1491-1499.
- Baines, C.P. 2009, "The molecular composition of the mitochondrial permeability transition pore", *Journal of Molecular and Cellular Cardiology*, vol. 46, no. 6, pp. 850-857.
- Baines, C.P., Kaiser, R.A., Sheiko, T., Craigen, W.J. & Molkenin, J.D. 2007, "Voltage-dependent anion channels are dispensable for mitochondrial-dependent cell death", *Nature cell biology*, vol. 9, no. 5, pp. 550-555.

- Bandi, N., Zbinden, S., Gugger, M., Arnold, M., Kocher, V., Hasan, L., Kappeler, A., Brunner, T. & Vassella, E. 2009, "miR-15a and miR-16 are implicated in cell cycle regulation in a Rb-dependent manner and are frequently deleted or down-regulated in non-small cell lung cancer", *Cancer research*, vol. 69, no. 13, pp. 5553-5559.
- Barrientos, A. 2002, "In vivo and in organello assessment of OXPHOS activities", *Methods (San Diego, Calif.)*, vol. 26, no. 4, pp. 307-316.
- Barringhaus, K.G. & Zamore, P.D. 2009, "MicroRNAs: regulating a change of heart", *Circulation*, vol. 119, no. 16, pp. 2217-2224.
- Belham, M., Kruger, A., Mephram, S., Faganello, G. & Pritchard, C. 2007, "Monitoring left ventricular function in adults receiving anthracycline-containing chemotherapy", *European journal of heart failure : journal of the Working Group on Heart Failure of the European Society of Cardiology*, vol. 9, no. 4, pp. 409-414.
- Bellomo, G., Mirabelli, F., DiMonte, D., Richelmi, P., Thor, H., Orrenius, C. & Orrenius, S. 1987, "Formation and reduction of glutathione-protein mixed disulfides during oxidative stress. A study with isolated hepatocytes and menadione (2-methyl-1,4-naphthoquinone)", *Biochemical pharmacology*, vol. 36, no. 8, pp. 1313-1320.
- Bengtsson, J., Gustafsson, T., Widegren, U., Jansson, E. & Sundberg, C.J. 2001, "Mitochondrial transcription factor A and respiratory complex IV increase in response to exercise training in humans", *Pflugers Archiv : European journal of physiology*, vol. 443, no. 1, pp. 61-66.
- Bernuzzi, F., Recalcati, S., Alberghini, A. & Cairo, G. 2009, "Reactive oxygen species-independent apoptosis in doxorubicin-treated H9c2 cardiomyocytes: role for heme oxygenase-1 down-modulation", *Chemico-biological interactions*, vol. 177, no. 1, pp. 12-20.
- Berthiaume, J.M. & Wallace, K.B. 2007a, "Adriamycin-induced oxidative mitochondrial cardiotoxicity", *Cell biology and toxicology*, vol. 23, no. 1, pp. 15-25.
- Berthiaume, J.M. & Wallace, K.B. 2007b, "Persistent alterations to the gene expression profile of the heart subsequent to chronic Doxorubicin treatment", *Cardiovascular toxicology*, vol. 7, no. 3, pp. 178-191.
- Bertinchant, J.P., Robert, E., Polge, A., Marty-Double, C., Fabbro-Peray, P., Poirey, S., Aya, G., Juan, J.M., Ledermann, B., de la Coussaye, J.E. & Dautat, M. 2000, "Comparison of the diagnostic value of cardiac troponin I and T determinations for detecting early myocardial damage and the relationship with histological findings after isoprenaline-induced cardiac injury in rats", *Clinica chimica acta; international journal of clinical chemistry*, vol. 298, no. 1-2, pp. 13-28.
- Bird, B.R. & Swain, S.M. 2008, "Cardiac toxicity in breast cancer survivors: review of potential cardiac problems", *Clinical cancer research : an official journal of the American Association for Cancer Research*, vol. 14, no. 1, pp. 14-24.
- Blais, J.D., Filipenko, V., Bi, M., Harding, H.P., Ron, D., Koumenis, C., Wouters, B.G. & Bell, J.C. 2004, "Activating transcription factor 4 is translationally regulated by hypoxic stress", *Molecular and cellular biology*, vol. 24, no. 17, pp. 7469-7482.
- Bohr, V.A., Stevnsner, T. & de Souza-Pinto, N.C. 2002, "Mitochondrial DNA repair of oxidative damage in mammalian cells", *Gene*, vol. 286, no. 1, pp. 127-134.
- Boldogh, I.R. & Pon, L.A. 2007, "Mitochondria on the move", *Trends in cell biology*, vol. 17, no. 10, pp. 502-510.

- Bolton, J.L., Trush, M.A., Penning, T.M., Dryhurst, G. & Monks, T.J. 2000, "Role of quinones in toxicology", *Chemical research in toxicology*, vol. 13, no. 3, pp. 135-160.
- Brandman, O., Liou, J., Park, W.S. & Meyer, T. 2007, "STIM2 is a feedback regulator that stabilizes basal cytosolic and endoplasmic reticulum Ca²⁺ levels", *Cell*, vol. 131, no. 7, pp. 1327-1339.
- Brown, J.M., Quinton, M.S. & Yamamoto, B.K. 2005, "Methamphetamine-induced inhibition of mitochondrial complex II: roles of glutamate and peroxynitrite", *Journal of neurochemistry*, vol. 95, no. 2, pp. 429-436.
- Brugger-Andersen, T., Aarsetoy, H., Grundt, H., Staines, H. & Nilsen, D.W. 2008, "The long-term prognostic value of multiple biomarkers following a myocardial infarction", *Thrombosis research*, vol. 123, no. 1, pp. 60-66.
- Bruneau, B.G. 2005, "Developmental biology: tiny brakes for a growing heart", *Nature*, vol. 436, no. 7048, pp. 181-182.
- Buffinton, G.D., Ollinger, K., Brunmark, A. & Cadenas, E. 1989, "DT-diaphorase-catalysed reduction of 1,4-naphthoquinone derivatives and glutathionyl-quinone conjugates. Effect of substituents on autoxidation rates", *The Biochemical journal*, vol. 257, no. 2, pp. 561-571.
- Calin, G.A., Dumitru, C.D., Shimizu, M., Bichi, R., Zupo, S., Noch, E., Aldler, H., Rattan, S., Keating, M., Rai, K., Rassenti, L., Kipps, T., Negrini, M., Bullrich, F. & Croce, C.M. 2002, "Frequent deletions and down-regulation of micro- RNA genes miR15 and miR16 at 13q14 in chronic lymphocytic leukemia", *Proceedings of the National Academy of Sciences of the United States of America*, vol. 99, no. 24, pp. 15524-15529.
- Callis, T.E. & Wang, D.Z. 2008, "Taking microRNAs to heart", *Trends in molecular medicine*, vol. 14, no. 6, pp. 254-260.
- Castoldi, M., Schmidt, S., Benes, V., Noerholm, M., Kulozik, A.E., Hentze, M.W. & Muckenthaler, M.U. 2006, "A sensitive array for microRNA expression profiling (miChip) based on locked nucleic acids (LNA)", *RNA (New York, N.Y.)*, vol. 12, no. 5, pp. 913-920.
- Chen, J.F., Callis, T.E. & Wang, D.Z. 2009, "microRNAs and muscle disorders", *Journal of cell science*, vol. 122, no. Pt 1, pp. 13-20.
- Chendrimada, T.P., Gregory, R.I., Kumaraswamy, E., Norman, J., Cooch, N., Nishikura, K. & Shiekhattar, R. 2005, "TRBP recruits the Dicer complex to Ago2 for microRNA processing and gene silencing", *Nature*, vol. 436, no. 7051, pp. 740-744.
- Cheng, E.H., Sheiko, T.V., Fisher, J.K., Craigen, W.J. & Korsmeyer, S.J. 2003, "VDAC2 inhibits BAK activation and mitochondrial apoptosis", *Science (New York, N.Y.)*, vol. 301, no. 5632, pp. 513-517.
- Chiaratti, M.R. & Meirelles, F.V. 2006, "Increase in mitochondrial DNA quantity and impairment of oxidative phosphorylation in bovine fibroblast cells treated with ethidium bromide for 15 passages in culture", *Genetics and molecular research : GMR*, vol. 5, no. 1, pp. 55-62.
- Chien, K.R. 2007, "Molecular medicine: microRNAs and the tell-tale heart", *Nature*, vol. 447, no. 7143, pp. 389-390.
- Childs, A.C., Phaneuf, S.L., Dirks, A.J., Phillips, T. & Leeuwenburgh, C. 2002, "Doxorubicin treatment in vivo causes cytochrome C release and cardiomyocyte apoptosis, as well as increased mitochondrial efficiency, superoxide dismutase activity, and Bcl-2:Bax ratio", *Cancer research*, vol. 62, no. 16, pp. 4592-4598.

Chinta, S.J. & Andersen, J.K. 2006, "Reversible inhibition of mitochondrial complex I activity following chronic dopaminergic glutathione depletion in vitro: implications for Parkinson's disease", *Free radical biology & medicine*, vol. 41, no. 9, pp. 1442-1448.

Chivukula, R.R. & Mendell, J.T. 2008, "Circular reasoning: microRNAs and cell-cycle control", *Trends in biochemical sciences*, vol. 33, no. 10, pp. 474-481.

Choi, Y.J., Rho, J.K., Lee, S.J., Jang, W.S., Lee, S.S., Kim, C.H. & Lee, J.C. 2009, "HIF-1 α modulation by topoisomerase inhibitors in non-small cell lung cancer cell lines", *Journal of cancer research and clinical oncology*, vol. 135, no. 8, pp. 1047-1053.

Clancy, J.L., Nusch, M., Humphreys, D.T., Westman, B.J., Beilharz, T.H. & Preiss, T. 2007, "Methods to analyze microRNA-mediated control of mRNA translation", *Methods in enzymology*, vol. 431, pp. 83-111.

Claycomb, W.C., Lanson, N.A., Jr, Stallworth, B.S., Egeland, D.B., Delcarpio, J.B., Bahinski, A. & Izzo, N.J., Jr 1998, "HL-1 cells: a cardiac muscle cell line that contracts and retains phenotypic characteristics of the adult cardiomyocyte", *Proceedings of the National Academy of Sciences of the United States of America*, vol. 95, no. 6, pp. 2979-2984.

Colombo, T., Parisi, I., Zucchetti, M., Sessa, C., Goldhirsch, A. & D'Incalci, M. 1999, "Pharmacokinetic interactions of paclitaxel, docetaxel and their vehicles with doxorubicin", *Annals of Oncology : Official Journal of the European Society for Medical Oncology / ESMO*, vol. 10, no. 4, pp. 391-395.

Cordes, K.R. & Srivastava, D. 2009, "MicroRNA regulation of cardiovascular development", *Circulation research*, vol. 104, no. 6, pp. 724-732.

Correa, G.A., Rumpf, R., Mundim, T.C., Franco, M.M. & Dode, M.A. 2008, "Oxygen tension during in vitro culture of bovine embryos: effect in production and expression of genes related to oxidative stress", *Animal Reproduction Science*, vol. 104, no. 2-4, pp. 132-142.

Croce, C.M. & Calin, G.A. 2005, "miRNAs, cancer, and stem cell division", *Cell*, vol. 122, no. 1, pp. 6-7.

Cullen, B.R. 2004, "Transcription and processing of human microRNA precursors", *Molecular cell*, vol. 16, no. 6, pp. 861-865.

Curtis, R.K., Oresic, M. & Vidal-Puig, A. 2005, "Pathways to the analysis of microarray data", *Trends in biotechnology*, vol. 23, no. 8, pp. 429-435.

Cutts, S.M., Parsons, P.G., Sturm, R.A. & Phillips, D.R. 1996, "Adriamycin-induced DNA adducts inhibit the DNA interactions of transcription factors and RNA polymerase", *The Journal of biological chemistry*, vol. 271, no. 10, pp. 5422-5429.

Danesi, R., Fogli, S., Gennari, A., Conte, P. & Del Tacca, M. 2002, "Pharmacokinetic-pharmacodynamic relationships of the anthracycline anticancer drugs", *Clinical pharmacokinetics*, vol. 41, no. 6, pp. 431-444.

Davies, R., Schuurman, A., Barker, C.R., Clothier, B., Chernova, T., Higginson, F.M., Judah, D.J., Dinsdale, D., Edwards, R.E., Greaves, P., Gant, T.W. & Smith, A.G. 2005, "Hepatic gene expression in protoporphyric Fech mice is associated with cholestatic injury but not a marked depletion of the heme regulatory pool", *The American journal of pathology*, vol. 166, no. 4, pp. 1041-1053.

de Groot, H., Noll, T. & Sies, H. 1985, "Oxygen dependence and subcellular partitioning of hepatic menadione-mediated oxygen uptake. Studies with isolated hepatocytes, mitochondria, and

microsomes from rat liver in an oxystat system", *Archives of Biochemistry and Biophysics*, vol. 243, no. 2, pp. 556-562.

de Jong, R.S., Mulder, N.H., Uges, D.R., Sleijfer, D.T., Hoppener, F.J., Groen, H.J., Willemse, P.H., van der Graaf, W.T. & de Vries, E.G. 1999, "Phase I and pharmacokinetic study of the topoisomerase II catalytic inhibitor fostriecin", *British journal of cancer*, vol. 79, no. 5-6, pp. 882-887.

Delgado, R.M., 3rd, Nawar, M.A., Zewail, A.M., Kar, B., Vaughn, W.K., Wu, K.K., Aleksic, N., Sivasubramanian, N., McKay, K., Mann, D.L. & Willerson, J.T. 2004, "Cyclooxygenase-2 inhibitor treatment improves left ventricular function and mortality in a murine model of doxorubicin-induced heart failure", *Circulation*, vol. 109, no. 11, pp. 1428-1433.

Demant, E.J. 1984, "Binding of adriamycin-Fe³⁺ complex to membrane phospholipids", *European journal of biochemistry / FEBS*, vol. 142, no. 3, pp. 571-575.

Deniaud, A., Sharaf el dein, O., Maillier, E., Poncet, D., Kroemer, G., Lemaire, C. & Brenner, C. 2008, "Endoplasmic reticulum stress induces calcium-dependent permeability transition, mitochondrial outer membrane permeabilization and apoptosis", *Oncogene*, vol. 27, no. 3, pp. 285-299.

Diwakar, L., Ray, A., Ravindranath, V. 2008, "Complex I assay in mitochondrial preparations from CNS", *Current protocols in toxicology*, vol. 17, no. 10, pp. 1-7.

Doroshov, J.H. & Davies, K.J. 1986, "Redox cycling of anthracyclines by cardiac mitochondria. II. Formation of superoxide anion, hydrogen peroxide, and hydroxyl radical", *The Journal of biological chemistry*, vol. 261, no. 7, pp. 3068-3074.

Doroshov, J.H., Locker, G.Y., Ifrim, I. & Myers, C.E. 1981, "Prevention of doxorubicin cardiac toxicity in the mouse by N-acetylcysteine", *The Journal of clinical investigation*, vol. 68, no. 4, pp. 1053-1064.

Doust, J.A., Pietrzak, E., Dobson, A. & Glasziou, P. 2005, "How well does B-type natriuretic peptide predict death and cardiac events in patients with heart failure: systematic review", *BMJ (Clinical research ed.)*, vol. 330, no. 7492, pp. 625.

Dykens, J.A. & Will, Y. 2007, "The significance of mitochondrial toxicity testing in drug development", *Drug discovery today*, vol. 12, no. 17-18, pp. 777-785.

Ekstrand, M.I., Falkenberg, M., Rantanen, A., Park, C.B., Gaspari, M., Hulthenby, K., Rustin, P., Gustafsson, C.M. & Larsson, N.G. 2004, "Mitochondrial transcription factor A regulates mtDNA copy number in mammals", *Human molecular genetics*, vol. 13, no. 9, pp. 935-944.

Elmore, S. 2007, "Apoptosis: a review of programmed cell death", *Toxicologic pathology*, vol. 35, no. 4, pp. 495-516.

Faustin, B., Rossignol, R., Rocher, C., Benard, G., Malgat, M. & Letellier, T. 2004, "Mobilization of adenine nucleotide translocators as molecular bases of the biochemical threshold effect observed in mitochondrial diseases", *The Journal of biological chemistry*, vol. 279, no. 19, pp. 20411-20421.

Fernandez-Vizarra, E., Tiranti, V. & Zeviani, M. 2009, "Assembly of the oxidative phosphorylation system in humans: what we have learned by studying its defects", *Biochimica et biophysica acta*, vol. 1793, no. 1, pp. 200-211.

Fink, S.L. & Cookson, B.T. 2005, "Apoptosis, pyroptosis, and necrosis: mechanistic description of dead and dying eukaryotic cells", *Infection and immunity*, vol. 73, no. 4, pp. 1907-1916.

- Fliss, H. & Gattinger, D. 1996, "Apoptosis in ischemic and reperfused rat myocardium", *Circulation research*, vol. 79, no. 5, pp. 949-956.
- Floreani, M. & Carpenedo, F. 1991, "Modifications of cardiac contractility by redox cycling alkylating and mixed redox cycling/alkylating quinones", *The Journal of pharmacology and experimental therapeutics*, vol. 256, no. 1, pp. 243-248.
- Force, T. & Kerkela, R. 2008, "Cardiotoxicity of the new cancer therapeutics--mechanisms of, and approaches to, the problem", *Drug discovery today*, vol. 13, no. 17-18, pp. 778-784.
- Fornari, F.A., Randolph, J.K., Yalowich, J.C., Ritke, M.K. & Gewirtz, D.A. 1994, "Interference by doxorubicin with DNA unwinding in MCF-7 breast tumor cells", *Molecular pharmacology*, vol. 45, no. 4, pp. 649-656.
- Forrest, G.L., Gonzalez, B., Tseng, W., Li, X. & Mann, J. 2000, "Human carbonyl reductase overexpression in the heart advances the development of doxorubicin-induced cardiotoxicity in transgenic mice", *Cancer research*, vol. 60, no. 18, pp. 5158-5164.
- Frederick, R.L. & Shaw, J.M. 2007, "Moving mitochondria: establishing distribution of an essential organelle", *Traffic (Copenhagen, Denmark)*, vol. 8, no. 12, pp. 1668-1675.
- Gant, T.W., Rao, D.N., Mason, R.P. & Cohen, G.M. 1988, "Redox cycling and sulphhydryl arylation; their relative importance in the mechanism of quinone cytotoxicity to isolated hepatocytes", *Chemico-biological interactions*, vol. 65, no. 2, pp. 157-173.
- Gant, T.W., Zhang, S.D. & Taylor, E.L. 2009, "Novel genomic methods for drug discovery and mechanism-based toxicological assessment", *Current opinion in drug discovery & development*, vol. 12, no. 1, pp. 72-80.
- Gellerich, F.N., Mayr, J.A., Reuter, S., Sperl, W. & Zierz, S. 2004, "The problem of interlab variation in methods for mitochondrial disease diagnosis: enzymatic measurement of respiratory chain complexes", *Mitochondrion*, vol. 4, no. 5-6, pp. 427-439.
- Gerszten, R.E. & Wang, T.J. 2008, "The search for new cardiovascular biomarkers", *Nature*, vol. 451, no. 7181, pp. 949-952.
- Glinka, Y., Tipton, K.F. & Youdim, M.B. 1998, "Mechanism of inhibition of mitochondrial respiratory complex I by 6-hydroxydopamine and its prevention by desferrioxamine", *European journal of pharmacology*, vol. 351, no. 1, pp. 121-129.
- Glinka, Y., Tipton, K.F. & Youdim, M.B. 1996, "Nature of inhibition of mitochondrial respiratory complex I by 6-Hydroxydopamine", *Journal of neurochemistry*, vol. 66, no. 5, pp. 2004-2010.
- Goormaghtigh, E., Huart, P., Brasseur, R. & Ruysschaert, J.M. 1986, "Mechanism of inhibition of mitochondrial enzymatic complex I-III by adriamycin derivatives", *Biochimica et biophysica acta*, vol. 861, no. 1, pp. 83-94.
- Goormaghtigh, E., Huart, P., Praet, M., Brasseur, R. & Ruysschaert, J.M. 1990, "Structure of the adriamycin-cardiolipin complex. Role in mitochondrial toxicity", *Biophysical chemistry*, vol. 35, no. 2-3, pp. 247-257.
- Gordaliza, M., Castro, M.A., del Corral, J.M. & Feliciano, A.S. 2000, "Antitumor properties of podophyllotoxin and related compounds", *Current pharmaceutical design*, vol. 6, no. 18, pp. 1811-1839.

- Gottlieb, R.A., Bureson, K.O., Kloner, R.A., Babior, B.M. & Engler, R.L. 1994, "Reperfusion injury induces apoptosis in rabbit cardiomyocytes", *The Journal of clinical investigation*, vol. 94, no. 4, pp. 1621-1628.
- Gourlay, C.W. & Ayscough, K.R. 2005, "The actin cytoskeleton in ageing and apoptosis", *FEMS yeast research*, vol. 5, no. 12, pp. 1193-1198.
- Gustafsson, A.B. & Gottlieb, R.A. 2008, "Heart mitochondria: gates of life and death", *Cardiovascular research*, vol. 77, no. 2, pp. 334-343.
- Gutierrez, P.L. 2000, "The role of NAD(P)H oxidoreductase (DT-Diaphorase) in the bioactivation of quinone-containing antitumor agents: a review", *Free radical biology & medicine*, vol. 29, no. 3-4, pp. 263-275.
- Guzy, R.D. & Schumacker, P.T. 2006, "Oxygen sensing by mitochondria at complex III: the paradox of increased reactive oxygen species during hypoxia", *Experimental physiology*, vol. 91, no. 5, pp. 807-819.
- Halestrap, A.P., Doran, E., Gillespie, J.P. & O'Toole, A. 2000, "Mitochondria and cell death", *Biochemical Society transactions*, vol. 28, no. 2, pp. 170-177.
- Hamilton, B.F., Stokes, A.H., Lyon, J. & Adler, R.R. 2008, "In vivo assessment of mitochondrial toxicity", *Drug discovery today*, vol. 13, no. 17-18, pp. 785-790.
- Hayashi, T., Arimura, T., Itoh-Satoh, M., Ueda, K., Hohda, S., Inagaki, N., Takahashi, M., Hori, H., Yasunami, M., Nishi, H., Koga, Y., Nakamura, H., Matsuzaki, M., Choi, B.Y., Bae, S.W., You, C.W., Han, K.H., Park, J.E., Knoll, R., Hoshijima, M., Chien, K.R. & Kimura, A. 2004, "Tcap gene mutations in hypertrophic cardiomyopathy and dilated cardiomyopathy", *Journal of the American College of Cardiology*, vol. 44, no. 11, pp. 2192-2201.
- He, L., He, X., Lowe, S.W. & Hannon, G.J. 2007, "microRNAs join the p53 network--another piece in the tumour-suppression puzzle", *Nature reviews.Cancer*, vol. 7, no. 11, pp. 819-822.
- Henry, T.R. & Wallace, K.B. 1995, "Differential mechanisms of induction of the mitochondrial permeability transition by quinones of varying chemical reactivities", *Toxicology and applied pharmacology*, vol. 134, no. 2, pp. 195-203.
- Hensley, M.L., Schuchter, L.M., Lindley, C., Meropol, N.J., Cohen, G.I., Broder, G., Gradishar, W.J., Green, D.M., Langdon, R.J., Jr, Mitchell, R.B., Negrin, R., Szatrowski, T.P., Thigpen, J.T., Von Hoff, D., Wasserman, T.H., Winer, E.P. & Pfister, D.G. 1999, "American Society of Clinical Oncology clinical practice guidelines for the use of chemotherapy and radiotherapy protectants", *Journal of clinical oncology : official journal of the American Society of Clinical Oncology*, vol. 17, no. 10, pp. 3333-3355.
- Heon, S., Bernier, M., Servant, N., Dostanic, S., Wang, C., Kirby, G.M., Alpert, L. & Chalifour, L.E. 2003, "Dexrazoxane does not protect against doxorubicin-induced damage in young rats", *American journal of physiology.Heart and circulatory physiology*, vol. 285, no. 2, pp. H499-506.
- Hirabayashi, N., Nishiyama, M., Niimi, K., Yamaguchi, M., Toge, T., Niimoto, M. & Hattori, T. 1987, "Effect of oxygen tension on the antitumor activity of mitomycin C assayed by human tumor clonogenic assay", *The Japanese journal of surgery*, vol. 17, no. 5, pp. 402-406.
- Hiraumi, Y., Iwai-Kanai, E., Baba, S., Yui, Y., Kamitsuji, Y., Mizushima, Y., Matsubara, H., Watanabe, M., Watanabe, K., Toyokuni, S., Matsubara, H., Nakahata, T. & Adachi, S. 2009, "Granulocyte colony-stimulating factor protects cardiac mitochondria in the early phase of cardiac injury", *American journal of physiology.Heart and circulatory physiology*, vol. 296, no. 3, pp. H823-32.

- Hodnett, E.M., Wongwiechintana, C., Dunn, W.J., 3rd & Marrs, P. 1983, "Substituted 1,4-naphthoquinones vs. the ascitic sarcoma 180 of mice", *Journal of medicinal chemistry*, vol. 26, no. 4, pp. 570-574.
- Hom, J. & Sheu, S.S. 2009, "Morphological dynamics of mitochondria--a special emphasis on cardiac muscle cells", *Journal of Molecular and Cellular Cardiology*, vol. 46, no. 6, pp. 811-820.
- Horan, P.G., McMullin, M.F. & McKeown, P.P. 2006, "Anthracycline cardiotoxicity", *European heart journal*, vol. 27, no. 10, pp. 1137-1138.
- Huart, P., Brasseur, R., Goormaghtigh, E. & Ruysschaert, J.M. 1984, "Antimitotics induce cardiolipin cluster formation. Possible role in mitochondrial enzyme inactivation", *Biochimica et biophysica acta*, vol. 799, no. 2, pp. 199-202.
- Hudson, G., Carelli, V., Spruijt, L., Gerards, M., Mowbray, C., Achilli, A., Pyle, A., Elson, J., Howell, N., La Morgia, C., Valentino, M.L., Huoponen, K., Savontaus, M.L., Nikoskelainen, E., Sadun, A.A., Salomao, S.R., Belfort, R., Jr, Griffiths, P., Man, P.Y., de Coo, R.F., Horvath, R., Zeviani, M., Smeets, H.J., Torroni, A. & Chinnery, P.F. 2007, "Clinical expression of Leber hereditary optic neuropathy is affected by the mitochondrial DNA-haplogroup background", *American Journal of Human Genetics*, vol. 81, no. 2, pp. 228-233.
- Humphries, A.D., Streimann, I.C., Stojanovski, D., Johnston, A.J., Yano, M., Hoogenraad, N.J. & Ryan, M.T. 2005, "Dissection of the mitochondrial import and assembly pathway for human Tom40", *The Journal of biological chemistry*, vol. 280, no. 12, pp. 11535-11543.
- Huss, J.M. & Kelly, D.P. 2005, "Mitochondrial energy metabolism in heart failure: a question of balance", *The Journal of clinical investigation*, vol. 115, no. 3, pp. 547-555.
- Iguchi, N., Tobias, J.W. & Hecht, N.B. 2006, "Expression profiling reveals meiotic male germ cell mRNAs that are translationally up- and down-regulated", *Proceedings of the National Academy of Sciences of the United States of America*, vol. 103, no. 20, pp. 7712-7717.
- Ino, M., Yoshinaga, T., Wakamori, M., Miyamoto, N., Takahashi, E., Sonoda, J., Kagaya, T., Oki, T., Nagasu, T., Nishizawa, Y., Tanaka, I., Imoto, K., Aizawa, S., Koch, S., Schwartz, A., Niidome, T., Sawada, K. & Mori, Y. 2001, "Functional disorders of the sympathetic nervous system in mice lacking the alpha 1B subunit (Cav 2.2) of N-type calcium channels", *Proceedings of the National Academy of Sciences of the United States of America*, vol. 98, no. 9, pp. 5323-5328.
- Ishigami, T., Uzawa, K., Higo, M., Nomura, H., Saito, K., Kato, Y., Nakashima, D., Shiiba, M., Bukawa, H., Yokoe, H., Kawata, T., Ito, H. & Tanzawa, H. 2007, "Genes and molecular pathways related to radioresistance of oral squamous cell carcinoma cells", *International journal of cancer. Journal international du cancer*, vol. 120, no. 10, pp. 2262-2270.
- Ishihara, Y., Shiba, D. & Shimamoto, N. 2006, "Enhancement of DMNQ-induced hepatocyte toxicity by cytochrome P450 inhibition", *Toxicology and applied pharmacology*, vol. 214, no. 2, pp. 109-117.
- Jason, T.L., Koropatnick, J. & Berg, R.W. 2004, "Toxicology of antisense therapeutics", *Toxicology and applied pharmacology*, vol. 201, no. 1, pp. 66-83.
- Jeyaseelan, R., Poizat, C., Wu, H.Y. & Kedes, L. 1997, "Molecular mechanisms of doxorubicin-induced cardiomyopathy. Selective suppression of Reiske iron-sulfur protein, ADP/ATP translocase, and phosphofructokinase genes is associated with ATP depletion in rat cardiomyocytes", *The Journal of biological chemistry*, vol. 272, no. 9, pp. 5828-5832.

- Kamburov, A., Wierling, C., Lehrach, H. & Herwig, R. 2009, "ConsensusPathDB--a database for integrating human functional interaction networks", *Nucleic acids research*, vol. 37, no. Database issue, pp. D623-8.
- Kang, Y.J., Chen, Y. & Epstein, P.N. 1996, "Suppression of doxorubicin cardiotoxicity by overexpression of catalase in the heart of transgenic mice", *The Journal of biological chemistry*, vol. 271, no. 21, pp. 12610-12616.
- Kang, Y.J., Chen, Y., Yu, A., Voss-McCowan, M. & Epstein, P.N. 1997, "Overexpression of metallothionein in the heart of transgenic mice suppresses doxorubicin cardiotoxicity", *The Journal of clinical investigation*, vol. 100, no. 6, pp. 1501-1506.
- Kasap, S., Gonenc, A., Sener, D.E. & Hisar, I. 2007, "Serum cardiac markers in patients with acute myocardial infarction: oxidative stress, C-reactive protein and N-terminal probrain natriuretic Peptide", *Journal of clinical biochemistry and nutrition*, vol. 41, no. 1, pp. 50-57.
- Kawasaki, N., Lee, J.D., Shimizu, H., Ishii, Y. & Ueda, T. 1996, "Cardiac energy metabolism at several stages of adriamycin-induced heart failure in rats", *International journal of cardiology*, vol. 55, no. 3, pp. 217-225.
- Kaye, S., McKetin, R., Duflo, J. & Darke, S. 2007, "Methamphetamine and cardiovascular pathology: a review of the evidence", *Addiction (Abingdon, England)*, vol. 102, no. 8, pp. 1204-1211.
- Kelly, D.P. & Scarpulla, R.C. 2004, "Transcriptional regulatory circuits controlling mitochondrial biogenesis and function", *Genes & development*, vol. 18, no. 4, pp. 357-368.
- Kerr, J.F., Wyllie, A.H. & Currie, A.R. 1972, "Apoptosis: a basic biological phenomenon with wide-ranging implications in tissue kinetics", *British journal of cancer*, vol. 26, no. 4, pp. 239-257.
- Kim, V.N. & Nam, J.W. 2006, "Genomics of microRNA", *Trends in genetics : TIG*, vol. 22, no. 3, pp. 165-173.
- Kim, Y., Ma, A.G., Kitta, K., Fitch, S.N., Ikeda, T., Ihara, Y., Simon, A.R., Evans, T. & Suzuki, Y.J. 2003, "Anthracycline-induced suppression of GATA-4 transcription factor: implication in the regulation of cardiac myocyte apoptosis", *Molecular pharmacology*, vol. 63, no. 2, pp. 368-377.
- King, T.E., Yong, F.C. & Takemori, S. 1967, "Studies on cytochrome oxidase. 3. Ligand reactions and Schiff base formation of heme a", *The Journal of biological chemistry*, vol. 242, no. 5, pp. 819-829.
- Kmita, H., Antos, N., Wojtkowska, M. & Hryniewiecka, L. 2004, "Processes underlying the upregulation of Tom proteins in *S. cerevisiae* mitochondria depleted of the VDAC channel", *Journal of Bioenergetics and Biomembranes*, vol. 36, no. 2, pp. 187-193.
- Kogan, N.M., Schlesinger, M., Peters, M., Marincheva, G., Beeri, R. & Mechoulam, R. 2007, "A cannabinoid anticancer quinone, HU-331, is more potent and less cardiotoxic than doxorubicin: a comparative in vivo study", *The Journal of pharmacology and experimental therapeutics*, vol. 322, no. 2, pp. 646-653.
- Kogan, N.M., Schlesinger, M., Priel, E., Rabinowitz, R., Berenshtein, E., Chevion, M. & Mechoulam, R. 2007, "HU-331, a novel cannabinoid-based anticancer topoisomerase II inhibitor", *Molecular cancer therapeutics*, vol. 6, no. 1, pp. 173-183.
- Kowaltowski, A.J., Castilho, R.F. & Vercesi, A.E. 2001, "Mitochondrial permeability transition and oxidative stress", *FEBS letters*, vol. 495, no. 1-2, pp. 12-15.

- Krek, A., Grun, D., Poy, M.N., Wolf, R., Rosenberg, L., Epstein, E.J., MacMenamin, P., da Piedade, I., Gunsalus, K.C., Stoffel, M. & Rajewsky, N. 2005, "Combinatorial microRNA target predictions", *Nature genetics*, vol. 37, no. 5, pp. 495-500.
- Kulshreshtha, R., Ferracin, M., Wojcik, S.E., Garzon, R., Alder, H., Agosto-Perez, F.J., Davuluri, R., Liu, C.G., Croce, C.M., Negrini, M., Calin, G.A. & Ivan, M. 2007, "A microRNA signature of hypoxia", *Molecular and cellular biology*, vol. 27, no. 5, pp. 1859-1867.
- Kurosaka, K., Takahashi, M., Watanabe, N. & Kobayashi, Y. 2003, "Silent cleanup of very early apoptotic cells by macrophages", *Journal of immunology (Baltimore, Md.: 1950)*, vol. 171, no. 9, pp. 4672-4679.
- Ladha, J.S., Tripathy, M.K. & Mitra, D. 2005, "Mitochondrial complex I activity is impaired during HIV-1-induced T-cell apoptosis", *Cell death and differentiation*, vol. 12, no. 11, pp. 1417-1428.
- Latronico, M.V., Catalucci, D. & Condorelli, G. 2008, "MicroRNA and cardiac pathologies", *Physiological genomics*, vol. 34, no. 3, pp. 239-242.
- Latronico, M.V. & Condorelli, G. 2009, "MicroRNAs and cardiac pathology", *Nature reviews.Cardiology*, vol. 6, no. 6, pp. 419-429.
- Latronico, M.V., Elia, L., Condorelli, G. & Catalucci, D. 2008, "Heart failure: targeting transcriptional and post-transcriptional control mechanisms of hypertrophy for treatment", *The international journal of biochemistry & cell biology*, vol. 40, no. 9, pp. 1643-1648.
- Law, R.H., Manon, S., Devenish, R.J. & Nagley, P. 1995, "ATP synthase from *Saccharomyces cerevisiae*", *Methods in enzymology*, vol. 260, pp. 133-163.
- Lawrie, C.H., Gal, S., Dunlop, H.M., Pushkaran, B., Liggins, A.P., Pulford, K., Banham, A.H., Pezzella, F., Boultonwood, J., Waincoat, J.S., Hatton, C.S. & Harris, A.L. 2008, "Detection of elevated levels of tumour-associated microRNAs in serum of patients with diffuse large B-cell lymphoma", *British journal of haematology*, vol. 141, no. 5, pp. 672-675.
- Lebrecht, D., Geist, A., Ketelsen, U.P., Haberstroh, J., Setzer, B. & Walker, U.A. 2007, "Dexrazoxane prevents doxorubicin-induced long-term cardiotoxicity and protects myocardial mitochondria from genetic and functional lesions in rats", *British journal of pharmacology*, vol. 151, no. 6, pp. 771-778.
- Lebrecht, D., Setzer, B., Ketelsen, U.P., Haberstroh, J. & Walker, U.A. 2003, "Time-dependent and tissue-specific accumulation of mtDNA and respiratory chain defects in chronic doxorubicin cardiomyopathy", *Circulation*, vol. 108, no. 19, pp. 2423-2429.
- L'Ecuyer, T., Sanjeev, S., Thomas, R., Novak, R., Das, L., Campbell, W. & Heide, R.V. 2006, "DNA damage is an early event in doxorubicin-induced cardiac myocyte death", *American journal of physiology.Heart and circulatory physiology*, vol. 291, no. 3, pp. H1273-80.
- LeMoine, C.M., McClelland, G.B., Lyons, C.N., Mathieu-Costello, O. & Moyes, C.D. 2006, "Control of mitochondrial gene expression in the aging rat myocardium", *Biochemistry and cell biology = Biochimie et biologie cellulaire*, vol. 84, no. 2, pp. 191-198.
- Li, Q.J., Chau, J., Ebert, P.J., Sylvester, G., Min, H., Liu, G., Braich, R., Manoharan, M., Soutschek, J., Skare, P., Klein, L.O., Davis, M.M. & Chen, C.Z. 2007, "miR-181a is an intrinsic modulator of T cell sensitivity and selection", *Cell*, vol. 129, no. 1, pp. 147-161.
- Liang, H. & Ward, W.F. 2006, "PGC-1alpha: a key regulator of energy metabolism", *Advances in Physiology Education*, vol. 30, no. 4, pp. 145-151.

Lim, S.Y., Davidson, S.M., Hausenloy, D.J. & Yellon, D.M. 2007, "Preconditioning and postconditioning: the essential role of the mitochondrial permeability transition pore", *Cardiovascular research*, vol. 75, no. 3, pp. 530-535.

Lipshultz, S.E., Giantris, A.L., Lipsitz, S.R., Kimball Dalton, V., Asselin, B.L., Barr, R.D., Clavell, L.A., Hurwitz, C.A., Moghrabi, A., Samson, Y., Schorin, M.A., Gelber, R.D., Sallan, S.E. & Colan, S.D. 2002, "Doxorubicin administration by continuous infusion is not cardioprotective: the Dana-Farber 91-01 Acute Lymphoblastic Leukemia protocol", *Journal of clinical oncology : official journal of the American Society of Clinical Oncology*, vol. 20, no. 6, pp. 1677-1682.

Lipshultz, S.E., Rifai, N., Dalton, V.M., Levy, D.E., Silverman, L.B., Lipsitz, S.R., Colan, S.D., Asselin, B.L., Barr, R.D., Clavell, L.A., Hurwitz, C.A., Moghrabi, A., Samson, Y., Schorin, M.A., Gelber, R.D. & Sallan, S.E. 2004, "The effect of dexrazoxane on myocardial injury in doxorubicin-treated children with acute lymphoblastic leukemia", *The New England journal of medicine*, vol. 351, no. 2, pp. 145-153.

Liu, Z., Sall, A. & Yang, D. 2008, "MicroRNA: an Emerging Therapeutic Target and Intervention Tool", *International journal of molecular sciences*, vol. 9, no. 6, pp. 978-999.

Lodes, M.J., Caraballo, M., Suci, D., Munro, S., Kumar, A. & Anderson, B. 2009, "Detection of cancer with serum miRNAs on an oligonucleotide microarray", *PloS one*, vol. 4, no. 7, pp. e6229.

Long, D.J., 2nd & Jaiswal, A.K. 2000, "NRH:quinone oxidoreductase2 (NQO2)", *Chemico-biological interactions*, vol. 129, no. 1-2, pp. 99-112.

Lopez, M., Vici, P., Di Lauro, K., Conti, F., Paoletti, G., Ferraironi, A., Sciuto, R., Giannarelli, D. & Maini, C.L. 1998, "Randomized prospective clinical trial of high-dose epirubicin and dexrazoxane in patients with advanced breast cancer and soft tissue sarcomas", *Journal of clinical oncology : official journal of the American Society of Clinical Oncology*, vol. 16, no. 1, pp. 86-92.

Lu, J., Getz, G., Miska, E.A., Alvarez-Saavedra, E., Lamb, J., Peck, D., Sweet-Cordero, A., Ebert, B.L., Mak, R.H., Ferrando, A.A., Downing, J.R., Jacks, T., Horvitz, H.R. & Golub, T.R. 2005, "MicroRNA expression profiles classify human cancers", *Nature*, vol. 435, no. 7043, pp. 834-838.

Lu, X., de la Pena, L., Barker, C., Camphausen, K. & Tofilon, P.J. 2006, "Radiation-induced changes in gene expression involve recruitment of existing messenger RNAs to and away from polysomes", *Cancer research*, vol. 66, no. 2, pp. 1052-1061.

Lukiw, W.J. 2007, "Micro-RNA speciation in fetal, adult and Alzheimer's disease hippocampus", *Neuroreport*, vol. 18, no. 3, pp. 297-300.

Luo, C., Long, J. & Liu, J. 2008, "An improved spectrophotometric method for a more specific and accurate assay of mitochondrial complex III activity", *Clinica chimica acta; international journal of clinical chemistry*, vol. 395, no. 1-2, pp. 38-41.

Maeno, Y., Iwasa, M., Inoue, H., Koyama, H. & Matoba, R. 2000, "Methamphetamine induces an increase in cell size and reorganization of myofibrils in cultured adult rat cardiomyocytes", *International journal of legal medicine*, vol. 113, no. 4, pp. 201-207.

Malakhova, L., Bezlepkin, V.G., Antipova, V., Ushakova, T., Fomenko, L., Sirota, N. & Gaziev, A.I. 2005, "The increase in mitochondrial DNA copy number in the tissues of gamma-irradiated mice", *Cellular & Molecular Biology Letters*, vol. 10, no. 4, pp. 721-732.

Malone, C.D., Brennecke, J., Dus, M., Stark, A., McCombie, W.R., Sachidanandam, R. & Hannon, G.J. 2009, "Specialized piRNA pathways act in germline and somatic tissues of the Drosophila ovary", *Cell*, vol. 137, no. 3, pp. 522-535.

- Mamane, Y., Petroulakis, E., LeBacquer, O. & Sonenberg, N. 2006, "mTOR, translation initiation and cancer", *Oncogene*, vol. 25, no. 48, pp. 6416-6422.
- Marian, A.J. & Nambi, V. 2004, "Biomarkers of cardiac disease", *Expert review of molecular diagnostics*, vol. 4, no. 6, pp. 805-820.
- Markert, C.D., Ning, J., Staley, J.T., Heinzke, L., Childers, C.K., Ferreira, J.A., Brown, M., Stoker, A., Okamura, C. & Childers, M.K. 2008, "TCAP knockdown by RNA interference inhibits myoblast differentiation in cultured skeletal muscle cells", *Neuromuscular disorders : NMD*, vol. 18, no. 5, pp. 413-422.
- Marks, A.R. 2003, "Calcium and the heart: a question of life and death", *The Journal of clinical investigation*, vol. 111, no. 5, pp. 597-600.
- Marnett, L.J. 1999, "Lipid peroxidation-DNA damage by malondialdehyde", *Mutation research*, vol. 424, no. 1-2, pp. 83-95.
- Matkovich, S.J., Van Booven, D.J., Youker, K.A., Torre-Amione, G., Diwan, A., Eschenbacher, W.H., Dorn, L.E., Watson, M.A., Margulies, K.B. & Dorn, G.W., 2nd 2009, "Reciprocal regulation of myocardial microRNAs and messenger RNA in human cardiomyopathy and reversal of the microRNA signature by biomechanical support", *Circulation*, vol. 119, no. 9, pp. 1263-1271.
- Matsson, H., Eason, J., Bookwalter, C.S., Klar, J., Gustavsson, P., Sunnegardh, J., Enell, H., Jonzon, A., Vikkula, M., Gutierrez, I., Granados-Riveron, J., Pope, M., Bu'Lock, F., Cox, J., Robinson, T.E., Song, F., Brook, D.J., Marston, S., Trybus, K.M. & Dahl, N. 2008, "Alpha-cardiac actin mutations produce atrial septal defects", *Human molecular genetics*, vol. 17, no. 2, pp. 256-265.
- McClintock, D.S., Santore, M.T., Lee, V.Y., Brunelle, J., Budinger, G.R., Zong, W.X., Thompson, C.B., Hay, N. & Chandel, N.S. 2002, "Bcl-2 family members and functional electron transport chain regulate oxygen deprivation-induced cell death", *Molecular and cellular biology*, vol. 22, no. 1, pp. 94-104.
- Meder, B., Katus, H.A. & Rottbauer, W. 2008, "Right into the heart of microRNA-133a", *Genes & development*, vol. 22, no. 23, pp. 3227-3231.
- Meirhaeghe, A., Crowley, V., Lenaghan, C., Lelliott, C., Green, K., Stewart, A., Hart, K., Schinner, S., Sethi, J.K., Yeo, G., Brand, M.D., Cortright, R.N., O'Rahilly, S., Montague, C. & Vidal-Puig, A.J. 2003, "Characterization of the human, mouse and rat PGC1 beta (peroxisome-proliferator-activated receptor-gamma co-activator 1 beta) gene in vitro and in vivo", *The Biochemical journal*, vol. 373, no. Pt 1, pp. 155-165.
- Meister, G. 2007, "miRNAs get an early start on translational silencing", *Cell*, vol. 131, no. 1, pp. 25-28.
- Melamed, D. & Arava, Y. 2007, "Genome-wide analysis of mRNA polysomal profiles with spotted DNA microarrays", *Methods in enzymology*, vol. 431, pp. 177-201.
- Menna, P., Salvatorelli, E. & Minotti, G. 2007, "Doxorubicin degradation in cardiomyocytes", *The Journal of pharmacology and experimental therapeutics*, vol. 322, no. 1, pp. 408-419.
- Meyer, D. & Birchmeier, C. 1995, "Multiple essential functions of neuregulin in development", *Nature*, vol. 378, no. 6555, pp. 386-390.
- Milagros Rocha, M. & Victor, V.M. 2007, "Targeting antioxidants to mitochondria and cardiovascular diseases: the effects of mitoquinone", *Medical science monitor : international medical journal of experimental and clinical research*, vol. 13, no. 7, pp. RA132-45.

- Miller, M.G., Rodgers, A. & Cohen, G.M. 1986, "Mechanisms of toxicity of naphthoquinones to isolated hepatocytes", *Biochemical pharmacology*, vol. 35, no. 7, pp. 1177-1184.
- Minotti, G., Cairo, G. & Monti, E. 1999, "Role of iron in anthracycline cardiotoxicity: new tunes for an old song?", *The FASEB journal : official publication of the Federation of American Societies for Experimental Biology*, vol. 13, no. 2, pp. 199-212.
- Minotti, G., Menna, P., Salvatorelli, E., Cairo, G. & Gianni, L. 2004, "Anthracyclines: molecular advances and pharmacologic developments in antitumor activity and cardiotoxicity", *Pharmacological reviews*, vol. 56, no. 2, pp. 185-229.
- Mishra, P.K., Tyagi, N., Kumar, M. & Tyagi, S.C. 2009, "MicroRNAs as a therapeutic target for cardiovascular diseases", *Journal of Cellular and Molecular Medicine*, vol. 13, no. 4, pp. 778-789.
- Miskon, A., Ehashi, T., Mahara, A., Uyama, H. & Yamaoka, T. 2009, "Beating behavior of primary neonatal cardiomyocytes and cardiac-differentiated P19.CL6 cells on different extracellular matrix components", *Journal of artificial organs : the official journal of the Japanese Society for Artificial Organs*, vol. 12, no. 2, pp. 111-117.
- Mitchell, P.S., Parkin, R.K., Kroh, E.M., Fritz, B.R., Wyman, S.K., Pogosova-Agadjanyan, E.L., Peterson, A., Noteboom, J., O'Briant, K.C., Allen, A., Lin, D.W., Urban, N., Drescher, C.W., Knudsen, B.S., Stirewalt, D.L., Gentleman, R., Vessella, R.L., Nelson, P.S., Martin, D.B. & Tewari, M. 2008, "Circulating microRNAs as stable blood-based markers for cancer detection", *Proceedings of the National Academy of Sciences of the United States of America*, vol. 105, no. 30, pp. 10513-10518.
- Molitor, H. & Robinson, H. 1940, "Oral and parental toxicity of vitamin K1, phthiocol and 2-methyl-1, 4, naphthoquinone", *Proceedings-society for experimental biology and medicine*, vol. 43, pp. 125-128.
- Molkentin, J.D. & Robbins, J. 2009, "With great power comes great responsibility: using mouse genetics to study cardiac hypertrophy and failure", *Journal of Molecular and Cellular Cardiology*, vol. 46, no. 2, pp. 130-136.
- Monks, T.J. & Jones, D.C. 2002, "The metabolism and toxicity of quinones, quinonimines, quinone methides, and quinone-thioethers", *Current Drug Metabolism*, vol. 3, no. 4, pp. 425-438.
- Mudd, J.O. & Kass, D.A. 2008, "Tackling heart failure in the twenty-first century", *Nature*, vol. 451, no. 7181, pp. 919-928.
- Munday, R. 2001, "Concerted action of DT-diaphorase and superoxide dismutase in preventing redox cycling of naphthoquinones: an evaluation", *Free radical research*, vol. 35, no. 2, pp. 145-158.
- Muravchick, S. & Levy, R.J. 2006, "Clinical implications of mitochondrial dysfunction", *Anesthesiology*, vol. 105, no. 4, pp. 819-837.
- Murchison, E.P. & Hannon, G.J. 2004, "miRNAs on the move: miRNA biogenesis and the RNAi machinery", *Current opinion in cell biology*, vol. 16, no. 3, pp. 223-229.
- Muslin, A.J. 2008, "MAPK signalling in cardiovascular health and disease: molecular mechanisms and therapeutic targets", *Clinical science (London, England : 1979)*, vol. 115, no. 7, pp. 203-218.
- Naguibneva, I., Ameyar-Zazoua, M., Polesskaya, A., Ait-Si-Ali, S., Groisman, R., Souidi, M., Cuvellier, S. & Harel-Bellan, A. 2006, "The microRNA miR-181 targets the homeobox protein Hox-A11 during mammalian myoblast differentiation", *Nature cell biology*, vol. 8, no. 3, pp. 278-284.

Naraoka, H., Ito, K., Suzuki, M., Naito, K. & Tojo, H. 2005, "Evaluation of H-FABP as a marker of ongoing myocardial damage using hGH transgenic mice", *Clinica chimica acta; international journal of clinical chemistry*, vol. 361, no. 1-2, pp. 159-166.

Ning, X.H., Zhang, J., Liu, J., Ye, Y., Chen, S.H., From, A.H., Bache, R.J. & Portman, M.A. 2000, "Signaling and expression for mitochondrial membrane proteins during left ventricular remodeling and contractile failure after myocardial infarction", *Journal of the American College of Cardiology*, vol. 36, no. 1, pp. 282-287.

Nowak, G., Clifton, G.L. & Bakajsova, D. 2008, "Succinate ameliorates energy deficits and prevents dysfunction of complex I in injured renal proximal tubular cells", *The Journal of pharmacology and experimental therapeutics*, vol. 324, no. 3, pp. 1155-1162.

O'Brien, P.J. 2008, "Cardiac troponin is the most effective translational safety biomarker for myocardial injury in cardiotoxicity", *Toxicology*, vol. 245, no. 3, pp. 206-218.

O'Brien, P.J. 1991, "Molecular mechanisms of quinone cytotoxicity", *Chemico-biological interactions*, vol. 80, no. 1, pp. 1-41.

O'Brien, P.J., Dameron, G.W., Beck, M.L., Kang, Y.J., Erickson, B.K., Di Battista, T.H., Miller, K.E., Jackson, K.N. & Mittelstadt, S. 1997, "Cardiac troponin T is a sensitive, specific biomarker of cardiac injury in laboratory animals", *Laboratory animal science*, vol. 47, no. 5, pp. 486-495.

Oliveira, P.J., Bjork, J.A., Santos, M.S., Leino, R.L., Froberg, M.K., Moreno, A.J. & Wallace, K.B. 2004, "Carvedilol-mediated antioxidant protection against doxorubicin-induced cardiac mitochondrial toxicity", *Toxicology and applied pharmacology*, vol. 200, no. 2, pp. 159-168.

Oliveira, P.J. & Wallace, K.B. 2006, "Depletion of adenine nucleotide translocator protein in heart mitochondria from doxorubicin-treated rats--relevance for mitochondrial dysfunction", *Toxicology*, vol. 220, no. 2-3, pp. 160-168.

Olson, R.D., Mushlin, P.S., Brenner, D.E., Fleischer, S., Cusack, B.J., Chang, B.K. & Boucek, R.J., Jr 1988, "Doxorubicin cardiotoxicity may be caused by its metabolite, doxorubicinol", *Proceedings of the National Academy of Sciences of the United States of America*, vol. 85, no. 10, pp. 3585-3589.

Outomuro, D., Grana, D.R., Azzato, F. & Milei, J. 2007, "Adriamycin-induced myocardial toxicity: new solutions for an old problem?", *International journal of cardiology*, vol. 117, no. 1, pp. 6-15.

Ozcelik, C., Erdmann, B., Pilz, B., Wettschureck, N., Britsch, S., Hubner, N., Chien, K.R., Birchmeier, C. & Garratt, A.N. 2002, "Conditional mutation of the ErbB2 (HER2) receptor in cardiomyocytes leads to dilated cardiomyopathy", *Proceedings of the National Academy of Sciences of the United States of America*, vol. 99, no. 13, pp. 8880-8885.

Pacher, P., Liaudet, L., Bai, P., Mabley, J.G., Kaminski, P.M., Virag, L., Deb, A., Szabo, E., Ungvari, Z., Wolin, M.S., Groves, J.T. & Szabo, C. 2003, "Potent metalloporphyrin peroxynitrite decomposition catalyst protects against the development of doxorubicin-induced cardiac dysfunction", *Circulation*, vol. 107, no. 1, pp. 896-904.

Pajic, A., Spitkovsky, D., Christoph, B., Kempkes, B., Schuhmacher, M., Staeger, M.S., Brielmeier, M., Ellwart, J., Kohlhuber, F., Bornkamm, G.W., Polack, A. & Eick, D. 2000, "Cell cycle activation by c-myc in a burkitt lymphoma model cell line", *International journal of cancer. Journal international du cancer*, vol. 87, no. 6, pp. 787-793.

- Palmeira, C.M., Rolo, A.P., Berthiaume, J., Bjork, J.A. & Wallace, K.B. 2007, "Hyperglycemia decreases mitochondrial function: the regulatory role of mitochondrial biogenesis", *Toxicology and applied pharmacology*, vol. 225, no. 2, pp. 214-220.
- Palmieri, F. 2004, "The mitochondrial transporter family (SLC25): physiological and pathological implications", *Pflugers Archiv : European journal of physiology*, vol. 447, no. 5, pp. 689-709.
- Pan, C.J., Schmitz, D.A., Cho, A.K., Froines, J. & Fukuto, J.M. 2004, "Inherent redox properties of diesel exhaust particles: catalysis of the generation of reactive oxygen species by biological reductants", *Toxicological sciences : an official journal of the Society of Toxicology*, vol. 81, no. 1, pp. 225-232.
- Panov, A., Dikalov, S., Shalbuyeva, N., Taylor, G., Sherer, T. & Greenamyre, J.T. 2005, "Rotenone model of Parkinson disease: multiple brain mitochondria dysfunctions after short term systemic rotenone intoxication", *The Journal of biological chemistry*, vol. 280, no. 51, pp. 42026-42035.
- Paradies, G., Petrosillo, G., Pistolese, M., Di Venosa, N., Federici, A. & Ruggiero, F.M. 2004, "Decrease in mitochondrial complex I activity in ischemic/reperfused rat heart: involvement of reactive oxygen species and cardiolipin", *Circulation research*, vol. 94, no. 1, pp. 53-59.
- Park, S.Y., Lee, J.H., Ha, M., Nam, J.W. & Kim, V.N. 2009, "miR-29 miRNAs activate p53 by targeting p85 alpha and CDC42", *Nature structural & molecular biology*, vol. 16, no. 1, pp. 23-29.
- Parker, B.J. & Wen, J. 2009, "Predicting microRNA targets in time-series microarray experiments via functional data analysis", *BMC bioinformatics*, vol. 10 Suppl 1, pp. S32.
- Parry, J.D., Pointon, A.V., Lutz, U., Teichert, F., Charlwood, J.K., Chan, P.H., Athersuch, T.J., Taylor, E.L., Singh, R., Luo, J., Phillips, K.M., Vetillard, A., Lyon, J.J., Keun, H.C., Lutz, W.K. & Gant, T.W. 2009, "Pivotal role for two electron reduction in 2,3-dimethoxy-1,4-naphthoquinone and 2-methyl-1,4-naphthoquinone metabolism and kinetics in vivo that prevents liver redox stress", *Chemical research in toxicology*, vol. 22, no. 4, pp. 717-725.
- Perkins, D.O., Jeffries, C.D., Jarskog, L.F., Thomson, J.M., Woods, K., Newman, M.A., Parker, J.S., Jin, J. & Hammond, S.M. 2007, "microRNA expression in the prefrontal cortex of individuals with schizophrenia and schizoaffective disorder", *Genome biology*, vol. 8, no. 2, pp. R27.
- Petersen, C.P., Bordeleau, M.E., Pelletier, J. & Sharp, P.A. 2006, "Short RNAs repress translation after initiation in mammalian cells", *Molecular cell*, vol. 21, no. 4, pp. 533-542.
- Pickering, B.M. & Willis, A.E. 2005, "The implications of structured 5' untranslated regions on translation and disease", *Seminars in cell & developmental biology*, vol. 16, no. 1, pp. 39-47.
- Pickering, M.T., Stadler, B.M. & Kowalik, T.F. 2009, "miR-17 and miR-20a temper an E2F1-induced G1 checkpoint to regulate cell cycle progression", *Oncogene*, vol. 28, no. 1, pp. 140-145.
- Pillai, R.S., Bhattacharyya, S.N. & Filipowicz, W. 2007, "Repression of protein synthesis by miRNAs: how many mechanisms?", *Trends in cell biology*, vol. 17, no. 3, pp. 118-126.
- Pogribny, I.P., Tryndyak, V.P., Boyko, A., Rodriguez-Juarez, R., Beland, F.A. & Kovalchuk, O. 2007, "Induction of microRNAome deregulation in rat liver by long-term tamoxifen exposure", *Mutation research*, vol. 619, no. 1-2, pp. 30-37.
- Popat, S. & Smith, I.E. 2008, "Therapy Insight: anthracyclines and trastuzumab--the optimal management of cardiotoxic side effects", *Nature clinical practice.Oncology*, vol. 5, no. 6, pp. 324-335.

- Powis, G. & Appel, P.L. 1980, "Relationship of the single-electron reduction potential of quinones to their reduction by flavoproteins", *Biochemical pharmacology*, vol. 29, no. 19, pp. 2567-2572.
- Provenzani, A., Fronza, R., Loreni, F., Pascale, A., Amadio, M. & Quattrone, A. 2006, "Global alterations in mRNA polysomal recruitment in a cell model of colorectal cancer progression to metastasis", *Carcinogenesis*, vol. 27, no. 7, pp. 1323-1333.
- Puigserver, P. & Spiegelman, B.M. 2003, "Peroxisome proliferator-activated receptor-gamma coactivator 1 alpha (PGC-1 alpha): transcriptional coactivator and metabolic regulator", *Endocrine reviews*, vol. 24, no. 1, pp. 78-90.
- Radjendirane, V., Joseph, P., Lee, Y.H., Kimura, S., Klein-Szanto, A.J., Gonzalez, F.J. & Jaiswal, A.K. 1998, "Disruption of the DT diaphorase (NQO1) gene in mice leads to increased menadione toxicity", *The Journal of biological chemistry*, vol. 273, no. 13, pp. 7382-7389.
- Ramachandran, V. & Chen, X. 2008, "Degradation of microRNAs by a family of exoribonucleases in Arabidopsis", *Science (New York, N.Y.)*, vol. 321, no. 5895, pp. 1490-1492.
- Rau, J. & Stolz, A. 2003, "Oxygen-insensitive nitroreductases NfsA and NfsB of Escherichia coli function under anaerobic conditions as lawsone-dependent Azo reductases", *Applied and Environmental Microbiology*, vol. 69, no. 6, pp. 3448-3455.
- Reeve, J.L., Szegezdi, E., Logue, S.E., Chonghaile, T.N., O'Brien, T., Ritter, T. & Samali, A. 2007, "Distinct mechanisms of cardiomyocyte apoptosis induced by doxorubicin and hypoxia converge on mitochondria and are inhibited by Bcl-xL", *Journal of Cellular and Molecular Medicine*, vol. 11, no. 3, pp. 509-520.
- Reymann, S. & Borlak, J. 2008, "Topoisomerase II inhibition involves characteristic chromosomal expression patterns", *BMC genomics*, vol. 9, pp. 324.
- Richter, J.D. & Sonenberg, N. 2005, "Regulation of cap-dependent translation by eIF4E inhibitory proteins", *Nature*, vol. 433, no. 7025, pp. 477-480.
- Ringner, M. 2008, "What is principal component analysis?", *Nature biotechnology*, vol. 26, no. 3, pp. 303-304.
- Robert, J. 2007, "Preclinical assessment of anthracycline cardiotoxicity in laboratory animals: predictiveness and pitfalls", *Cell biology and toxicology*, vol. 23, no. 1, pp. 27-37.
- Ross, D., Thor, H., Orrenius, S. & Moldeus, P. 1985, "Interaction of menadione (2-methyl-1,4-naphthoquinone) with glutathione", *Chemico-biological interactions*, vol. 55, no. 1-2, pp. 177-184.
- Rossi, L., Bonmassar, E. & Faraoni, I. 2007, "Modification of miR gene expression pattern in human colon cancer cells following exposure to 5-fluorouracil in vitro", *Pharmacological research : the official journal of the Italian Pharmacological Society*, vol. 56, no. 3, pp. 248-253.
- Rouault, T.A. 2006, "The role of iron regulatory proteins in mammalian iron homeostasis and disease", *Nature chemical biology*, vol. 2, no. 8, pp. 406-414.
- Rouault, T.A. 2001, "Iron on the brain", *Nature genetics*, vol. 28, no. 4, pp. 299-300.
- Roussel, D., Chainier, F., Rouanet, J. & Barre, H. 2000, "Increase in the adenine nucleotide translocase content of duckling subsarcolemmal mitochondria during cold acclimation", *FEBS letters*, vol. 477, no. 1-2, pp. 141-144.

- Russo, P., Arzani, D., Trombino, S. & Falugi, C. 2003, "c-myc down-regulation induces apoptosis in human cancer cell lines exposed to RPR-115135 (C31H29NO4), a non-peptidomimetic farnesyltransferase inhibitor", *The Journal of pharmacology and experimental therapeutics*, vol. 304, no. 1, pp. 37-47.
- Saraste, M. 1999, "Oxidative phosphorylation at the fin de siecle", *Science (New York, N.Y.)*, vol. 283, no. 5407, pp. 1488-1493.
- Sardao, V.A., Oliveira, P.J., Holy, J., Oliveira, C.R. & Wallace, K.B. 2009, "Morphological alterations induced by doxorubicin on H9c2 myoblasts: nuclear, mitochondrial, and cytoskeletal targets", *Cell biology and toxicology*, vol. 25, no. 3, pp. 227-243.
- Sathyan, P., Golden, H.B. & Miranda, R.C. 2007, "Competing interactions between micro-RNAs determine neural progenitor survival and proliferation after ethanol exposure: evidence from an ex vivo model of the fetal cerebral cortical neuroepithelium", *The Journal of neuroscience : the official journal of the Society for Neuroscience*, vol. 27, no. 32, pp. 8546-8557.
- Savill, J. & Fadok, V. 2000, "Corpse clearance defines the meaning of cell death", *Nature*, vol. 407, no. 6805, pp. 784-788.
- Savina, A., Furlan, M., Vidal, M. & Colombo, M.I. 2003, "Exosome release is regulated by a calcium-dependent mechanism in K562 cells", *The Journal of biological chemistry*, vol. 278, no. 22, pp. 20083-20090.
- Scalbert, E. & Bril, A. 2008, "Implication of microRNAs in the cardiovascular system", *Current opinion in pharmacology*, vol. 8, no. 2, pp. 181-188.
- Scarpulla, R.C. 2008, "Nuclear control of respiratory chain expression by nuclear respiratory factors and PGC-1-related coactivator", *Annals of the New York Academy of Sciences*, vol. 1147, pp. 321-334.
- Scarpulla, R.C. 2006, "Nuclear control of respiratory gene expression in mammalian cells", *Journal of cellular biochemistry*, vol. 97, no. 4, pp. 673-683.
- Scatena, R., Bottoni, P., Botta, G., Martorana, G.E. & Giardina, B. 2007, "The role of mitochondria in pharmacotoxicology: a reevaluation of an old, newly emerging topic", *American journal of physiology. Cell physiology*, vol. 293, no. 1, pp. C12-21.
- Schagger, H., de Coo, R., Bauer, M.F., Hofmann, S., Godinot, C. & Brandt, U. 2004, "Significance of respirasomes for the assembly/stability of human respiratory chain complex I", *The Journal of biological chemistry*, vol. 279, no. 35, pp. 36349-36353.
- Scortegagna, M., Ding, K., Oktay, Y., Gaur, A., Thurmond, F., Yan, L.J., Marck, B.T., Matsumoto, A.M., Shelton, J.M., Richardson, J.A., Bennett, M.J. & Garcia, J.A. 2003, "Multiple organ pathology, metabolic abnormalities and impaired homeostasis of reactive oxygen species in Epas1^{-/-} mice", *Nature genetics*, vol. 35, no. 4, pp. 331-340.
- Seidman, A., Hudis, C., Pierri, M.K., Shak, S., Paton, V., Ashby, M., Murphy, M., Stewart, S.J. & Keefe, D. 2002, "Cardiac dysfunction in the trastuzumab clinical trials experience", *Journal of clinical oncology : official journal of the American Society of Clinical Oncology*, vol. 20, no. 5, pp. 1215-1221.
- Selbach, M., Schwanhaussner, B., Thierfelder, N., Fang, Z., Khanin, R. & Rajewsky, N. 2008, "Widespread changes in protein synthesis induced by microRNAs", *Nature*, vol. 455, no. 7209, pp. 58-63.

- Shaw, J.M. & Nunnari, J. 2002, "Mitochondrial dynamics and division in budding yeast", *Trends in cell biology*, vol. 12, no. 4, pp. 178-184.
- Shen, L., Zhi, L., Hu, W. & Wu, M.X. 2009, "IEX-1 targets mitochondrial F1Fo-ATPase inhibitor for degradation", *Cell death and differentiation*, vol. 16, no. 4, pp. 603-612.
- Shen, M., Zhang, L., Bonner, M.R., Liu, C.S., Li, G., Vermeulen, R., Dosemeci, M., Yin, S. & Lan, Q. 2008, "Association between mitochondrial DNA copy number, blood cell counts, and occupational benzene exposure", *Environmental and molecular mutagenesis*, vol. 49, no. 6, pp. 453-457.
- Shivdasani, R.A. 2006, "MicroRNAs: regulators of gene expression and cell differentiation", *Blood*, vol. 108, no. 12, pp. 3646-3653.
- Sirvent, P., Mercier, J. & Lacampagne, A. 2008, "New insights into mechanisms of statin-associated myotoxicity", *Current opinion in pharmacology*, vol. 8, no. 3, pp. 333-338.
- Siu, P.M., Donley, D.A., Bryner, R.W. & Alway, S.E. 2003, "Citrate synthase expression and enzyme activity after endurance training in cardiac and skeletal muscles", *Journal of applied physiology (Bethesda, Md.: 1985)*, vol. 94, no. 2, pp. 555-560.
- Smith, M.T. 1985, "Quinones as mutagens, carcinogens, and anticancer agents: introduction and overview", *Journal of toxicology and environmental health*, vol. 16, no. 5, pp. 665-672.
- Sparagna, G.C. & Lesnefsky, E.J. 2009, "Cardiolipin remodeling in the heart", *Journal of cardiovascular pharmacology*, vol. 53, no. 4, pp. 290-301.
- Spence, J., Duggan, B.M., Eckhardt, C., McClelland, M. & Mercola, D. 2006, "Messenger RNAs under differential translational control in Ki-ras-transformed cells", *Molecular cancer research : MCR*, vol. 4, no. 1, pp. 47-60.
- Stanley, W.C. & Hoppel, C.L. 2000, "Mitochondrial dysfunction in heart failure: potential for therapeutic interventions?", *Cardiovascular research*, vol. 45, no. 4, pp. 805-806.
- Stanley, W.C., Lopaschuk, G.D., Hall, J.L. & McCormack, J.G. 1997, "Regulation of myocardial carbohydrate metabolism under normal and ischaemic conditions. Potential for pharmacological interventions", *Cardiovascular research*, vol. 33, no. 2, pp. 243-257.
- Stoneley, M. & Willis, A.E. 2004, "Cellular internal ribosome entry segments: structures, trans-acting factors and regulation of gene expression", *Oncogene*, vol. 23, no. 18, pp. 3200-3207.
- Sun, L., Shukair, S., Naik, T.J., Moazed, F. & Ardehali, H. 2008, "Glucose phosphorylation and mitochondrial binding are required for the protective effects of hexokinases I and II", *Molecular and cellular biology*, vol. 28, no. 3, pp. 1007-1017.
- Sun, X., Zhou, Z. & Kang, Y.J. 2001, "Attenuation of doxorubicin chronic toxicity in metallothionein-overexpressing transgenic mouse heart", *Cancer research*, vol. 61, no. 8, pp. 3382-3387.
- Swain, S.M., Whaley, F.S., Gerber, M.C., Ewer, M.S., Bianchine, J.R. & Gams, R.A. 1997, "Delayed administration of dexrazoxane provides cardioprotection for patients with advanced breast cancer treated with doxorubicin-containing therapy", *Journal of clinical oncology : official journal of the American Society of Clinical Oncology*, vol. 15, no. 4, pp. 1333-1340.

- Swift, L.P., Rephaeli, A., Nudelman, A., Phillips, D.R. & Cutts, S.M. 2006, "Doxorubicin-DNA adducts induce a non-topoisomerase II-mediated form of cell death", *Cancer research*, vol. 66, no. 9, pp. 4863-4871.
- Taft, R.J., Glazov, E.A., Cloonan, N., Simons, C., Stephen, S., Faulkner, G.J., Lassmann, T., Forrest, A.R., Grimmond, S.M., Schroder, K., Irvine, K., Arakawa, T., Nakamura, M., Kubosaki, A., Hayashida, K., Kawazu, C., Murata, M., Nishiyori, H., Fukuda, S., Kawai, J., Daub, C.O., Hume, D.A., Suzuki, H., Orlando, V., Carninci, P., Hayashizaki, Y. & Mattick, J.S. 2009, "Tiny RNAs associated with transcription start sites in animals", *Nature genetics*, vol. 41, no. 5, pp. 572-578.
- Takemura, G. & Fujiwara, H. 2007, "Doxorubicin-induced cardiomyopathy from the cardiotoxic mechanisms to management", *Progress in cardiovascular diseases*, vol. 49, no. 5, pp. 330-352.
- Takemura, G. & Fujiwara, H. 2004, "Role of apoptosis in remodeling after myocardial infarction", *Pharmacology & therapeutics*, vol. 104, no. 1, pp. 1-16.
- Tanaka, T., Tohyama, S., Murata, M., Nomura, F., Kaneko, T., Chen, H., Hattori, F., Egashira, T., Seki, T., Ohno, Y., Koshimizu, U., Yuasa, S., Ogawa, S., Yamanaka, S., Yasuda, K. & Fukuda, K. 2009, "In vitro pharmacologic testing using human induced pluripotent stem cell-derived cardiomyocytes", *Biochemical and biophysical research communications*, vol. 385, no. 4, pp. 497-502.
- Tarr, M. & van Helden, P.D. 1990, "Inhibition of transcription by adriamycin is a consequence of the loss of negative superhelicity in DNA mediated by topoisomerase II", *Molecular and cellular biochemistry*, vol. 93, no. 2, pp. 141-146.
- Taylor, E.L. & Gant, T.W. 2008, "Emerging fundamental roles for non-coding RNA species in toxicology", *Toxicology*, vol. 246, no. 1, pp. 34-39.
- Thannickal, V.J. & Fanburg, B.L. 2000, "Reactive oxygen species in cell signaling", *American journal of physiology. Lung cellular and molecular physiology*, vol. 279, no. 6, pp. L1005-28.
- Thorburn, A. & Frankel, A.E. 2006, "Apoptosis and anthracycline cardiotoxicity", *Molecular cancer therapeutics*, vol. 5, no. 2, pp. 197-199.
- Thum, T., Galuppo, P., Wolf, C., Fiedler, J., Kneitz, S., van Laake, L.W., Doevendans, P.A., Mummery, C.L., Borlak, J., Haverich, A., Gross, C., Engelhardt, S., Ertl, G. & Bauersachs, J. 2007, "MicroRNAs in the human heart: a clue to fetal gene reprogramming in heart failure", *Circulation*, vol. 116, no. 3, pp. 258-267.
- Thum, T., Gross, C., Fiedler, J., Fischer, T., Kissler, S., Bussen, M., Galuppo, P., Just, S., Rottbauer, W., Frantz, S., Castoldi, M., Soutschek, J., Koteliensky, V., Rosenwald, A., Basson, M.A., Licht, J.D., Pena, J.T., Rouhanifard, S.H., Muckenthaler, M.U., Tuschl, T., Martin, G.R., Bauersachs, J. & Engelhardt, S. 2008, "MicroRNA-21 contributes to myocardial disease by stimulating MAP kinase signalling in fibroblasts", *Nature*, vol. 456, no. 7224, pp. 980-984.
- Tokarska-Schlattner, M., Wallimann, T. & Schlattner, U. 2006, "Alterations in myocardial energy metabolism induced by the anti-cancer drug doxorubicin", *Comptes rendus biologiques*, vol. 329, no. 9, pp. 657-668.
- Tokarska-Schlattner, M., Zaugg, M., da Silva, R., Lucchinetti, E., Schaub, M.C., Wallimann, T. & Schlattner, U. 2005, "Acute toxicity of doxorubicin on isolated perfused heart: response of kinases regulating energy supply", *American journal of physiology. Heart and circulatory physiology*, vol. 289, no. 1, pp. H37-47.

Tokarska-Schlattner, M., Zaugg, M., Zuppinger, C., Wallimann, T. & Schlattner, U. 2006, "New insights into doxorubicin-induced cardiotoxicity: the critical role of cellular energetics", *Journal of Molecular and Cellular Cardiology*, vol. 41, no. 3, pp. 389-405.

Toogood, P.L. 2008, "Mitochondrial drugs", *Current opinion in chemical biology*, vol. 12, no. 4, pp. 457-463.

Toxopeus, C., van Holsteijn, I., de Winther, M.P., van den Dobbelsteen, D., Horbach, G.J., Blaauboer, B.J. & Noordhoek, J. 1994, "Role of thiol homeostasis and adenine nucleotide metabolism in the protective effects of fructose in quinone-induced cytotoxicity in rat hepatocytes", *Biochemical pharmacology*, vol. 48, no. 9, pp. 1682-1692.

Toxopeus, C., van Holsteijn, I., Thuring, J.W., Blaauboer, B.J. & Noordhoek, J. 1993, "Cytotoxicity of menadione and related quinones in freshly isolated rat hepatocytes: effects on thiol homeostasis and energy charge", *Archives of Toxicology*, vol. 67, no. 10, pp. 674-679.

Tsang, W.P. & Kwok, T.T. 2009, "The miR-18a* microRNA functions as a potential tumor suppressor by targeting on K-Ras", *Carcinogenesis*, vol. 30, no. 6, pp. 953-959.

Urva, S.R., Shin, B.S., Yang, V.C. & Balthasar, J.P. 2009, "Sensitive high performance liquid chromatographic assay for assessment of doxorubicin pharmacokinetics in mouse plasma and tissues", *Journal of chromatography.B, Analytical technologies in the biomedical and life sciences*, vol. 877, no. 8-9, pp. 837-841.

Valadi, H., Ekstrom, K., Bossios, A., Sjostrand, M., Lee, J.J. & Lotvall, J.O. 2007, "Exosome-mediated transfer of mRNAs and microRNAs is a novel mechanism of genetic exchange between cells", *Nature cell biology*, vol. 9, no. 6, pp. 654-659.

Valen, G. 2009, "Extracardiac approaches to protecting the heart", *European journal of cardio-thoracic surgery : official journal of the European Association for Cardio-thoracic Surgery*, vol. 35, no. 4, pp. 651-657.

Valencia-Sanchez, M.A., Liu, J., Hannon, G.J. & Parker, R. 2006, "Control of translation and mRNA degradation by miRNAs and siRNAs", *Genes & development*, vol. 20, no. 5, pp. 515-524.

van den Beucken, T., Koritzinsky, M. & Wouters, B.G. 2006, "Translational control of gene expression during hypoxia", *Cancer biology & therapy*, vol. 5, no. 7, pp. 749-755.

van Rooij, E., Marshall, W.S. & Olson, E.N. 2008, "Toward microRNA-based therapeutics for heart disease: the sense in antisense", *Circulation research*, vol. 103, no. 9, pp. 919-928.

van Rooij, E. & Olson, E.N. 2007, "MicroRNAs: powerful new regulators of heart disease and provocative therapeutic targets", *The Journal of clinical investigation*, vol. 117, no. 9, pp. 2369-2376.

van Rooij, E., Sutherland, L.B., Liu, N., Williams, A.H., McAnally, J., Gerard, R.D., Richardson, J.A. & Olson, E.N. 2006, "A signature pattern of stress-responsive microRNAs that can evoke cardiac hypertrophy and heart failure", *Proceedings of the National Academy of Sciences of the United States of America*, vol. 103, no. 48, pp. 18255-18260.

van Rooij, E., Sutherland, L.B., Thatcher, J.E., DiMaio, J.M., Naseem, R.H., Marshall, W.S., Hill, J.A. & Olson, E.N. 2008, "Dysregulation of microRNAs after myocardial infarction reveals a role of miR-29 in cardiac fibrosis", *Proceedings of the National Academy of Sciences of the United States of America*, vol. 105, no. 35, pp. 13027-13032.

- Vega, R.B., Huss, J.M. & Kelly, D.P. 2000, "The coactivator PGC-1 cooperates with peroxisome proliferator-activated receptor alpha in transcriptional control of nuclear genes encoding mitochondrial fatty acid oxidation enzymes", *Molecular and cellular biology*, vol. 20, no. 5, pp. 1868-1876.
- Vile, G.F. & Winterbourn, C.C. 1989, "Microsomal lipid peroxidation induced by adriamycin, epirubicin, daunorubicin and mitoxantrone: a comparative study", *Cancer chemotherapy and pharmacology*, vol. 24, no. 2, pp. 105-108.
- Vitko, I., Shcheglovitov, A., Baumgart, J.P., Arias-Olguin, I.I., Murbartian, J., Arias, J.M. & Perez-Reyes, E. 2008, "Orientation of the calcium channel beta relative to the alpha(1)2.2 subunit is critical for its regulation of channel activity", *PloS one*, vol. 3, no. 10, pp. e3560.
- Volinia, S., Calin, G.A., Liu, C.G., Ambs, S., Cimmino, A., Petrocca, F., Visone, R., Iorio, M., Roldo, C., Ferracin, M., Prueitt, R.L., Yanaihara, N., Lanza, G., Scarpa, A., Vecchione, A., Negrini, M., Harris, C.C. & Croce, C.M. 2006, "A microRNA expression signature of human solid tumors defines cancer gene targets", *Proceedings of the National Academy of Sciences of the United States of America*, vol. 103, no. 7, pp. 2257-2261.
- Wagner, B.K., Kitami, T., Gilbert, T.J., Peck, D., Ramanathan, A., Schreiber, S.L., Golub, T.R. & Mootha, V.K. 2008, "Large-scale chemical dissection of mitochondrial function", *Nature biotechnology*, vol. 26, no. 3, pp. 343-351.
- Walker, D.B. 2006, "Serum chemical biomarkers of cardiac injury for nonclinical safety testing", *Toxicologic pathology*, vol. 34, no. 1, pp. 94-104.
- Wallace, D.C. 2005, "A mitochondrial paradigm of metabolic and degenerative diseases, aging, and cancer: a dawn for evolutionary medicine", *Annual Review of Genetics*, vol. 39, pp. 359-407.
- Wallace, K.B. 2008, "Mitochondrial off targets of drug therapy", *Trends in pharmacological sciences*, vol. 29, no. 7, pp. 361-366.
- Wallace, K.B. 2003, "Doxorubicin-induced cardiac mitochondrionopathy", *Pharmacology & toxicology*, vol. 93, no. 3, pp. 105-115.
- Wallace, K.B., Hausner, E., Herman, E., Holt, G.D., MacGregor, J.T., Metz, A.L., Murphy, E., Rosenblum, I.Y., Sistare, F.D. & York, M.J. 2004, "Serum troponins as biomarkers of drug-induced cardiac toxicity", *Toxicologic pathology*, vol. 32, no. 1, pp. 106-121.
- Wallace, K.B. & Starkov, A.A. 2000, "Mitochondrial targets of drug toxicity", *Annual Review of Pharmacology and Toxicology*, vol. 40, pp. 353-388.
- Wang, L.L., Zhang, Z., Li, Q., Yang, R., Pei, X., Xu, Y., Wang, J., Zhou, S.F. & Li, Y. 2009, "Ethanol exposure induces differential microRNA and target gene expression and teratogenic effects which can be suppressed by folic acid supplementation", *Human reproduction (Oxford, England)*, vol. 24, no. 3, pp. 562-579.
- Wang, N., Zhou, Z., Liao, X. & Zhang, T. 2009a, "Role of microRNAs in cardiac hypertrophy and heart failure", *IUBMB life*, vol. 61, no. 6, pp. 566-571.
- Wang, S., Tian, C., Xiao, T., Xing, G., He, F., Zhang, L. & Chen, H. 2009b, "Differential regulation of Apak by various DNA damage signals", *Molecular and cellular biochemistry*, .
- Wang, Y., Liang, Y. & Lu, Q. 2008, "MicroRNA epigenetic alterations: predicting biomarkers and therapeutic targets in human diseases", *Clinical genetics*, vol. 74, no. 4, pp. 307-315.

- Weinstein, D.M., Mihm, M.J. & Bauer, J.A. 2000, "Cardiac peroxynitrite formation and left ventricular dysfunction following doxorubicin treatment in mice", *The Journal of pharmacology and experimental therapeutics*, vol. 294, no. 1, pp. 396-401.
- Weiss, R.B. 1992, "The anthracyclines: will we ever find a better doxorubicin?", *Seminars in oncology*, vol. 19, no. 6, pp. 670-686.
- White, S.M., Constantin, P.E. & Claycomb, W.C. 2004, "Cardiac physiology at the cellular level: use of cultured HL-1 cardiomyocytes for studies of cardiac muscle cell structure and function", *American journal of physiology. Heart and circulatory physiology*, vol. 286, no. 3, pp. H823-9.
- Wilkie, G.S., Dickson, K.S. & Gray, N.K. 2003, "Regulation of mRNA translation by 5'- and 3'-UTR-binding factors", *Trends in biochemical sciences*, vol. 28, no. 4, pp. 182-188.
- Williams, A.E. 2007, "Functional aspects of animal microRNAs", *Cellular and Molecular Life Sciences*, vol. 18, no. 7, pp. 7355-7359.
- Winter, J., Jung, S., Keller, S., Gregory, R.I. & Diederichs, S. 2009, "Many roads to maturity: microRNA biogenesis pathways and their regulation", *Nature cell biology*, vol. 11, no. 3, pp. 228-234.
- Wong, C.F. & Tellam, R.L. 2008, "MicroRNA-26a targets the histone methyltransferase Enhancer of Zeste homolog 2 during myogenesis", *The Journal of biological chemistry*, vol. 283, no. 15, pp. 9836-9843.
- Wu, A.H. 2008, "Cardiotoxic drugs: clinical monitoring and decision making", *Heart (British Cardiac Society)*, vol. 94, no. 11, pp. 1503-1509.
- Wu, L., Fan, J. & Belasco, J.G. 2006, "MicroRNAs direct rapid deadenylation of mRNA", *Proceedings of the National Academy of Sciences of the United States of America*, vol. 103, no. 11, pp. 4034-4039.
- Xiao, J., Luo, X., Lin, H., Zhang, Y., Lu, Y., Wang, N., Zhang, Y., Yang, B. & Wang, Z. 2007, "MicroRNA miR-133 represses HERG K⁺ channel expression contributing to QT prolongation in diabetic hearts", *The Journal of biological chemistry*, vol. 282, no. 17, pp. 12363-12367.
- Xu, C., Lu, Y., Pan, Z., Chu, W., Luo, X., Lin, H., Xiao, J., Shan, H., Wang, Z. & Yang, B. 2007, "The muscle-specific microRNAs miR-1 and miR-133 produce opposing effects on apoptosis by targeting HSP60, HSP70 and caspase-9 in cardiomyocytes", *Journal of cell science*, vol. 120, no. Pt 17, pp. 3045-3052.
- Xu, L.J., Jin, L., Pan, H., Zhang, A.Z., Wei, G., Li, P.P. & Lu, W.Y. 2006, "Deferiprone protects the isolated atria from cardiotoxicity induced by doxorubicin", *Acta Pharmacologica Sinica*, vol. 27, no. 10, pp. 1333-1339.
- Xu, T., Zhu, Y., Xiong, Y., Ge, Y.Y., Yun, J.P. & Zhuang, S.M. 2009, "MicroRNA-195 suppresses tumorigenicity and regulates G1/S transition of human hepatocellular carcinoma cells", *Hepatology (Baltimore, Md.)*, vol. 50, no. 1, pp. 113-121.
- Yang, B., Lu, Y. & Wang, Z. 2008, "Control of cardiac excitability by microRNAs", *Cardiovascular research*, vol. 79, no. 4, pp. 571-580.
- Yang, Y.P., Liang, Z.Q., Gu, Z.L. & Qin, Z.H. 2005, "Molecular mechanism and regulation of autophagy", *Acta Pharmacologica Sinica*, vol. 26, no. 12, pp. 1421-1434.

- Yi, X., Bekeredjian, R., DeFilippis, N.J., Siddiquee, Z., Fernandez, E. & Shohet, R.V. 2006, "Transcriptional analysis of doxorubicin-induced cardiotoxicity", *American journal of physiology.Heart and circulatory physiology*, vol. 290, no. 3, pp. H1098-102.
- Yin, X., Wu, H., Chen, Y. & Kang, Y.J. 1998, "Induction of antioxidants by adriamycin in mouse heart", *Biochemical pharmacology*, vol. 56, no. 1, pp. 87-93.
- York, M., Scudamore, C., Brady, S., Chen, C., Wilson, S., Curtis, M., Evans, G., Griffiths, W., Whayman, M., Williams, T. & Turton, J. 2007, "Characterization of troponin responses in isoproterenol-induced cardiac injury in the Hanover Wistar rat", *Toxicologic pathology*, vol. 35, no. 4, pp. 606-617.
- Young, J. 2001, "Healing the heart with ventricular assist device therapy: mechanisms of cardiac recovery", *The Annals of thoracic surgery*, vol. 71, pp. 210-219.
- Yu, L., Wan, F., Dutta, S., Welsh, S., Liu, Z., Freundt, E., Baehrecke, E.H. & Lenardo, M. 2006, "Autophagic programmed cell death by selective catalase degradation", *Proceedings of the National Academy of Sciences of the United States of America*, vol. 103, no. 13, pp. 4952-4957.
- Zhang, A., Wu, Y., Lai, H. W. L., Yew, D. T. 2004, "Apoptosis-A Brief Review", *Neuroembryology*, , no. 3, pp. 47-59.
- Zhang, C. 2008, "MicroRNAs: role in cardiovascular biology and disease", *Clinical Science*, vol. 114, pp. 699-706.
- Zhang, J., Clark, J.R., Jr, Herman, E.H. & Ferrans, V.J. 1996, "Doxorubicin-induced apoptosis in spontaneously hypertensive rats: differential effects in heart, kidney and intestine, and inhibition by ICRF-187", *Journal of Molecular and Cellular Cardiology*, vol. 28, no. 9, pp. 1931-1943.
- Zhang, S.D. & Gant, T.W. 2005, "Effect of pooling samples on the efficiency of comparative studies using microarrays", *Bioinformatics (Oxford, England)*, vol. 21, no. 24, pp. 4378-4383.
- Zhang, Y., Xiao, J., Wang, H., Luo, X., Wang, J., Villeneuve, L.R., Zhang, H., Bai, Y., Yang, B. & Wang, Z. 2006, "Restoring depressed HERG K⁺ channel function as a mechanism for insulin treatment of abnormal QT prolongation and associated arrhythmias in diabetic rabbits", *American journal of physiology.Heart and circulatory physiology*, vol. 291, no. 3, pp. H1446-55.
- Zhang, S.D. & Gant, T.W. 2004, "A statistical framework for the design of microarray experiments and effective detection of differential gene expression", *Bioinformatics (Oxford, England)*, vol. 20, no. 16, pp. 2821-2828.
- Zhao, Y. & Srivastava, D. 2007, "A developmental view of microRNA function", *Trends in biochemical sciences*, vol. 32, no. 4, pp. 189-197.
- Zheng, J. & Ramirez, V.D. 1999, "Piceatannol, a stilbene phytochemical, inhibits mitochondrial F₀F₁-ATPase activity by targeting the F₁ complex", *Biochemical and biophysical research communications*, vol. 261, no. 2, pp. 499-503.
- Zhou, S., Starkov, A., Froberg, M.K., Leino, R.L. & Wallace, K.B. 2001, "Cumulative and irreversible cardiac mitochondrial dysfunction induced by doxorubicin", *Cancer research*, vol. 61, no. 2, pp. 771-777.